

SACRAMENTO/SAN JOAQUIN RIVER DELTA
REGIONAL SALMON OUTMIGRATION STUDY PLAN:
DEVELOPING UNDERSTANDING FOR MANAGEMENT AND RESTORATION

Jon Burau, Aaron Blake and Russell Perry

December 10, 2007

1. INTRODUCTION

The Sacramento-San Joaquin Delta (Delta) is used as a migration corridor and as rearing habitat by juvenile Chinook salmon (*Oncorhynchus tshawytscha*) that emigrate from Central Valley Rivers on their annual migration to the Pacific Ocean. Four runs of Chinook salmon (fall, late-fall, winter, and spring runs) utilize the Sacramento basin, while fall Chinook use portions of east-side streams and the San Joaquin Basin. Winter-run Chinook are federally listed as an endangered species; spring-run Chinook are listed as threatened. Collectively, these species use the Delta for rearing and outmigration over a period from approximately November through May, with considerable variability attributed to genetic characteristics and watershed attributes (e.g. hydrology).

The migratory behavior of young salmon on the Sacramento River system is complex and not well understood (Kreeger and McNeil 1992). The specific timing of natural smolt migration depends on the physiological state of the fish and on local hydrologic conditions. Abiotic factors that are known to have a primary influence on young salmon migration include photoperiod/date, water temperature, and flow. Other factors which may affect migration include barometric pressure, turbidity, flooding, rainfall, species, stock (e.g., fall-run or spring-run), life history stage, degree of smoltification, parental origin (e.g., hatchery or wild), size of juveniles, location (e.g. distance from the ocean), food availability, etc. (Burgner 1991, as cited by Kreeger and McNeil 1992). In addition to all of these factors that make it difficult to predict outmigration behavior, there is limited understanding of the factors that control the pathways taken by juvenile salmonids as they migrate through the complex of channels that make up the geometry of the Delta.

Relevance

The interaction between seasonal timescale variations in upstream hydrology and strong tidal forcing within the Delta's complex network of channels has made it difficult to clearly identify the effects of water management actions on survival and recovery of endangered juvenile salmon populations. Nonetheless, long-term studies (e.g., Anadromous Fish Restoration Program's (AFRP) Delta Action 8) have generated working hypotheses that water exports reduce survival of juvenile salmon migrating through the central and southern Delta. Although these studies have historically been a key source of information for water project and fisheries agency managers, what remains unclear is the proportion of the population subject to these lower survival rates and, more generally, how survival rates compare between channels and between regions under a wide variety of physical conditions, such as Sacramento River flow rates, Delta Cross Channel (DCC) gate operations and export rates.

The need to understand the effects of current and proposed water project operations on survival of endangered salmon populations is vital and time critical. While salmon runs have been on the rise in recent years, the 2008 returns of fall run Chinook at Sacramento and San Joaquin River hatcheries are at all time lows (San Francisco Chronicle, 10/30/2007). Thus, it is important to conduct process-level studies on salmon now, before their numbers are reduced to levels which further constrain water supplies and make scientific inquiries difficult (as is currently the case with delta smelt). This information is needed to better understand how existing operations (reservoir releases and DCC gate operations) effect fish populations to determine if current operations can be improved to enhance the overall survival of outmigrants as the move through the delta. Beyond this immediate need, information on salmon outmigration is needed to assess the efficacy of ongoing and planned large-scale restoration efforts throughout the Central Valley and within the Delta that are designed to improve habitats for salmonids and increase their populations. Moreover, this information is needed to design, and determine operational criteria, for proposed structural changes in the Delta, such as those proposed in the Bay-Delta Conservation Plan (BDCP)(<http://www.resources.ca.gov/bdcp/>), the Through Delta Facility (TDF), and barriers/gates at Threemile Slough and False River, among others. The results from this effort will provide information that is essential for ongoing management actions and future political processes such as Governor Schwarzenegger's Blue Ribbon Delta Vision task force, and agency planning processes such as DWR's Delta Risk Management Strategy (DRMS), and CALFED's Bay-Delta Conservation Plan (BDCP) and Delta Regional Ecosystem Restoration Implementation Plan (DRERIP). Finally, these results should provide valuable information needed to manage the salmon fishery in the face of possible changes associated with global warming, such as changes in the quantity and timing of fresh water entering the Delta, and sea level rise and temperature increases.

Unfortunately, with our current level of understanding of salmon outmigration and survival we cannot predict, with any degree of certainty, the impacts of proposed significant physical and operational changes on the survival of juvenile salmon in the Delta. This lack of understanding could significantly delay/constrain the implementation of proposed changes in the system. Or, worse yet, this lack of understanding could lead to significant after-the-fact negative unintended consequences caused by ill-informed structural or operational changes.

This study is motivated by the following question:

How do we manage the bay/delta system, using changes in water project operations, changes in geometry and plumbing (barriers, tide gates, canals), or through restoration efforts, to maintain or improve the survival of Sacramento River salmon outmigrants within the Delta in the face of potentially dramatic changes, such as changes in delta conveyance and global climate change?

Physical Setting

The Delta is a complex network of natural and man-made channels confined behind levees that are, for the most part, covered with rock. From the air, the delta appears incredibly complex, yet the geomorphology within individual channels is typically devoid of the bathymetric variability characteristic of natural river channels - deep areas on the outsides of bends and point bars on the insides of bends are rare. For example, the Clarksburg bend, described in detail later, is one of the few deep channel/point bar systems in the delta. Moreover, the narrow shallow vegetated environments that typically border the deeper water areas in natural channels are virtually non-

existent in the delta. Thus, the channels in the delta are essentially prismatic, armored **canals** that have been optimized, over the years, to convey water and to protect adjacent lands from flooding. As a consequence, many of the channels in the delta provide little in the way of suitable refugia and rearing habitat for Sacramento River salmon outmigrants

Juvenile salmon traversing the network of channels in the delta may take any number of migration routes on their journey to the ocean. For example, Steamboat and Sutter Slough, entering the Sacramento River upstream of the Delta Cross Channel (DCC), is one major route through which juvenile salmon may migrate. The Sacramento River and numerous secondary routes through the Delta also exist; including the Delta Cross Channel and Georgiana Slough, both of which may divert fish into the central and southern Delta, where previous studies have shown reduced survival (U.S. Fish and Wildlife Service, 1996; Newman and Rice, 1997; Brandes and McLain, 2001).

Added to the physical complexity of the Delta is hydrodynamic complexity that varies significantly at daily to seasonal timescales due to natural processes, such as the tides and hydrologic cycle, and human influences, such as reservoir releases, DCC gate operations, and export rates. Discharge and water velocities within the Delta channels are not only influenced by the river flows but are strongly influenced by the tidal flow and stage, which can vary both at daily and fortnightly (14-day) time scales. The influence of the tidal flows and stage varies directly with proximity to the ocean and inversely with river flows: at a given location, the influence of the tidal flows and stage decreases as the river flow increases. The tidal flows and stage not only affect the discharges and water velocities within a given channel, they also affect how the total river discharge is distributed among the channels at junctions (Dinehart and Burau, 2005b). For instance Dinehart and Burau (2005a), found that water enters the Delta Cross Channel from downstream during flood tides and the flow in the Sacramento River virtually bypasses the DCC altogether during ebb tides.

The Delta is also affected by numerous human demands on its water resources. In addition to in-Delta agricultural use, the State Water Project (SWP) and Central Valley Project (CVP) export water out of the southern Delta for agriculture and human consumption in the southern regions of the State. Water project operations affect the net (tidally-averaged) discharge throughout the south, central and western Delta, and at some locations, water can flow in a net upstream direction (depending on the difference between exports and inflows). The Delta Cross Channel, a man-made channel used to divert flow from the Sacramento River into the central and southern Delta, is a critical component of the CVP and is also relevant to SWP and Contra Costa Water District (CCWD) exports, especially in the late summer and early winter periods. The diversion of Sacramento River water through the DCC into the central delta reduces salinities in the central and southern Delta so that water can be exported by the water projects.

Flow into the DCC is controlled by radial gates; changes in the position of the DCC gates has the principal effect of significantly, and in a step function fashion, changing the geometry of the north delta. When the gates are closed, the north delta is completely isolated from the Mokelumne system, as it was historically. When the gates are closed the net flows in the Sacramento River downstream of Georgiana Slough, and the net flow in Sutter and Steamboat Sloughs (in channels upstream of the DCC) and in Georgiana Slough increase (see [appendix A](#)), potentially influencing the routes taken by outmigrating juvenile salmon. Indeed, preliminary results from the north delta pilot, discussed in the next section, suggest this is the case. Conversely, when the DCC gates are open, the hydrodynamics of the north delta and Mokelumne River system interact, resulting in a decrease in the net flow in Sutter, Steamboat, Georgiana Sloughs and the Sacramento River downstream of Georgiana Slough. The primary impact of DCC gate operations on the north delta is a step function (and predictable – see [appendix A](#)) change in how the flows are distributed among the channels in the north delta. The

Mokelumne River system, on the other hand, is transformed from a system that is dominated by the tides when the gates are closed, to a system that is dominated by advection of water that passes through the DCC when the gates are open. The step function change in the hydrodynamics of the Mokelumne system due to gate operations has unknown consequences for Mokelumne River salmon and steelhead outmigrants (J. Miyamoto, personal communication).

Fisheries Impacts

As migrating fish enter the Delta from the Sacramento River, the population is distributed within the delta's complex network of channels. Each migratory pathway has a unique set of biotic and abiotic processes that affect migration rates, predation rates, feeding and growth rates, and ultimately, survival. For example, fish entering the central and southern Delta must traverse longer routes and are subject to entrainment at the CVP and SWP, both of which may decrease survival of juvenile salmon using this migratory pathway (Brandes and McLain, 2001). Population-level survival rates of juvenile salmon migrating through the Delta are driven by 1) the proportion of the population using each migratory pathway, and 2) the survival rates arising from a suite of processes unique to each migratory pathway. Many of these processes vary at scales that are relevant over the period of the outmigration within a given year and between years. For example, the locations where predators congregate and feed are thought to vary seasonally and between years, although very little work has been done on this issue. Researchers have long speculated that striped bass, in particular, migrate between channels and between regions at daily to seasonal timescales (Vogel, personal communication). Finally, natural and human-imposed variations in discharge, water velocities, and water routing affect the distribution of salmon outmigrants among channels, and affect survival within each channel, ultimately affecting survival of the outmigrant population as a whole.

2. SUMMARY OF PREVIOUS WORK

Currently, there is poor understanding of how human-imposed and natural changes in water distribution affect route selection and route-specific survival of outmigrating juvenile salmon. Historically, salmon outmigration studies have been conducted at the scale of the Delta: single one-time large releases of coded-wire tagged salmon into the Sacramento River between the city of Sacramento and Walnut Grove (with release times governed by trucking logistics) followed by trawling conducted at Chipps Island. This approach treats the entire Delta as if it were a “black box”. Results from studies conducted in this way tells us nothing about how the population was distributed among the various channels in the Delta, where the mortality occurred and what caused the mortality. The proposed study seeks to get inside the “box”; it is specifically designed to monitor where the salmon went, what their survival was within individual channels and how the things that we can control, such as Sacramento River flows, DCC gate operations and export rates, affect the ultimate survival to Chipps Island on a junction-by-junction, reach-by-reach basis. Moreover, past studies have often been conducted without regard to controlling physical factors such as tidal current phase, spring/neap cycle, solar cycles and turbidity (Brandes and McLain, 2001). More recently, however, studies began to integrate the movement of salmon outmigrants with hydrodynamic and meteorological measurements (Blake and Horn (in press)^{a,b}, Dinehart and Burau, 2005^{a,b}). For example, recent work by the USGS has shown that operation of the DCC not only affects the discharge in the Sacramento River, but the discharge in Sutter, Steamboat and Georgiana Sloughs (see [appendix A](#)) suggesting that the impacts of DCC gate operations on salmon outmigrants is regional in scale and that these impacts must be studied, at a minimum, throughout the north Delta region.

Moreover, the entrainment of juvenile salmon in junctions can be quite complex, owing to the spatial complexity and temporal unsteadiness of the tidally driven current structures within junctions (Dinhart and Burau, 2005). For example, Vogel (2004) showed that reversing tidal flows in the Sacramento River can advect juvenile salmon past a junction, only to have these same fish entrained into other channels such as the DCC or Georgiana Slough on the next tide. Because of these observations we hypothesize that changes in DCC operations (1) *primarily* influence the distribution of juvenile salmon among the various north Delta channels (e.g. route selection) because the DCC gates *primarily* influences the flow splits within the north delta junctions, and, (2) *secondarily*, the survival within these channels because of the changes in the net flows caused by gate operations (see [appendix A](#)).

Results from North Delta Pilot

The primary goals of the north delta pilot studies were aimed at testing a variety of state-of-the art measurement techniques and analytical approaches in preparation for the study described in this study plan. To account for variations in tidal conditions, fish were released over a 24 hour period. A total of 96 fish were released when the DCC was open (December 14, 2004) and the net Sacramento River flow at Freeport was approximately 19,600 cfs. An additional 150 fish were released at the same location when the DCC was closed (January, 2007), and the net Freeport flow was approximately 11,300 cfs. A brief description of the statistical models applied to these data is described in [Appendix B](#). These investigations were limited in scope; notably, detailed measurements at Clarksburg Bend in the Sacramento River and the deployment of a handful of acoustic telemetry stations in the north delta. Nevertheless, preliminary results for the North Delta Pilot study, in which ~16 hydrophones were deployed in two different configurations based on DCC gate position ([figures 2.1 and 2.2](#)), showed that both route selection and reach-specific survival depend upon Sacramento River discharge and DCC gate position. These preliminary conclusions are based on a total of ~250 acoustically-tagged fish released near the city of Sacramento. [Figure 2.3](#) summarizes the principal results from the two pilot study releases. From [figure 2.3](#) we can see the data strongly suggest: (1) when the DCC gates are closed the probability that salmon are entrained in Sutter, Steamboat and Georgiana Sloughs increases, which is consistent with increases in discharge in each of these channels when the gates are closed ([see appendix A](#)), (2) survival in every channel was higher at the higher discharge: survival in the Sacramento River increased by ~20% between the city of Sacramento and Sutter Slough, by ~8% in the reach between Steamboat Slough and the DCC, and ~15% between Georgiana Slough and Cache Slough. (3) Survival in Georgiana Slough is consistently lower than in any other channel where survivals were estimated. And, finally, (4) the precision in the survival estimates are progressively lower (error bars increase) farther into the system because the number of fish passing through the lower reaches is less. The sample size in channels farther from the release sites are reduced because: (1) the total number of fish are progressively distributed into a greater number of pathways, and (2) mortality occurs as fish traverse the system, leaving fewer viable fish to traverse channels at greater distances from the release site. To our knowledge these are the first estimates of juvenile salmon route selection and survival probabilities in the bay/Delta system.

There were a couple of channels for which we had survival rates from both pilot study releases and thus we can plot the survival in each channel versus the Sacramento River flow as is shown in [figure 2.4](#). The two survival estimates computed from the pilot study data are plotted with their associated error bars (at the 95% confidence interval) within each panel for each reach – the dashed lines are fictitious relations that fit the data. Ultimately, we propose to establish survival vs the individual

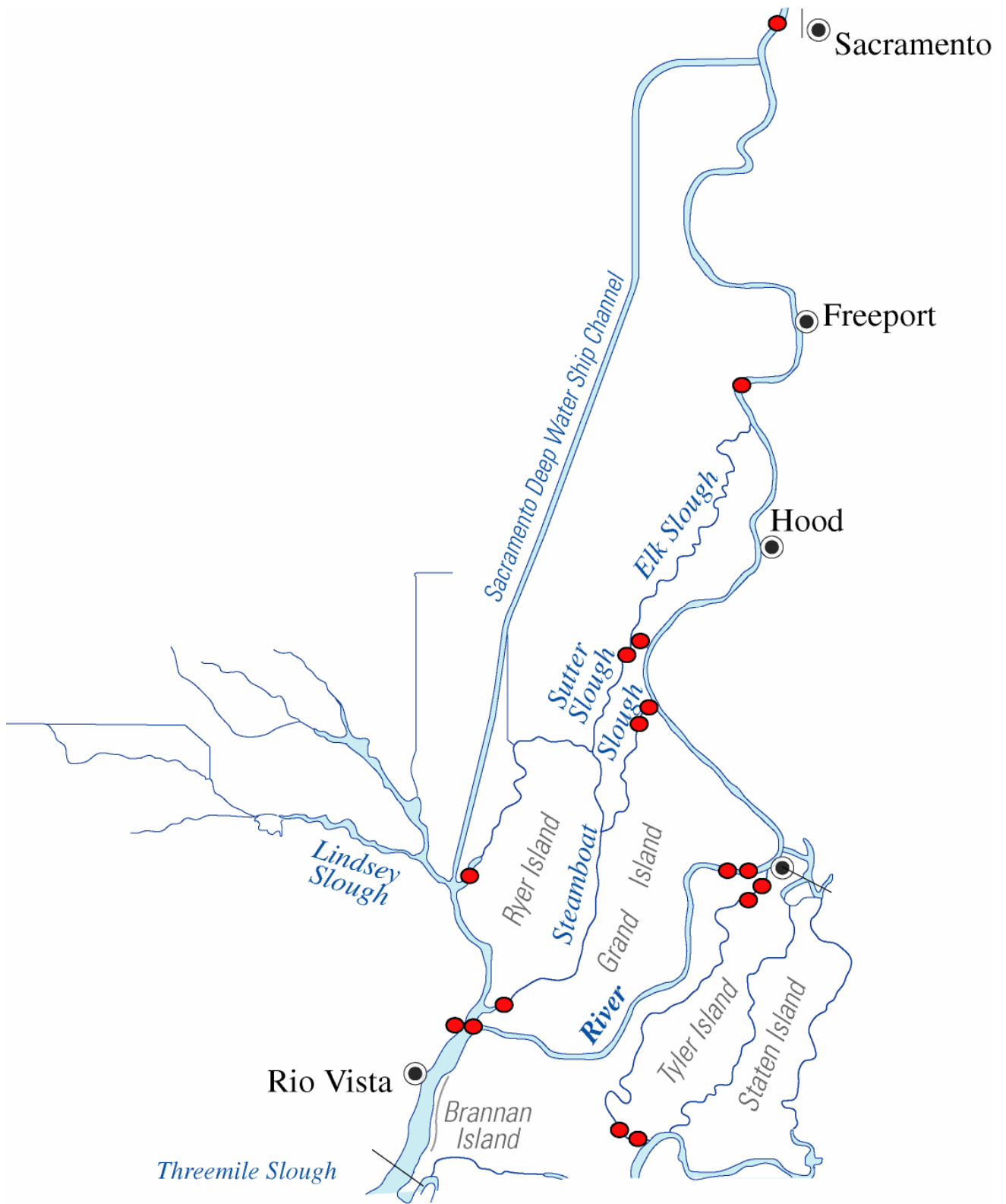


Figure 2.1 – Acoustic tag receiver locations for the 2006-2007 pilot study – DCC gate closed configuration.

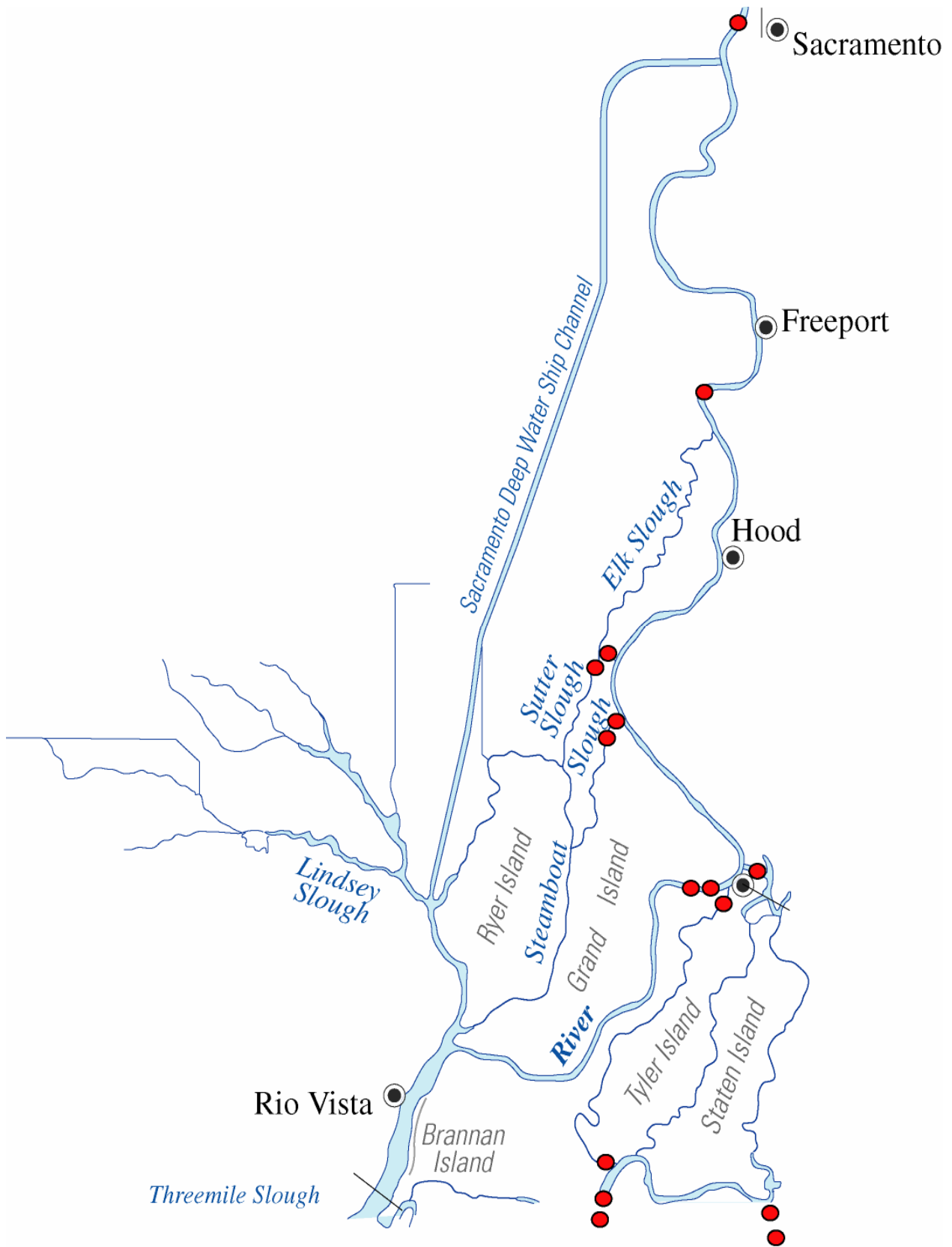


Figure 2.2 – Acoustic tag detection locations for the 2006-2007 pilot study – DCC gate open configuration.

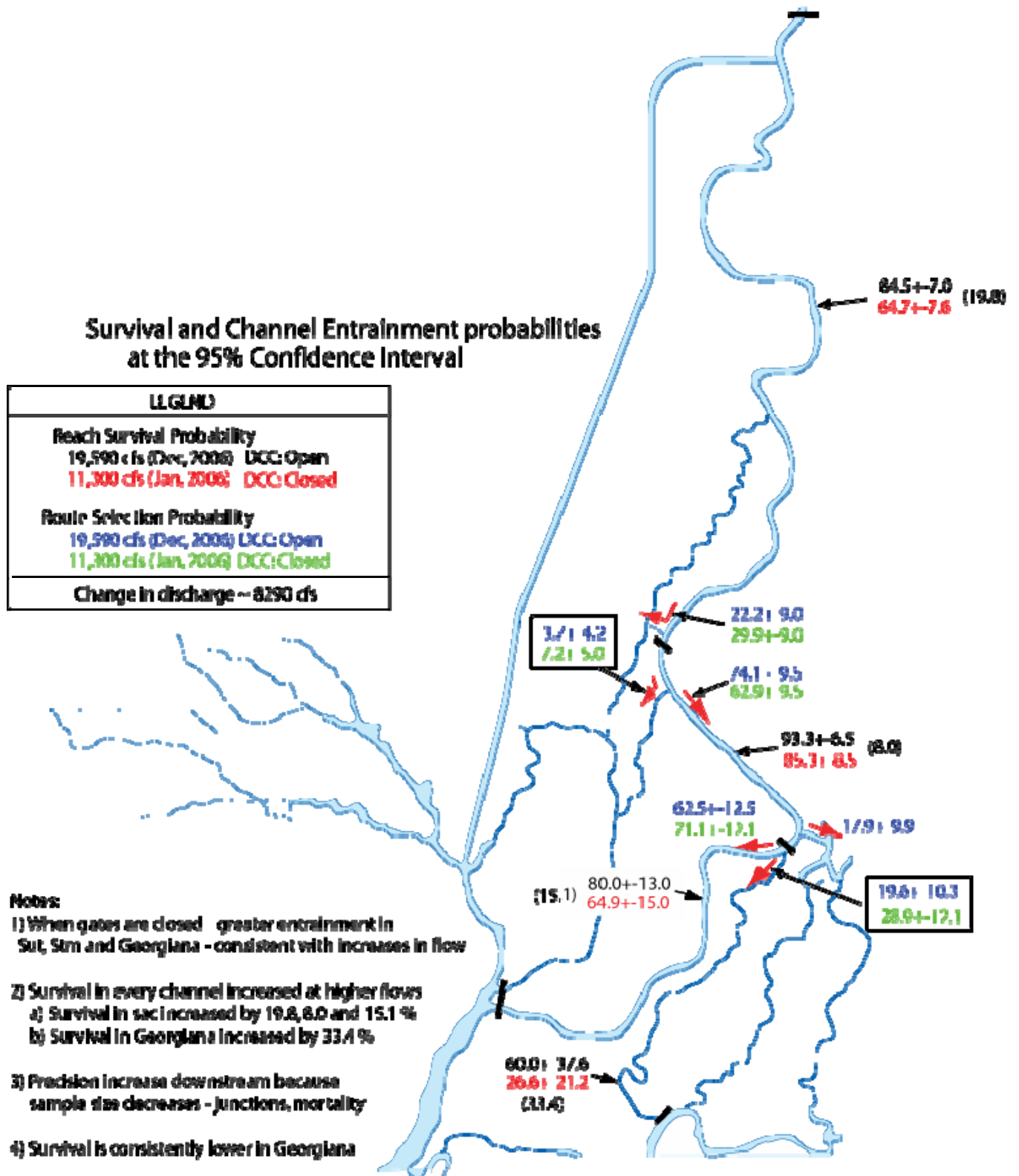


Figure 2.3 – Summary of the survival and entrainment probability estimates for the 2006-2007 pilot study.

Survival/Discharge relations 2006-07 Pilot study results

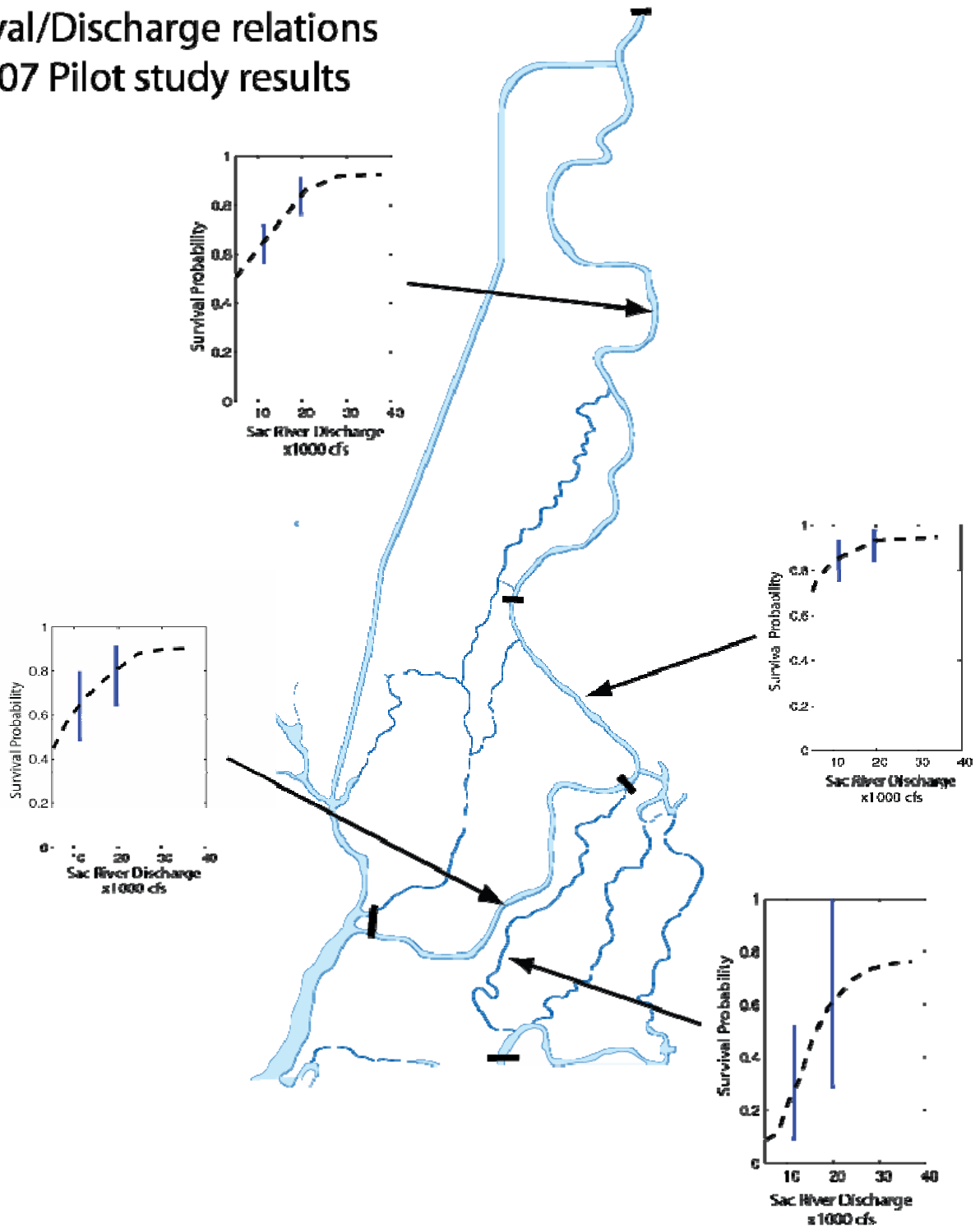


Figure 2.4 – Survival versus discharge relations for several reaches based on the 2006-07 pilot study results. The dashed lines are purely for illustrative purposes and are intended to show that obtaining survival discharge relations is one of many possible analytical approaches we propose to use in this investigation.

channel discharge relations over a broad range of flows and DCC gate operations for every reach where data are available from the proposed 2008-09 regional study as a first step in the development of predictive management tools. Relationships like this will form the statistical linkage between the tidally averaged hydrodynamics, which we can model accurately now, and salmon outmigration in a management tool to be discussed.

These preliminary results suggest that survival increased with increasing discharge in every channel where comparisons between releases could be made. From these results, we hypothesize that the increased travel time through the system associated with the lower Sacramento River flow rates may be responsible for the reduced overall survival. However, at this writing these conclusions are preliminary, particularly when the error bars associated with these results are taken into account (figure 2.4). The error bars shown in figure 2.4 are primarily a function of the small number of acoustically tagged fish used in the pilot study. Detection probabilities at the receivers can also play a role in the precision of the survival estimates (as is discussed in Appendix B), however, during the pilot the detection probabilities were very good (~1.0). Indeed, one of the principal objectives of the proposed study is to: (1) further investigate the implications of discharge dependent route selection and survival rates in relation to proposed structural and operational changes and (2) reduce the uncertainty in the survival rate estimates by using a larger sample size (e.g. more fish)(see “*Estimating Sample Size and Precision of Survival Estimates*” for details). It is important to note that unlike the coded-wire-tag studies of the past (Brandes and McLain, 2001), the statistical power (e.g. error bars) associated with the survival estimates are an intrinsic feature of the statistical models that will be used in this investigation.

The possible inverse relation between juvenile salmon survival and discharge at low flows implies that existing instream withdrawals, as well as proposed withdrawals from the Sacramento River through a number of options considered under the BDCP, an expanded DCC, or a Through Delta Facility (TDF), could increase mortality within the channels in the north Delta (see figure 2.4). Although very preliminary, the pilot study results suggest that decreases in survival associated with any withdrawals from the Sacramento River (DCC, TDF or a number of BDCP options) may need to be taken into account in the design and operation of these facilities, if they are built. Hopefully, significant decreases in survival, if they exist, will be limited to withdrawals that occur during low flow periods. The proposed studies aim to document the dependency of reach specific survival on discharge and DCC gate operations, if it exists. Reach-specific survival, as well as route selection, will be studied using mark-recapture models based on the data collected from an array of roughly 40 listening stations deployed throughout the north, western and central Delta described in detail in section 6 (“*Mark-recapture modeling*”) (figure 4.1).

Total discharge is not the only factor effecting survival. For example, the correlation between day/night behaviors with the tidal currents may also control transit time, at shorter timescales (Appendix C). The relative phase between the solar cycle (day/night/crepuscular periods) and the tidal cycle (flood vs ebb) may also influence transit times and exposures to predators. The predator field is likely to also be non-stationary at a variety of timescales and may also vary in relation to hydrodynamic conditions. Since many predators are associated with structure (docks, sharp bends, etc.), local, spatially distinct, and, perhaps hydrodynamically driven, “hot spots” may, in fact, substantially contribute to overall reach survival. Thus, predation is likely not continuous along a given reach but may occur in discrete highly localized areas. Although this study is not intended to directly address these “hot spots”, some level of site specific information will be obtained through

proposed mobile tracking efforts. Still, these “hot spots” could be very important as a management tool - potentially forming the basis of site specific restoration efforts, and/or design of future facilities or reconfiguration of existing facilities aimed at reducing predation of juvenile salmon.

Clarksburg Bend Experiment

Recent research by Blake and Horn ([in press; a, b](#)) has shown that juvenile salmon approaching channel junctions are not entrained in proportion to distribution of the flows (e.g. net discharges) in junctions. For fish to “go with the flow” salmon outmigrant spatial distributions would, on average, have to be homogeneous. These authors hypothesized that salmon are not homogeneously distributed in the water column and that secondary circulation (Dinehart and Burau, 2005b) concentrate juvenile salmon on the outside of river bends ([figure 2.5](#)) where they are more likely to become entrained in channels located on the outside of river bends. Every single junction in the Sacramento River is located on the outside of a bend in the river ([figure 2.6](#)) and thus secondary circulation may play a role in how salmon are distributed among the channels of the north delta.

Preliminary results from a recent study conducted in Clarksburg bend in the winter of 2006-07, showed that fish were predominately distributed on the outside of bend at night, while significant “holding” and “milling” behavior occurred during the day ([see Appendix C](#)).

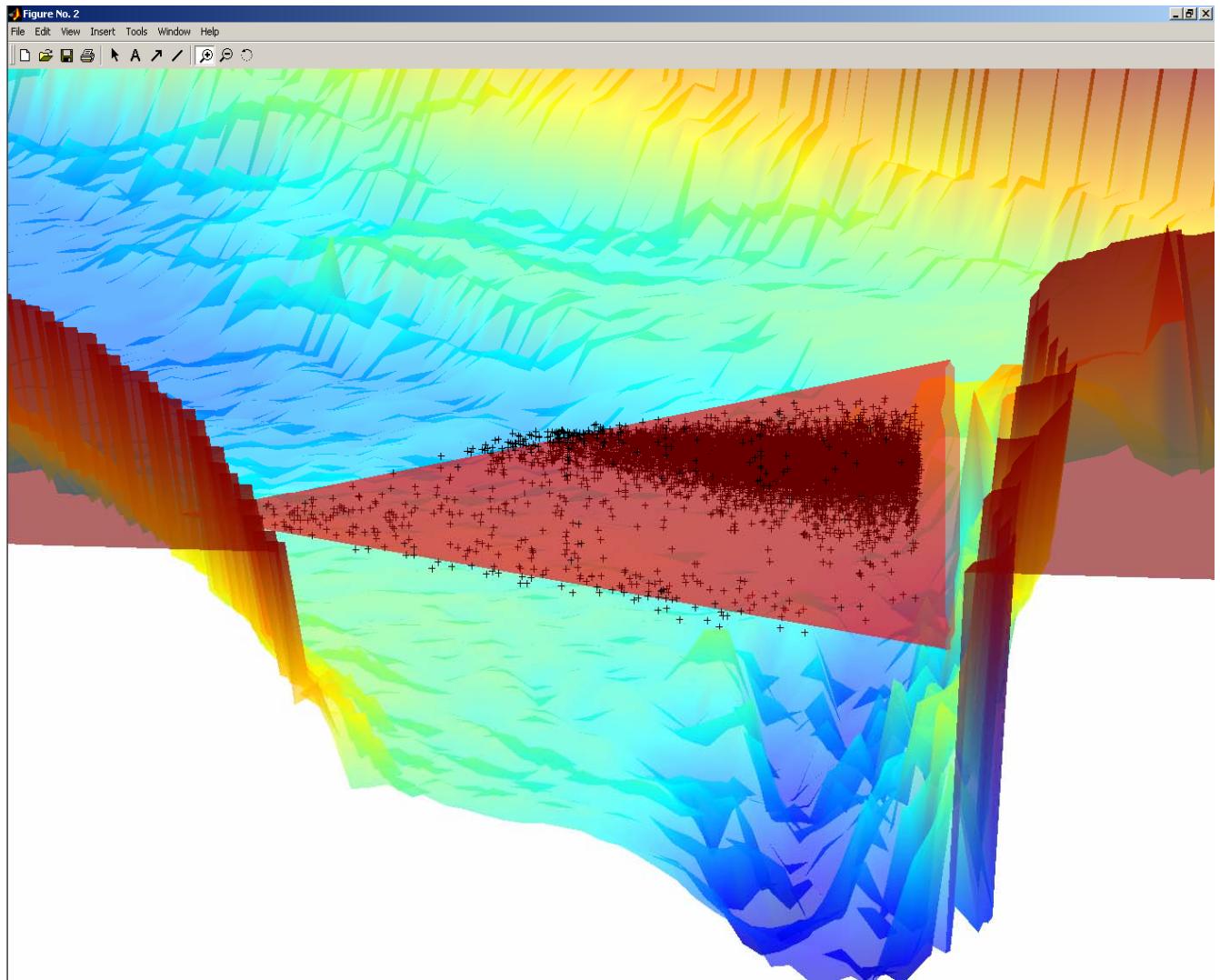


Figure 2.5 – Detections of juvenile salmon on the outside of a bend in the Sacramento River immediately downstream its junction with Georgiana Slough (Courtesy of Blake and Horn, in press)

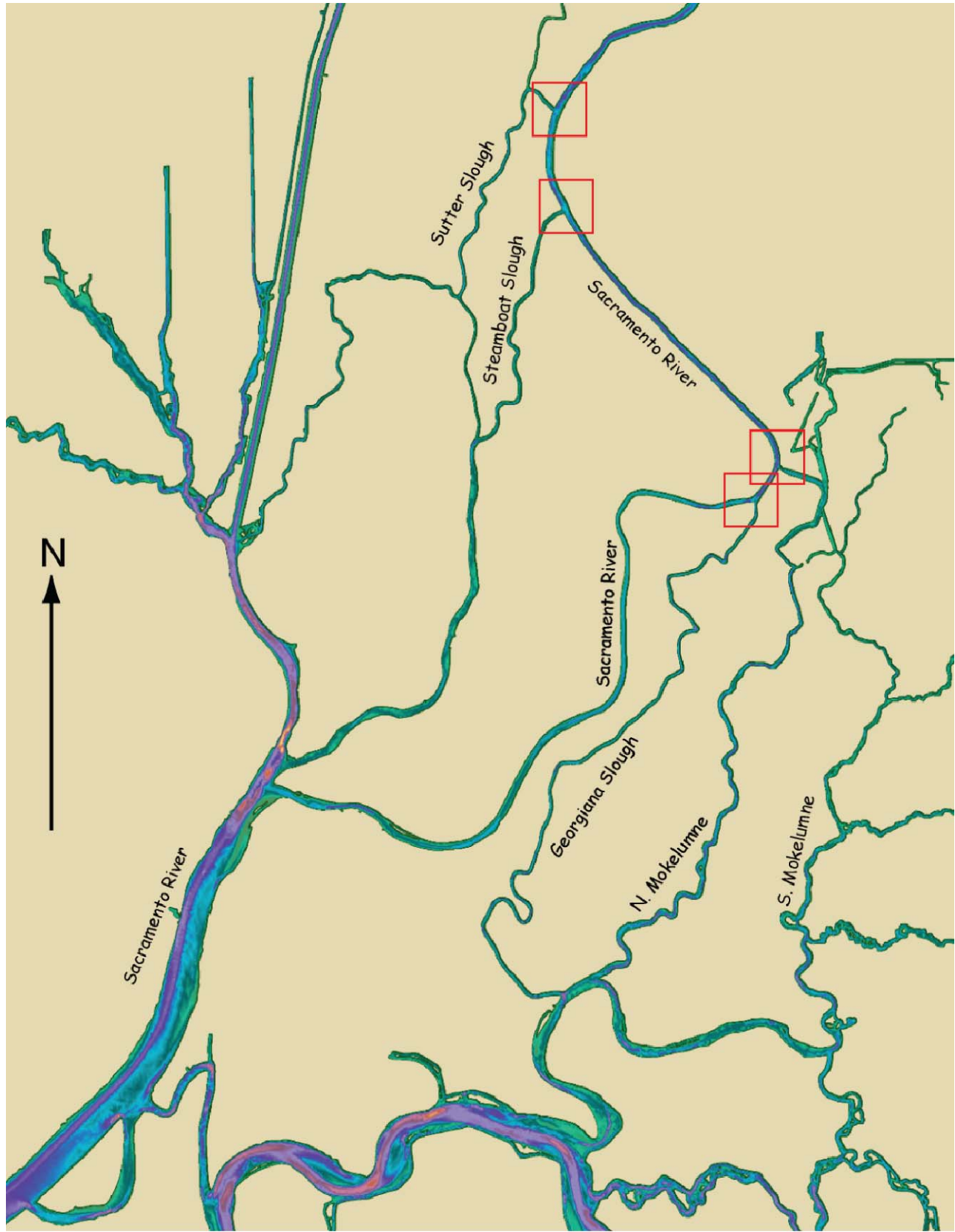


Figure 2.6 – All of the junctions on the Sacramento River are located on the outside of river bends.

3. PURPOSE

The overarching goal of this salmon outmigration study is to:

Develop a management model to predict the impacts of management actions on salmon survival.

Management actions include changes in geometry, such as modification of channel alignments at junctions, barriers/gates in Franks Tract and elsewhere, as well as changes in operations, such as changes in reservoir releases, export rates, DCC re-operations, and the Through Delta Facility (TDF) and an expanded Delta Cross Channel (DCC) and numerous options proposed in the BDCP. This management model, based on synthesis of the field data and computer models described in this section, will also be needed to manage the salmon fishery in the face of possible changes associated with climate change; such as changes in hydrology (quantity and timing of river inputs), sea level rise and temperature increases. To be predictive over a broad range of conditions, these management tools will need to incorporate a process-level understanding of the principal mechanisms that control juvenile salmon route selection and survival. This, of course, will not be easy, particularly in the tidally dominated and heavily managed bay/Delta system. Nonetheless, with multi-billion dollar modifications to the Delta being seriously considered in the wake of Katrina and the possibility of climate change, this process-level understanding will be needed to predict impacts on the salmon fishery from both natural and human-induced changes. Indeed, the central challenge of this investigation is the distillation of those processes that control salmon outmigration into the proposed management tools.

The intent of this study is to associate salmon movements with physical factors such as current speed, solar radiation, etc., and to incorporate field data and statistical sub-models directly into numerical hydrodynamic transport models. This mechanistic approach makes the tacit assumption that physical factors, such as river inputs, current speeds, turbidity and solar radiation are first order drivers of the outmigration process and that biotic factors, such as species, stock (e.g., fall-run or spring-run), life history stage, degree of smoltification, parental origin (e.g., hatchery or wild), size of juveniles, location (e.g. distance from the ocean), food availability, and non-stationary predator fields are second order drivers that can be “layered on”, or taken into account, after the impacts of the first order processes are fully investigated. With process-based predictive tools, water project managers and policy makers, will be able to evaluate the impacts of operational and physical changes on overall salmon survival that fall outside the current physical and operational paradigms.

The way in which we propose to characterize the impacts of proposed management actions is through the linkage of a series of statistical and mechanistic sub-models representing key processes, such as salmon migration timing, route selection, and survival ([Figure 3.1](#)) using the following methods.

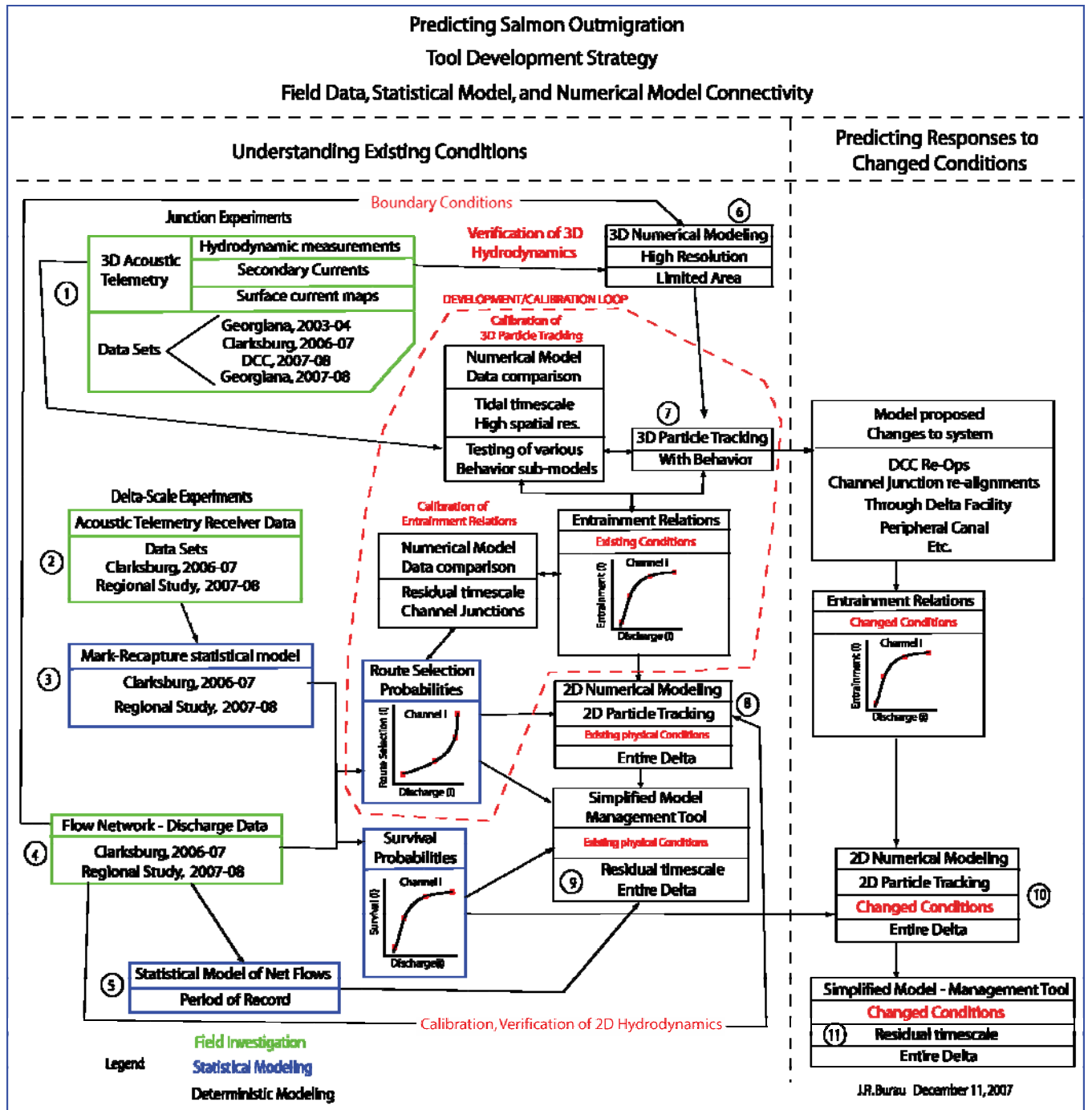


Figure 3.1 – Schematic representation of the interrelationships between the field experiments, statistical modeling, deterministic (hydrodynamic) models and simplified management models.

4. METHODS

A combination of field experiments and numerical modeling will be used in this investigation. Both the field work and modeling will be investigated at two principal scales: (1) at the scale of the junction, where mechanisms critical to route selection will be studied, and (2) at the scale of the channel network, where reach-specific survival will be studied. This separation is partly for conceptual and computational convenience, however, it is also based on data that suggests that outmigrants spend very little time in junctions (order of minutes) (Vogel, 2004; Blake and Horn, in press, a) compared to the time spent within each reach. For example, the outmigration time from the City of Sacramento to Chipps Island is typically on the order of weeks (Brandes and McLain, 2001), although transit times obviously vary with the Sacramento River flow. Thus, mortality within junctions is assumed to be zero (although we know it occurs) so that junctions are studied and modeled as a place where route selection, (or entrainment) occurs and mortality, wherever it occurs, is assigned exclusively to the channel-segments. If this assumption is violated, we will know it from the mobile tracking component of the proposed experiment in which location of defecated tags is determined.

Overview – Combining the field data collection and numerical modeling

The field experiments, and the way in which information is exchanged from more complex models to progressively simpler models, is based on separating the overall process of salmon outmigration into route selection at junctions and survival within reaches. Ultimately, we hope to develop relations for route selection and survival that depend on physical variables, such as flow splits and transit times, respectively; variables that are well predicted by existing numerical models. Thus, the field experiments will provide the data necessary to inform the development of a hierarchy of models, beginning with state of the art high resolution numerical 3D models, which will inform, in a natural progression, simplified models appropriate for use in a management setting ([figure 3.1](#)).

This study marks a significant increase in scale (spatial and temporal resolution) and cost over previous salmon outmigration investigations, due in part to newly emerging technologies (Vogel, 2006). Given the large scale and interdisciplinary nature of the proposed field investigations, the field work will, of necessity, be an integrated interagency endeavor; involving two USGS disciplines (Water Resources, California Water Science Center (CAWSC); Biological Resources, Columbia River Research Lab (CRRL)), the US Fish and Wildlife Service, California Department of Fish and Game, and numerous private contractors (Dave Vogel, Natural Resources Scientists), in consultation with US Bureau of Reclamation and California Department of Water Resources water project operators. This increase in scale is based on the recognition that certain intransigent management problems cannot be solved through years of small-scale, low budget, low statistical-power investigations. Results from studies with a high degree of uncertainty are simply not very useful. If investments are not made at the appropriate scale, solutions may never be found - no matter how many years the problem is studied. To be successful, the scale of the study must match the intrinsic scale of the problem. Experiments aimed at understanding the inherent complexity of salmon outmigration, which necessarily involves numerous abiotic factors and behavioral responses that occur at a variety of timescales within the context of a highly managed, tidally dominated, incredibly complex network of channels, require a commensurate level of sophistication in their design, and in their temporal and spatial coverage.

The proposed investigation is unique in that it involves concurrent measurements of hydrodynamic processes and salmon movements at a variety of spatial and temporal scales that are specifically intended to develop and calibrate a hierarchy of interconnected statistical and deterministic models (figure 3.1). The complex interactions between fish behavior, hydrodynamics and water management actions occur at fine temporal and spatial scales which, when integrated over space and time, determine the population distribution throughout the delta and overall survival rates that occur over the duration of the juvenile salmonid migration season. It is our intention to develop simplified management tools for predicting the impacts of various actions on the out-migration population, based on a hierarchy of detailed models that explicitly encompass appropriate temporal and spatial averages of behavioral responses of salmon outmigrants to the salient hydrodynamic processes. Therefore, this study is designed to: (1) understand the fundamental mechanisms that govern how salmon move through, and survive within the existing system and (2) use field data to develop mechanistic models that predict how salmon will move through the system under substantially changed conditions, such as a Delta that includes a various BDCP options or through delta facility. None of the physical and biological models proposed in this investigation will be developed in the absence of data collected at the appropriate scale. For example, at the scale of the junction, surface current maps and transects of secondary circulation will be made at the junction of the Sacramento River and the DCC as well as the junction of the Sacramento River and Georgiana Slough (see section 5 “junction experiments”). Concurrently, acoustically-tagged salmon will be monitored at these junctions so that behavioral responses to the hydrodynamic environment can be deduced. These data will be used to: (1) calibrate and validate high resolution 3D numerical model simulations of these processes at these junctions, (2) provide the 3D current structure for understanding the role of bathymetric variations in the entrainment of juvenile salmon at junctions. The field data and detailed 3D numerical model simulations will hopefully lead to mechanistically based entrainment relations at these and other junctions in the Delta. Similarly, at the scale of the Delta, flow stations, operated by the USGS, will collect hydrodynamic information that will (1) provide the boundary condition data for the detailed 3D hydrodynamic calculations, (2) provide the data needed for the calibration and validation of 2D numerical hydrodynamic model (RMA) (see section 6 “flow network”) and (3) provide measures of the hydrodynamic conditions at many of the acoustic telemetry receiver locations (see section 6 “delta scale experiment”).

Most of the acoustic tag listening stations (figure 4.1) will be placed at the flow station locations (figure 4.2) so that correlations between current speed and the movements of acoustic tag salmon can be made. The acoustic tag listening stations will allow us to develop statistical models based on well known mark-recapture models. The mark-recapture models will provide route selection and survival probabilities for the balance of the model development, and so on. To our knowledge this is the first time, the field data, in terms of both the physical and biological measurements, and the statistical and deterministic modeling efforts have been so tightly integrated, with the specific aim of developing simplified management tools.

The field experiment proposed for the winter of 2008-2009 will involve detailed investigations at two junctions (e.g. DCC and Georgiana Slough, figure 4.3), the so-called “junction experiments” (component (1) in figure 3.1), where the mechanisms that control route selection will be studied in detail, and a large network of acoustic tag listening stations (figure 4.1), where route selection probabilities will be computed for numerous other junctions, and survival probabilities will be estimated (components (2) and (3) in figure 3.1) throughout the Delta. The hydrodynamic data from the junction experiments will be used to calibrate and verify a 3D numerical model (component (6) in figure 3.1), applied to a limited area of the Sacramento River (figure 4.4) and the measured 3D tracks

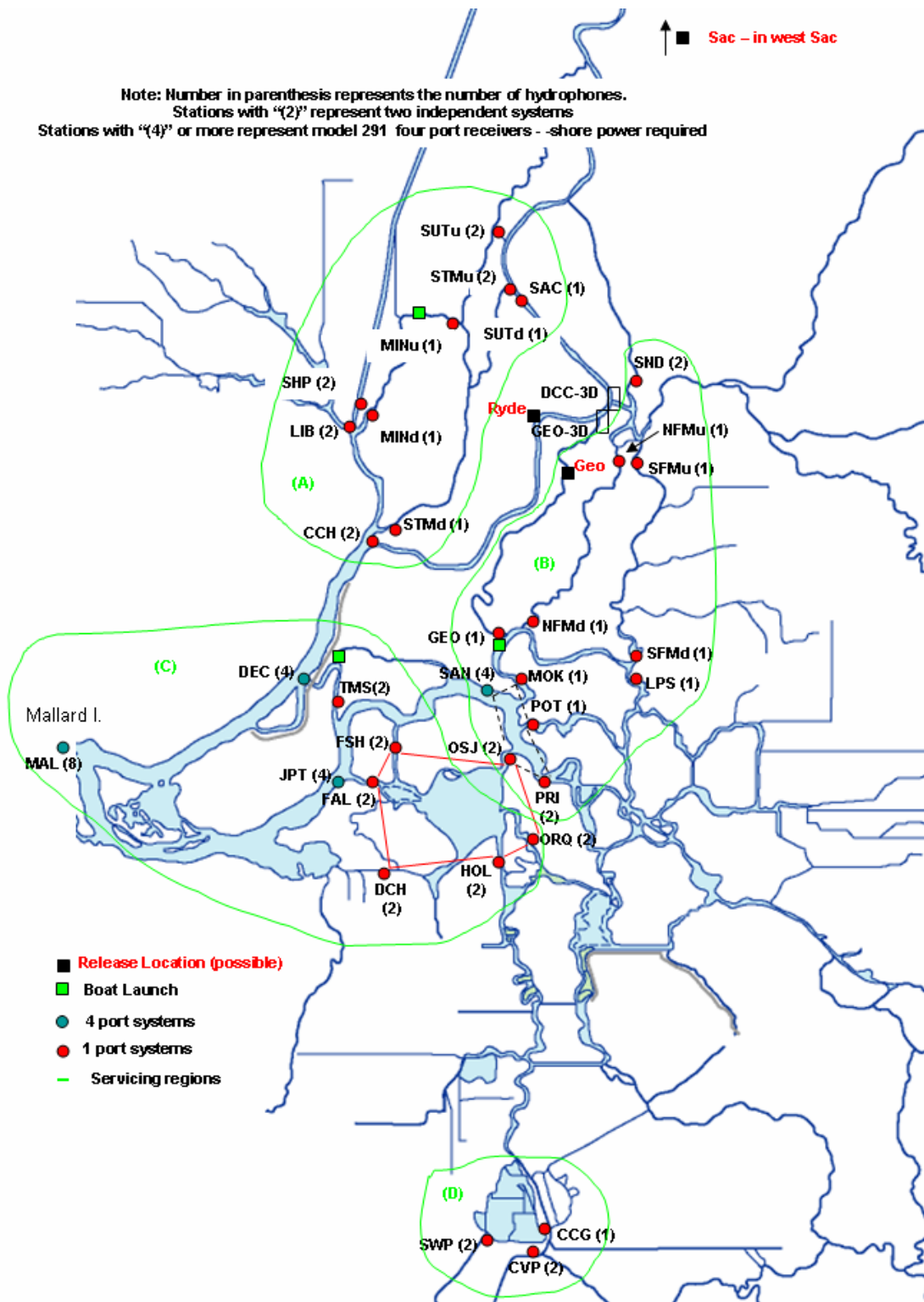
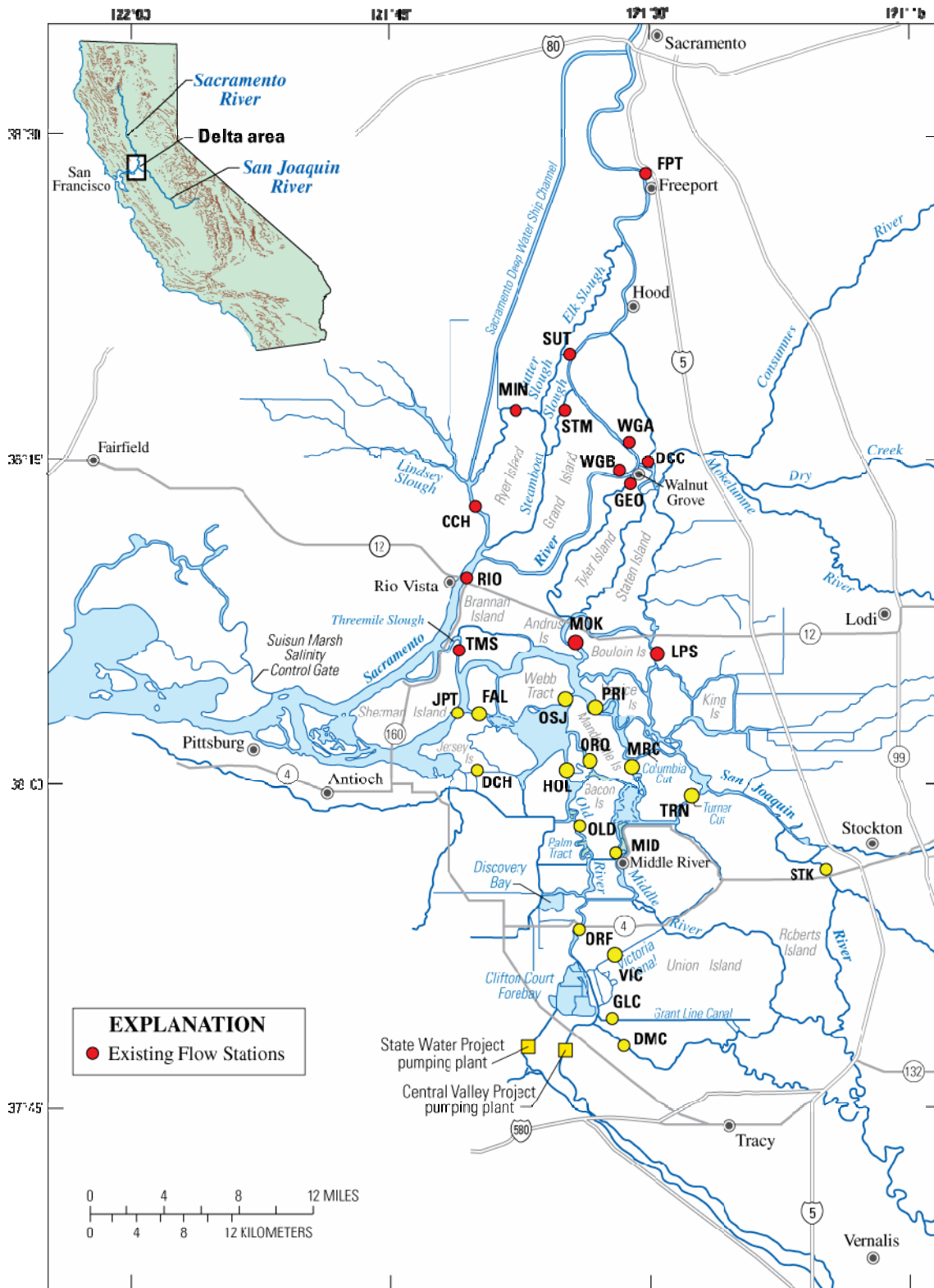


Figure 4.1 – Proposed acoustic tag receiver locations for the 2007-2008 regional study.



Location of flow station sites in the Delta Area of California.

Figure 4.2 – USGS flow station network.

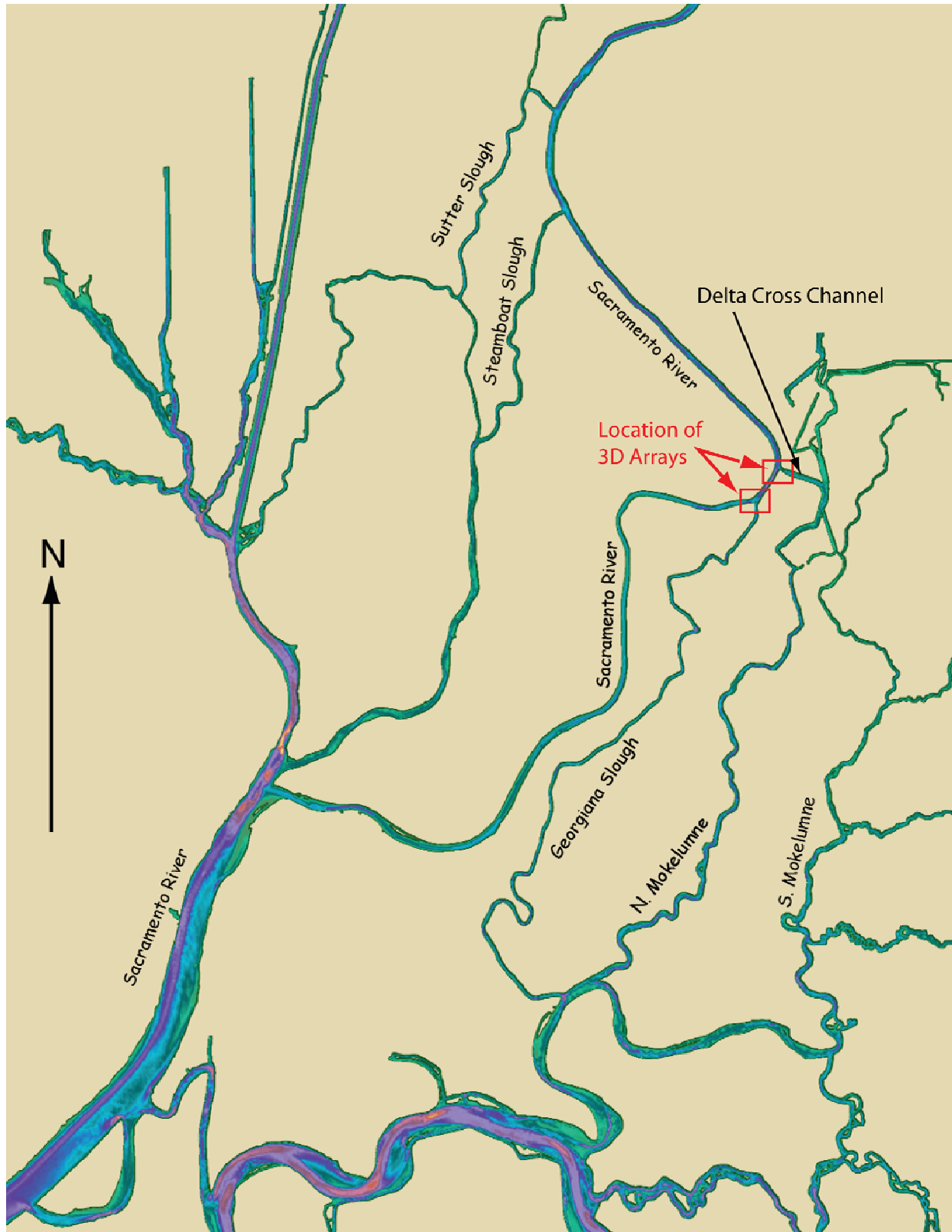


Figure 4.3 - Site location map. Location of the 3-D acoustic telemetry arrays. Deployments are proposed in the Sacramento River at the junctions of the DCC and Georgiana Slough.

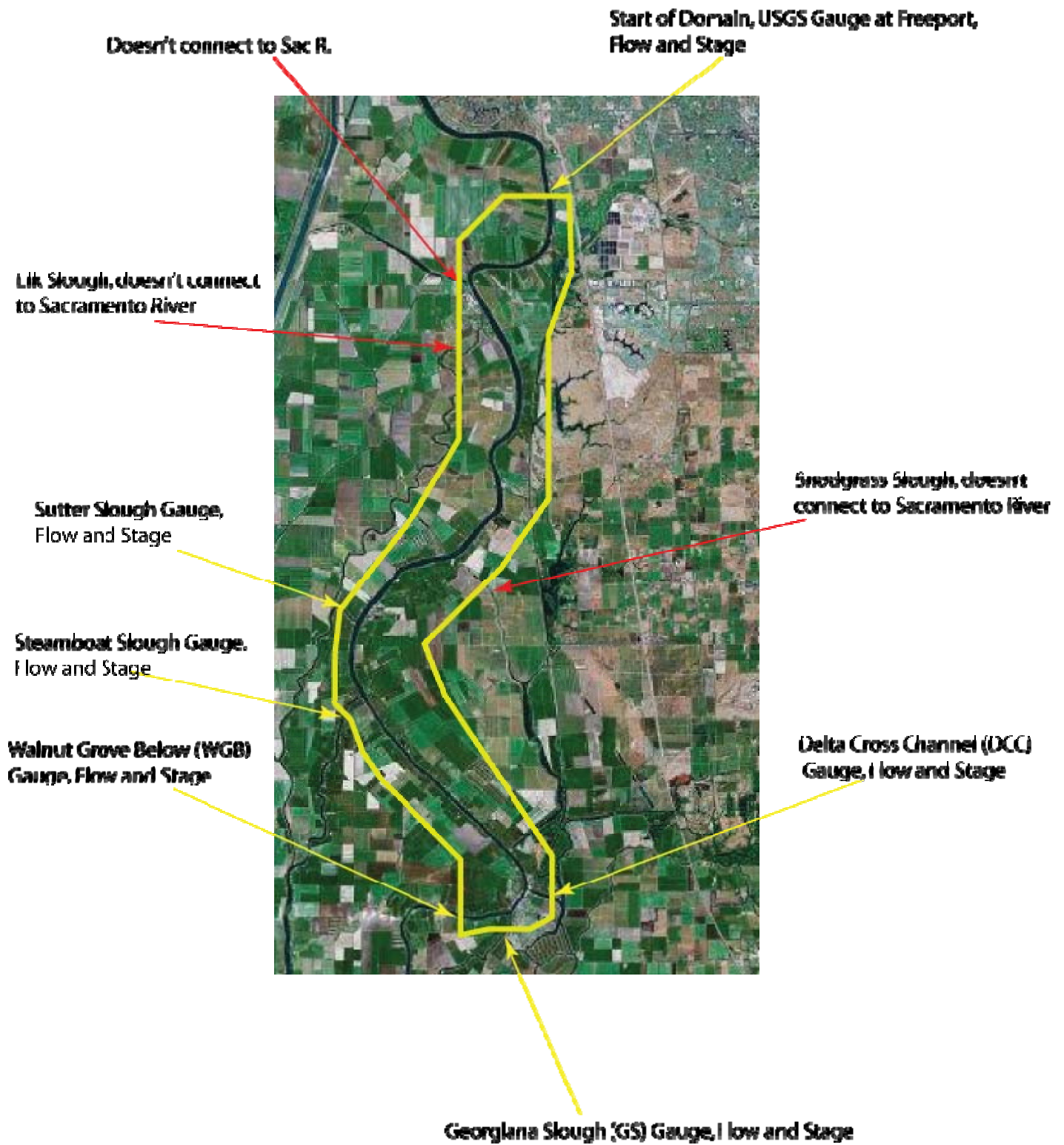


Figure 4.4 – Proposed 3D model domain in yellow, model boundaries are conveniently located at existing USGS flow station locations, which will be used to supply the necessary boundary conditions for the model.

of acoustically tagged fish will be used to develop/calibrate the behavioral sub-models used in the 3D particle tracking algorithms (component (7) in [figure 3.1](#)). The data from the receivers ([figure 4.1](#)) will be used to develop route selection and survival probabilities for a range of discharges that will be used to: (1) confirm the entrainment relations developed with the 3D particle tracking code, (2) develop/calibrate route selection within the delta-scale 2D particle tracking model, and (3) provide survival probabilities versus discharge curves for all of the channels covered by the receiver data shown in [figure 4.1](#) to be used by the 2D particle tracking model, (4) as necessary, provide route selection and survival probabilities versus discharge curves for the simplified management model.

Finally, the proposed approach is, from start-to-finish, fully integrated across disciplines and between the field work, the analytical tools and modeling efforts, which will allow us to link, hierarchically, nine basic project elements as shown in [figure 3.1](#). The following sections describe the component parts shown in [figure 3.1](#), which include a large field experiment (components (1),(2) in [figure 3.1](#)), proposed for the winter of 2008-2009, involving 5000 acoustic tagged juvenile salmon, statistical modeling (components (3),(5) in [figure 3.1](#)), numerical modeling (components (6),(7),(8) in [figure 3.1](#)), the development of simplified models (component (9) in [figure 3.1](#)), and their linkages.

The following sections, where the various component parts are described in detail, are organized by process; all of the work associated with route selection (both the field work and modeling) will be discussed first, then the work associated with survival will be discussed next, followed by the fish release strategy and the experiment timeline. We begin with route selection.

5. ROUTE SELECTION

Route selection depends upon the tidal average of the interaction between (a) the spatial distribution of salmon outmigrants up-current of a junction and (b) the tidal timescale evolution of the current structure within the junction. Spatial distributions of salmon up-current of a junction depend upon the interaction between local hydrodynamic processes (e.g. secondary currents) and subtle behaviors that play out in a Lagrangian reference frame. These spatial structures evolve over fractions of an hour to hours. Junction interactions, on the other hand, happen very rapidly, typically within minutes. Thus, route selection may only minimally depend on behavioral responses that occur within the junction, depending to a greater degree on spatial distributions that are created by subtle behavioral responses/interactions to geometry-mediated current structures that occur up-current of a given junction. If this is true, changes in geometry could provide viable management alternatives for controlling entrainment at junctions and thus overall survival.

The Junction Experiments (1)

The junction experiments are specifically designed to collect the data needed to understand the mechanisms that control route selection. The goal of the junction experiments is to:

Understand the physical processes that control fine-scale movement and entrainment of juvenile salmon in the Walnut Grove region (e.g. in Sacramento River junctions with the DCC and Georgiana Slough).

To study route selection in the field we propose to simultaneously measure the: (1) hydrodynamic conditions (e.g. current structures) and (2) the positions of acoustically tagged fish in three dimensions within the junctions of the Sacramento River at the DCC and Georgiana Slough (schematic [figure 5.1](#); detailed deployments, [figures 5.2, 5.3](#)).

Hydrodynamic measurements

In terms of the hydrodynamic measurements, we propose to (1) measure the surface currents at half hour intervals using high frequency radar (e.g. a CODAR, Seasonde) ([figure 5.1](#)), and (2) measure the internal velocity structures using an autonomous survey vessel (e.g. SeaRobotics, USV1000) ([Figure 5.4](#)) outfitted with a downward-looking ADCP.

Surface Current maps

The surface currents will be measured at ten-minute intervals using high frequency radar (e.g. CODAR, Seasonde). CODAR's SeaSonde system uses two radar antenna ([figure 5.5](#)) to triangulate velocity vectors over an entire region ([figure 5.6](#)) based on Bragg scattering of small amplitude surface waves (Cheng et.al., 2007). This approach has several advantages over the use of boat-mounted systems that have been used in previous studies: (1) simultaneity of the measurements, (2) minimal manpower requirements, and (3) no physical contact with the water by the measurement device. Previous studies of the flow structures in the DCC used boat-mounted downward-looking ADCP's to traverse a set route within the junction. In order to minimize the standard deviation in the velocity measurements the transecting boat should move slowly (particularly during periods near slack water), the boat should move at a fraction of the water velocity whenever possible so that bottom tracking

errors in the measured boat are minimized (see RDI manual, <http://www.rdinstruments.com>). Thus, measurements of the velocity distributions measured in the Sacramento River in front of the DCC took on the order of 1 hour to measure in previous investigations. Given the unsteadiness of the tidal flows in this region, the velocities within the mapped region clearly changed over this 1 hour measurement period. The use of high frequency radar collects data over the entire region at very high frequency and so simultaneous measurements are achieved. To make measurements using a boat-mounted system requires two people in the boat (one to drive the other to run the ADCP). Making measurements continuously over several days, as is proposed in this study, would require an inordinate amount of manpower and expense. The use of the high frequency (hf) radar requires a single person to make sure it is running, dramatically reducing the manpower requirements and greatly increasing the safety of this experiment (e.g. people are not needed out on the water for long hours under nasty conditions when surface current measurements are made using hf radar). The non-contact aspect of this measurement technique is particularly noteworthy in the context of salmon outmigration studies, since it keeps boats out of the water that could potentially alter behavior.

Internal velocity structures - Secondary Currents

The internal velocity structures, such as secondary currents (see [figures 5.7](#), and Dinehart and Burau, 2005b), will be measured at multiple discrete cross sections up-current of each junction using an unmanned, autonomous survey vessel (e.g. SeaRobotics, USV1000). ([figure 5.4](#)). These survey vessels will dramatically reduce the manpower required to measure the internal velocity structures and will improve the data collected (e.g. minimize hull affects, good side-bad side, etc.). Moreover, these vessels will minimally disturb salmon as they move through each junction since the vessels are small (~12 feet long, 12 in diameter), and are powered by an electric trolling motor.



Figure 5.1 – Proposed experimental layout in the Sacramento River at junctions with the DCC and Georgiana Slough.

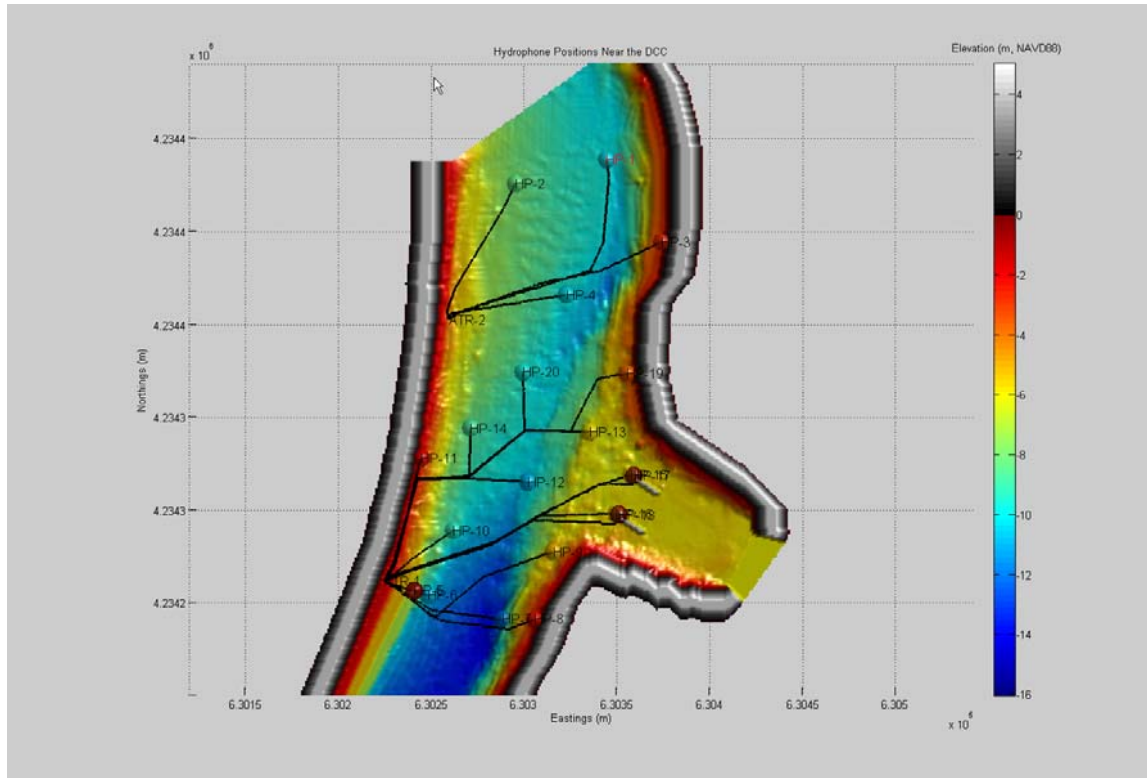


Figure 5.2 - Hydrophone and communication cable locations for arrays deployed in the Sacramento River/DCC. Exact hydrophone and cable locations will be determined through detailed field reconnaissance and testing conducted in the summer/fall of 2007.

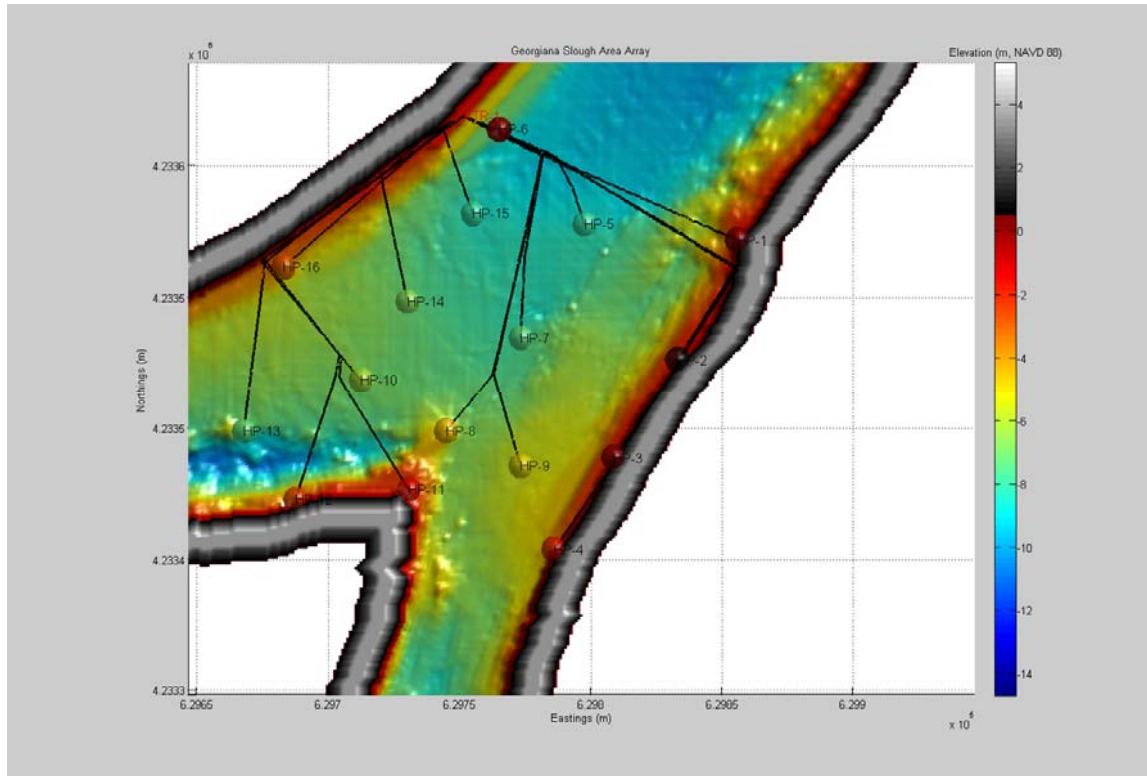


Figure 5.3 - Hydrophone and communication cable locations for arrays deployed in the Sacramento River/Georgiana Slough junction. Exact hydrophone and cable locations will be determined through detailed field reconnaissance.



Figure 5.4 - SeaRobotics USV-1000 unmanned survey vessel, which will be used to collect detailed transects of the velocity structure upcurrent of the DCC and Georgiana Slough junctions.



Figure 5.5 - Radar antenna installed at Three-mile slough gage.

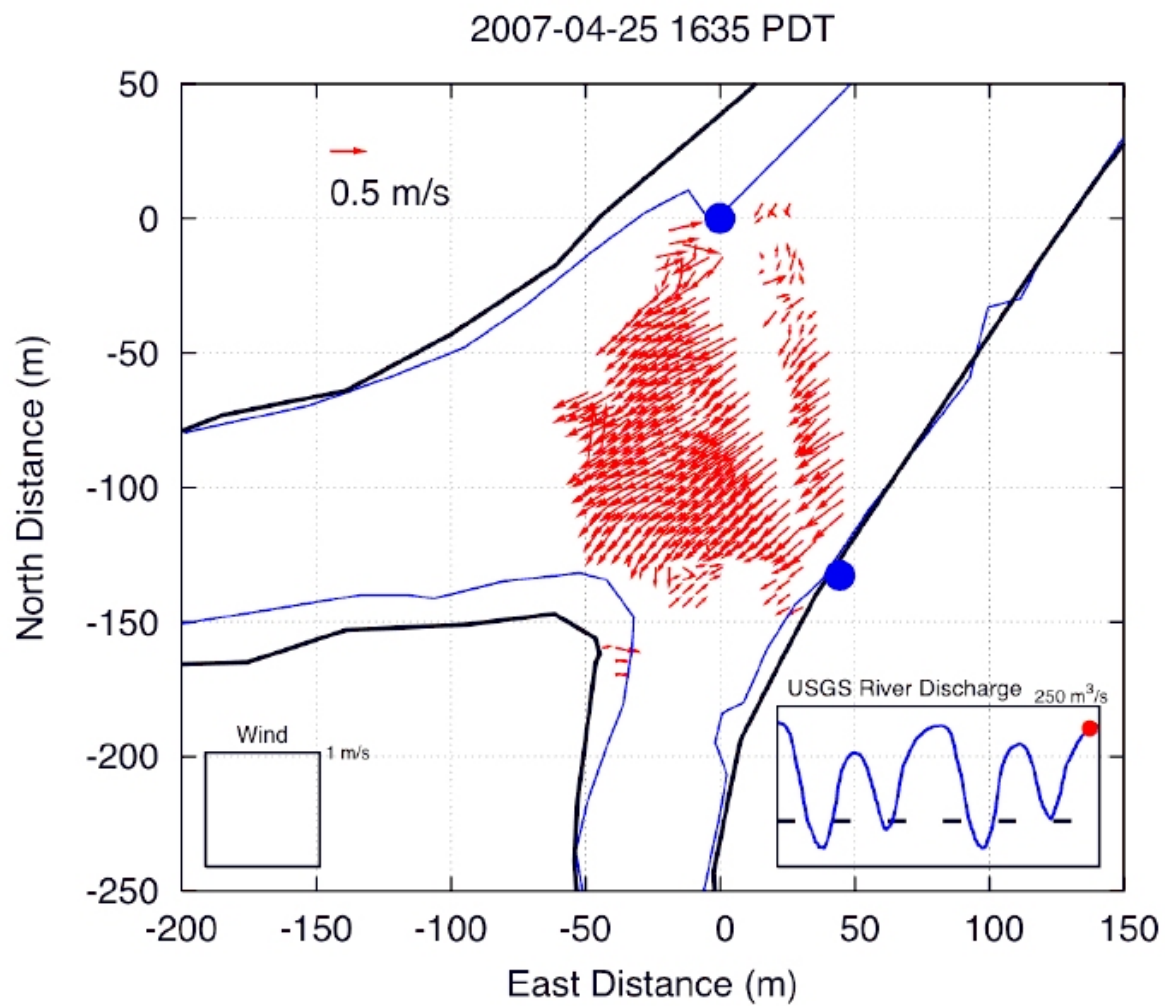


Figure 5.6 – CODAR measurements of surface current distributions measured at Georgiana Slough.

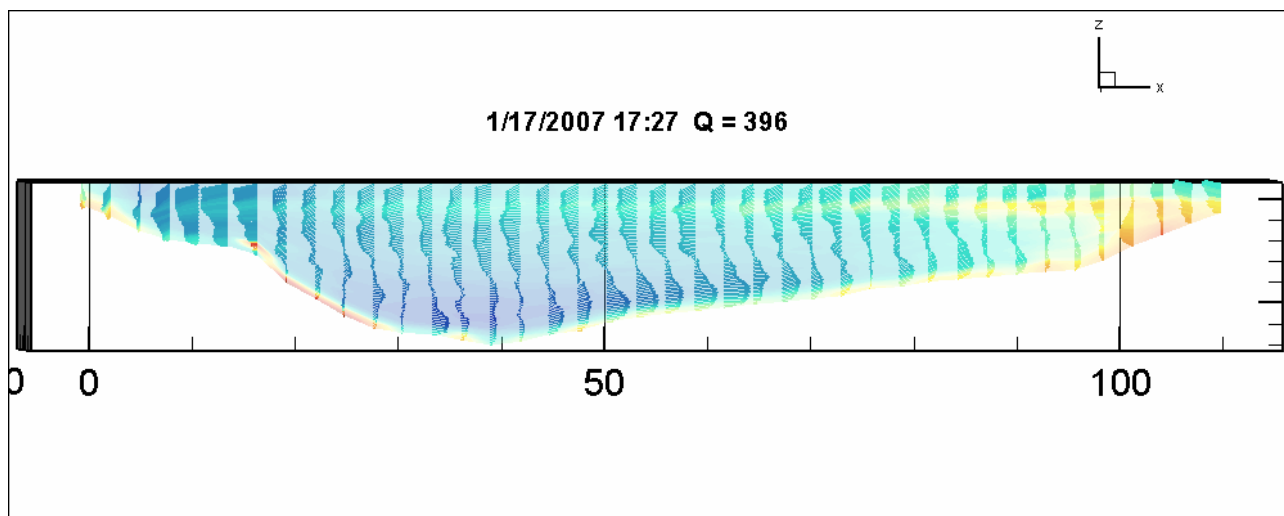


Figure 5.7 – Example of secondary circulation measurement made in the Sacramento River at the Clarksburg Bend. View is looking upstream; outside of the bend is to the left.

Turbulence measurements

If the management agencies allow a ½ open DCC gate operation, 2-3 upward-looking ADCP’s will be deployed in the entrance channel of the DCC to measure the vertical shear and increased turbulence intensity associated with an ½ open DCC operation. Turbulence intensity will be computed using the variance technique outlined in Stacey, 2003 and compared in space and time to observed behavior of tagged fish.

3D tracking of acoustically tagged fish

Juvenile salmon fitted with acoustic tags released into the Sacramento River near the I Street Bridge will be tracked in three dimensions within Sacramento River junctions with the DCC and Georgiana Slough (see schematic in [figure 5.1](#)). Currently, estimates of the 3D location of transmitter positions is computed based on time of travel information recorded at a minimum of four hydrophones within the tracking array (we may work on this algorithm as part of this investigation). Thus, hydrophones will be arranged within each of these junctions in a configuration that permits transmissions from the ultrasonic micro-transmitters implanted in the test fish to be received on a minimum of four hydrophones as they move through the junctions ([figures 5.2 and 5.3 – detailed deployment maps](#)). The 3D tracks of individual salmon within each junction will be related to the hydrodynamic measurements within the Walnut Grove region using the “Data Fusion” 4D analytical framework developed by Sonardata. The hydrophone arrays will be operated continuously for minimum of ten days after each release. If the management agencies allow a ½ gate open operation, additional hydrophones will be placed in the entrance channel of the DCC ([figure 5.8](#)) to capture the response of the tagged fish to the increased water column turbulence associated with flow under the submerged gate.

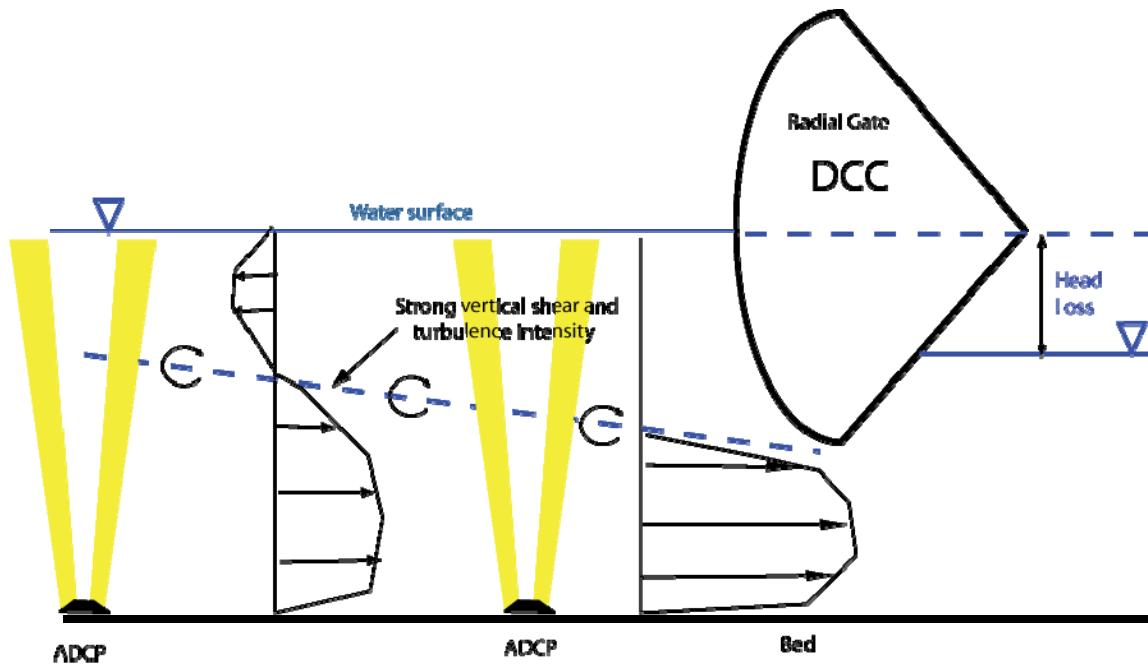


Figure 5.8 – Side view of the DCC entrance channel showing the DCC radial gates in a half closed position. This operation will create intense vertical shear and turbulence intensity which a series of upward-looking bottom mounted ADCP’s will be deployed to capture.

3D Numerical Modeling (6)

At this writing, 1D particle tracking models (e.g. DSM2), that do not conserve momentum at junctions and do not currently include particle behavior, are used to predict “fish movements” as part of the decision-making process routinely used to manage water project operations in the delta. The particle tracking models developed as part of this study plan will be based on 2D and 3D formulations (which do conserve momentum at junctions) and will include particle behavioral sub-models based on the field data collected as part of this study plan. Ultimately, the numerical modeling will provide the conceptual *framework* for developing an increased understanding of how salmon outmigration works in this system by explicitly testing various salmon outmigration models against actual outmigration data.

The fisheries data (3D acoustic tag tracks) from the Clarksburg Bend pilot study (conducted in winter 2006-2007) and the data from the proposed study at the DCC and Georgiana Slough during the winter of 2008-2009 will be used to develop behavioral sub-models for use in individual-based particle tracking models. Pete Smith and others (in review), have successfully simulated the observed secondary circulation in the Walnut Grove area using a semi-implicit 3D model known as Si3D (Smith, 1997). The SI3D model uses a semi-implicit, three-time-level, leapfrog-trapezoidal finite difference scheme on a staggered Cartesian grid (Arakawa C-grid) to solve the layered-averaged form of the governing equations. The semi-implicit approach is based on treating the gravity-wave and vertical-diffusion terms implicitly to prevent limitations on the size of the model time step for these

terms from affecting the stability of the method. All other terms, including advection, are treated explicitly. The approach avoids using mode splitting to solve the problem posed by a system of equations that supports both fast (barotropic or external) and slow (baroclinic or internal) waves. The iterative leapfrog-trapezoidal algorithm for time stepping gives second order accuracy in both time and space. The objective of using trapezoidal iterations is to remove the well-known computational mode associated with the leapfrog discretization (Durran, 1998) and to increase the stability of the code. Further details of the algorithm were reported by Smith (2006).

We propose to use a version of Si3D, a fully three-dimensional hydrodynamic model, developed by Dr. Francisco Rueda, currently a professor at the Universidad de Granada, Spain, to generate the 3D velocity fields for the particle tracking experiments. Dr. Rueda's version of Si3D, includes numerous advanced turbulence closure schemes as well as memory mapping (Rueda, 2001), which will allow us to simulate the region shown in [figure 4.4](#) to the desired resolution. Francisco, and a post-doc, will run Si3D based on bathymetry data and boundary condition data supplied by the USGS. They will calibrate and validate the flow fields against data collected in Clarksburg Bend, the DCC and Georgiana Slough junctions.

3D Particle Tracking (7)

Once the modeled flow fields satisfactorily match the field data (specifically the CODAR surface current maps and the down-ward-looking ADCP transects made by the Searobotics USV-100's and using averaging following the procedures discussed in Dinehart and Burau, 2005b), numerous particle tracking experiments will be run with differing particle behaviors in an attempt to match (in some statistical sense) the observed three dimensional movements of tagged juvenile salmon within the Sacramento River junctions at the DCC and Georgiana Slough. Measured flow fields, model generated flow fields, 3D tracks of acoustic-tagged juvenile salmon and model generated particle tracks will be compared within the "Data Fusion" 4D analytical framework developed by Sonardata. If the 3D movements of juvenile salmon can be modeled using individual-based particle tracking algorithms within the flow fields generated by Si3D, we propose to: (1) experiment with different channel alignments as a means of altering entrainment at a given junction and (2) develop add-hoc 2D junction entrainment relations that can be incorporated into RMA's 1D-2D model to look at system wide impacts of various management strategies on route-selection and survival. Finally, while it is not practical with existing computer resources to run large scale simulations of salmon outmigration in a management context, we hope, as discussed earlier, to collapse the results of the field data and numerical modeling into a simple tool that would allow managers to quantify the effects of various day-to-day management actions on salmon outmigration survival, such as DCC gate and/or Delta Conveyance operations.

6. SURVIVAL

Unlike junction interactions, which occur at timescales of minutes, survival within a given reach depends on transit times (exposures) that, in the north Delta, are on the order of days (Vogel, 2004), and, in the central and western Delta can be on the order of weeks (Brandes and McLain, 2001). Transit times to a large extent depend on hydrodynamic processes, which in the case of reach survival, most likely depend upon the discharge (velocity) in a given reach. The velocity in a given channel is, in turn, primarily a function of the Sacramento River inputs, and secondarily, DCC gate operations (Appendix A).

Delta Scale Experiment (1): A Distributed network of acoustic telemetry receivers

The goal of the delta scale experiment is to:

Estimate reach-specific survival probabilities and junction-specific route selection probabilities for juvenile salmon outmigrants in response to a range of discharge and DCC operations.

Receiver placement strategy

The proposed network of receivers shown in figure 4.1 was specifically designed to (1) estimate route selection probabilities at each junction and (2) survival probabilities within each reach. To accomplish this, (1) receivers are placed within each channel at each junction to estimate route selection probabilities and (2) at the upper and lower ends of each reach to estimate the route selection probabilities. In the case of the junction of the Sacramento River with the DCC and Georgiana Slough, the 3D systems shown in figure 5.1 will be used instead of the deployment of individual receivers. The network shown in figure 4.1 will allow us to compare total survival (e.g. to Chipps Island) under a variety of conditions at a number of different spatial scales: between reaches, between regions and against losses at the export facilities, Snodgrass Slough and within the Cache Slough/Liberty Island complex.

Station redundancy

A number of sites will have multiple receivers, often for different reasons. For example, completely redundant stations will be placed at several locations because they are absolutely critical for computing route selection and survival probabilities on key junctions and reaches, respectively. These stations include SUTu, STMu, TMS, and all of the sites that encircle Franks Tract. At other locations, the statistical model requires multiple sites to compute both survival and detection probabilities (Appendix B). These sites are located at the boundaries of the network and include: MAL, LIB, SHP, SND, PRI, ORQ, HOL, DCH, SWP, CVP. At sites with very wide cross sections, four hydrophones are needed to ensure acoustic “coverage”. For example, two completely separate 4-hydrophone systems will be needed at the Mallard Island station, (MAL, figure 6.1) so that survival and detection probabilities can be computed. Individual four-hydrophone systems will also be needed at stations DEC (figure 6.2), JPT (figure 6.3), and SAN (figure 6.4) for complete acoustical coverage in these locations because they also have “wide” cross sections.

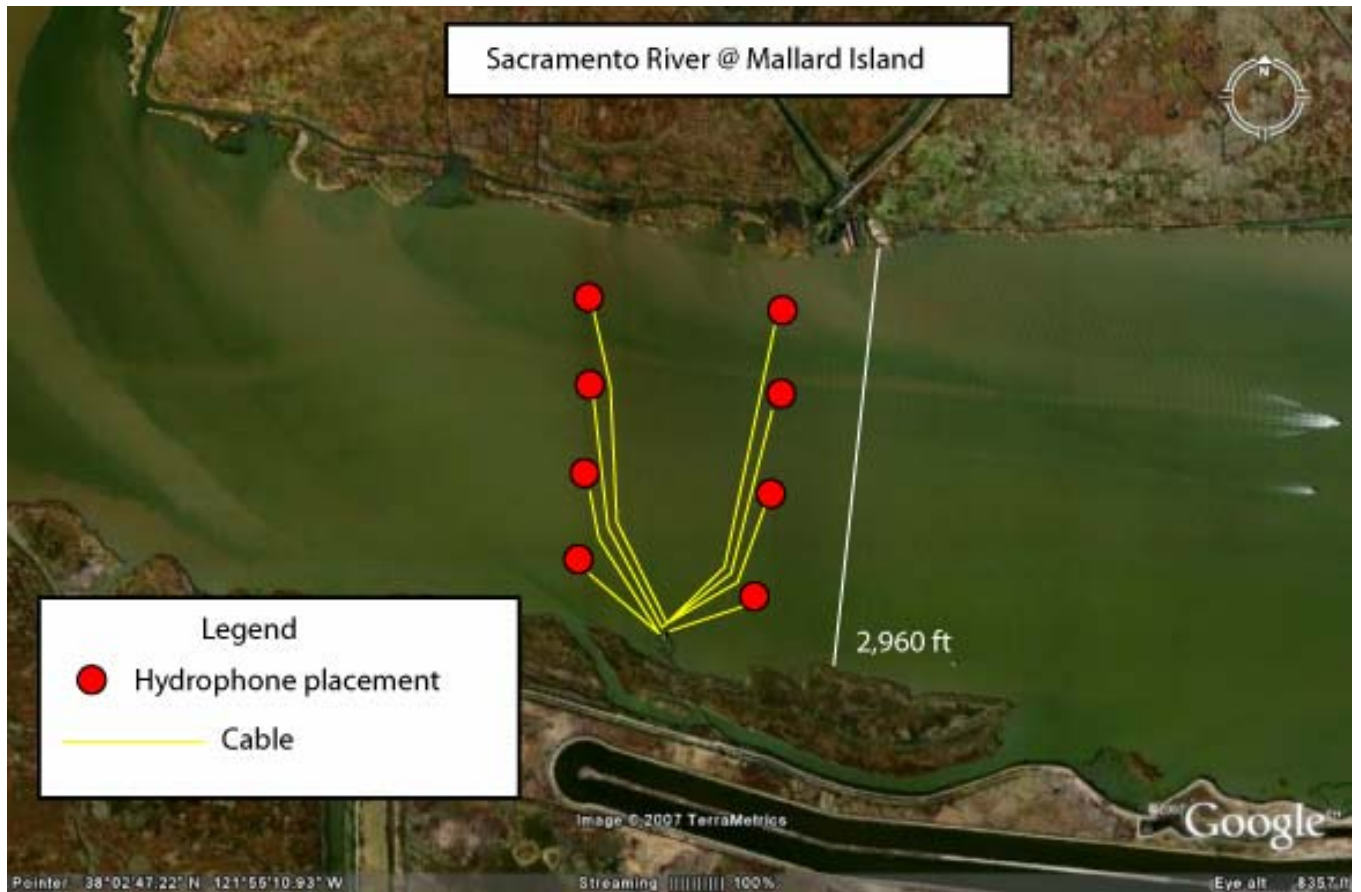


Figure 6.1 - Proposed 4-port system: hydrophone and communication cable locations in the Sacramento River at Mallard Island (MAL). Exact hydrophone and cable locations will be determined through detailed field reconnaissance and testing conducted in the summer/fall of 2007.

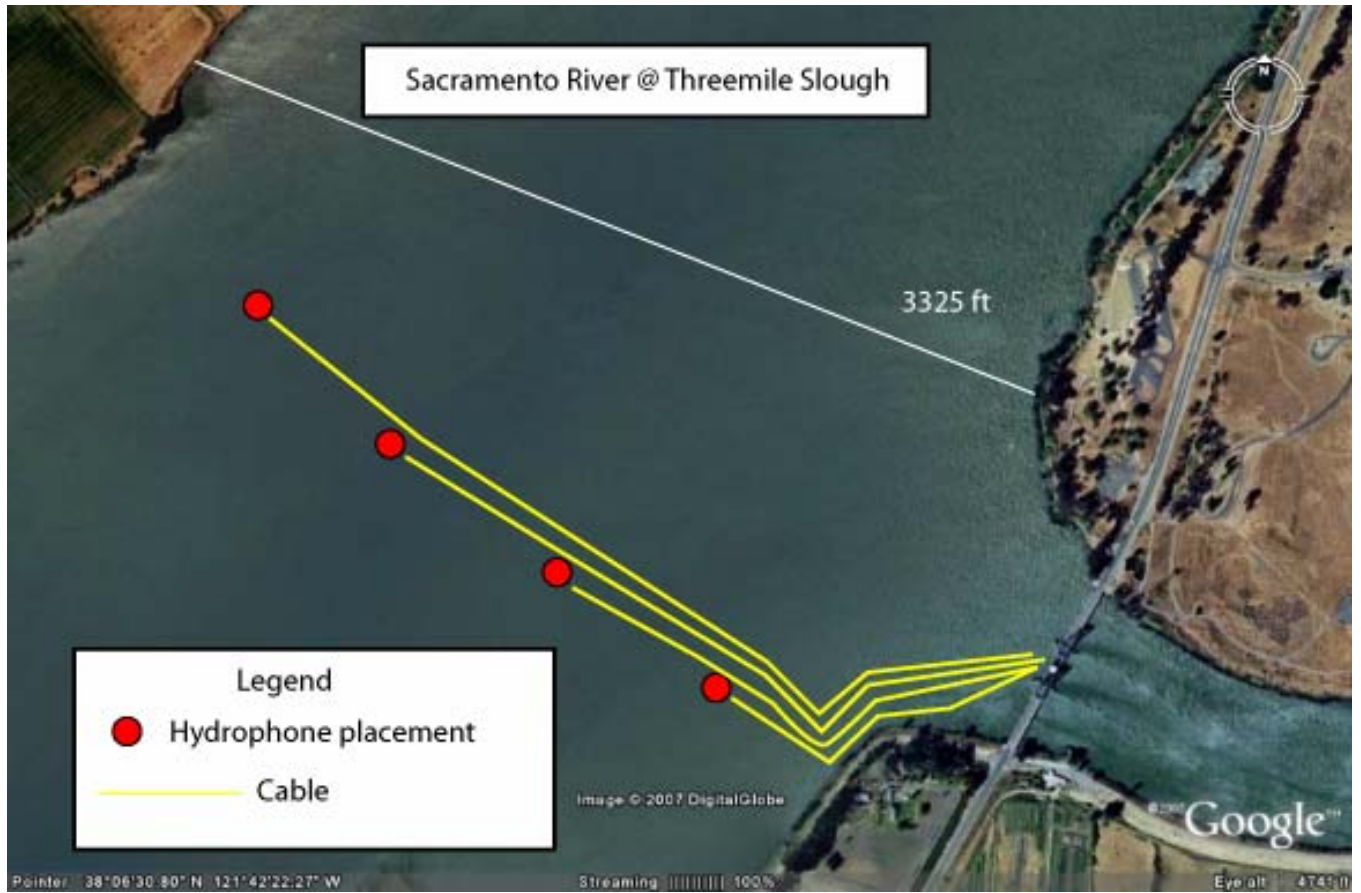


Figure 6.2 - Proposed 4-port system: hydrophone and communication cable locations in the Sacramento River at Three-Mile Slough (DEC). Exact hydrophone and cable locations will be determined through detailed field reconnaissance and testing conducted in the summer/fall of 2007.



Figure 6.3 - Proposed 4-port system: hydrophone and communication cable locations in the San Joaquin River, at Jersey Point (JER). Exact hydrophone and cable locations will be determined through detailed field reconnaissance and testing conducted in the summer/fall of 2007.



Figure 6.4 - Proposed 4-port system: hydrophone and communication cable locations in the San Joaquin River, at San Andreas Point (SAN). Exact hydrophone and cable locations will be determined through detailed field reconnaissance and testing conducted in the summer/fall of 2007.

Station Servicing

Servicing roughly 40 sites spread throughout the Delta (figure 4.1) will be a very large logistical challenge, involving lots of people and multiple boats. Thus, we've spent a great deal of time experimenting with a number of different ways of powering the receivers to extend the required servicing interval for each site. The multiport sites at MAL, DEC, JPT, and SAN (figure 4.1) require shore (A/C) power, so powering and servicing these sites will be relatively easy, although they will be susceptible to power outages. After extensive testing, we've decided to power each receiver using two 72 pound, Trojan t145 batteries. This configuration will give us about 9.5 days of battery life, which allows for a weekly (7 day) servicing interval for the receivers, giving us about 2.5 days of cushion for bad weather, staffing or mechanical problems, etc. We plan on using two crews to service the receivers on three consecutive days in the three regions indicated by the green lines on figure 4.1. Barring extremely bad weather, servicing each region should take a day (given the short days in mid-winter). We plan on telemetering all of the data (including battery voltage) from all of the receivers, so that instrument malfunctions can be quickly identified and corrected. "Sentinel" tags will be placed adjacent to each site, to verify the equipment is working properly. The data integrity from

each station will be remotely evaluated on a daily basis using the telemetered data downloads from each station. Telemetry of the data will also allow us to process the data as the experiment proceeds. This will be particularly useful at stations that border Cache Slough and the lower Mokelumne, the data from these stations will be critical for determining if a change in gate position is possible. A separate boat and crew will be available 7 days a week during the execution of the experiment to make receiver repairs as necessary. Crews will launch at Happy Isles marina on Miner Slough to service region (A), at B&K Marina on the Mokelumne to service region (B), and at Brannan Island State Park, to service region (C). The four port systems require AC power, and, thus, servicing of these stations will involve downloading the data and a check of system integrity. Stations DEC and MAL will be accessed by vehicle, all other stations (except the receivers at the export facilities) will be accessed by boat. For information on receiver testing and data processing, see Vogel, 2004.

Regional Differences

Based on hydrodynamic/geometric considerations, we expect salmon will “move” differently within different regions in the system (figure 6.5), which we expect will influence survival within these regions. For example, hydrodynamic conditions change dramatically as salmon pass from the north Delta into Cache Slough, and, similarly, when they pass from the Mokelumne system into the San Joaquin River (Vogel, 2004). At these transitions, the net currents fall off dramatically while the tidal currents increase: in both cases the tidal to net current ratio, $u'/\langle u \rangle$, goes from about 1 to 10 (see figure 6.6). As a consequence, salmon move relatively rapidly though both the north Delta and Mokelumne systems. However, once salmon outmigrants enter either Cache Slough or the San Joaquin River, their net movement downstream is arrested and they tend to be moved large distances by the tidal currents (Vogel, 2004). Thus, changes in the net currents have relatively less influence on outmigration, once salmon reach the strongly tidally influenced regions in the Delta. We propose to operate the gates up until the time we believe the acoustic-tagged salmon will have entered the San Joaquin or Cache Slough, about 10 days. In order to change gate operations as soon as is practical, we plan to process the data from the listening stations that border Cache Slough and the listening station in the lower Mokelumne River in real time which will allow us to make a change in the gate position significantly *after* the observed peak migration past these stations has occurred.

Referring to figure 6.6, we expect salmon to “move” relatively rapidly in the north Delta and Mokelumne regions. Both the Snodgrass and Cache/Lindsey regions are dead end sloughs, the net currents are near zero in these areas and, as a result, these areas could be locations of either long residence (e.g. these areas could be good rearing areas) or high mortality (e.g. good predator habitat). Two receiver stations are placed in these locations so that both survival and detection probabilities can be computed. The west Sacramento and San Joaquin regions are characterized by weak net flows and strong tidal currents and thus the transit times through these regions are likely to be long. Exchange into and out of Franks Tract and survival within Franks Tract is totally unknown at this time; however, we expect both exchange into Franks Tract and survival to be strongly governed by the tides. Thus, each of the entrance channels to Franks Tract will have two receivers for: (a) redundancy, and (b) to determine direction of travel and potentially speed ([distance between stations]/[time between detections]). One of the receivers in each of the entrance channels to Franks Tract will be associated with a flow station (compare figures 4.1 and 4.2), so that water velocity measurements can be compared to the “fish speeds”. Finally, once salmon “move” into the south Delta region, export rates will likely begin to influence their movements. Transit times to the pumps from stations HOL, ORQ, PRI (figure 4.2) will be compared to the net velocities measured at USGS flow stations at Old and Middle River (stations OLD and MID in figure 4.2). Finally, receivers will

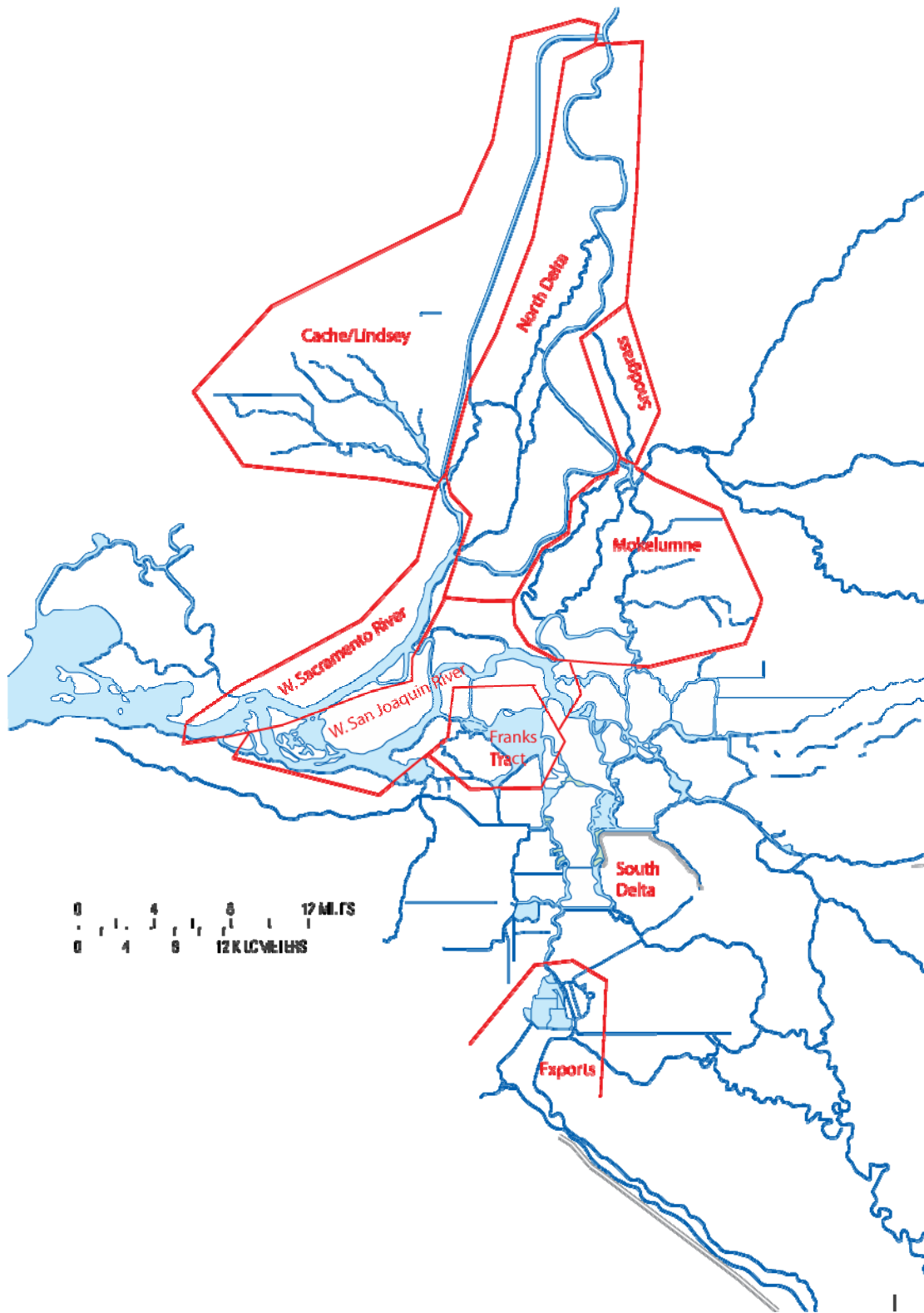


Figure 6.5 – Hydrodynamically distinct outmigration regions.

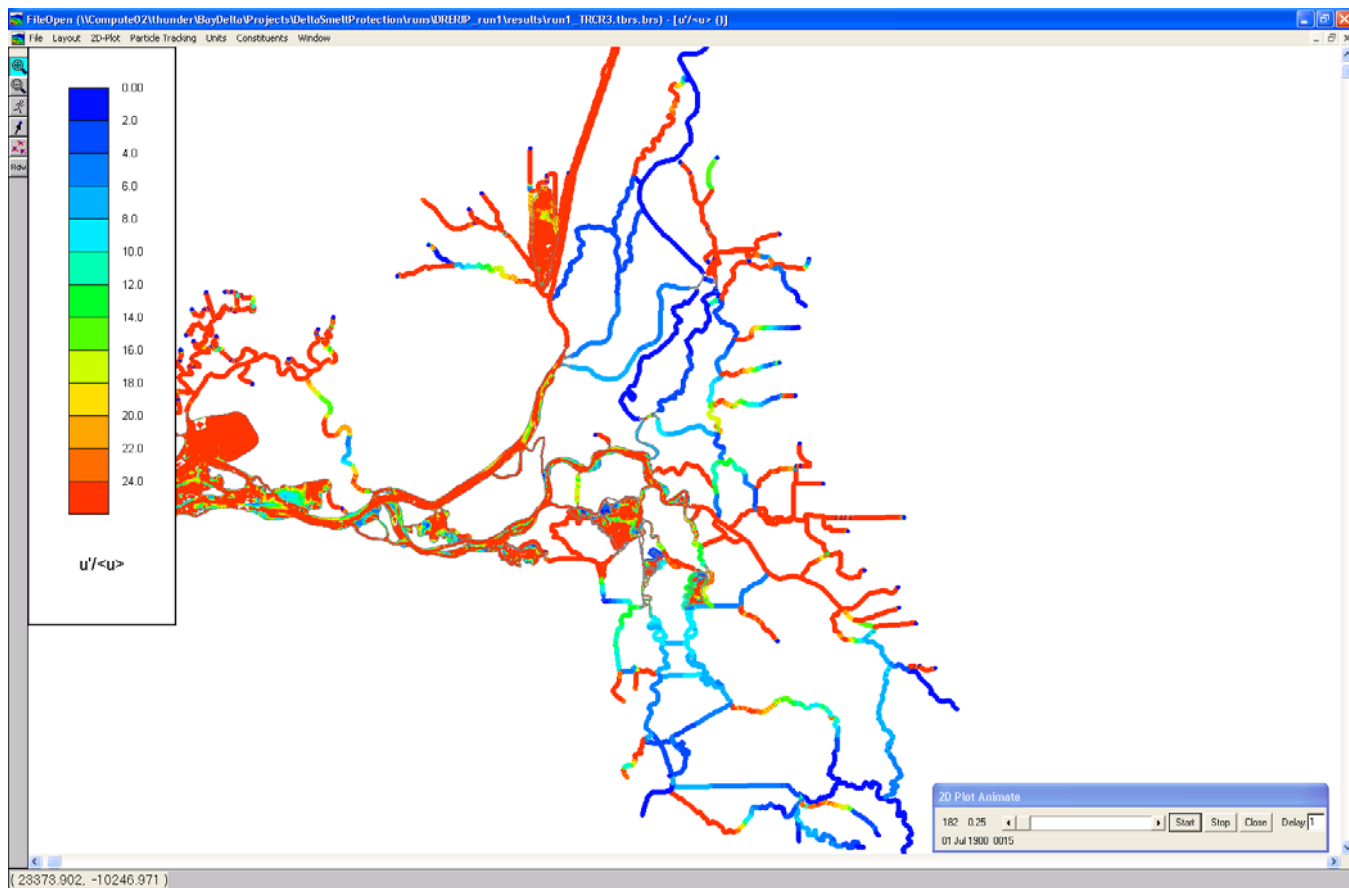


Figure 6.6 – Color plot of the ratio of the tidal current amplitude, u' , to the residual current $\langle u \rangle$ ratio, $u'/\langle u \rangle$. In this plot regions of warmer colors are dominated by the tides; whereas, regions with cooler colors are dominated by advection (river inputs and export rates).

be placed in the export facilities to monitor “entrainment” at the pumps. In summary, regional differences in transit times and survival will be compared to hydrodynamic measurements (e.g. discharges and velocities) made throughout the system (figure 4.1).

Site Specific Details

There are a number of site-specific details inherent in the network shown in figure 4.1. In what follows, we discuss these details. Relatively few receivers (16) were available during the 2006-07 pilot study, so we set up the network to compute aggregate survivals. For example, we set up the receiver network to compute the aggregate survival in both Sutter and Steamboat Sloughs (figure 2.1). And, similarly, the 2006-07 network on the Mokelumne system was set up to compute the combined survival from both the north and south forks (figure 2.2). For the 2008-09 study, we propose to add a number of stations that will allow us to compute the survival within individual reaches. In the case of the north Delta, we’ve added stations MINu and SUTd, which will allow us to compute reach-specific survival in Sutter, Steamboat and Miner Sloughs. On the Mokelumne system, we’ve added

stations at NFMu and SFMu, which will allow us to compute reach specific survival down each fork of the Mokelumne system.

(1) Cache/Lindsey Region

Particle tracking and radio tagging results have shown that salmon outmigrants that exit Miner Slough, Steamboat Slough and the Sacramento River into Cache Slough can be advected into the Sacramento Deep Water Ship Channel and Liberty Island area on a single flood tide (Vogel, 2004). Thus, we propose to install receivers at stations SHP and LIB to monitor the extent to which salmon outmigrants use these areas and the survival rates within them. High predation rates in this region could suggest the need for restoration (for example, increasing the size of the levee breach openings).

(2) Mokelumne Region

Given proposed changes in conveyance in the Mokelumne system, such as: (1) the TDF, (2) changes in inlet geometries at the DCC and Georgiana Slough, (3) widening of the North and South Forks of the Mokelumne River for flood protection and increased conveyance, (4) changes in DCC gate operations, and (5) impacts of reduced diversion due to a TDF and a variety of BDCP options, additional sites were added in the Mokelumne system (NFMu, SFMu, NFMd, SFMd), to explicitly separate out travel times and survival rates between the north and south Forks.

(3) Snodgrass Slough

Roughly 30% of the flow that enters the DCC initially exchanges into Snodgrass Slough. This exchange could “move” salmon outmigrants into this area. We’ve propose a station at SND, a dual receiver site, to monitor exchange into, and predation within, Snodgrass Slough.

(4) Threemile Slough

The California Department of Water Resources is evaluating a barrier on Threemile Slough as an element of the Franks Tract Project. A barrier operated tidally in this location could be used to repel salinity intrusion from the Bay into the western San Joaquin River by creating a net flow from the Sacramento River to the San Joaquin through Threemile Slough by closing the tide gates on flood tides. This tidal operation has the potential to increase entrainment of salmon outmigrants traversing the Sacramento River near Decker Island into the San Joaquin River. To collect baseline data on entrainment of salmon outmigrants into Threemile Slough, two stations are proposed: (1) a pair of receivers within Threemile Slough to monitor exchange through Threemile Slough and (2) a four port system which will monitor the lateral spatial distributions of salmon outmigrants in the Sacramento River ([figure 6.2](#)). Understanding the lateral distribution of juvenile salmon outmigrants within the Sacramento River near its junction with Threemile Slough will help us assess the likelihood of entrainment of salmon into the San Joaquin based due to gate operations. For example, if outmigrants move through this area predominantly within the Sacramento River on the side opposite Threemile Slough, then we can conclude that gate operations are likely to have a minimal impact on outmigrants in this region.

(5) Junction of Mokelumne with San Joaquin River (dashed lines in [figure 4.1](#))

The Mokelumne River, where it meets the San Joaquin River, is nearly perfectly phase locked with the San Joaquin. However, the tidal currents in the Mokelumne do turn about an hour later than on the San Joaquin. Therefore, salmon outmigrants that exit the Mokelumne at the beginning of an ebb tide are advected toward the bay in the San Joaquin to about False River on a single ebb tide, which is a significant “push” towards the ocean. On the other hand, those outmigrants that exit the Mokelumne at the end of ebb can be advected towards Old River and the pumps for the roughly hour period

when the Mokelumne and San Joaquin are out of phase. The group of stations highlighted by the dashed lines in [figure 4.1](#) will be used to document the extent to which tidal current phase determines the fate of salmon that traverse the Mokelumne.

(6) Franks Tract (red lines in [figure 4.1](#))

The California Department Water Resources is evaluating a number of different barriers in the Franks Tract region, the data from these stations will provide a first look at the role Franks Tract plays in salmon outmigration and will provide critical base line data for assessing these projects.

The stations connected by red lines in [figure 4.1](#) (FAL, OSJ, ORQ, HOL, DCH) will be used to monitor the exchange into, and survival within, Franks Tract. All of these stations will have two receivers for redundancy and to determine direction of travel. All of the Franks Tract stations will be associated with USGS flow stations.

(7) Export facilities

The number of acoustic tagged fish that reach the facilities will be monitored by stations CCG, CVP, and SWP. Travel time and survival across Clifton Court Forebay will be computed as the difference between detections at stations CCG and SWP.

Mark-recapture Modeling (3)

Based on the network of acoustic telemetry receivers shown in [figure 4.1](#), we propose to develop a mark-recapture model that will estimate both population distribution and survival rates within the Delta. To fully understand population-level responses to both natural variation and human-imposed management actions, we've proposed the Delta-wide approach shown in [figure 4.1](#) (and just discussed) that will explicitly estimate how juvenile salmonid populations distribute through the Delta and survive within each migratory pathway. The goal of the mark-recapture model is to:

Develop estimates of parameters of population distribution through the Delta, including route selection probabilities, survival probabilities of juvenile salmonids traversing different migratory pathways, survival probabilities within regions in the Delta ([figure 6.5](#)) and overall survival probabilities of the population migrating through the Delta.

Ultimately, this approach will combine information about population distribution and route-specific survival rates to estimate the overall survival rate of the population migrating through the Delta. Under this framework, researchers will gain a better understanding of population-level responses to changes in water distribution, and resource managers will gain better information on which to base important decisions affecting water and aquatic resources. With an emphasis on hydrodynamic forcing we ask the following question:

How does the distribution of the net flows in the delta effect: 1) distribution of juvenile salmon migrating through the Delta, 2) survival rates of juvenile salmonids negotiating different migratory pathways, and consequently 3) survival of the population as a whole?

Traditional mark-recapture techniques that depend on the physical recapture of fish are incapable of providing the level of detailed information needed to understand the complex physical and biological processes acting on survival of juvenile salmonid populations migrating through the Delta. In contrast, telemetry is a passive recapture technique that can provide detailed information on the movement of individual fish. In addition, recent advances in telemetry technology have progressively

reduced the size of transmitters, making it possible to study movements of juvenile salmonids without significantly altering their behavior or survival (Hockersmith et al. 2003). Strategic placement of telemetry arrays in the Delta will allow for individual-specific information on routes used by juvenile salmon and migration timing through those routes. Specifically, telemetry arrays, like the network proposed in [figure 4.1](#), can be implemented under a mark-recapture framework to estimate survival probabilities through various routes of the Delta.

Description of survival models

Historically, simple recapture rates of marked animals have been used as a survival “index”, but this approach does not account for imperfect recovery of all marked animals alive at subsequent sampling occasions (Nichols 1992). As a consequence, recapture rates will almost always underestimate the probability of survival since the recapture rate is the product of both the capture probability (p) and survival probability (S). Furthermore, if the capture probability is not constant over sampling occasions then inferences about changes in survival will be invalid. The classical works of Cormack (1964), Jolly (1965), and Seber (1965) developed the “CJS” model, which estimates both capture and survival probabilities allowing for an unbiased estimate of survival probability. Since the ground-breaking work of Cormack, Jolly, and Seber, much advancement has taken place in both the structure of survival models and the framework within which they are implemented (Lebreton et al. 1992, Williams et al. 2002).

Although numerous mark-recapture models have been tailored to meet the specific needs of fisheries research (see Burnham et al. 1987, Pevan et al. 2006), the route-specific survival model (Skalski et al. 2002) comes closest to emulating the model structure that is needed for the Delta. This mark-recapture model was developed to estimate survival probabilities of juvenile salmon as they migrate through the Columbia River and pass through a hydroelectric project (for examples, see Counihan et al. 2003 and Perry et al. 2006). This model estimates survival probabilities of fish migrating through the reservoir (S_{pool}) between an upstream release point (R_u) and the dam ([Figure 6.7](#)). Once fish arrive at the dam, they may pass the dam through a number of available routes such as the turbines or the spillway. By monitoring passage routes with telemetry equipment and recording detections of tagged fish in each passage route, the model estimates the probability of survival through each passage route (S_{By} , S_{Tur} , and S_{Sp} ; [Figure 6.7](#)) as well as conditional probabilities of passing through each route (Sp , Tu , and By ; [Figure 6.7](#)). Both the passage distribution through all routes and the overall probability of surviving dam passage can be estimated as functions of conditional survival and passage probabilities. Specifically, the overall probability of surviving passage through the dam is estimated as the average probability of survival through all routes weighted by the probability of passing each route.

Clearly, the physical settings of the Columbia River and the Sacramento – San Joaquin Delta could not differ more, but conceptually, the problem is the same. What is the survival of fish passing each route (i.e., passage route at a dam or migratory route through a specific channel in the Delta)? What is the proportion of the population that is subject to each route-specific survival probability? And, what is the overall survival probability through all routes? Most importantly, in both cases this approach allows managers and researchers to explicitly answer the important question, “How do management actions in the Delta (e.g., reservoir releases, DCC gate operations, export rates) affect the distribution of fish passing available routes and in turn, how are survival probabilities affected by

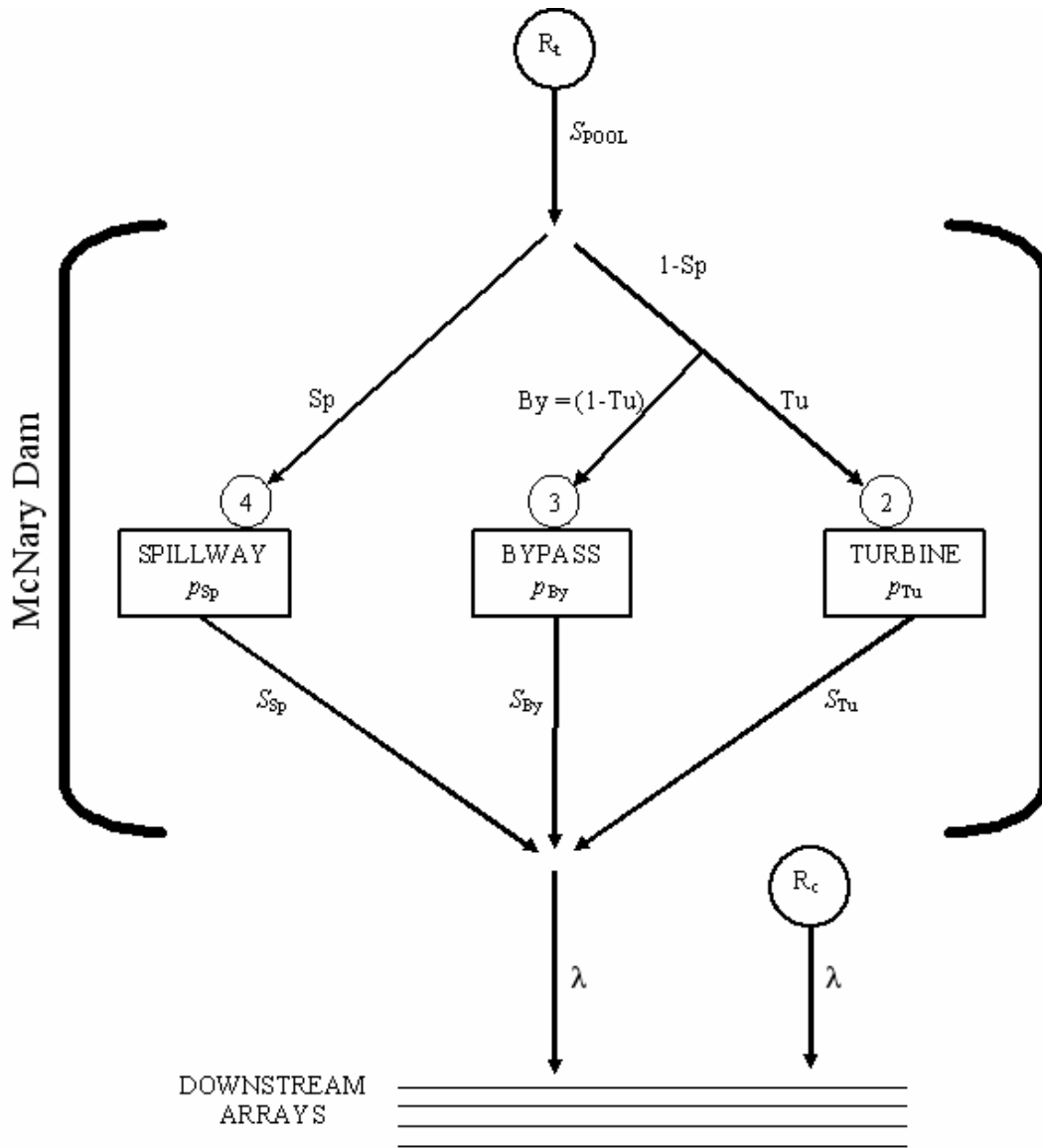


Figure 6.7 – Schematic of the route-specific survival model developed by Skalski et al. (2002) and used by Perry et al. (2006). Shown are fish release locations and R_c (R_t and R_c) and passage (S_p , B_y , and T_u), detection (P_{sp} , P_{by} , and P_{tu}) and survival probabilities (S_{pool} , S_{sp} , S_{by} , and S_{tu}). Circles numbers show coding used in detection histories to indicate the route of passage of each fish. Lambda (λ) is the joint probability of surviving and being detected by telemetry arrays downriver of the dam.

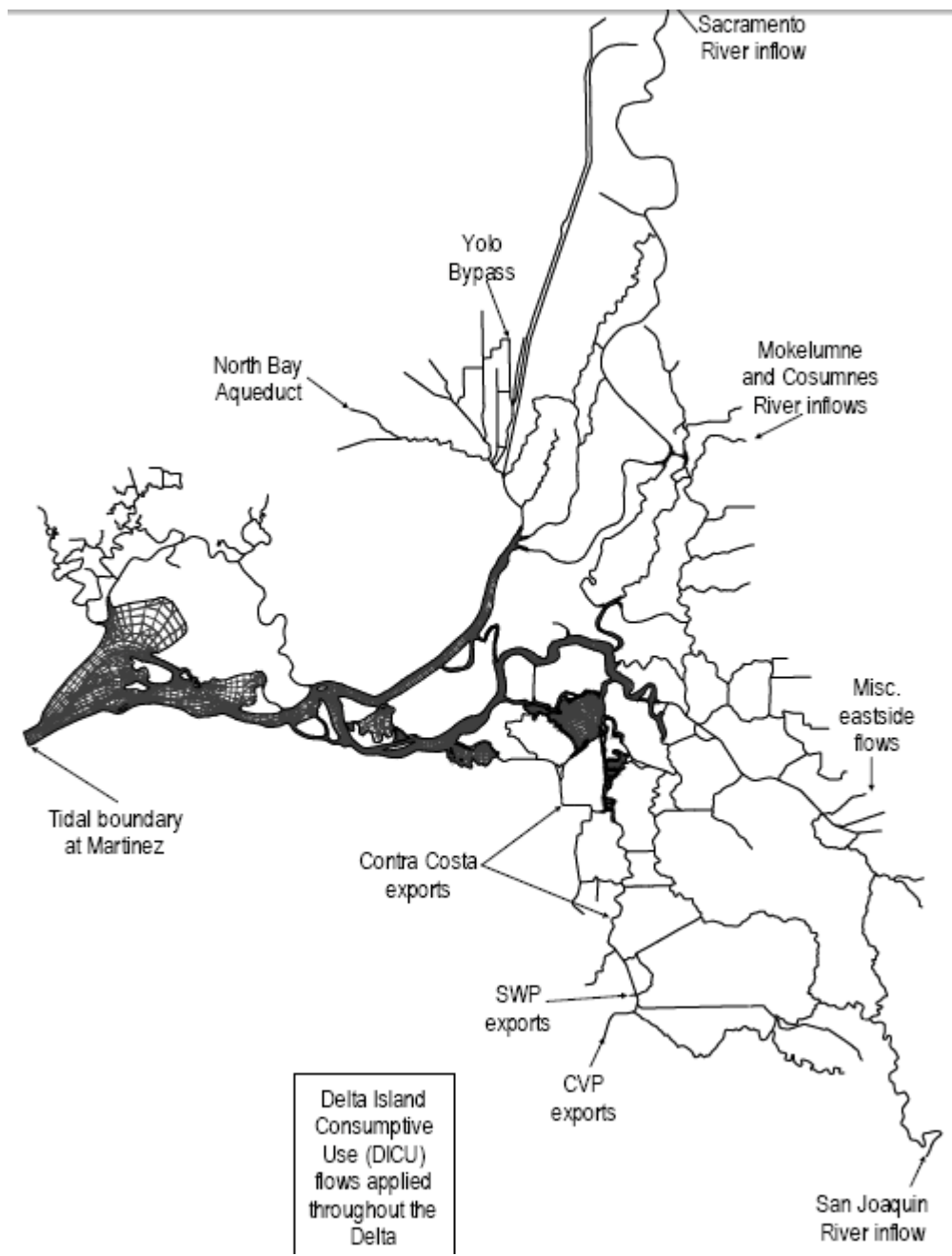


Figure 6.8 – Example RMA 1D-2D finite-element model grid.

these operations. Moreover, the spatial distribution of survival probabilities could suggest optimal locations for restoration efforts aimed at increasing overall salmon survival.

Statistical approach and modeling framework

The foundation of the proposed mark-recapture model is based on the classic single release-recapture models of Cormack (1964), Jolly (1965), and Seber (1965). Detection (or “capture”) histories of each fish form the basis of these models and allow for the estimation of route-specific survival, detection, and passage probabilities. In general, survival and detection probabilities are estimated by:

- 1) Creating detection histories for each fish.
- 2) Estimating the probability of each possible detection history from the number of fish with that detection history (i.e., from the observed frequencies of each detection history).
- 3) Using maximum likelihood methods to find parameter estimates of survival, passage, and detection probabilities that were most likely, given the observed data set of detection histories.

We will apply the USER software program (User Specified Estimation Routine) to implement the mark-recapture survival model and estimate survival, detection, route-specific passage parameters (Lady et al. 2003). To prepare the data for input into USER, telemetry records for each fish will be summarized into detection histories to indicate the migratory-route of each fish and whether fish were detected or not detected at receivers located throughout the Delta. For example, the route-specific model uses a primary likelihood to estimate survival and passage probabilities and a secondary likelihood to estimate route-specific detection probabilities. At Columbia River dams, the detection history for the primary likelihood is typically composed of 3 digits indicating 1) the release site (1 = upstream of the dam, 0 = tailrace), 2) the route of passage for each fish coded by numbers ranging from 0 to 4 (see Figure 6.7), and 3) whether fish were detected (1) or not detected (0) at telemetry arrays downriver of the dam. For example, the detection history 140 indicates a fish that was released upstream of the dam and passed the dam via the spillway, but was not subsequently detected by downriver telemetry arrays.

Each unique detection history has a probability of occurrence that can be completely specified in terms of the survival, route-specific passage, and detection probabilities. For example, if a fish was detected passing the spillway, then it survived through the preceding reach. Thus, the probability of this event is the joint probability that it survived through the reservoir (S_{Pool}), passed the spillway (S_p), and was detected in the spillway (P_{Sp}). However, if this fish was not subsequently detected at an array downriver of the dam, then two possibilities arise, 1) the fish died ($1-S_{Sp}$, the probability of not surviving through the spillway), or 2) the fish survived the spillway but was not detected by downriver telemetry arrays, $S_{Sp}(1-\lambda)$, the joint probability of surviving and not being detected. Therefore, the probability of detection history 130 can be specified as $S_{Pool} * S_p * P_{Sp} * (1-S_{Sp} + S_{Sp}(1-\lambda))$.

The expected probability of each detection history is then estimated from the observed frequencies of fish with that detection history. Given the expected probability of each detection history and its probability function in terms of survival, route-specific passage, and detection probabilities, maximum

likelihood methods are used to find the combination of survival, passage, and detection probabilities most likely to occur, given the observed frequencies of each detection history. The maximum likelihood function to be maximized is simply the joint probability of all possible detection histories.

Sampling variances for parameters estimated by maximum likelihood are calculated using the inverse Hessian matrix provided by the USER software. Further details on the maximum likelihood methods for estimating survival and detection probabilities, including estimation of theoretical variances, can be found in Burnham et al. (1987), Lebreton et al. (1992), and Skalski et al. (2001). Additional parameters, such as overall survival through multiple routes, can be estimated as functions of model parameters. Variances for these parameters are calculated using the Delta method (Seber 1982). Confidence intervals for all model parameters will be calculated using likelihood profile methods as supplied in the USER software. Likelihood profile confidence intervals are presented as ranges because profile likelihood intervals may not be symmetrical about the point estimate due to asymmetrical likelihood distributions.

Dual detection arrays are another important aspect of the route-specific survival model that would likely need to be implemented in this study. To estimate the proportion of fish choosing various routes through the Delta, two independent telemetry arrays would be deployed closely-spaced together at the entrance to each channel just downstream of a channel junction. These dual arrays serve two important functions. First, the dual arrays allow for the estimation of detection probabilities at the entrance to each channel by using the Lincoln/Petersen mark-recapture model (Seber 1982). Without estimating the detection probability of arrays located at the entrance to each channel, estimates of the proportion of fish using each channel may become biased if detection probabilities differ between arrays at each channel entrance (e.g., arrays with lower detection probabilities at one channel entrance will underestimate the proportion of fish passing into that channel). Second, dual arrays will provide information on the direction of movement (upstream or downstream) when fish are detected at both arrays. This information may be critical to minimize errors in assigning fish to a migratory pathway in cases when fish are advected upstream during a flood tide and enter and different migratory pathway.

The dual array is implemented as a secondary likelihood in the mark-recapture model and within-route detection histories are used to calculate the detection probability of each dual array. Within-route histories are composed of two digits and indicate whether fish passing through a dual array were detected by the first array (10), the second array (01), or both arrays (11) within each route.

Assumptions of survival models

All survival models are subject to assumptions for valid interpretation of parameter estimates. These assumptions relate to inferences to the population of interest, error in interpreting telemetry signals, and statistical fit of the data to the model's structure. Some of these assumptions can be explicitly tested, while others can be fulfilled through careful study design. Where possible, we propose to assess model assumptions to validate estimates obtained from mark-recapture survival models. Assumptions are as follows:

- 1) Tagged individuals are representative of the population of interest. For example, if tagged fish are larger on average than the population of interest, then inferences may not apply to the unsampled fraction of the population.
- 2) Survival probabilities of tagged fish are the same as that of untagged fish. For example, the tagging procedures should not influence survival or detection probabilities. If the transmitter negatively affects survival, then estimates of survival rates will be biased accordingly.
- 3) All sampling events are instantaneous. That is, sampling should take place over a short distance relative to the distance between telemetry arrays so that the chance of mortality at a telemetry array is minimized. This assumption is necessary to correctly attribute mortality to a specific river reach. This assumption is usually satisfied by the location of telemetry arrays and the downstream migration rates of juvenile salmonids.
- 4) The fate of each tagged fish is independent of the fate of other tagged fish. In other words, survival or mortality of one fish has no effect on that of others.
- 5) The prior detection history of a tagged fish has no effect on its subsequent survival. This assumption could be violated if there are portions of the river that are not monitored for tagged fish. For telemetry, this assumption is usually satisfied by the passive nature of detecting tags and by monitoring the entire channel cross-section of the river.
- 6) All tagged fish alive at a sampling location have the same detection probability. This assumption could also be violated as described in assumption 5, but is usually satisfied with telemetry by monitoring the entire channel cross-section.
- 7) All tags are correctly identified and the status of tagged fish (i.e., alive or dead) is known without error. This assumes fish do not lose their tags and that the tag is functioning while the fish is in the study area. Additionally, this assumes that all detections are of live fish and that dead fish are not detected and interpreted as live (i.e., false positive detections).
- 8) The dual detection arrays within each route are independent. This assumption is necessary to obtain valid estimates of route-specific detection probabilities. To fulfill this assumption, fish detected in one array should have the same probability of detection in the second array compared to fish not detected in the first array.
- 9) Routes of tagged fish are known without error. This assumption is important to avoid bias in route-specific passage and survival probabilities.

Assumptions 5 and 6 can be formally tested using χ^2 Goodness of Fit tests known as Test 2 and Test 3 (Burnham et al. 1987). Both Test 2 and 3 are implemented as a series of contingency tables. Test 2 is informally known as the “recapture test” because it assesses whether detection at an upstream array affects detections at subsequent downstream arrays (assumption 6). Test 3 is known as the “survival test” because it assesses assumption 5 that fish alive at array i have the same probability of surviving to array $i+1$ as fish not detected at array i . The pooled χ^2 value from Test 2 and 3 provides an overall test of overdispersion in the parameter estimates.

Assumption 7 can be tested empirically. To test for false positive detections, a subsample of euthanized tagged fish can be released and subsequent detection monitored. To test whether fish exited the study area within the battery life of the transmitter, a controlled tag life study can be conducted to estimate the probability of tag failure at any point in time after tags were turned on.

The methods of Townsend et al. (In Press) can be used to estimate the average probability that a tag was alive while fish were in the study area. If tags fail prior to exiting the study area, then information from the tag life study can be used to correct survival estimates for the probability of tag failure.

Finally, application of this approach was applied to the pilot data collected in 2006-2007, these results are summarized in [appendix B](#).

Flow Network – Discharge Data (4)

We expect the flow station data will be used in the analysis of the data obtained from the acoustic telemetry receivers and in the management model. As of this writing, the current configuration of the flow station network is shown in [figure 4.2](#) and is comprised of 38 stations spread throughout the Delta. Water level, cross sectionally averaged velocity, and discharge are all measured at the circles shown in [figure 4.2](#). Temperature and conductivity (e.g. salinity) are also measured, in addition to stage, the cross sectionally averaged velocity and discharge at the yellow circles in [figure 4.2](#). In the context of this study, these data will be used to supply boundary condition information and calibration and validation data for both the 3D and 2D numerical hydrodynamic models and will, additionally, provide velocity data for use in the analysis of the acoustic telemetry (receiver) data. Fifteen minute averages of the data are telemetered to the USGS offices at Sacramento State University in real time. These stations are calibrated to deliver discharge data following standard USGS protocols (Simpson, 2001; Ruhl and Simpson, 2005).

Statistical Model of Net Flows (5)

Fortunately, the distribution of the net flows within the channels of the north Delta are remarkably stable (time invariant) and predictable, depending almost entirely on the Sacramento River inputs (as measured at Freeport) and DCC gate operations ([Appendix A](#)). This inherent predictability could provide the foundation on which simplified management models could be built. The central challenge in developing these tools will be in collapsing high frequency variability, such as created by the tides and behavioral responses to ambient light (day, night, crepuscular), into tidally-averaged constructs. Considerable effort will be made in the collection of the data in the field to account for tidal timescale variations (e.g. releasing fish over a 24 hour period, etc.), so tidal averages can be computed with the aim of using these averages in simplified management models.

2D Numerical Modeling/Particle Tracking (8)

Whereas the detailed simulation of the distribution of salmon outmigrants within the water column, and the impact of these distributions on entrainment in junctions will be studied and quantified using the 3D modeling described above, we propose to use a suite of finite element models, RMA2 (a 2D depth averaged hydrodynamic transport model) and RMA11 (a 2D depth averaged water quality model), to address salmon outmigration from a delta-wide perspective. Multi-month, full 3D model simulations of the entire Delta are currently impractical, and thus junction entrainment relations developed with the 3D model described above (and possibly the route selection probabilities developed in the mark-recapture statistical model just described) will be incorporated into the 2D models described in this section.

RMA2, is a generalized free surface hydrodynamic model, developed by Ian King in the early 1990's, and is based on the two-dimensional depth averaged Shallow water equations (King, 1992). This

model solves primitive form of the shallow water equations to compute temporal and spatial descriptions of velocities and water levels within a specified model domain. This model uses a Galerkin approach of minimizing the weighted residuals over the entire domain using 6-node triangular and 8-node quadrilateral elements. Three node line elements are used for approximating one-dimensional channel flow. Quadratic shape functions are used to interpolate the velocity variables while linear shape functions are used for the depth, h . The quadratic functions allow for curved element edge geometry. Because these equations are non-linear, they are solved by a Newton-Raphson iterative technique. Time integration in this model follows a Crank-Nicholson implicit finite difference scheme. Values of the time integration constant, θ , can be varied by user input. Typically a value of 0.526 is used for the RMA2 time dependent simulations. The time step used for modeling the depth-averaged flow and water quality transport in the Delta is 7.5 minutes. The model uses the Smagorinsky formulation for modeling of turbulent momentum transfer. RMA2, capable of simulating the de-watering of tidal flats, is well suited for modeling of inter-tidal hydrodynamics in the marshes and mudflats characteristic of the Bay-Delta system.

RMA11 (King, 1995) is a generalized two dimensional depth-averaged water quality model which computes a temporal and spatial description of conservative and non-conservative water quality parameters. RMA11 uses the results from RMA2 for its description of the flow field. Vertical gradients in salinity, generally limited to regions seaward of Chipps Island may lead to three dimensional circulation patterns that will not be represented by a two dimensional depth-averaged model. Instead, the three dimensional processes are approximated by two-dimensional mixing parameters. Calibration results presented in DeGeorge, 2005 show that this model is able to very accurately transport salinity from the tidal boundary at Martinez, through Suisun Bay, to Jersey Point and False River for the 2002 period simulated.

A “salinity-coupled” version of the RMA2 program has been developed, and will be used for the work proposed here, which includes the relevant water quality transport routines from the RMA11 program to compute the salinity distribution throughout the model domain during the hydrodynamic simulations. The salinities values are used in the computation of the depth averaged baroclinic pressure gradient terms in the momentum equations. Salinity transport and flow are not computed simultaneously in the model; rather, the salinities from the previous computational time step are used to compute the fluid densities for the current hydrodynamic time step. Once a converged solution for the flow computation is achieved, the resulting flow field is utilized for the computation of the salt transport, and so on.

In addition, RMA2-11 also employs one-dimensional channel elements for computational efficiency. Special “transition” elements allow the one dimensional elements to be readily interfaced to the two-dimensional depth-averaged elements. One dimensional depth-averaged elements are used in the “simple” channels of the delta, primarily within the north delta, Mokelumne River system and south Delta. An example grid of the entire Delta is shown in [figure 6.8](#).

In anticipation of this work, the geometry used in this model has been recently updated to include newly collected bathymetry data collected in: Liberty Island, Elk Slough, and the north and south Forks of the Mokelumne River, Beaver, Hog, Sycamore and Snodgrass Sloughs. The model has since been recalibrated in the north Delta and model results have been compared to USGS flow station data (a calibration document is in preparation).

Finally, particle tracking has recently been implemented for use with the RMA2 generated flow fields. These routines are currently being tested and will be fully documented before particle tracking results generated from this effort are presented. Moreover, “listening stations” (e.g. numerical acoustic telemetry listening stations) have been implemented in the particle tracking model, in much the same way data are collected in the field, so that particle tracking results can be directly compared to the receiver data collected in the field. The “numerical” listening stations will be used to compute tidally averaged Lagrangian transit times for the individual channel segments based on a large number of particle releases.

7. EXPERIMENTAL TREATMENTS – RELEASE STRATEGY

A total of 5000 late-fall Chinook salmon smolts from Coleman National Fish Hatchery will be surgically implanted with individually-identifiable, miniature (~ 0.65-g weight in air) acoustic transmitters (307.2 kHz) by the USGS-CRRL and will be released during four separate experiments that will be specifically designed to capture a range of hydrodynamic conditions (e.g. Sacramento River flow rates and DCC gate operations) so that we can produce discharge versus survival curves (e.g. [figure 2.4](#)) and route selection relations (e.g. [figure 2.3](#)).

General assumptions associated with this approach

As with any study there are a host of explicit and implicit assumptions. The following is a list of assumptions associated with this study design:

- (1) The hatchery raised surrogates used in the study will mimic the behavior of wild fish. To minimize the influence of the use of hatchery raised fish, the acoustically-tagged fish will be acclimated for 24 hours in the Delta prior to release and fish will be released roughly 24 hours transit time upstream of the receiver locations.
- (2) Surgical implantation of the acoustic tags will not significantly affect fish behavior or movement.
- (3) The size of the surrogates will approximate the size of naturally occurring fish in the system.
- (4) Extreme weather and/or other conditions at the time of our experiments will not impair our ability to detect the impacts of the parameters for which we are testing.

Since the same fish will be used for the junction experiments (component (1) in [figure 3.1](#)) and the delta-scale experiment (component (2) in [figure 3.1](#)) in this experiment, we begin with a discussion of the release strategy, which applies to both efforts.

DCC gate operations

The operation of the DCC gates plays a critical role in the management of water supplies, water quality and the Sacramento River salmon fishery. During the late-fall and winter months, juvenile salmon, including winter, late-fall and tributary spring-run, migrate past the DCC on their way to the ocean. These fish are generally 120-150 mm in length and initiate their outmigration due to a combination of (1) storm-induced increases in flow and/or turbidity in the streams of the upper watershed and (2) physiological/behavioral changes associated with smoltification. Studies with 70-90 mm smolts in spring months suggest that outmigrant survival is substantially poorer for fish that pass through the central delta rather than staying in the main river channel (USFWS, 1996 and Newman and Rice, 1997). Wintertime experiments using larger late-fall run (110-120mm) as surrogates for winter run have also shown a survival rate between 5 to 70% for fish in the interior delta relative to fish that remain in the Sacramento River (Delta Action 8 studies). Thus, we plan on using late-fall run Chinook salmon for our study. Based on these smolt survival data, the DCC gates are now required by the 1995 Water Quality Control Plan to be closed from February 1 through May 20 of every year, and the DCC gates can be closed for half of the days in the November-January period at the discretion of the fishery management agencies. The DCC also plays a central role in controlling the distribution of the flows among the channels of the north Delta ([appendix A](#)), and thus, the operation of the DCC gates, understandably, plays a central role in the design of the proposed field experiments.

Pending approval of the various management agencies the gate operations we propose are: (1) DCC gates open, (2) DCC gates closed, (3) DCC gates closed at night, (4) DCC gates half open. Releases involving alternative scenarios may be conducted depending on consultations with the management agencies. For each of four different study periods in December 2008 and January 2009, 1250 acoustic-tagged salmon will be transported to the Delta by USFWS and placed in a series of live pens (figure 7.1) in the Sacramento River at Old Sacramento and at the northern end of Georgiana Slough for overnight acclimation prior to release. Each release group of 1250 fish will be acclimated for a period of 24 hours. The tags will be programmed in the fish (figure 7.2), on site, during the acclimation period, to save battery life, and to allow greater flexibility in the timing of each release. Fish with malfunctioning tags will be used as a control group and kept in pens for a period of approximately 10 days. In addition, a small number of fish with functioning tags (~10 per release) will be set aside and used to determine tag life (tag life depends on a variety of factors, such as tag lot, shelf life, water temperature, etc.). As part of normal operation, the DCC gates are anticipated to be open during the lower-flow conditions in December and early January and closed during high-flow conditions in mid- to late-January. We expect to organize our experiments to be as consistent with normal operations as possible to minimize the impacts on water project operations to the greatest extent possible. During each river condition, the ~1200 acoustic-tagged salmon will be released over a 24-hour period (either hourly or every half hour depending on release logistics). This approach ensures salmon will be released at daytime, nighttime, and during morning and evening crepuscular periods, to avoid tidal and diel-cycle aliasing. We are hopeful that the 24 hour, in-river acclimation period, prior to interaction with our monitoring equipment, will be sufficient to allow the hatchery raised salmon to begin natural behavioral patterns.

Releases will be made at two locations: (1) near the Tower Bridge in Sacramento, and (2) within Georgiana Slough (black squares in Figure 4.1). Georgiana Slough releases are intended to insure “adequate” numbers of acoustically tagged salmon traverse the Franks Tract region. The exact numbers of fish released at each site for each release is under consideration, since we know next to nothing about route selection and survival in the central Delta. However, pilot study results will allow us to address sample size issues in the North Delta (Appendix B).

Open vs Closed operations

Currently the DCC gates are required to be closed when juvenile salmon are in the system, under the hypothesis that salmon that enter the central Delta through the DCC experience reduced survival to Chipps Island. Fish that enter Georgiana Slough also end up in the central Delta and would theoretically experience similarly reduced survival as those that enter the DCC. Gate closures increase the net flow in Georgiana Slough (Appendix A) and thus the possibility of increased entrainment in Georgiana Slough needs to be weighed against zero entrainment in the DCC when the gates are closed. The current management strategy is essentially based on trawling data that compared mass releases made at Ryde, in the Sacramento River, versus releases made in Georgiana Slough (Brandes and McLain, 2001). Placing fish directly in the channel at Ryde and in Georgiana Slough completely ignores the effect that gate operations have on route selection and, moreover, the changes that gate operations may have on reach-specific survival elsewhere in the system (e.g. in Sutter and Steamboat Sloughs). For example, the net flows in Sutter, Steamboat and Georgiana Sloughs all increase when the gates are closed for a given Sacramento River input (Appendix A), with unknown consequences for both route selection and overall survival to Chipps Island. Thus, the impact on overall survival to Chipps Island of gate operations is not simply a matter of survival from



Figure 7.1 - Acclimation and holding pen used for acoustic-telemetry studies.

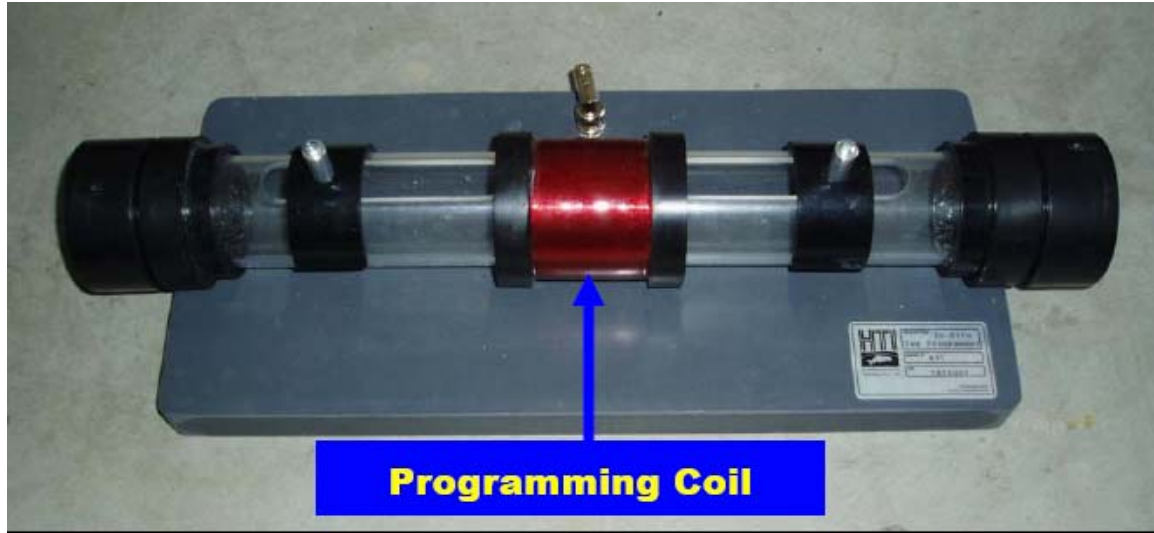


Figure 7.2 - In situ tag programmer.

Ryde and through Georgiana Slough, one must also consider the impacts of gate operations on the changes in *distribution* of salmon outmigrants and survival within the entire network. For example, if the numbers of salmon outmigrants that enter Sutter and Steamboat Sloughs increases and survival there is low, closing the gates could conceivably decrease overall survival to Chipps Island, in direct conflict with current management objectives associated with gate operations at the DCC. Comparing gate open versus closed conditions in the context of this study will allow us to take a first-time look at the regional scale impacts of gate operations on overall survival of juvenile salmon to Chipps Island, in part, as an evaluation of current management practices.

Nighttime Closures

Research on juvenile salmon migratory behavior indicates that fish respond differently during diel periods (and the preliminary results from the study conducted at Clarksburg Bend confirm this – appendix C). For example, juvenile salmon have been shown to exhibit a different vertical distribution in the water column with respect to day and night (Schaffter, 1980; Horn and Mueller, 2001). Also, lateral fish distributions within river channels have been shown to vary with diel period (Schaffter, 1980). Moreover, previous north Delta studies (Blake and Horn, in press, a,b, appendix C) have shown that salmon outmigrants tend to be higher in the water column and “move” more during crepuscular periods and at night, preferring to “hold” during the day. If diel patterns of spatial variability occur in the vicinity of the DCC, then the gates could be operated with respect to the diel cycle to minimize fish movements into the central Delta while at the same time minimizing water quality impacts in the central Delta. These observations motivate the idea of closing the gates at night, presumably a period when salmon outmigrants are more vulnerable to entrainment into the DCC. Using this operational strategy, the DCC would be allowed to convey water into the central Delta during the day (and recreational boaters could move freely from the central to northern Delta through the DCC), where it would presumably alleviate water quality concerns and allow increased exports over fully closed conditions. If this operational strategy minimizes the entrainment of juvenile salmon in the DCC in the context of this experiment, it would suggest that diel operation of either a TDF or some of the BDCP options (e.g. take water on big ebb tides during the day during low flow periods – do not take water at night when salmon are present) could minimize impacts on salmon outmigrants, provided either of these proposed facilities were built in such a way as to be able to do this (e.g. larger capacity and capable of handling flow transients (e.g. water hammer)).

DCC gates half closed

This scenario is the least likely of the gate treatments to be approved by the management agencies because of concerns associated with undermining the DCC gate support structure and boating safety issues. The idea behind this scenario is to keep salmon outmigrants out of the DCC via a “startle response” – fish respond to sudden changes in flow, turbulence or vertical position by swimming away from it because they are unsure of what lies ahead. This type of response has been seen at bypass structures in the Columbia River (Noah Adams, USGS, personal communication). With the gate half closed salmon outmigrants will be swept from the surface layers, where they typically reside, into a region of large shears and increased turbulence intensity, which could provide the necessary behavioral cues for them to swim back toward the Sacramento River and out of the DCC. If this scenario is approved by the USBR, we would add additional hydrophones within the mouth of the

DCC and would deploy a series of upward-looking ADCP's to measure vertical shear and turbulence intensities following the methodology of Stacey, 2003. (see [figure 5.1](#), for a plan view – ADCP positions at magenta squares; and [figure 5.8](#) for a profile view). Behavioral responses of acoustically tagged salmon within the confines of the mouth of the DCC will be compared to observed water column shear and turbulence intensity measured by the upward-looking ADCP's. This would allow us to determine if we see a behavior response associated with increased vertical shear and turbulence intensity.

Finally, the impact of all of the gate operation scenarios on water supplies, water quality (e.g. salinity), and survival to Chipps Island will be evaluated and compared.

Water Project Operations, Study duration and the need for stable hydrodynamic conditions

The principal investigators will coordinate with project operators to provide stable operational conditions, to the extent possible, during the period the acoustic tag fish are expected to be traversing the north Delta. In addition to stable DCC gate operations, this includes stable reservoir releases and export rates. We will request that the gates be placed in the desired position 1.5 days before fish are released to avoid hydrodynamic transients and to avoid oscillations in the computed net flows due to tidal filter response time ([Figure 7.3](#), see [appendix A](#)). Furthermore, we will be requesting that operations remain steady until the last fish released is projected to have either (1) entered Cache Slough or (2) entered the San Joaquin from the Mokelumne River – on the order of 10 days during low flow conditions. Based on past experience, and particularly under the expected drought conditions that might occur during the winter of 2008-2009, we do not expect them to be able to do this – we will likely get what nature gives us. The tidal flows are so strong in Cache Slough and on the San Joaquin west of the Mokelumne River that changes in the net flows due to DCC gate operations are expected to have relatively little affect on salmon outmigrants once they reach these areas.

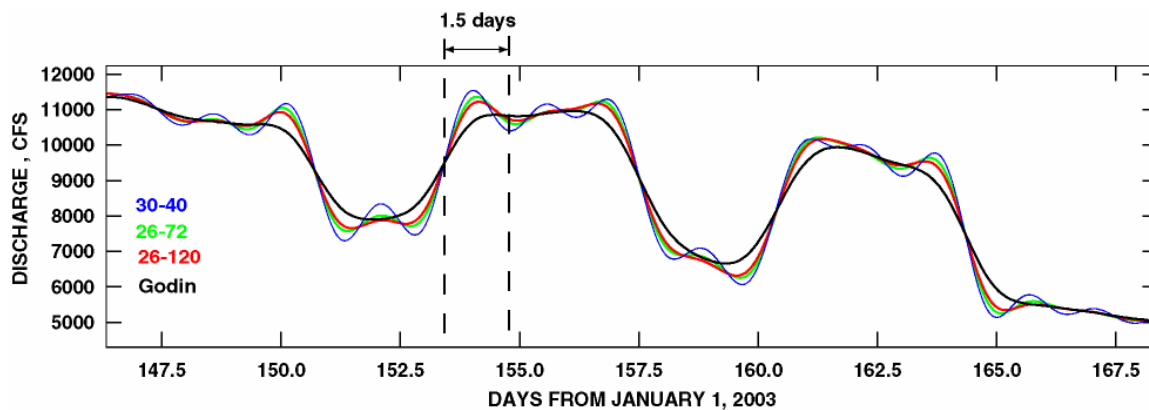


Figure 7.3 – Time series of responses to gate operations from various filters applied to flow data collected on the Sacramento River below Georgiana Slough (station WGB) : the digital filter described in Walters and Heston 1989 with stop: pass periods of 30-40 hours (blue), 26-72 hours (green), 26-120 (red) and the Godin filter (black). The digital filter with the stop:pass periods of 30-40 hours oscillated the most and the Godin filter is the most damped. The Godin filter takes approximately 1.5 days to “settle” after a change in gate operation.

Estimating Sample Size and Precision of Survival Estimates

So how did we come up with the need to release approximately 1,000 fish per treatment (5,000 fish total)? To estimate sample sizes for this study, we assumed values for all parameters of a survival model and then estimated the precision (\pm 95% confidence interval) of these parameter values over a range of sample sizes. The goals of this analysis were to understand how precision of survival estimates varied over sample size among 1) different areas of the Delta, 2) different scenarios of “high” versus “low” survival, and 3) different release strategies (i.e., one versus two release sites). Since the survival outcomes of a future study are uncertain, this approach also allowed us to examine the robustness of a given sample size in response to different survival outcomes and release strategies. Our intent was to select a sample size and release strategy for each release that would achieve approximately \pm 5% for a 95% confidence interval of survival estimates for the Delta as whole, as well as the “North Delta”, and “South Delta”. Here, the Delta included the release site at Sacramento to Chipps Island, the North Delta included the Sacramento River and Steamboat and Sutter Slough from their junction with the Sacramento to Rio Vista, and the South Delta included from the Delta Cross Channel and Georgiana Slough to Jersey Point.

We examined scenarios of “low” survival, a “base case”, and “high” survival, each under two release scenarios. Under the first release scenario, all fish were released at Sacramento, and for the second, one-third of the fish were released in Georgiana Slough to supplement the sample size of fish entering the South Delta (Table 4.1). Parameter values for the base case scenario were based partly on survival estimates obtained during the USGS pilot study conducted during the winter of 2006/2007. Some survival estimates were unknown (e.g., the South Delta) at the time of this analysis, and arbitrary (but “best-guess”) values were chosen for these parameters. From the base case, parameter values were adjusted both lower and higher to obtain the other scenarios. The proportion of fish migrating through Steamboat and Sutter Slough and the South Delta was held constant over all scenarios. In addition, we assumed a detection probability of 0.90 for all telemetry stations in this analysis (which is conservative since the detection probabilities from the pilot study were generally greater than this). We then generated estimates of standard errors of survival probabilities that would be obtained over a range sample sizes. It is important to note that these precision estimates include only simple multinomial variation and thus should be viewed as the precision that would be obtained under stable environmental conditions (e.g., stable discharge, exports, and gate operations). Thus, this analysis was used to determine the sample size for each release group, where each release group would be migrating under a given set of environmental and operational conditions.

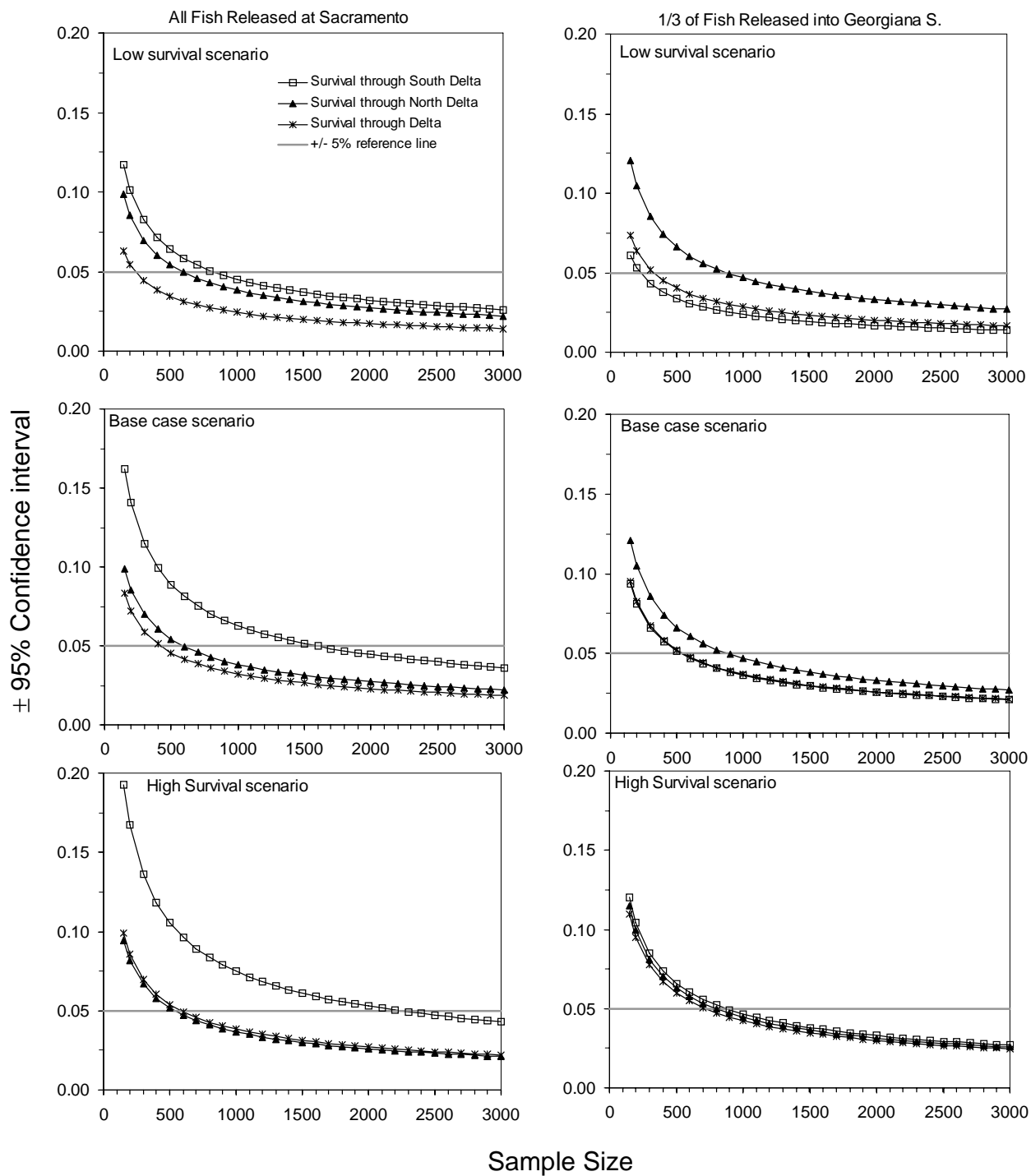


Figure 7.4 - Precision as a function of sample size for three survival scenarios (see Table 4.1) and two release scenarios for the proposed telemetry study in 2008.

The sample size analysis revealed two important patterns. First, since only about 25% of surviving fish entered the South Delta, precision of the South Delta survival estimate was lower than the other two survival estimates when all fish are released at Sacramento (Figure 7.4). Under two of the survival scenarios, we found that sample sizes required to obtain $\pm 5\%$ confidence intervals for the South Delta were exceedingly large when all fish are released at Sacramento. However, releasing one-third of the fish into Georgiana Slough balances the sample size of fish for the North and South Delta, resulting in comparable precision curves for all three scenarios. Second, we found that increasing sample size initially leads to a large reduction in confidence intervals, but the marginal benefit of increasing sample decreases at larger sample sizes. The nonlinear relationship between sample size and precision suggests that the optimal size occurs where the curve changes from a steep to a shallow slope. For sample sizes on the steep part of the curve (e.g., 200-500 fish), we can expect large fluctuations in precision if observed survival differs substantially from the values assumed here (possibly resulting in failure to achieve precision goals). However, sample sizes on the “flat” part of the curve will be robust to deviations in assumptions about survival. That is, we would expect precision to vary less if observed survival differed from the values used here. However, precision improves little with sample size exceeding about 1500 fish, suggesting little additional benefit of further increases in sample size. This analysis suggests a sample size in the range of 1000 to 1500 fish for each release to obtain a high likelihood achieving $\pm 5\%$ confidence intervals or better. With one-third of fish released into Georgiana Slough, these precision goals were achieved for all three summary survival estimates under all three survival scenarios beginning at a sample size of about 1000 fish. Therefore, we selected a sample size of 1250 fish per release to incorporate a buffer against uncertainty of future survival outcomes and to insure that we would achieve our precision goal of $\pm 5\%$ confidence intervals or better.

Parameter Description	Base case	Low survival	High survival
Proportion entering Sutter and Steamboat Slough	0.300	0.300	0.300
Proportion remaining in Sacramento at DCC and Georgiana	0.650	0.650	0.650
Survival from release to Junction with Sutter/Steamboat Slough	0.750	0.650	0.850
Survival from entry to exit of Sutter/Steamboat Slough	0.583	0.415	0.796
Survival in Sac. from Sutter/Steamboat to DCC	0.853	0.793	0.928
Survival in Sac. from DCC to confluence w/ Cache S	0.649	0.507	0.828
Survival of fish from exit of Sac and Sutter/Steamboat to Rio Vista	0.867	0.813	0.935
Survival of fish from Jersey point and from Rio Vista to Chipps I.	0.499	0.345	0.635
<u>Summary Survivals:</u>			
North Delta survival combined for Sac. and Sutter/Steamboat	0.370	0.250	0.550
South Delta survival from DCC and Georgiana to Jersey point	0.150	0.050	0.350
Delta survival of all fish to Chipps Island	0.200	0.100	0.400

Table 4.1. Parameter values used to generate precision curves under three different survival scenarios.

8. SIMPLIFIED MANAGEMENT TOOL (9)

The final outcome of this study is a management tool that can predict the impacts of management actions on salmon survival. In this section we provide a glimpse of a possible organizational structure for this tool. The envisioned management tool must be simple to be useful to managers because it is not feasible to run sophisticated, time consuming, multi-dimensional particle tracking models, or conduct juvenile salmon outmigrant experiments every time a change in policy or management decision is needed. Yet, the movements of salmon outmigrants in the Delta is complex, due, in part, to the diversity of possible outmigration pathways and the differential survival between pathways. The following is a modeling exercise that attempts to capture the essence of the detailed numerical model results and field experiments in a simple and useful decision-making tool. As a first step, this model simply accounts for, and distributes among the north Delta channels, an initial quantity of Sacramento River juvenile salmon, N_0 , based on: (1) an entrainment function, α_j , at each junction, j , and (2) the survival rate, γ_i , within each channel, i . Both the entrainment function α_j and survival rate γ_i are functions that vary between 0 and 1 in the model, and, in the case of the entrainment function, can be thought of as a ratio or probability. Coming up with these relations is key to the success of this entire approach. The form of the entrainment relations are unknown, but they are likely to be junction specific (depending on approach channel curvature, specific junction geometry, etc.) and will likely depend on flow rate, degree of tidal forcing, salmon run, smoltification, etc. Survival rates will also likely depend on flow rate because flow rate, to a large degree, determines travel times (or exposure times) within individual channel segments. Flow rate may also influence the predation rate, for example, by creating greater lateral shears that have the possibility of disorienting juvenile outmigrants and favoring predators. The entrainment relations and survival rates will be determined through particle tracking experiments and through tracking of acoustically tagged juvenile salmon as described previously.

Fortunately, the distribution of the net flows among the north Delta channels at the tidally-averaged timescale is relatively straightforward, and, remarkably stable and predictable ([Appendix A](#)) even though the flow dynamics at tidal timescales are generally complex at individual channel junctions (Dinehart and Burau, 2005a). Thus, we will begin formulating a simplified North Delta Juvenile Salmon Survival Model at the tidally-averaged timescale using net flow relations, even though we know it is the tidal timescale evolution of the distribution of outmigrants in the water column and velocity structure within junctions that controls the entrainment of juvenile salmon within individual junctions. Bridging the temporal divide between the tidally-averaged, or management timescale, and the tidal timescale, is one of the greatest challenges we will face in this effort. However, the tidal timescale dynamics are intimately tied to the Sacramento River flows ([Appendix A](#)), so we hypothesize that a relation between the net flows and entrainment rate exists and is attainable using this approach. With the exception of Clifton Court Forebay gate operations and proposed tidal operation of the DCC gates, project operators only really have control at the tidally-averaged timescale: through reservoir releases, changes in export rates at the Bill Jones Pumping Plant and by operating the DCC gates for periods of a day or longer. Our hope is that by releasing acoustically tagged juvenile salmon over 24 hour periods in synchrony with the tides, under a wide variety of Sacramento River flow rates and gate operations, we will be able to bridge the gap between the tidal and residual timescales. Essentially, we hope that the particle tracking experiments and field investigations of entrainment at the tidal timescale using acoustic tags will allow us to build

sufficiently accurate entrainment and survival sub-models at the tidally averaged timescale for use in this management tool.

Simplified Management Tool - Model formulation: A simple example

The starting point for the envisioned model is really a glorified accounting scheme that keeps track of where fish go and where they die at residual timescales. The heavy lifting is done by the entrainment and survival sub-models. Similar to the development of most numerical models, a channel network invariant numbering scheme, which at first blush looks unnecessarily complicated, is used that allows changes to the model network through simple changes to the input files not the code (e.g. modification of the channel network does not require a change in the calculation routines). The accounting scheme envisioned in the model assumes that: (1) fish are conserved in a junction (e.g. in = out and no mortality in junctions) and (2) reach specific mortality is dependent on the time spent in that reach, (3) fish, in a regional sense, move downstream with the net flows. We'll account for tidal exchanges later. To see how these assumptions are implemented consider [figure 8.1](#), a simple network that includes all of the elements needed to model the north Delta, where a single channel is split into two channels, one of which has a dead-end slough attached. These channels then reconnect. For clarity, and to assure that fish are conserved in each junction, the network relations are derived and implemented on a channel junction basis (the order of the junction calculations is stored in variable `jord(j)` in the code). Two types of junctions are specified: (1) a “split” junction (`jtype=1`), and a (2) “combine” junction (`jtype=2`) ([Figure 8.2](#)). For a “split” junction, k , the entrainment relation, α_k , (remember: $0 \leq \alpha_k \leq 1$) is specified for one of the two channels leaving the junction, call it the primary exit channel. Note that the junction designation, k , is the number of the primary exit channel, $k = j_{k,1}$. To conserve fish, the entrainment in the secondary channel, $J_{k,2}$, is simply $1 - \alpha_k$. For example, if $\alpha_k = 1$ at a given junction, then all of the juvenile salmon would be diverted into the primary channel and none would be diverted into secondary channel. If $\alpha_k = 0.8$, then 80% of the fish entering this junction would go down the primary channel and 20% down the secondary channel. Thus, the relation between the entry channel and primary and secondary channels in each junction (connectivity) need to be mapped. So, for each “split” junction, k , the incoming channel is $J_{k,0}$, the primary exit channel is $J_{k,1}$ and the secondary exit channel is $J_{k,2}$ ([Figure 8.2](#)). In the case of junction 1 in [figure 8.1](#) this connectivity is: $J_{1,0} = 0$, $J_{1,1} = 1$, $J_{1,2} = 2$. For a “combine” junction an entrainment function isn't needed and the junction number is specified as the exit channel number. So for junction 5 in [figure 8.1](#), the connectivity is $J_{5,0} = 5$, $J_{5,1} = 1$, $J_{5,2} = 4$. Finally, the survival rate, γ_i , (remember: $0 \leq \gamma_i \leq 1$) for each channel, i , must be specified or calculated. If the survival rate γ_i were 1.0, then all of the juvenile salmon in that reach would survive, if it were zero than none would survive. For a complete list of terms see appendix A.

Now, for each channel reach, j : (1) the number of fish entering the reach, $N_{j,1}$, is computed, (2) the number of fish leaving the reach, $N_{j,2}$, is computed (e.g. survival), and finally (3) the mortality, M_j is computed. Thus, to be clear: for $N_{j,k}$, $k=1$ are fish entering the j 'th reach, $k=2$ are fish leaving the reach, which, incidentally, is consistent with the way in which data will be collected in the field to

Numbering Scheme Example

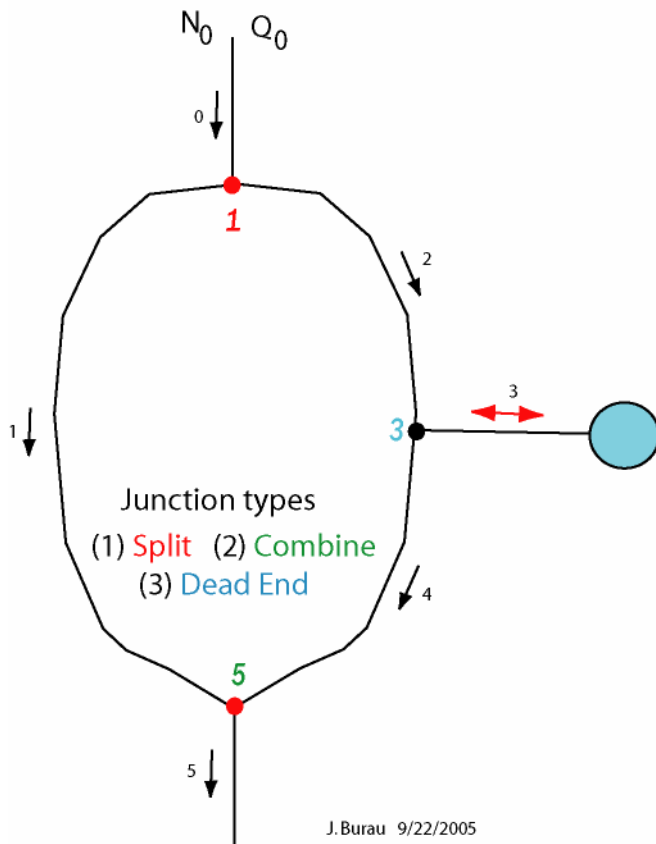
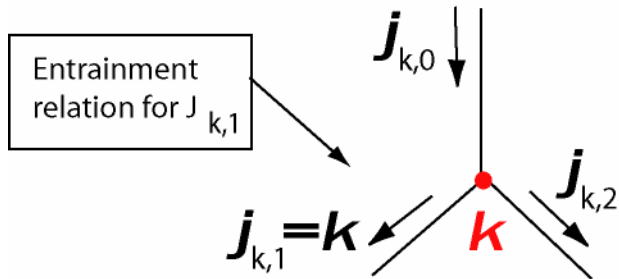


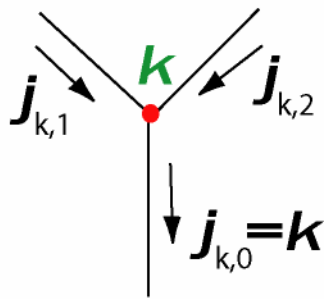
Figure 8.1 – Schematic of archetypal network of channel and junction elements.

Junction Numbering

(1) Split



(2) Combine



J.Burau 9/22/2005

Figure 8.2 –Schematic of junction numbering schemes. Two types of junctions are specified: (1) split, (2) combine.

North Delta Salmon Survival Model

Numbering Scheme

Model - 1

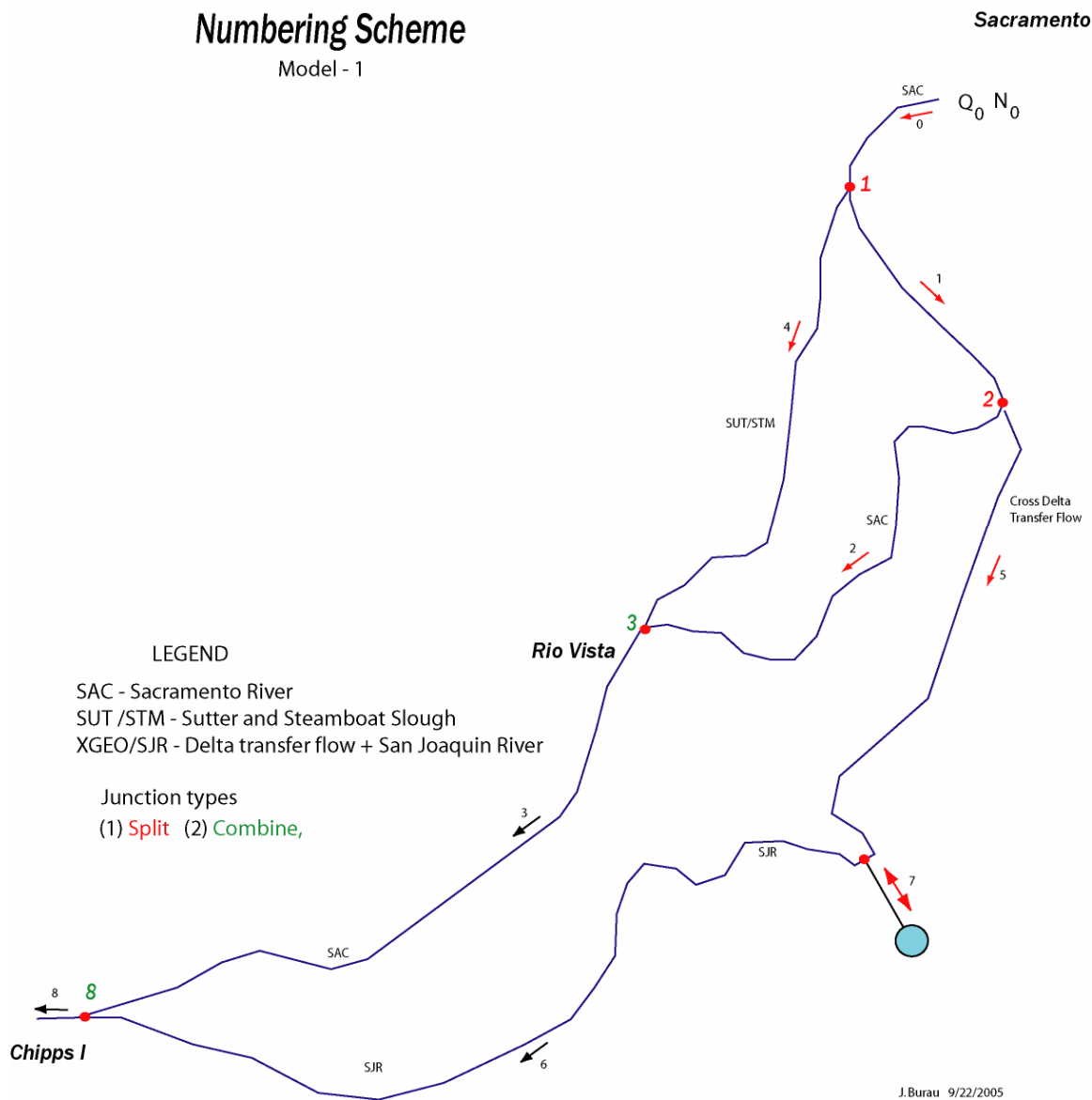


Figure 8.3 – Simple first-order salmon survival model of north Delta. This model includes three basic migration pathways: (1) Sutter/Steamboat, (2) Sacramento River, (3) Mokelumne/Georgiana.

develop these relations (e.g. an array of acoustic tag listening stations). The relations for the first junction in figure 8.1 are given in example 1 below, where the number of fish entering channel 1, $N_{1,1}$, is simply the product of the number of fish entering the junction, N_0 , and the entrainment relation, α_1 , for junction 1. To conserve fish in the junction, the number of fish entering channel 2, the secondary channel, is simply the product of $(1 - \alpha_1)$ and the number of fish entering the junction, N_0 . The survival and mortality in the reach are computed in a manner identical to reach 1.

We've used the simple numbering scheme outlined above to represent complex channel network systems such as the network shown in [figure 8.3](#). And, we've experimented with a number of different graphical user interfaces. At this point in their development, the simplified management tools are based on the net flow relations described in [appendix A](#), with user selectable assumed (essentially made up) entrainment relations and survival probabilities. As an end goal, we hope to replace the assumed entrainment relations and survival probabilities in these experimental simplified management tools with actual relations developed through the analysis of field data and/or model results described in the balance of this study plan. The ultimate end goal of this project is to develop a relatively easy to use graphical tool that can be used *directly* by resource managers to explore scenarios of interest.

9. STUDY TIMELINE

Pre-experiment Deployments

(1) Deploy 3-D HTI hydrophone systems in the junction of the Sacramento River with the DCC and Georgiana Slough: October 15 through November 7, 2008.

(2) Deploy the single- and four- hydrophone HTI receivers: October 5 through November 7, 2008.

First experiment (DCC gates open)

- Transport of 1250 acoustic-tagged from Coleman Hatchery for release at two sites: the Sacramento River at Old Sacramento and in upper Georgiana Slough on November 7, 2008.
- Release of fish over a 24-hr period beginning early morning November 9, 2008.
- Fish will be tracked in 3D for 10 days November 10- November 20, 2008
- Single- and four- hydrophone HTI receivers will be turned on November 10, 2008.

Second Experiment (DCC gates closed at night)

- Transport of 1250 acoustic-tagged from Coleman Hatchery for release at two sites: the Sacramento River at Old Sacramento and in upper Georgiana Slough on December 5, 2008.
- Release of fish over a 24-hr period beginning early morning December 7, 2008.
- Fish will be tracked in 3D for 10 days December 8- December 18, 2008
- Single- and four- hydrophone HTI receivers will be run continuously from November 8, 2008 until they run out of batteries after a final servicing on Dec. 22-23 before a recess for Christmas.

Third Experiment (DCC gates ½ open if approved)

- Transport of 1250 acoustic-tagged from Coleman Hatchery for release at two sites: the Sacramento River at Old Sacramento and in upper Georgiana Slough on January 9, 2009.
- Release of fish over a 24-hr period beginning early morning January 11, 2009.
- Fish will be tracked in 3D for 10 days January 12-22, 2009
- Single- and four- hydrophone HTI receivers will be turned on January 12, 2009.

Forth Experiment (DCC gates closed)

- Transport of 1250 acoustic-tagged from Coleman Hatchery for release at two sites: the Sacramento River at Old Sacramento in upper Georgiana Slough on January 30, 2009.
- Release of fish over a 24-hr period beginning early morning February 1, 2009.
- Fish will be tracked in 3D for 10 days February 2-12, 2009.
- Single- and four- hydrophone HTI receivers will be run continuously from February 2, 2009 until they run out of batteries after a final servicing on February 18,19, 2009.

Post-experiment equipment recoveries

(1) Recover 3-D HTI hydrophone systems in the junction of the Sacramento River with the DCC and Georgiana Slough: February 23-March 12, 2009.

(2) Recover the single- and four- hydrophone HTI receivers: February 23-March 12, 2009.

Field activities in the Delta are expected to be complete by March 13, 2009.

REFERENCES

- Blake, A. and M.J. Horn. In Press(a), "Acoustic Tracking of Juvenile Chinook Salmon Movement in the Vicinity of the Delta Cross Channel, Sacramento River, California - 2001 Study Results". USGS SIR -XXXX
- Blake, A, and M.J. Horn. In Press (b), "Acoustic Tracking of Juvenile Chinook Salmon Movement in the Vicinity of Georgiana Slough, Sacramento River, California - 2003 Study Results". USGS SIR-XXXX
- Blumberg, A. F., and G. L. Mellor (1987). "A description of a three-dimensional coastal ocean circulation model." Three-Dimensional Coastal Ocean Models, S. Heaps, ed., American Geophysical Union, Washington, DC., 1-16.
- Brandes, P.L. and J.S. McLain. 2001. Juvenile Chinook salmon abundance, distribution, and survival in the Sacramento-San Joaquin Estuary. Pages 39 – 138 *in* R.L. Brown, Editor. Contributions to the Biology of Central Valley Salmonids, Volume 2, Fish Bulletin 179. California Department of Fish and Game, Sacramento, California.
- Burgner, R.L. 1991. Life history of sockeye salmon (*Oncorhynchus nerka*). pp. 3-117. In C. Groot and L. Margolis (Eds.). Pacific Salmon Life Histories. Univ. British Columbia Press. Vancouver.
- Burnham, K. P., D. R. Anderson, G. C. White, C. Brownie, and K. H. Pollock. 1987. Design and Analysis Methods for Fish Survival Experiments Based on Release-Recapture, American Fisheries Society Monograph 5, Bethesda, Maryland.
- Casulli, V., and R. T. Cheng (1992). "Semi-implicit finite difference methods for threedimensional shallow water flow." International Journal for Numerical Methods in Fluids, 15, 629-648.
- Durrant, D. R., 1998, Numerical Methods for Wave Equations in Geophysical Fluid Dynamics, Springer, New York, 465 p.
- Cormack, R. M. 1964. Estimates of survival from the sighting of marked animals. *Biometrika* 51:429-438.
- Counihan, T. D., Holmberg, G. S., Walker, C. E., and Hardiman, J. M. 2003. Survival estimates of migrant juvenile salmonids in the Columbia River through John Day Dam using radio-telemetry, 2003. Final Report of Research by the U.S. Geological Survey to the U.S. Army Corps of Engineers, Portland District, Portland, Oregon.
- DeGeorge J, 2005. Flooded Island Pre-Feasibility Study: RMA Delta Model Calibration Report, Prepared for the California Department of Water Resources
- Dinehart R.L. and J.R. Burau. 2005a Repeated surveys by acoustic Doppler current profiler for flow and sediment dynamics in a tidal river, *Journal of Hydrology* 314 (2005) 1–21
- Dinehart R.L. and J.R. Burau. 2005b. Averaged indicators of secondary flow in repeated acoustic Doppler current profiler crossing of bends. *Water Resources Research*, VOL. 41, W09405, doi:10.1029/2005WR004050
- Durrant, D. R. (1999). Numerical Methods for Wave Equations in Geophysical Fluid Dynamics, Springer.
- Gross, E.S., Koseff, J.R. Koseff, and S.G. Monismith, (1999a) "Evaluation of advective schemes for estuarine salinity simulations," *J. Hyd. Div. ASCE* , 125(1), pp. 32-46.
- Gross, E.S., J.R. Koseff, and S.G. Monismith, (1999b) "Three-dimensional salinity simulations in South San Francisco Bay," *J. Hyd. Div. ASCE* , 125(11), pp. 1199-1209.

- Hockersmith, E. E., W. D. Muir, S. G. Smith, B. P. Sandford, R. W. Perry, N. S. Adams, and D. W. Rondorf. 2003. Comparison of migration rate and survival between radio-tagged and PIT-tagged migrant yearling chinook salmon in the Snake and Columbia Rivers. *North American Journal of Fisheries Management* 23:404-413.
- Jolly, G. M. 1965. Explicit estimates from capture-recapture data with both death and immigration-stochastic model. *Biometrika* 52:225-247.
- King, I. P., 1986, "Finite Element Model for Two-Dimensional Depth Averaged Flow, RMA2V, Version 3.3", Resource Management Associates.
- King, I. P., 1995, "RMA11 – A Two-Dimensional Finite Element Quality Model", Resource Management Associates.
- Kreeger, K.Y. and W.J. McNeil. 1992. A literature review of factors associated with migration of juvenile salmonids. Unpublished manuscript for Direct Service Industries, Inc. October 23, 1992. 46 pp.
- Horn, M. and G. Mueller. 2001. Acoustic Tracking of Chinook Salmon Smolts in the Sacramento River, California (in draft).
- Lady, J. M., P. Westhagen, and J. R. Skalski. 2003. USER 2.1: User specified estimation routine. Prepared for U.S. Department of Energy, Bonneville Power Administration, Project No. 198910700, Portland, Oregon.
- Lebreton, J. D., K. P. Burnham, J. Clobert, and D. R. Anderson. 1992. Modeling survival and testing biological hypotheses using marked animals: A unified approach with case studies. *Ecological Monographs* 62:67-118.
- Newman, K. and J. Rice. 1997. Statistical Model for Survival of Chinook Salmon Smolts Outmigrating through the Lower Sacramento-San Joaquin System. Technical Report 59, Interagency Ecological Program for the San Francisco Bay/Delta Estuary.
- Nichols, J.D. 1992. Capture-recapture models: using marked animals to study population dynamics. *Bioscience*. 42: 94-102.
- Perry, R.W., A.C. Braatz, S.D. Fielding, J.N. Lucchesi, J.M. Plumb, N.S. Adams, and D.W. Rondorf. 2006. Survival and migration behavior of juvenile salmonids at McNary Dam, 2004. Final Report of Research by the U. S. Geological Survey to the U.S. Army Corps of Engineers, Walla Walla District, Contract W68SBV40271050, Walla Walla, Washington.
- Pevan, C., A. Giorgi, J. Skalski, M. Langesley, A. Grassel, S. G. Smith, T. Counihan., R.W. Perry, and S. Bickford. 2006. Guidelines and Recommended Protocols For Conducting, Analyzing, and Reporting Juvenile Salmonid Survival Studies in the Columbia River Basin. Report to the U.S. Army Corps of Engineers, Portland District, Portland, Oregon.
- Ruhl, C.A., Simpson, M. R., 2005, Computation of discharge using the index-velocity Method in tidally affected areas: U.S. Geological Survey [SIR 2005-5004](#).
- Schaffter, R. G. 1980. Fish Occurrence, Size, and Distribution in the Sacramento River Near Hood, California During 1973 and 1974. Administrative Report No. 80-3, California Department of Fish and Game.
- Seber, G. A. F. 1965. A note on the multiple recapture census. *Biometrika* 52:249-259.
- Seber, G. A. F. 1982. The estimation of animal abundance and related parameters. Macmillan, New York.
- Simpson, Michael R., 2002, Discharge measurements using a broad-band acoustic Doppler current profiler: U.S. Geological Survey [Open-File Report 2001-1](#).

- Smith, P. E., 2006, A semi-implicit, three-dimensional model for estuarine circulation: U.S. Geological Survey Open-File Report 2006-1004, 176 p. (accessed December 2, 2007 at the URL <http://pubs.usgs.gov/of/2006/1004/>).
- Smith, P.E., and Larock, B.E., 1997, Semi-implicit numerical schemes for 3-D flow modeling, *in* Proceedings of the 27th Congress of the International Association for Hydraulic Research: San Francisco, Calif., August 11-15, 1997, v. 1, p. 773-778.
- Skalski, J.R., J. Lady, R. Townsend, A.E. Giorgi, J.R. Stevenson, C.M. Peven, and R.D. McDonald. 2001. Estimating in-river survival of migrating salmonid smolts using radiotelemetry. *Canadian Journal of Fisheries and Aquatic Sciences*. 58: 1987-1997.
- Skalski, J. R., R. Townsend, J. Lady, A. E. Giorgi, J. R. Stevenson, and R.S. McDonald. 2002. Estimating route-specific passage and survival probabilities at a hydroelectric project from smolt radiotelemetry studies. *Canadian Journal of Fisheries and Aquatic Sciences* 59:1385-1393.
- Stacey, M.T.. 2003. Estimation of Diffusive Transport of Turbulent Kinetic Energy from Acoustic Doppler Current Profiler data, *J. Atmos. Ocean. Tech.*, Vol. 20 (6), pp. 927-935, 2003.
- Sommer, T.R., M.L. Nobriga, W.C. Harrell, W. Batham, and W.J. Kimmerer. 2001. Floodplain rearing of juvenile Chinook salmon: evidence of enhanced growth and survival. *Canadian Journal of Fisheries and Aquatic Sciences*. 58: 325-333.
- Rueda, F. J. (2001). "A three-dimensional hydrodynamic and transport model for lake environments." Ph.D. Dissertation, University of California, Davis.
- Townsend, R. L., J. R. Skalski, P. Dillingham, and T. W. Steig. In Press. Correcting bias in survival estimation resulting from tag failure in acoustic and radiotelemetry studies. *Journal of Agricultural, Biological, and Environmental Statistics*.
- Vogel, D.A. 2004. Juvenile Chinook salmon radio-telemetry studies in the Northern and Central Sacramento-San Joaquin Delta 2002-2003. Final Report by Natural Resource Scientists, Inc. to National Fish and Wildlife Foundation, San Francisco, California.
- Vogel, D.A. 2006. Evaluation of Acoustic Telemetry Equipment for Monitoring Juvenile Chinook Salmon. Final Report by Natural Resource Scientists, Inc. to California Department of Water Resources, Sacramento, CA.
- U.S. Fish and Wildlife Service. 1996. Abundance and Survival of Juvenile Chinook Salmon in the Sacramento-San Joaquin Estuary. Annual progress report. Sacramento San Joaquin Fishery Resource Office, Stockton, CA.
- Williams, B.K., J.D. Nichols, M.J. Conroy. 2002. Analysis and management of animal populations. Academic Press, San Diego, California.

Appendix A: North Delta Residual Flows – A Regional Perspective

In this section we develop a series of simple statistical relations that surprisingly accurately predict the net flows in the north Delta that we hope to use as the hydrodynamic underpinning of simplified salmon outmigration management tools. As we will see these relations are fairly tight and stationary, at least over the ten years of data used in the analysis, which is directly related to the geometry of the North Delta. First, then, we begin this appendix with a basic discussion of the north Delta geometry and hydraulics as an introduction to the net flow relations.

(A.1) Physical setting and Scope

The temporal and spatial distribution of discharges, transport, mixing characteristics and residence times within the north Delta are primarily a function of the interaction between the Sacramento River inputs and the tides within a geometric framework characterized by a network of narrow, rip-rapped, prismatic channels. With a few notable exceptions, the north Delta is a network (Figure 1.1) of armored (Figures 1.2-1.5), prismatic canals (Figures 1.6-1.9) whose physical characteristics have been optimized, through anthropogenic manipulation, to control flooding of adjacent lands and to convey water to the central Delta, where it is subsequently exported to Southern California from the SWP and CVP pumping facilities in the southern Delta. Except for the epic dredging operation that occurred in the lower Sacramento River near Decker Island in the 1920-30's, where it is "traditionally said" that more material was removed than in the construction of the Panama Canal (Kelley, 1989; pg 281), the current north Delta geometry evolved from channel alignments that were locked in place when the levees were first constructed.

The distribution of discharges throughout the north Delta are controlled by water surface slopes (barotropic pressure gradients), that interact with physical factors such as the channel width, channel capacity (cross sectional area) and the channel roughness. These physical factors are collectively known as the conveyance,

$$K = \frac{A * R^{2/3}}{n} , \quad (1)$$

which is a measure of the carrying capacity, where A is the cross sectional area, $R = \frac{WP}{A}$ is the hydraulic radius, WP is the wetted perimeter, and n is the Manning's friction coefficient. The conveyance relates the total discharge, Q , in a given channel section to the water surface slope, $\frac{\partial \zeta}{\partial x}$, through the simple and well know relation (Chow, 1959)

$$Q = K \sqrt{\frac{\partial \zeta}{\partial x}} = \frac{A * R^{2/3}}{n} \sqrt{\frac{\partial \zeta}{\partial x}} \quad (2)$$

where ζ are water level fluctuations, x is the along-channel direction and ∂ is the partial derivative.

In most cases, the conveyance of channels in the north Delta (and elsewhere) have been slowly and significantly increased to enhance the flood control and water delivery aspects of the system through increases in cross sectional area and through reductions in channel

roughness (removal of tules, bushes, trees etc. from banks). This process has significantly reduced within-channel bathymetric variability throughout the north Delta over time. Channels in the north Delta are, for the most part, confined behind levees that are armored with rock (Figures 1.2-1.4) and thus the geometry of most north Delta channels are functionally somewhere between a concrete-lined canal and a natural river channel. For example, Sutter and Steamboat Sloughs, are not “sloughs” in the traditional sense, but are leveed and riprapped channels (Figure 1.5) that significantly contribute to the overall conveyance in the north Delta. In fact, at high Sacramento River flow rates, roughly half of the discharge passing Freeport travels down Sutter and Steamboat Sloughs. The name “Slough”, in this case, is purely a historical artifact, not a description of the current conditions there. Despite significant spatial differences in channel capacity, the stability of the flow relations derived in this paper suggest the conveyance within individual reaches and the conveyance between reaches have been stable over at least the last 10 years. Thus, processes such as changes in channel alignments, and changes in cross sectional areas and bed roughness due to sedimentation and erosion have been significantly constrained by levees - individual channel capacities have remained nearly static because a change in the conveyance in any single channel would change the *distribution* of flows among all the channels in the north Delta which we do not see (section A.4).

(A.2) Flow splits – Qualitative description/motivation

In this appendix we examine the impacts of DCC gate operations on three main flow paths in the north Delta based on long-term (> 10 years) data collected at six sites in the north Delta (Figure 1.1): (1) the Sutter-Steamboat corridor (SS), (2) the Cross Delta Transfer flow, which we alternatively refer to as the Mokelumne system, encompassing the combined flow in Georgiana Slough and the north and south forks of the Mokelumne River, and (3) the Sacramento River, which is, for the purposes of this appendix, separated into three distinct reaches: (1) the reach above Sutter Slough whose flow is represented by the discharge measured at Freeport, (2) the Vorden reach, between Steamboat Slough and the Delta Cross Channel whose flow is characterized by the discharge measured above the DCC (Station WGA) and (3) the Isleton reach whose flow is characterized by the discharge measured below Georgiana Slough (Station WGB).

The DCC is an important “feature” of the north Delta’s hydraulic landscape. As we will see, gate operations can significantly change the net discharges in all of the channels in the north Delta, including channels upstream of the DCC. For example, even though the Sacramento River inputs dominate the variability in the roughly two-year period shown in Figure 2.1A, discharges measured in all of the reaches shown are virtually completely coherent with the discharges measured in the Sacramento River at Freeport. However, the effects of DCC gate operations are significant and obvious when the discharge in each reach is plotted as a percentage of the flow at Freeport (Figure 2.1B), particularly at low Sacramento River discharges. As expected, when the gates are open more water flows into the central Delta, the so-called delta transfer flow, XGEO (XGEO: ~45% of the Freeport flow compared to ~20% when the gates are closed) (Figure 2.1C) and less water flows down the Sacramento River in the Isleton reach (20% of the Freeport flow when the gates are open and 40% of the Freeport flow when closed). When the gates are open, less water flows through Sutter and Steamboat Sloughs (SS: ~35% of the Freeport flow when the gates are open versus 45% of the Freeport Flow when they are closed) and slightly more water flows through the Vorden Reach of the Sacramento River (65% of the Freeport flows when open, 55% when

closed) (Figure 2.1B). Interestingly, the combined net flows down Sutter and Steamboat Sloughs, at high discharge, are only slightly less than the net flows in Sacramento River's Vorden reach. Thus, Sutter and Steamboat Sloughs combine to create a significant north Delta conveyance pathway, where nearly half the water that flows past Freeport passes through Sutter and Steamboat Sloughs at high water (Figure 2.1B). Moreover, when the gates are open and the overall Sacramento River inputs are low, only about 30% of the water that passes Freeport is actually conveyed through the Sacramento River's Isleton reach (Figure 2.1B). When the gates are closed, only 30% of the water flowing in the Vorden reach is diverted into the central Delta through Georgiana Slough. In other words, under low flow conditions, when the gates are open, the combined flow down Sutter, Steamboat, and Georgiana Sloughs and the DCC takes roughly 70% of the total amount of water passing Freeport. Therefore, during low flow conditions, the Sacramento River *is not* the primary conveyance channel: the combined flow in both Sutter and Steamboat Sloughs and the Cross Delta transfer flow exceed the flows in the Sacramento River's Isleton reach.

The preceding observations (Figure 2.1) *qualitatively* describe the effects of gate operations on the flows within the north Delta channel network and are presented to demonstrate the profound impact DCC gate operations have on the hydrodynamics of the north Delta and to illustrate the complexity of the distributions of flows among the north Delta channels. However, the record shown in Figure 2.1 is short (~2 years) relative to the data available (~10 years) and there is considerable variability in the impacts that DCC gate operations have on the flow distributions in the north Delta (see, for example, Figure 2.1B). The remainder of this appendix seeks to quantify these relations on the complete period of record (~10 years of data). In the end, we find the north Delta flows are predictable, stable (because the geometry of the north Delta changed very little over this period as discussed above) and follow simple relations that are functions of the Sacramento River flow rates and DCC gate position. After a brief discussion of temporal variability in the hydrodynamics of the north Delta, we develop a set of net flow relations for the key conveyance pathways shown in Figure 2.1.

(A.3) Temporal variability

Water level time-series measured in the north Delta, and, the concomitant changes in discharge, respond at a variety of timescales (Figures 3.1-3.4). Timescales vary from high frequency episodic events, such as water level and flow transients (~ hours) that occur because of changes in DCC gate position (Figure 3.1), short lived (daily timescale) changes in discharge due to strong wind events (Figure 3.2) to low frequency modes of variability, such as changes in atmospheric pressure (Figure 3.3), the spring/neap and tropic/equatorial cycles (red line in Figure 3.4B,C,D), and responses to seasonal and inter-annual changes in river flows (Figure 3.4A). The flows in the north Delta are dominated, at seasonal timescales, by the Sacramento River inputs, and, when the Sacramento River flows are low, throughout the summer to early winter period, the tides have a remarkably strong influence, even though the north Delta (e.g. DCC) is roughly 75 miles from the Golden Gate, the source of tidal forcing in the bay/Delta system.

There is an important interplay between the hydrologic inputs and tidal forcing. In general, tidal forcing varies spatially with proximity to the ocean (with a couple of notable exceptions discussed below), seasonally and between years depending on the river inputs. Sacramento River flows vary with rainfall, snowmelt, agricultural withdrawals and returns and reservoir

operations. Variations in river flows are driven by a net barotropic pressure gradient (water surface slopes) where the large uncontrolled Sacramento River discharges are driven by increases in water levels and water surface gradients. Lower water levels and their concomitant relatively weaker water surface gradients, typical of low flow summertime conditions; allow tidal variations to propagate far upstream. For example, during very low flow periods, tidal water level oscillations can propagate well past the city of Sacramento. The gage at Freeport, ~12 miles downstream of the city of Sacramento (used in this appendix as the upstream Sacramento River watershed boundary condition) is very near the upstream limit of the tides affect on water levels. These seasonal variations and inter-annual variability in tide-induced changes in water levels are an important aspect of the aquatic environment in the Delta.

Tidal filters

Time series data are often separated into tidal and residual timescale components (Walters and Heston, 1982; Cheng and Gartner, 1984; Wang and Cheng, 1993), as is shown in [Figure 3.4A](#), even though, in reality, temporal variability in hydrodynamic responses result from a variety of interacting process that can, and do, occur over a broad range of timescales. For example, non-linearities in the equations of motion (Signell and Geyer, 1991; Parker, 1991; Speer and others, 1991) guarantee that forcing mechanisms that occur at different time scales will interact. Fortunately, however, many surface water systems, like the Delta, are weakly non-linear (Cheng and others, 1987), which implies that energy occurring at a particular timescale is only minimally transferred to other timescales; a partial justification for separating data into tidal and residual, or net, components. However, a more pragmatic and powerful justification for this time separation is a distinct “trough” in energy that occurs in frequency space between the tidal and residual timescales in nearly every physical variable one can measure in this estuary ([Figure 3.5](#)). Despite the physical realities inherent in the equations of motion, the separation in time between tidal and residual components has been used as a useful conceptual paradigm for decades in this estuary (Walters, 1982; Walters and Gartner, 1985; Monismith and others, 1996; Tobin and Burau, 1995; Warner and others, 1997; Lopez and others, 2006; Lucas and others, 2006) and in estuaries throughout the world (Jay and others, 1997): we continue to use this conceptual abstraction.

(A.4) Net flows

In this section we develop a set of simple relations, based on the net flows at Freeport and DCC gate position, which describe, and, ultimately allow us to predict, the net flow distributions among the channels in the north Delta, as specified in [Figure 1.1](#). These relations are surprisingly accurate descriptions (>93 % of the variability) of the distributions of the tidally averaged flows within the north Delta and are intended, among other things, to form the hydrodynamic under-pining of simplified salmon outmigration management tools. We begin with a brief description of the data used to develop these relations, followed by discussions of how the data were conditioned and how the flow relations were developed. The flow relations for the so-called Delta transfer flow (XGEO) derived in this paper, based on ~11 years of data, are then compared to flow relations developed in the late 1960’s and 1970’s by DWR based on a handful of tidal cycle measurements. Finally, with the flow relations in hand, we systematically discuss the north Delta system response to changes in the Freeport flows and DCC gate operations.

(A.4.1) The Data

The relations developed in the following section are based on long term (~ 10 year data sets) discharge records collected at 5 station locations: Sacramento River @ Freeport (FPT), the Sacramento River above the DCC (WGA), the Sacramento River below Georgiana Slough (WGB), the Sacramento River at Rio Vista (RIO), and Threemile Slough (TMS) (see Figure 2.1). The combined net flows in Sutter and Steamboat Sloughs (designated SS) are computed as the difference in flow between the Sacramento River at Freeport and the Sacramento River above the DCC ($Q_{SS} = Q_{FPT} - Q_{WGA}$). In this paper, the so-called Delta Transfer Flow (XGEO) is computed as the difference between flows in the Sacramento River above the DCC (WGA) and the Sacramento River flows below Georgiana Slough (WGB) ($Q_{XGEO} = Q_{WGA} - Q_{WGB}$). The Delta Transfer Flows is therefore treated in a bulk fashion (the sum of flows in the DCC and Georgiana Slough). The way in which the Delta Transfer flow (XGEO) is distributed within the Mokelumne system and how these flows are exchanged into the central Delta is beyond the scope of this appendix.

(A.4.2) Data conditioning – Developing the net flow relations

Discharge or flow data collected in the Sacramento/San Joaquin River Delta is not measured directly but is a computed quantity based the calibration of an index velocity measurement. Index velocity measurements are made at 15-minute intervals using acoustic signals (sound) at fixed sites in the Delta, either by comparing time of travel differences in acoustic signals (an Ultrasonic Velocity Meter or UVM) or by using Doppler shifts of an acoustic signal of known frequency, as is used in horizontal Acoustic Doppler Current Profiler (HADCP) (Simpson and Oltmann, 1993; Simpson and Bland, 2000; Simpson, 2002). The index velocity is then calibrated to compute discharge based on a series of boat-mounted downward-looking ADCP measurements made over a complete tidal cycle at each location under a variety of hydrologic conditions (Ruhl and Simpson, 2005).

The raw, or as-computed discharge data, contains both tidal and residual, or net, components as can be seen in Figure 3.4 and as is described in section A3.1. In this section we are interested in developing relations for the net flows based on data collected at our fixed monitoring stations, and, thus, some sort of averaging process must be applied to the data. In this estuary, and, in estuaries throughout the world, two basic approaches have been used. One, based on a sequence of time-domain moving averages, the Godin filter (Godin, 1972), and the other based on a frequency-domain approach that uses a digital filter based on Fourier series expansions (a process shown schematically in Figure 4.1)(Walters and Heston, 1982). All tidal filters have an inherent frequency response which implicitly involves a compromise between signal attenuation (e.g. smoothing) and the ability to detect modes of variability near the cutoff frequency (Figure 4.2).

The Godin filter operates in the time-domain and consists of consecutively applying three moving averages to hourly data. Therefore, the 15 minute raw data collected at flow station locations throughout the Delta is first decimated to an hourly time-series before the Godin filter is applied. The first two moving averages use 24 data points and the third uses a 25-point average. The application of the 25-point average eliminates aliasing problems that can occur when strictly 24-point moving averages are applied to time series that contain signals with even multiples near, but not exactly at, 24 hours, such as the M2 partial tide (with a period of 12.42 hours), by far the largest of the partial tides in the bay and Delta (Cheng and

Gartner, 1984). Unfortunately, the frequency response of the Godin filter has the undesirable effect of attenuating variability in the 1-3 day range (Figure 4.2). In the case of the digital filter, the amplitude response is set by specifying a stop and pass frequency as is shown in Figure 4.2. The amount of ringing in the filtered result is directly related to how broad the filter's transition band is (e.g. the difference between the stop and pass periods). The amplitude response for the Godin filter has a very broad transition band, and, thus, attenuation occurs instead of ringing when this filter is applied. For the purpose of this appendix, we are most interested in the filter response near periods when the DCC gates change positions or on either side of a data gap. Step function changes in system response, such as when the DCC gates are operated, or near a data gap are notoriously difficult to represent in frequency space (e.g. the summation of sinusoids). Tidal filters with a narrow transition band "ring" near step function changes. To illustrate the problem, fictitious data gaps were placed in a discharge record collected in the Sacramento River upstream of the DCC (station WGA). This record was specifically chosen because it contains a significant DCC gate operations signal (Figure 4.3A). Ringing at the "edges" of the step function changes at both the data gaps (Figure 4.3AA-CC) and during periods when the DCC gates were operated are clearly evident in the net flows computed using a digital filter with a 30 hour pass period and 40 hour stop period. Digital filters with stop and pass periods of 30 and 40 hours have been applied in this estuary to remove tidal signals for at least two decades (Walters and Heston, 1982). Oscillations can be particularly egregious near gaps, which would introduce significant noise into the net flow time series used to develop the flow relations in this appendix. The Godin filter was compared to the digital filter described in Walters and Heston 1982, using a variety of stop and pass period combinations in search of a filter that minimized oscillations near gaps. The ability of the various filters to "capture" the discharge response to gate operations is shown in Figure 4.4, and for data gaps in Figure 4.5. Although the Godin filter is not ideal for capturing modes of variability with periods of 1-3 days (Figure 4.2), it does a great job of minimizing oscillations near gate operations as is shown in Figure 4.5, and was therefore selected as the filter of choice for this application, even though, in theory we could have designed a digital filter that would have mimicked the frequency response of the Godin filter. Still, when the Godin filter is used, roughly 1.5 days on either side of the step function change (or data gap) (Figures 4.4 and 4.5) must be removed from the filtered time series to account for the attenuation associated with the Godin filter (Figure 4.2).

Once the time series were filtered using the Godin filter, data gaps were removed and the attenuation near gaps and near periods where the DCC gate changed positions were removed to generate a "clean" time series for the development of the flow relations. A series of data masks were used to unambiguously separate the discharge time series into (1) DCC open and (2) DCC closed time series and to (3) remove filter attenuation/ringing associated with both changes in gate operations and data gaps. Each time series used to develop the flow relations was multiplied by this series of masks. Each mask was created to retain data by multiplying by unity and removing data from consideration by multiplying by zero. The following series of masks was developed: one for gaps, one for isolating data collected during DCC closed periods and one for isolating data collected during DCC open periods. So, for example, the time series used to develop flow relations for the discharge at the Sacramento River above the DCC (Station WGA) involves the product of a series of masks and the original Godin filtered time series as follows,

$$\bar{Q}_{WGA}^{open}(t) = M_{DCC}^{open}(t)M_{WGA}^{gap}(t)M_{FPT}^{gap}(t)\bar{Q}_{WGA}(t) \quad (\text{for DCC gates open}) \quad (16)$$

$$\bar{Q}_{WGA}^{cls}(t) = M_{DCC}^{cls}(t)M_{WGA}^{gap}(t)M_{FPT}^{gap}(t)\bar{Q}_{WGA}(t) \quad (\text{for DCC gates closed}) \quad (17)$$

where $\bar{Q}_{WGA}^{open}(t)$ is the desired “clean” (e.g. all of the attenuated signals removed) time series of Godin filtered discharges at station WGA during DCC gate open conditions, $M_{DCC}^{open}(t)$ is a mask that contains 1’s during periods when the gates are open, zeros are placed in this time series 1.5 days before the gates are closed and 1.5 days after they are opened;

$M_{WGA}^{gap}(t)$ includes 1’s everywhere in the time series where viable data exists, zeros are placed in this time series 1.5 days before a gap and 1.5 days after a gap; $M_{FPT}^{gap}(t)$ contains 1’s everywhere in the Freeport discharge time series where viable data exists, zeros are placed in this time series 1.5 days before a gap and 1.5 days after a gap. Every discharge time series was multiplied by $M_{FPT}^{gap}(t)$ to register all of the time series to the same time base; and finally, $\bar{Q}_{WGA}(t)$, is the original Godin filtered time series. A year-long example of the original time series, filter masks, and resultant time series for station WGA during DCC gate opened conditions is shown in Figure 4.6. “Clean” DCC gates open and DCC gates closed time series are similarly generated for each of the other flow stations in this analysis.

Once each of the “clean” DCC gates open and DCC gates closed time series was generated, it was regressed against the Sacramento River flow at Freeport. Two models were fit to the data using commercially available curve fitting software, Tablecurve 2D:

(1) a linear model

$$Q_{RIO} = aQ_{FPT} + b \quad (18)$$

and (2) a simple non-linear model

$$1/Q_{RIO} = a + b/Q_{FPT} , \quad (19)$$

where Q_{FPT} , Q_{RIO} are the discharges at Freeport and at Rio Vista, respectively. Both models, equations 18,19, were fit to the remainder of the stations studied. Plots of the data, the curve fits, and regression coefficients are shown in Figures 4.7 to 4.12. Both models fit the data exceptionally well, with $R^2 > 0.93$, as is shown in table 4. The linear model fit the data exceptionally well over the mid-to-upper end of the discharge range at all stations.

Table 4 - Summary of north Delta discharge model parameters and Rsq.

Station	Open	Open	Open	Open	Open	Open	Closed	Closed	Closed	Closed	Closed	Closed
	linear	linear	linear	nonlinear	nonlinear	nonlinear	linear	linear	linear	nonlinear	nonlinear	nonlinear
	a	b	Rsq	a	b	Rsq	a	b	Rsq	a	b	Rsq
RIO	0.6824	-1900.17	0.982	-2.0748E-05	2.12408	0.98318	0.8574	-975.207	0.999	-7.64E-07	1.24	0.999416
SS	0.4492	-1668.638	0.984	-4.4815E-05	3.65423	0.979567	0.4801	-1252.639	0.996	-4.38E-06	2.46718	0.9984
WGA	0.5509	1666.194	0.989	1.4614E-05	1.27689	0.989449	0.5202	1235.9957	0.997	3.04E-06	1.64879	0.998624
WGB	0.2375	-287.8712	0.925	-2.3147E-05	4.86944	0.9248	0.3752	327.5638	0.996	2.84E-06	2.438109	0.99763
XGEO	0.3117	2016.0856	0.924	4.1552E-05	1.570164	0.93335	0.1424	976.5318	0.983	2.26E-05	4.7498	0.980995

The linear model was used because it is easy to implement and useful in analytical assessments of system response. The non-linear relation fits the data better at the lower end, for some stations (for example, stations XGEO, RIO, WGB). The non-linear model, [equation 19](#), was chosen because it naturally goes through the origin - our best guess at system response under extreme drought conditions. The distribution of net flows under very low flow conditions, however, are not likely to asymptote to zero as [equation 19](#) suggests due to tidal non-linearities (Parker, 1991; Speer and others, 1991). Nonetheless, a relationship that goes through zero is the best we can do in the absence of data collected at very low Sacramento River discharges.

The scatter of points about net flow relations shown in [Figures 4.7](#) and [4.12](#) is likely mostly due to variability caused by forcing mechanisms other than the Sacramento River flow rate and DCC gate operations such as non-linear tidal interactions (e.g. the spring/neap cycle), seasonal timescale and episodic meteorological events, and, at the DCC, nonlinear interaction between tides that independently propagate up the Mokelumne and Sacramento River systems. Scatter in these relations generally increases as one moves seaward, as the influence of the Sacramento River inputs decreases. For example, the net flow in Threemile Slough when the DCC gates are closed is completely uncorrelated ($R_{sq} = 0.000!$) with the Sacramento River flows at Freeport, for Freeport flow rates less than 60,000 cfs. As was noted by previous investigators in the 60's and 70's, the exchange through Threemile Slough is driven by water surface elevation differences between the Sacramento and San Joaquin Rivers which are virtually completely controlled by tidal non-linearities and meteorological forcings.

(A.4.3) Comparison to historical relations

The California Department of Water Resources began measuring and documenting the distribution of tidal and net flows in the north Delta at a variety of locations using standard river discharge techniques during the Great Depression, ~1929 (Bulletin 27, DWR). Measurements were made using anemometer-type (Price AA) velocity meters at 0.2 and 0.8 of the depth at 12-24 stations across the river section from a boat attached to a tag-line. Flow curves based on hourly measurements of the tidal discharges over roughly 30 hour periods were developed for each location. The net flow at each station was estimated graphically by summing the areas under the flow curves between tidal peaks, roughly 25 hours apart. Each data point on [Figures 4.13](#) and [4.14](#), is the result of 25 hourly measurements of the tidal discharge. These graphs represent a tremendous effort in the field. The following net flow relations

$$XGEO = 0.100*Q_{fpt} + 990 \quad \text{Closed} \quad (20)$$

$$XGEO = 0.222*Q_{fpt} + 2850 \quad \text{Open} \quad (21)$$

were published in 1962 (Bulletin 76, DWR) ([Figure 4.13](#)). These relations were updated in 1978 (Bulletin 27, DWR) ([Figure 4.14](#)) based on measurements made in the late 60's to mid-70's using virtually the same techniques used to collect the data in the Depression (e.g. boats attached to tag lines measuring current speeds using Price AA meters). The relations published in 1978 (Bulletin 27, DWR) are as follows

$$\text{XGEO} = 0.103 \cdot \text{Q}_{\text{fpt}} + 885 \quad \text{Closed} \quad (22)$$

$$\text{XGEO} = 0.293 \cdot \text{Q}_{\text{fpt}} + 2090 \quad \text{Open} \quad (23)$$

and, are similar to the relations derived in 1929 (Figure 4.15). The 1962 relations significantly under predict the Delta transfer flow, particularly at the higher Freeport flow rates, assuming there was no significant change in channel geometry within the north Delta system. As of this writing equations 22, 23 are used to compute the Delta transfer flow, XGEO, in the DAYFLOW program (ref DWR, <http://iep.water.ca.gov/dayflow/>) for water years 1956-2002. Beginning in water year 2003, the DAYFLOW program uses the sum of measured data collected at the DCC and in Georgiana Slough (<http://baydelta.wr.usgs.gov/>).

Figures 4.16-4.18 compare relations developed in this appendix (referred to as the 2004 relations) with the relations developed in 1978. DWR's 1978 relations, based on a handful of tidal cycle measurements collected using Price-AA and tag-line, compare remarkably well to the relations derived in this paper based on 10+ years of data computed using state-of-the-art acoustic measurement technologies and data processing techniques. The 1978 relations under predict the Delta Transfer flow by a maximum of about 1,000 cfs (Figure 4.17) or ~12% (Figure 4.18). The 1978 relations under predict the XGEO flows by a maximum of ~6%, if the linear equations are compared – a remarkable achievement for the DWR folks collecting the flow data in the late-1960's through mid 1970's, given the technology and data processing techniques available at the time the measurements were made.

References

Cheng, R. T., and J.W. Gartner, 1984, Tides, Tidal and Residual Currents in San Francisco Bay, California - Results of Measurements, Part 1, U.S. Geological Survey WRI Report 84-4339, 72 p.

Cheng R.T., S. Feng and P. Xi, 1987, On Lagrangian Residual Ellipse, in Lecture Notes on Coastal and Estuarine studies, J. van de Kreeke ed., Springer-Verlag, New York, pgs 102-113.

Chow, V.T., 1959, Open-channel hydraulics, McGraw-Hill, New York, pg. 680.

Godin, G, 1972, The Analysis of the Tides, University of Toronto Press, 264 pp.

Jay, D.A., W.R. Geyer, R.J. Uncles, J. Vallino, J. Largier, W.R. Boynton, 1997, A review of recent developments in estuarine scalar flux estimation, *Estuaries*, 20(2), p. 262-280.

Kelley, R. (1989) Battling the Inland Sea: Floods, Public Policy, and the Sacramento Valley, University of California Press, Berkeley, CA, USA, pp. 394.

- Lopez, C.B., Cloern, J.E., Schraga, T.S., Little, A.J., Lucas, L.V., Thompson, J.K., and Burau, J.R., 2006, Ecological values of shallow-water habitats: Implications for the restoration of disturbed ecosystems: *Ecosystems*, v. 9, p. 422-440. ([on-line abstract of journal article](#))
- Lucas, L.V., Sereno, D.M., Burau, J.R., Schraga, T.S., Lopez, C.B., Stacey, M.T., Parchevsky, K.V., and Parchevsky, V.P., 2006, Intratidal variability of water quality in a shallow tidal lagoon: Mechanisms and implications: *Estuaries and Coasts*, v. 29, p. 711-730. ([on-line abstract of journal article](#))
- Monismith, S.G., J.R. Burau, and M. Stacey, 1996, Hydrodynamic transport and mixing processes in Suisun Bay, Hollibaugh, J.T., editor, *San Francisco Bay: The ecosystem*, San Francisco, Pacific Division, American Association for the advancement of science, p.123-153.
- Parker, B.B., 1991, The Relative Importance of the Various Nonlinear Mechanisms in a Wide Range of Tidal Interactions, in *Tidal Hydrodynamics*, ed. B.B. Parker, pp. 521-543, Wiley Interscience.
- Ruhl C.A. and D.H. Schoellhamer, 1999, Time series of suspended-solids concentration in Honker Bay during water year 1997, SFEI. 1999. 1997 Annual Report: San Francisco Estuary regional Monitoring Program for Trace Substances. San Francisco Estuary Institute, Richmond, CA.
<http://www.sfei.org/rmp/1997/c0304.htm>
- Ruhl, C. A., Simpson M.R.,(2005) Computation of Discharge Using the Index-velocity Method in Tidally Affected Areas , [SIR 2005-5004](#)
- Signell R.P. & Geyer W.R. (1991). Transient eddy formation around headlands. *J. Geophys. Res.* 96(C2):2561-75.
- Simpson, M.R. and Oltmann, R.N., (1993). Discharge-Measurement System Using an Acoustic Doppler Current Profiler with Applications to Large Rivers and Estuaries, [USGS Water-supply Paper 2395](#), 32p.
- Simpson, M.R. and Bland, R., (2000). Methods for Accurate Estimation of Net Discharge in a Tidal Channel, [IEEE Journal of Oceanic Engineering](#), Special Issue on Current Measurement Technology.
- Simpson, M.R. (2002). Discharge Measurements Using a Broad-band Acoustic Doppler Current Profiler, [OFR 2001-1](#) also published in Chinese.
- Speer, P.E., D.G. Aubrey, and C.T. Friedrichs, 1991, Nonlinear hydrodynamics of shallow tidal inlet/bay systems, in *Tidal Hydrodynamics* edited by Bruce B. Parker, John Wiley and Sons, 883 pg.
- Tobin, A., Schoellhamer, and J.R. Burau, 1995, Suspended-solids flux in Suisun Bay,

California, In: Water Resources Engineering edited by W.H. Espey and P.G. Combs, proceedings of the ASCE sponsored first international conference on water resources engineering, San Antonio, Texas, August 14-18, 1995, pp. 1511-1515.

Walters, R.A., and J.W. Gartner, 1985, Subtidal sea level and current variations in the northern reach of San Francisco Bay, *Estuarine, Coastal and Shelf Science*, v.21, p. 17-32.

Walters, R.A. and C. Heston, 1982, Removing tidal-period variations from time-series data using low-pass digital filters, *Journal of Physical Oceanography*, V.12, No.1. pp. 112-115.

Walters, R.A., 1982, Low-frequency variations in sea level and currents in South San Francisco Bay, V.12, No.7, pp.658-668.

Wang J., and R.T. Cheng, (1993) On low-pass digital filters in oceanography, *Acta Oceanologica Sinica*, (12)2, pp. 183-196.

Warner J.C., D.H. Schoellhamer, J.R. Burau, 1997, A sediment transport pathway in the back of a nearly semi-enclosed subembayment of San Francisco Bay, California, In: environmental and coastal hydraulics: Protecting the aquatic habitat, edited by: Wang S.Y. and T. Carstens, proceeding of the 27th Congress of the International Association of Hydraulic Research, August 10-15, 1997, San Francisco, California. pg. 1096-1101.

Appendix A: North Delta Residual Flows - Figures

(A.1) Physical Setting and Scope

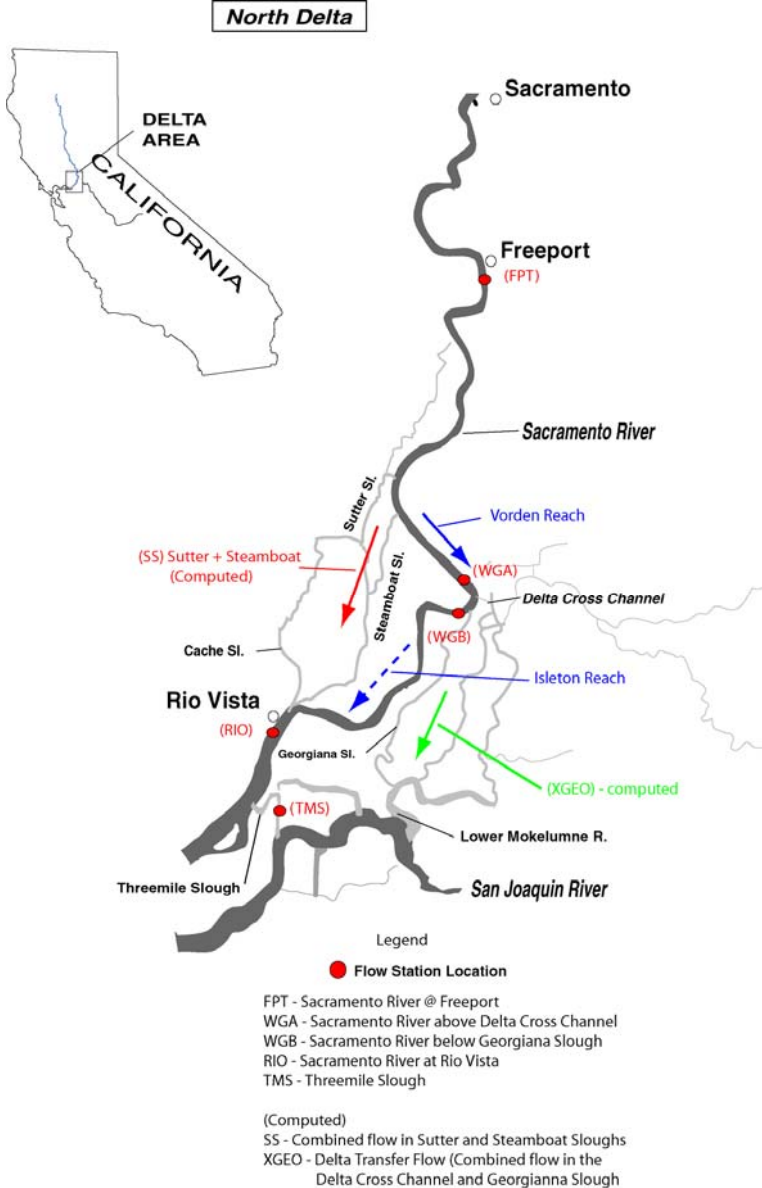


Figure 1.1 – Map of north Delta study area, flow station names and locations and a schematic of the three main flow paths in the north Delta examined in this paper: the Sutter steamboat corridor (SS, red arrow), (2) the Cross Delta Transfer flow (XGEO, green arrow), and (3) the mainstem Sacramento River, which is separated into three distinct reaches: (1) the reach above Sutter slough whose flow is represented by the discharge measured at Freeport, (2) the Vorden reach (Solid blue arrow), between steamboat slough and the Delta Cross Channel whose flow is characterized by the discharge measured above the DCC (Station WGA) and (3) the Isleton reach (Dashed blue arrow) whose flow is characterized by the discharge measured below Georgiana Slough (Station WGB).



Figure 1.2 – Photograph of the Sacramento River at station WGA. Flow monitoring equipment is mounted on the pilings shown.



Figure 1.3 – Photograph of the Sacramento River at station WGB. Flow monitoring equipment is mounted on the piling shown.



Figure 1.4 – Photograph of Threemile Slough: station TMS. Flow monitoring equipment is mounted on the piling shown.



Figure 1.5 – Photograph of the USGS flow station in Sutter Slough. Flow monitoring equipment is mounted on the pump stand shown.

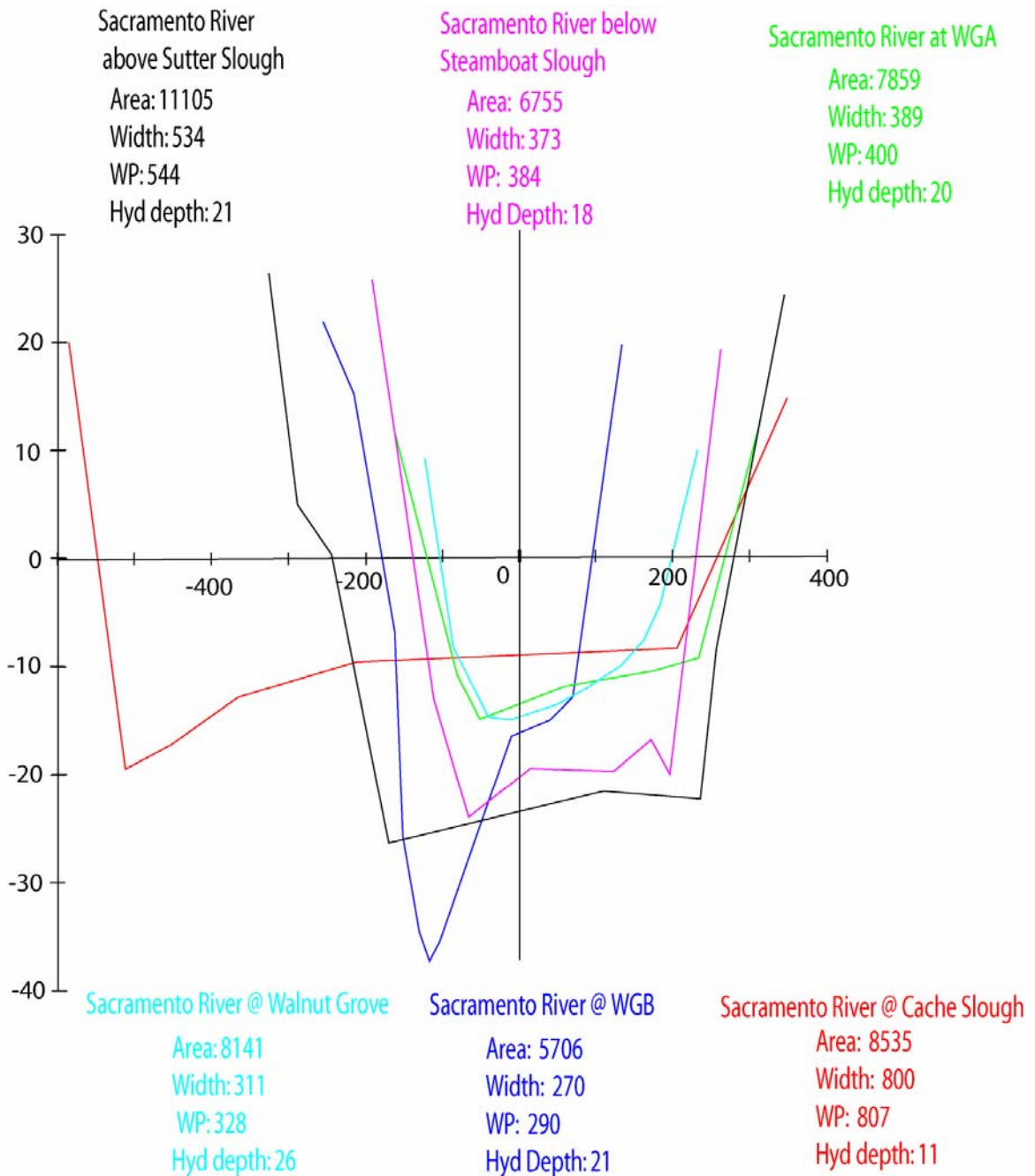


Figure 1.6 – Representative Sacramento River cross sections obtained from a Cross Section Development Program developed by DWR to generate numerical model geometry for DSM2 (<http://modeling.water.ca.gov/delta/models/dsm2/tools/csdp/index.html>). (See figure xx for cross section locations). All cross sections are referenced to NGVD. Cross sectional areas (A) are in feet²; top width in feet; Wetted perimeter (WP) in feet; Hydraulic depth = WP/A , in feet.

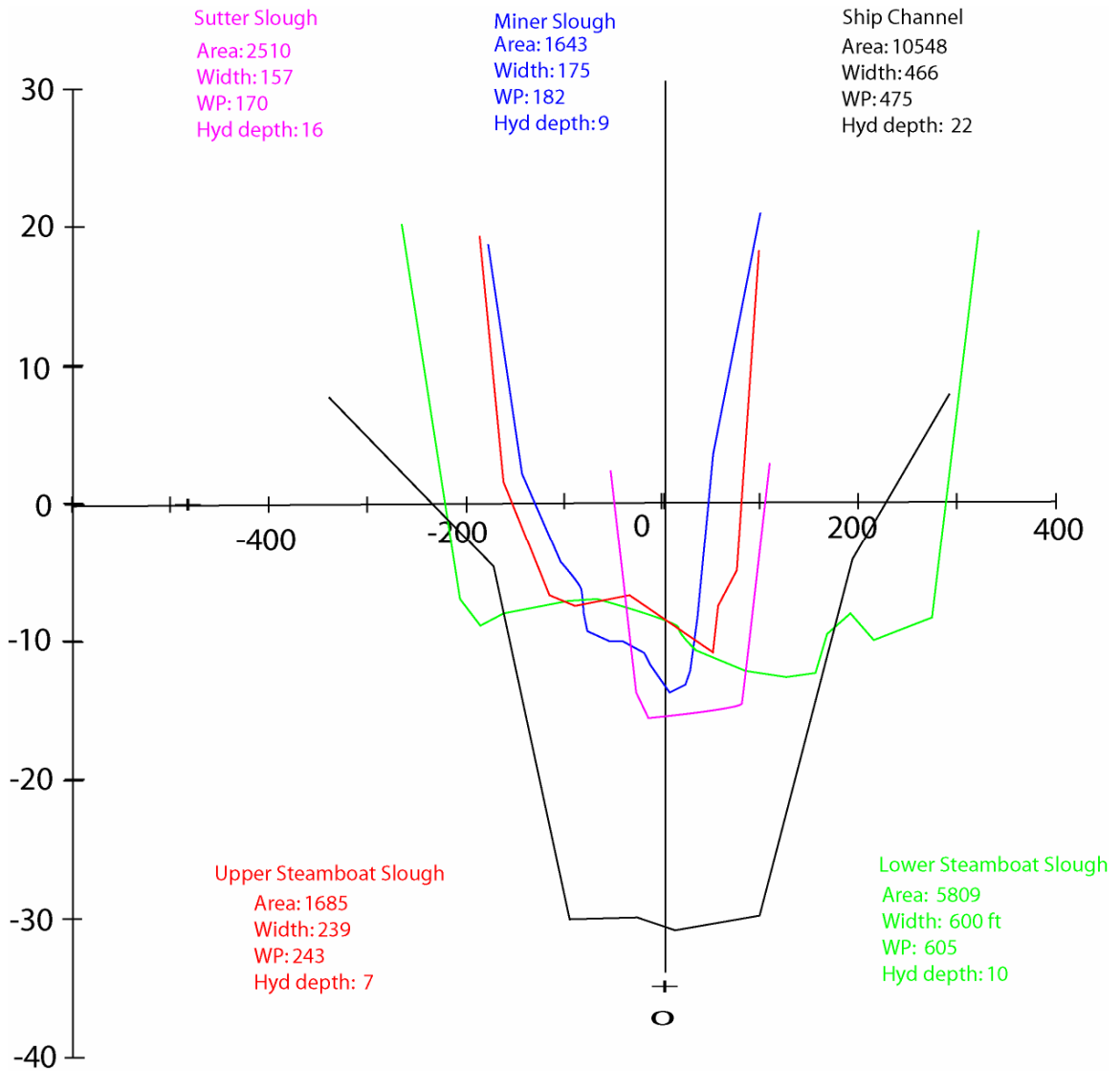


Figure 1.7 – Representative side slough and Ships channel cross sections obtained from a Cross Section Development Program developed by DWR to generate numerical model geometry for DSM2 (<http://modeling.water.ca.gov/delta/models/dsm2/tools/csdp/index.html>). (See figure xx for cross section locations). All cross sections are referenced to NGVD. Cross sectional areas (A) are in feet²; top width in feet; Wetted perimeter (WP) in feet; Hydraulic depth = WP/A , in feet.

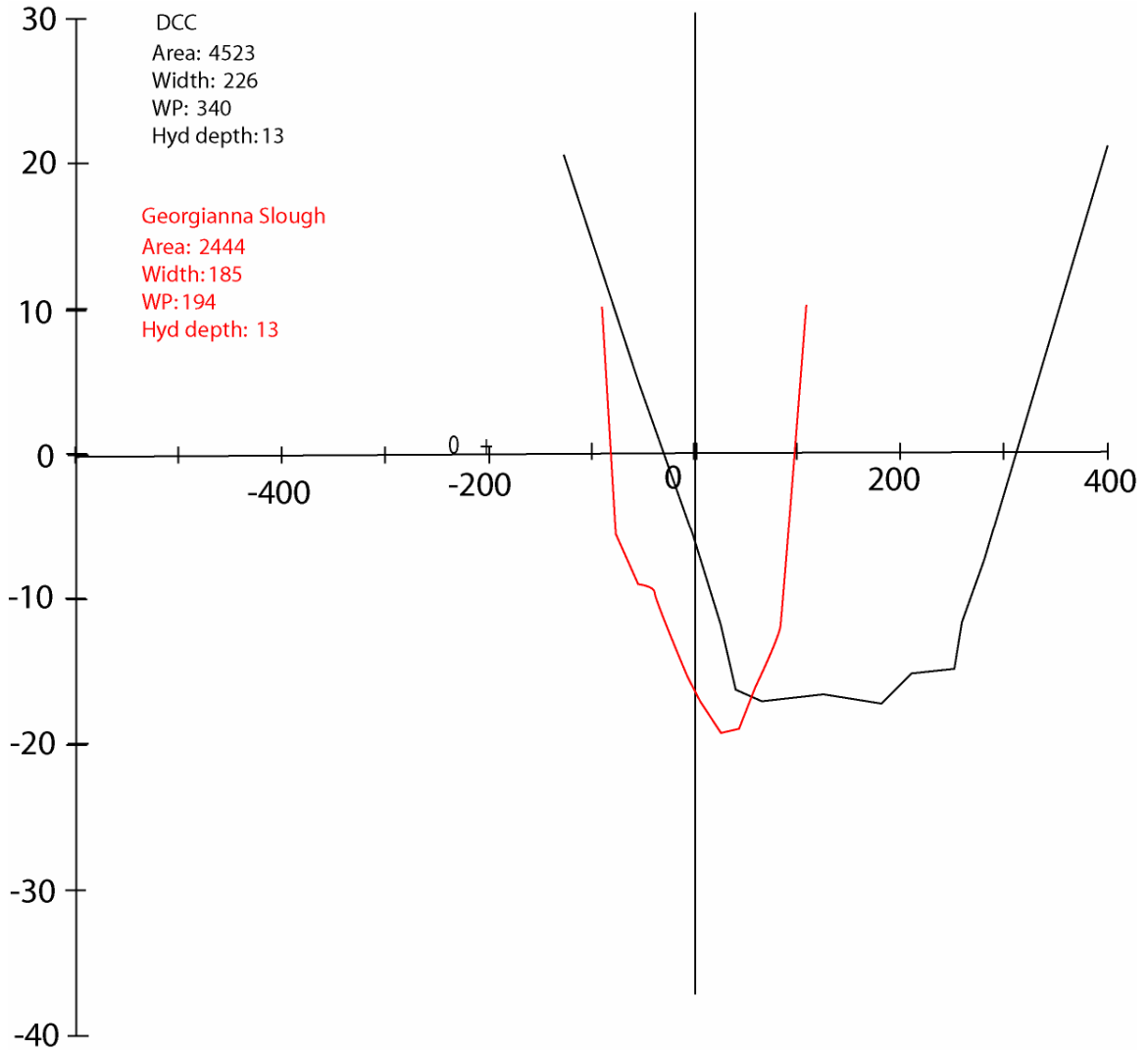


Figure 1.8 – Representative cross sections for the DCC and Georgianna Slough obtained from a Cross Section Development Program developed by DWR to generate numerical model geometry for DSM2 (<http://modeling.water.ca.gov/delta/models/dsm2/tools/csdp/index.html>). (See figure xx for cross section locations). All cross sections are referenced to NGVD. Cross sectional areas (A) are in feet²; top width in feet; Wetted perimeter (WP) in feet; Hydraulic depth = WP/A, in feet.

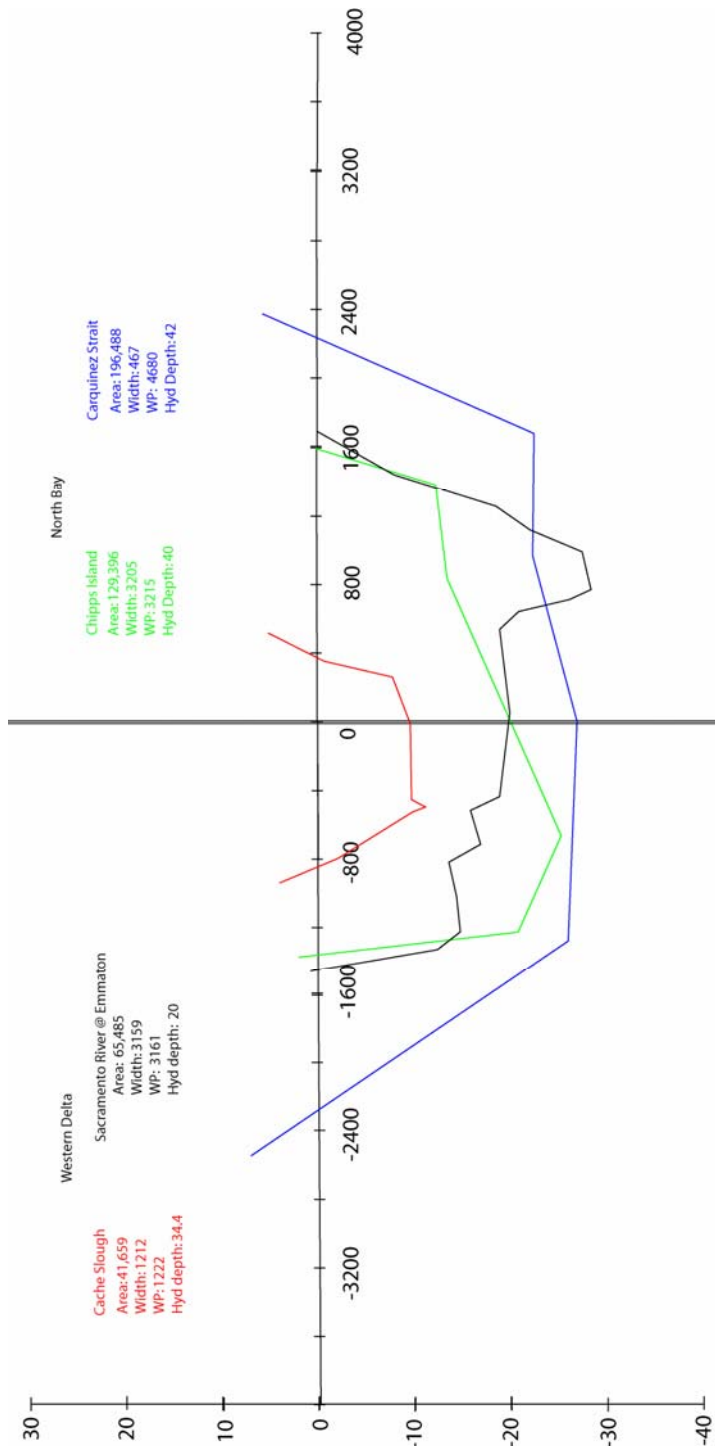


Figure 1.9 – Representative cross sections for the Western Delta and North Bay obtained from a Cross Section Development Program developed by DWR to generate numerical model geometry for DSM2 (<http://modeling.water.ca.gov/delta/models/dsm2/tools/csdp/index.html>). (See figure xx for cross section locations). All cross sections are referenced to NGVD. Cross sectional areas (A) are in feet²; top width in feet; Wetted perimeter (WP) in feet; Hydraulic depth = WP/A, in feet.

(A.2) Flow splits – Qualitative description/motivation

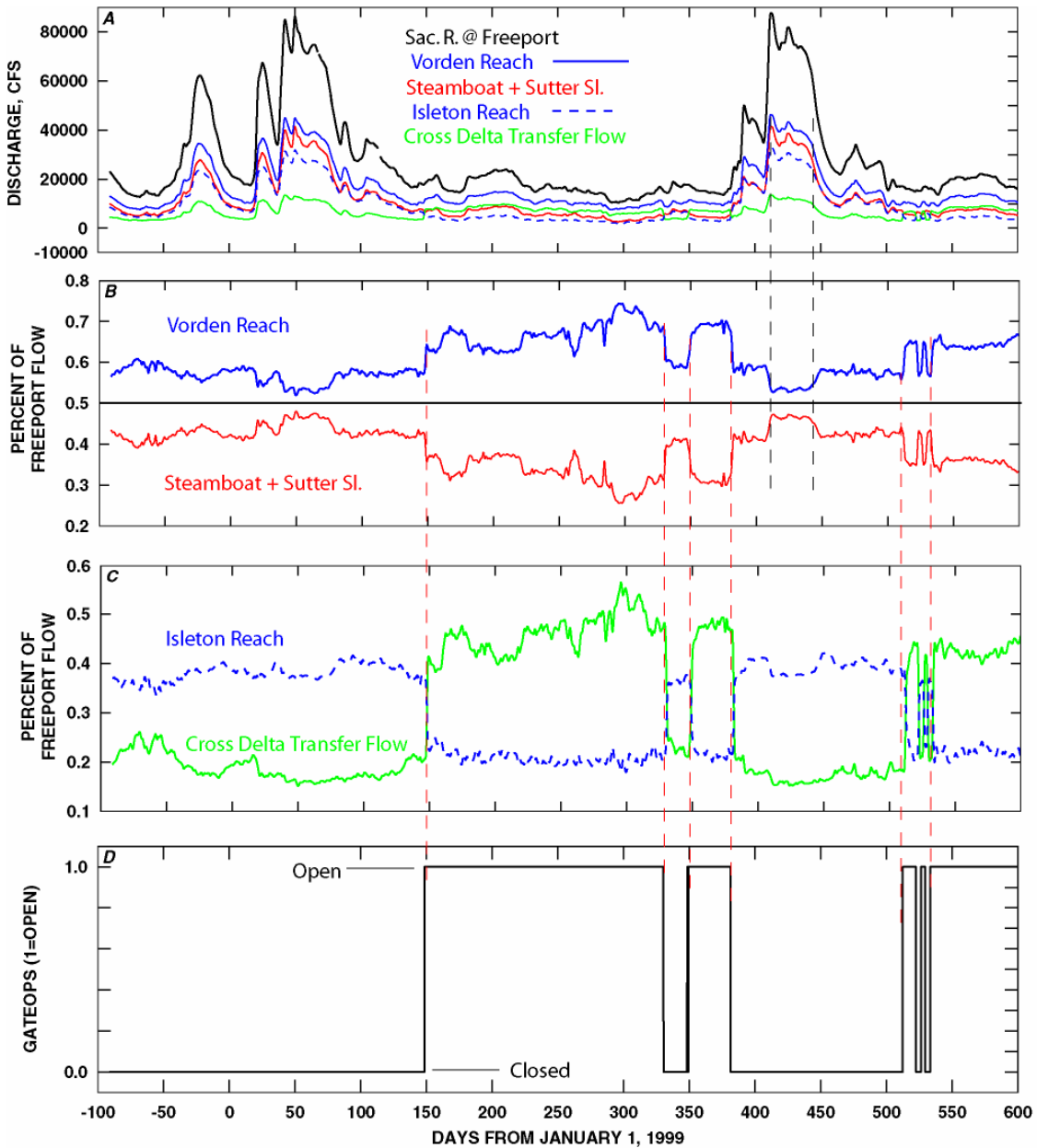


Figure 2.1 – Time series plots of (A) discharge for the Sacramento River @ Freeport, (black) , Sacramento River above the Delta Cross Channel (solid blue), the combined flow down steamboat and sutter sloughs (red), the Sacramento River below Georgiana Slough (dashed blue), the Cross Delta transfer flow (green), (B) the percentage of Freeport flow in the Sacramento River above the DCC (blue) and in Sutter and Steamboat Slough (red), (C) the percentage of flow in the Sacramento River below Georgiana Slough (dashed blue) and in the Cross Delta Transfer flow (green), (D) Delta Cross Channel Gate operations.

(A.3) Temporal Variability

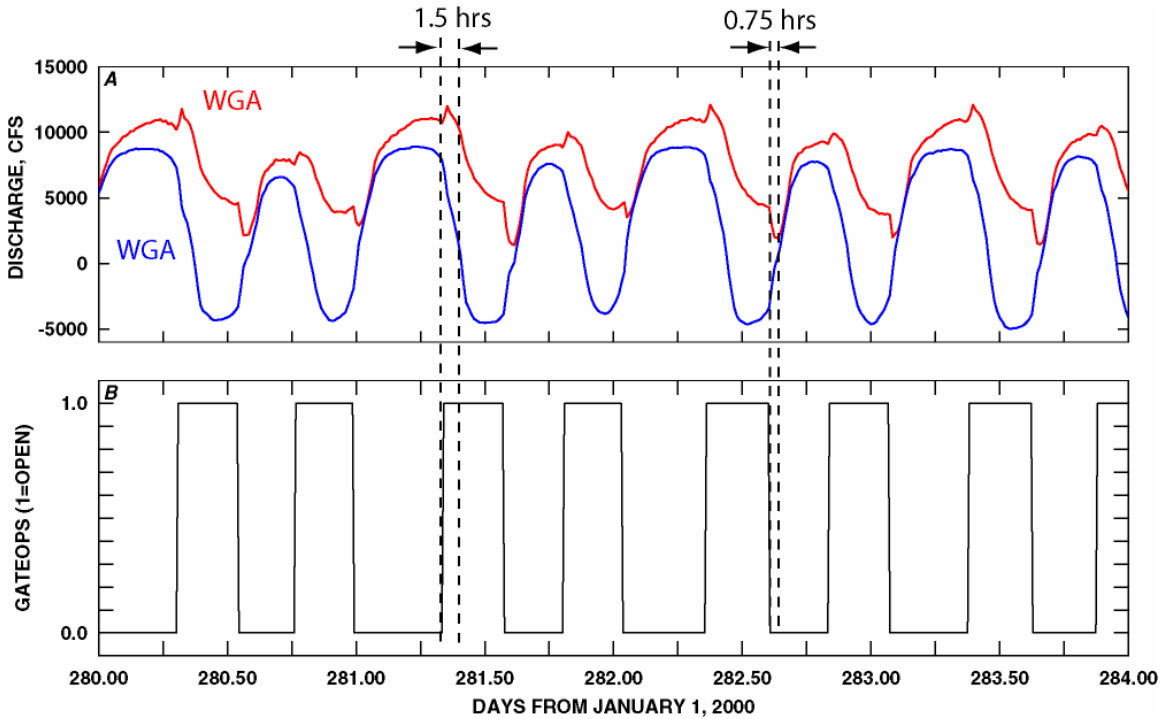


Figure 3.1 – Time series plots of (A) discharge in the Sacramento River above the DCC (red: station WGA) and in the Sacramento River downstream of Georgiana Slough (blue: station WGB), (B) DCC gate operations where 0 is closed and 1 is open. Panel (A) is an example of high frequency transients (\sim hour) that occur in discharges measured on the Sacramento River near the Delta Cross Channel during both flood and ebb tides. The transient response upstream of the DCC is fairly dramatic (changes on the order of 2300 cfs) with a weak response downstream of Georgiana Slough.

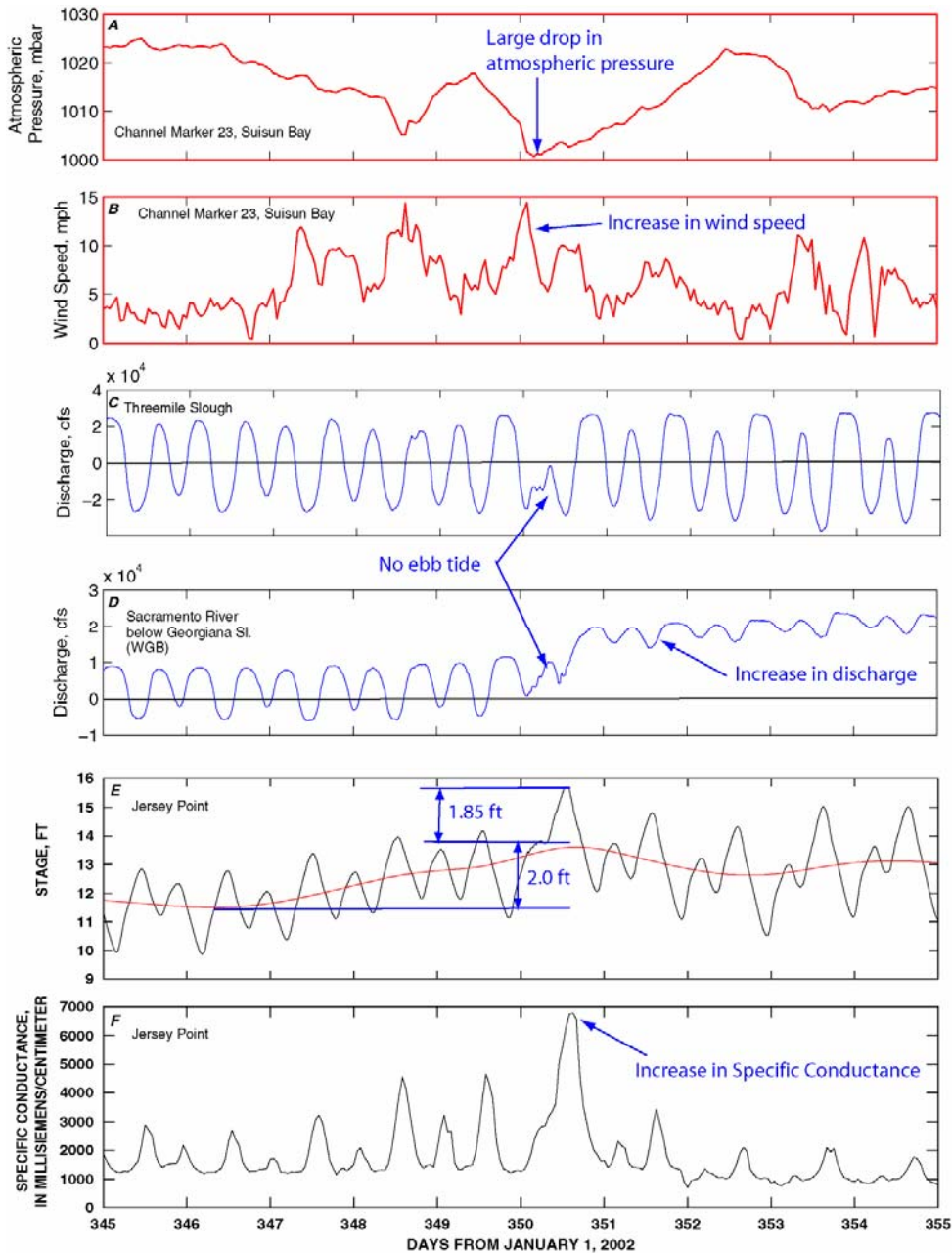


Figure 3.2 – Time series plots of (A) atmospheric pressure measured at channel marker 23 in Suisun Bay, (D) Wind speed measured at channel marker 23 in Suisun Bay, (C) discharge in Three mile Slough, (D) Discharge in the Sacramento River below Georgiana Slough (WGB), (E) Stage (water level) and (F) specific conductance measured at Jersey Point on the San Joaquin River. The large drop in atmospheric pressure (A) and sustained winds (B) that occurred on calendar day 350 increased mean water levels in the Delta by about 2 feet (E) causing salinity to intrude into the Delta from the Bay and a spike in specific conductance at Jersey point. The drop in atmospheric pressure on day 350 was immediately followed by the passage of a large storm which brought significant precipitation (not shown) to northern California which was followed by run-off that was measured in the Sacramento River below Georgiana Slough (station WGB).

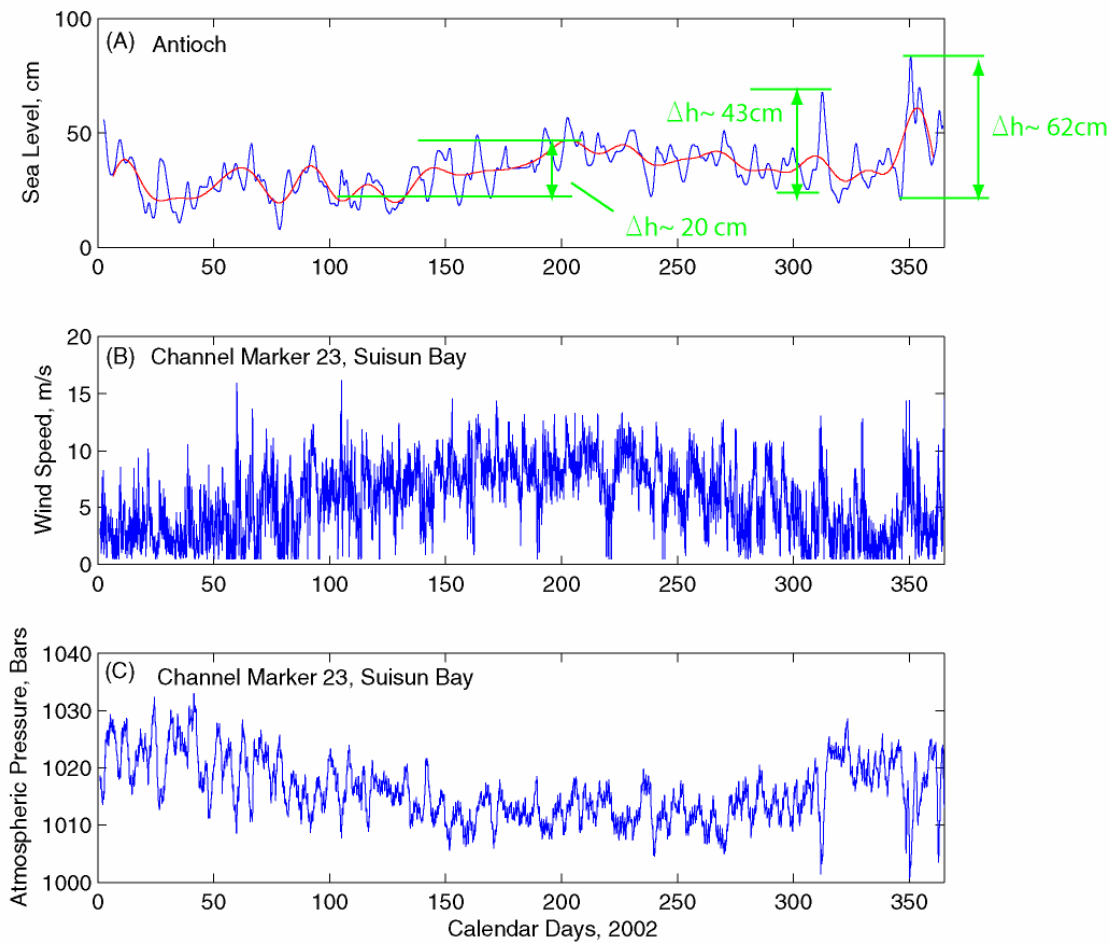


Figure 3.3 – Time series plots of (A) sea level at Antioch, (B) wind speed and (C) atmospheric pressure measured at channel marker 23 in Suisun Bay. Mean water levels in the Delta change inversely with atmospheric pressure on an annual cycle due to yearly low frequency changes in atmospheric pressure. Water levels also respond to episodic changes, usually rapid drops, in atmospheric pressure as is shown by a $\sim 43 \text{ cm}$ rise on day 305 and a rise of $\sim 62 \text{ cm}$ on day 350.

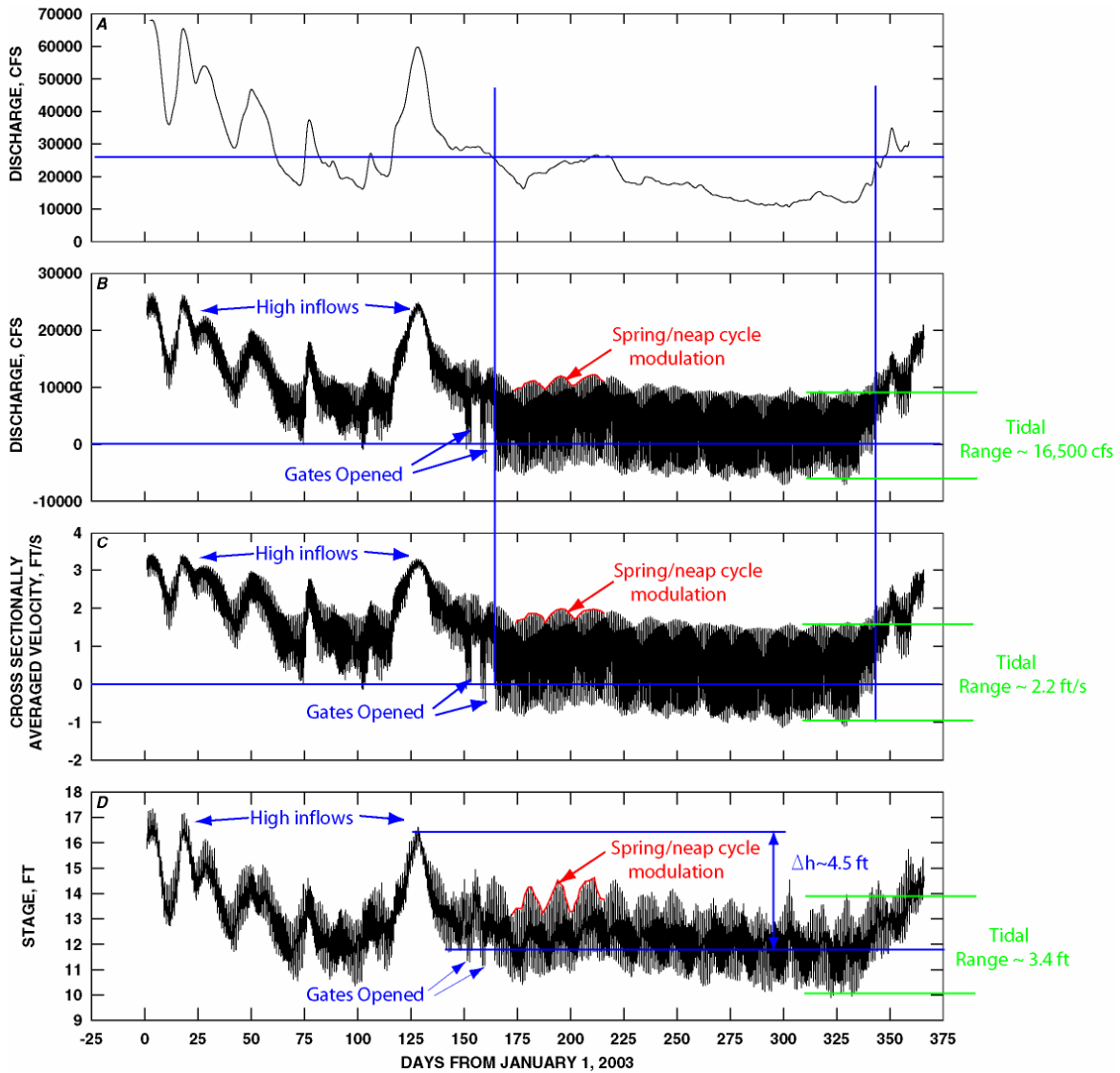


Figure 3.4 – Time series plots measured in the Sacramento River below Georgiana Slough (station WGB) of (A) the tidally-averaged, or net discharge, (B) the measured discharge, (C) the measured cross sectionally averaged velocity, and (D) stage (water level). These time series show that both the tides and Sacramento River flows influence water levels, the cross sectionally averaged velocity and discharge at this location. The net Sacramento River flows interact with the tides by raising water levels (an increase in the net water surface slope). As the Sacramento River flows increase the tidal discharges and velocities decrease. At this station (WGB), bi-directional, or reversing flows occur when the net flow measured at Freeport is less than approximately 28,000 cfs. DCC gate operations can have a profound affect on both the tidal and net flows as is indicated by arrows which that show where the gates were closed. In this figure we see a twofold increase in tidal discharge when the gates are opened near calendar day 151 and again on day 158.

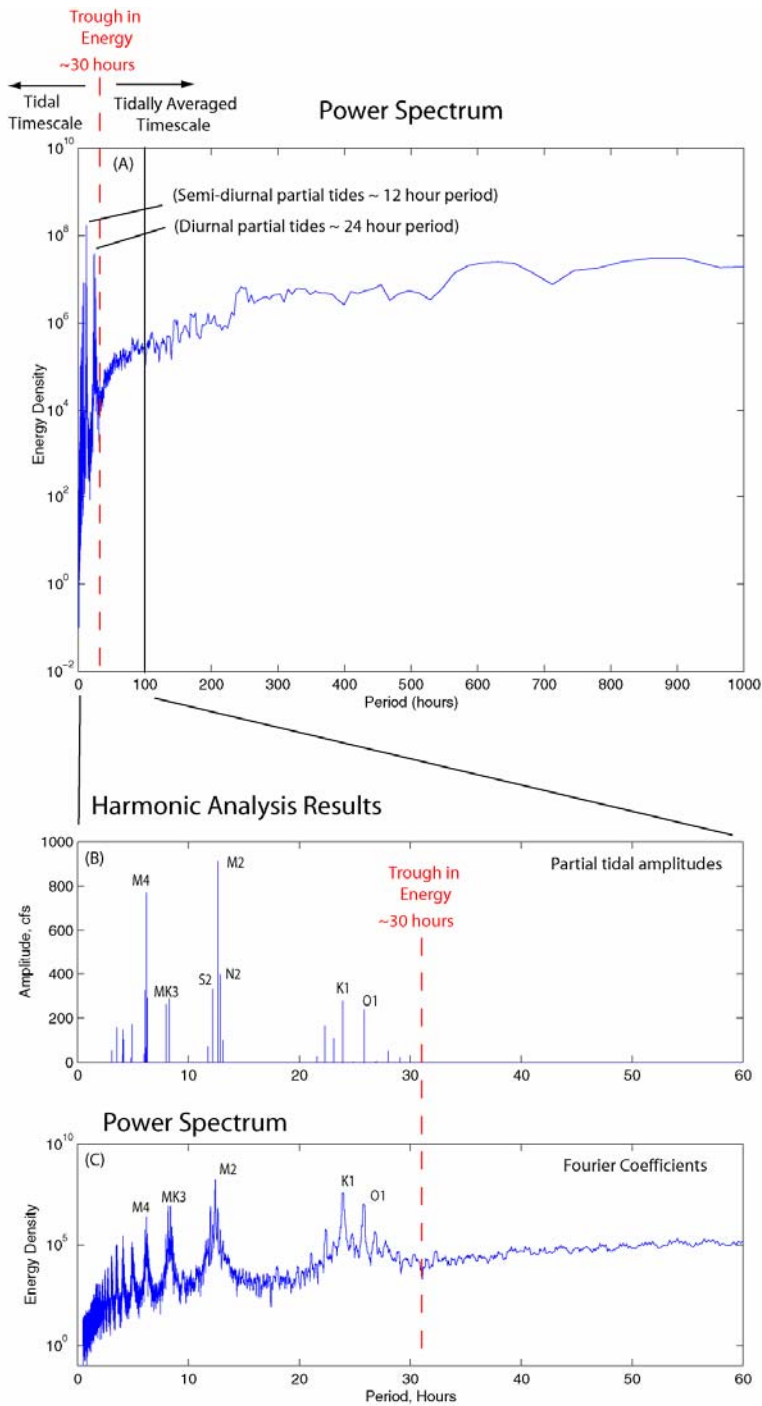


Figure 3.5 – Two frequency domain representations of 2003 data collected in the Sacramento River above the Delta Cross. Panel (A,B) is the power spectral density, in which the Fourier Coefficients, $|X_n^2|$, computed at a Δf intervals, are shown and panel (B) gives harmonic analysis results shown as line spectra of partial tidal amplitudes obtained from a least squares fit to the data. The power spectrum and harmonic analysis results are typical of most north Delta flow records, where there is a great deal of energy in a handful of line spectra (partial tides) representing the tidal energy and a broad spectrum of energy at lower

frequencies representing the influence of the Sacramento River. A trough in energy occurs around 30 hours, which provides a clear separation between the tidal and tidally averaged responses.

(4) Residual Flows

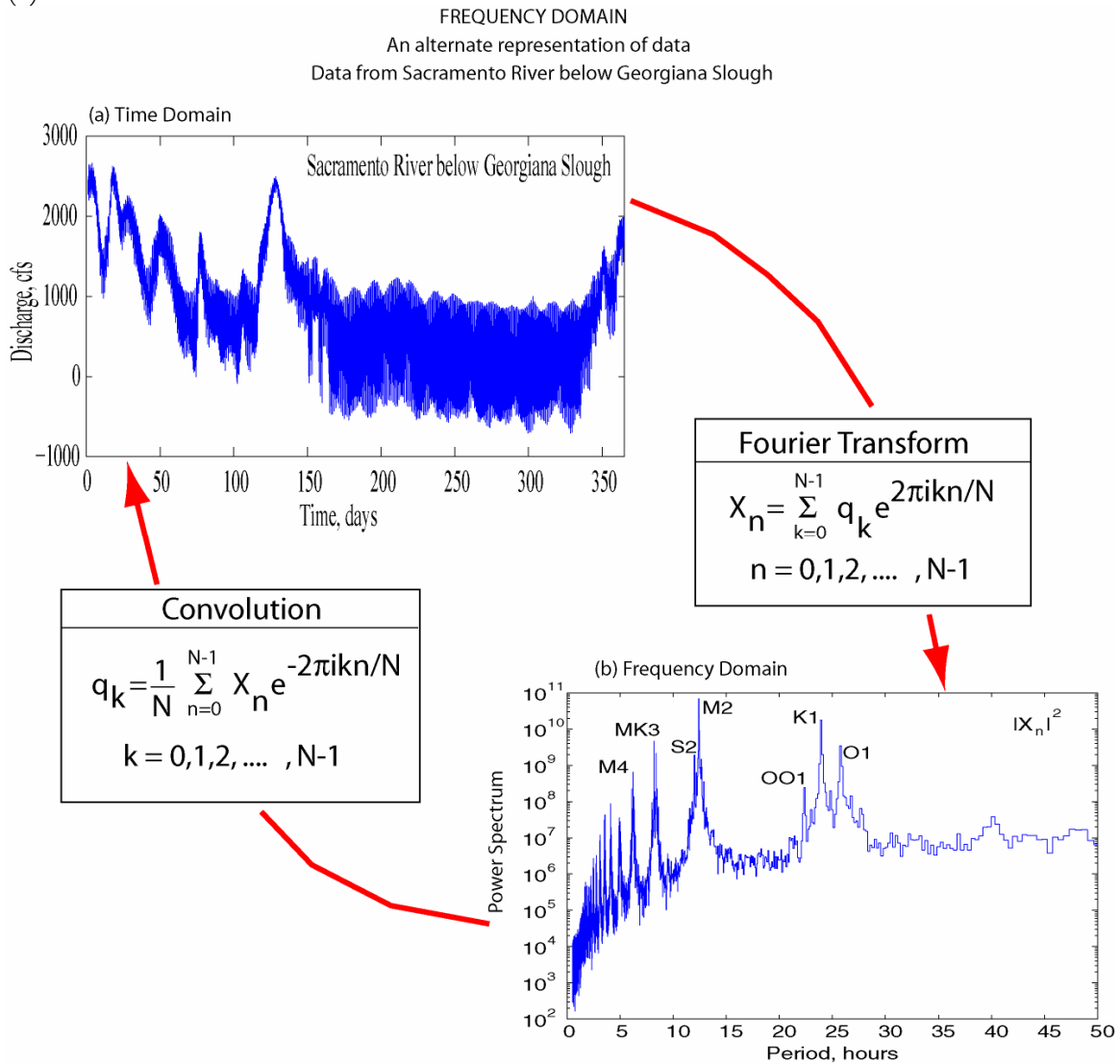


Figure 4.1 – Schematic that shows that time series data can be represented in the: (a) time domain and in the (b) frequency domain with identical information content. Moving from the time domain to frequency domain is accomplished by using Fourier Series and for transformations from frequency space to time space, the convolution is used.

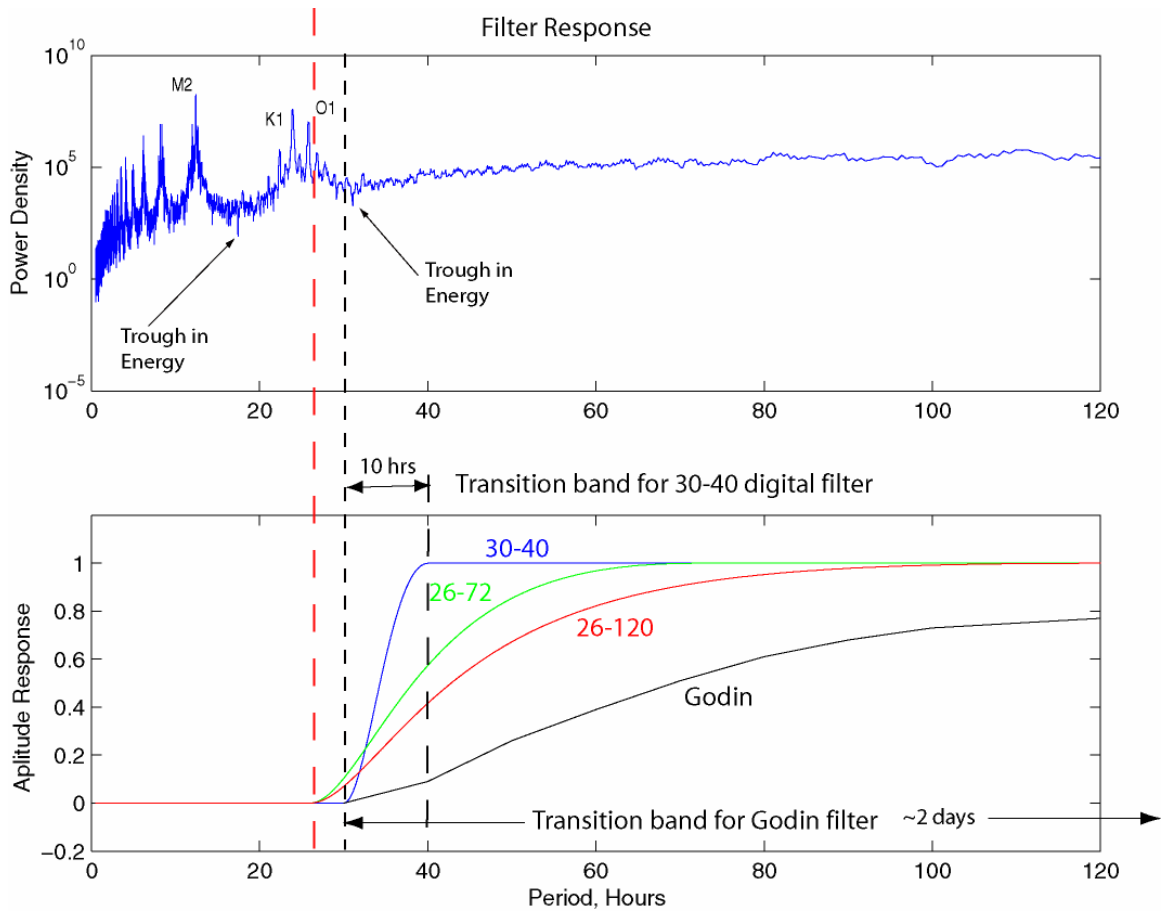


Figure 4.2 –Power spectrum (Top) for the Sacramento River discharge measured above Walnut Grove, (bottom) three different filter masks: (a) the standard (30-40) a stop period of 30 hours, pass period of 40 hours, (b) (26-40) a stop period of 26 hours, pass period of 40 hours, (c) (26-50) a stop period of 26 hours, pass period of 50 hours. Local troughs in the power spectrum occur at roughly 17 hours and at 32 hours. The M2, K1 and O1 partial tides are indicated in the top panel.

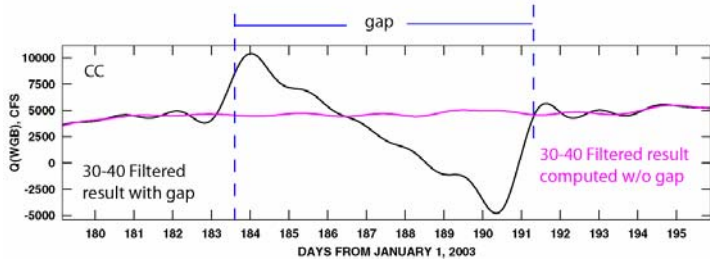
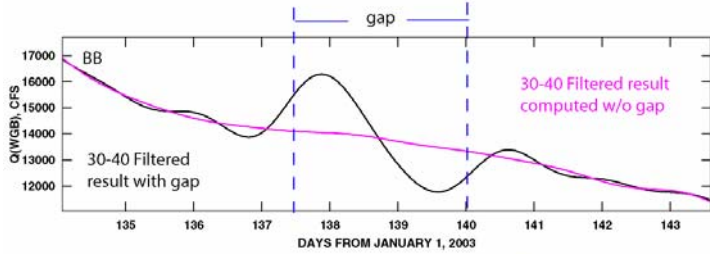
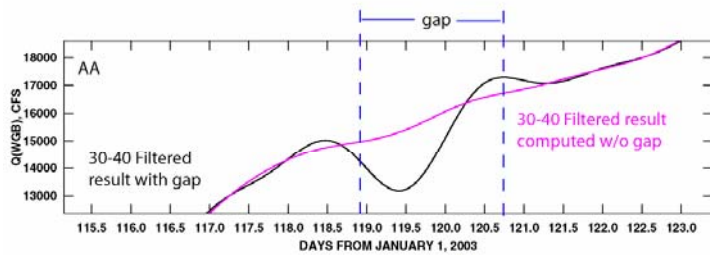
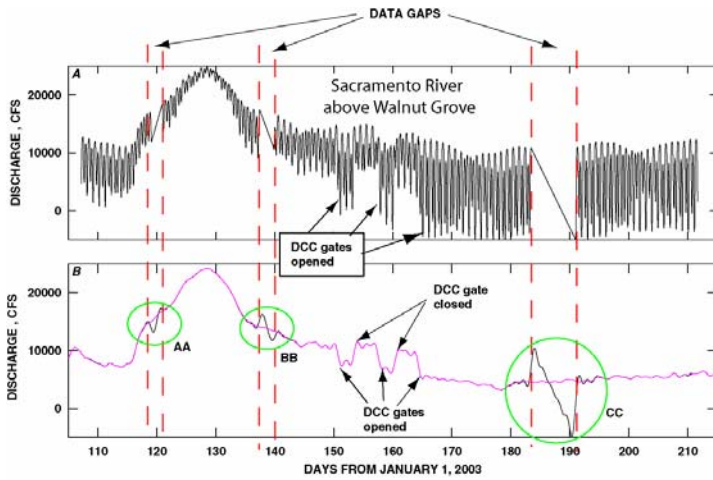


Figure 4.3 – Time series plots of (A) the as-measured Sacramento River discharge measured above Walnut Grove, (B) the tidally averaged discharge at the Sacramento River above Walnut Grove, (AA-CC) insets comparing the tidally averaged result with and without a gap where (AA) is on an ascending limb of the hydrograph, (BB) a descending limb and (CC) a steady limb. Data gaps cause the filter to “ring” at the edges of the gap: ringing creates spurious oscillations that propagate several days into the viable data. Any step function change in the data, such as DCC gate operations, is poorly represented in frequency space by a series of sinusoids. Our task is to minimize this ringing and then to remove data from the filtered time series where this ringing occurs.

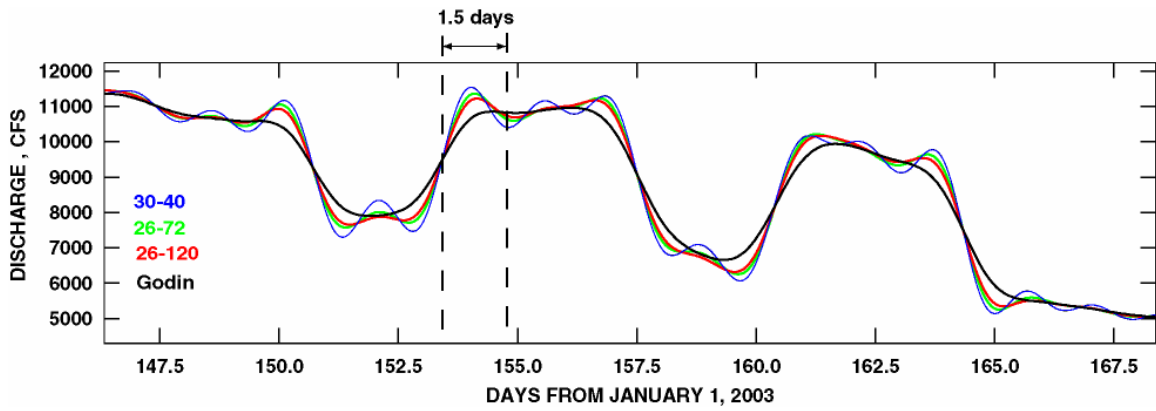


Figure 4.4 – Time series of responses to gate operations from various filters: the digital filter described in Walters and Heston 19xx with stop: pass periods of 30-40 hours (blue), 26-72 hours (green), 26-120 (red) and the Godin filter (black). The digital filter with the stop:pass periods of 30-40 hours oscillated the most and the Godin filter is the most damped.

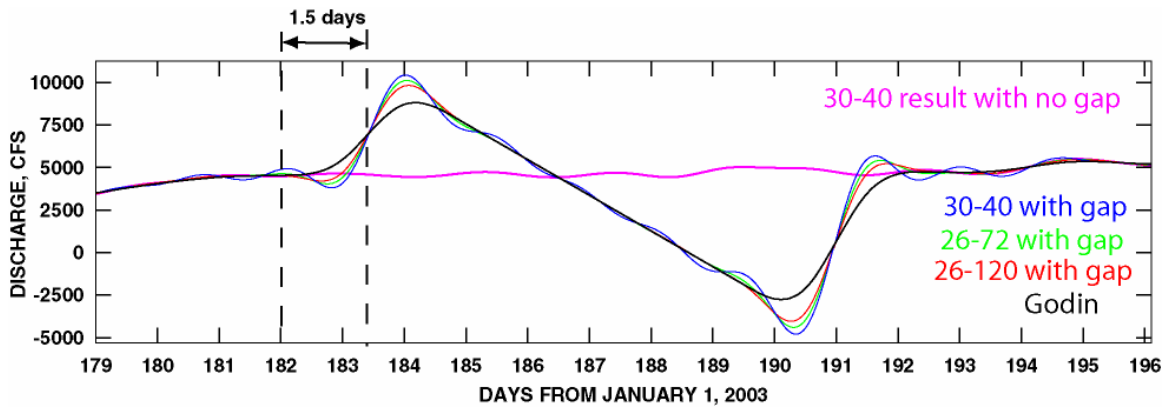


Figure 4.5 – Time series of responses to gate operations from various filters: the digital filter described in Walters and Heston 19xx with stop: pass periods of 30-40 hours (blue), 26-72 hours (green), 26-120 (red) and the Godin filter (black). The digital filter with the stop:pass periods of 30-40 hours oscillated the most and the Godin filter is the most damped. The magenta line represents the “true” tidal average.

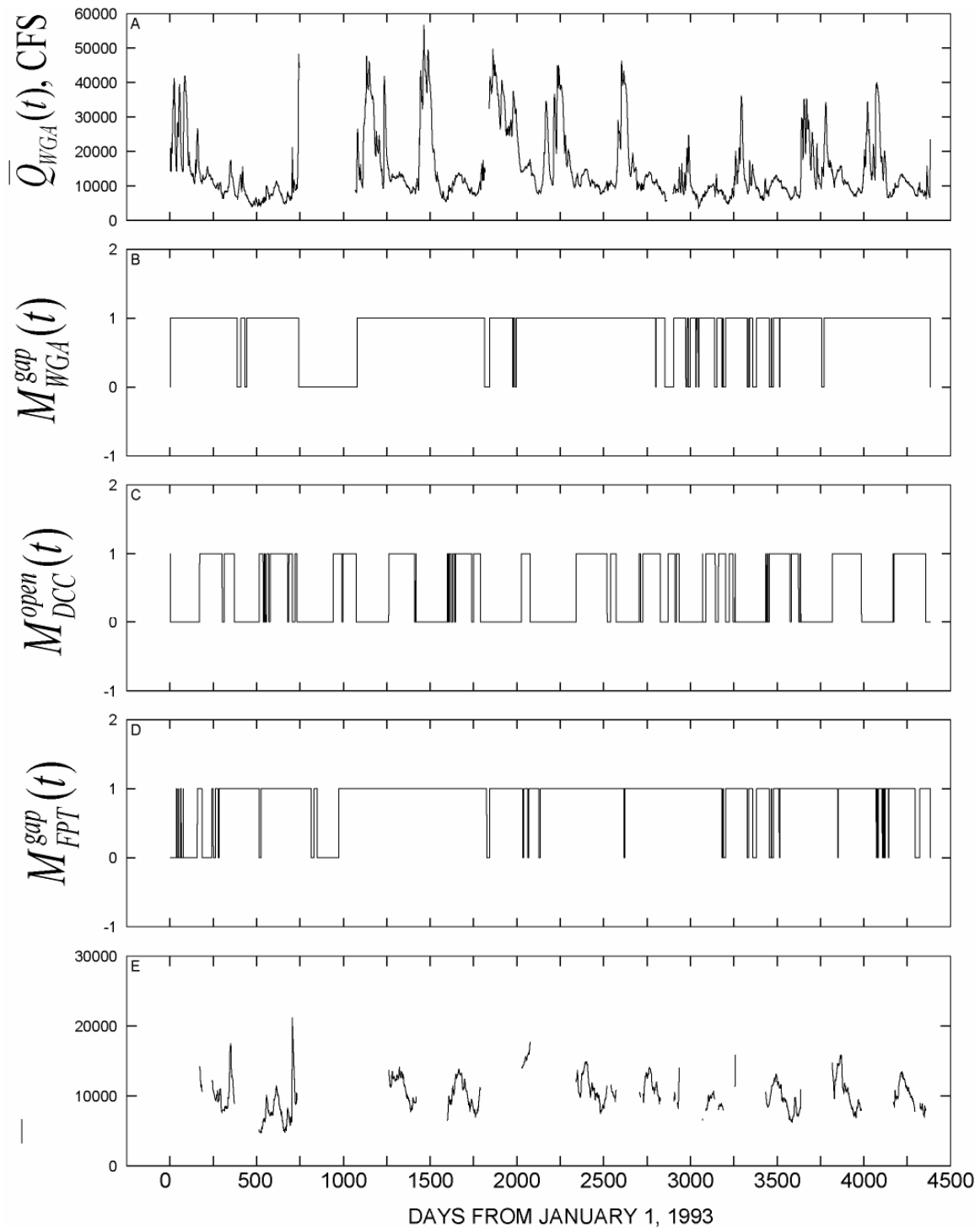


Figure 4.6 – Time series plots of (A) the Godin filtered discharge measured in the Sacramento River above the DCC (WGA), (B) gap mask for missing data at WGA, (C) DCC gates open mask, (D) gap mask for the net discharge collected in the Sacramento River at Freeport, (E) the “clean” net flow time series of net flow collected at station WGA.

Station RIO

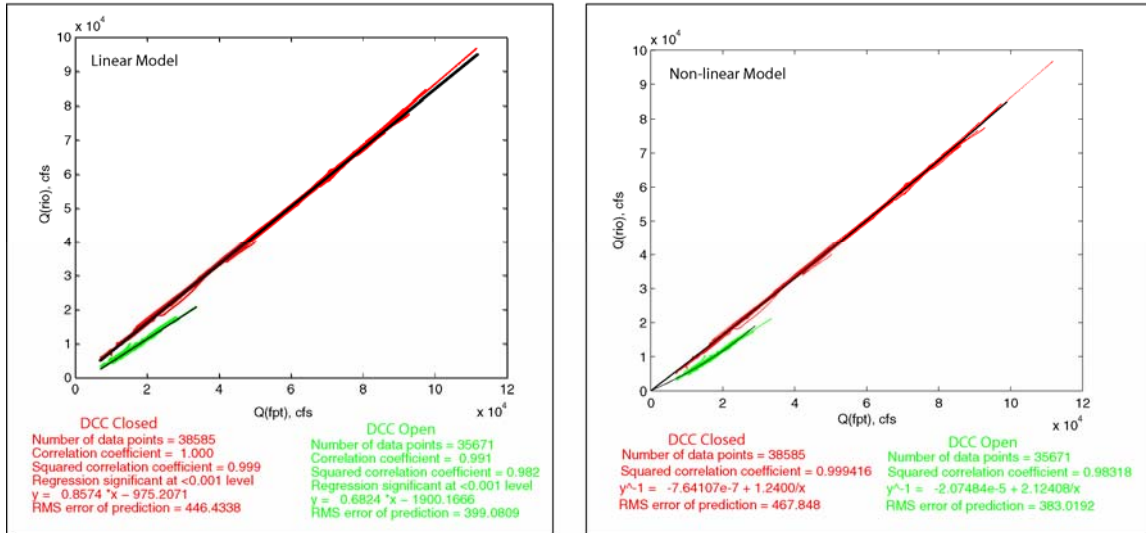


Figure 4.7 Scatter plots of the computed flow in the Sacramento River @ Rio Vista based on the sum of net flows measured in the Sacramento River below Georgiana Slough (WGB) and the combined flow down Sutter and Steamboat Sloughs (station SS). Data were separated on the basis of DCC gate position: green = open, red = closed. Two models based on the net flow at Freeport were applied to these data sets: a linear model $Q_{RIO} = aQ_{FPT} + b$ and a non-linear model $1/Q_{RIO} = a + b/Q_{FPT}$, where Q_{FPT} , Q_{RIO} are the discharges measured at Freeport and Rio Vista, respectively, The a's and b's were determined through least squares regression.

Station SS

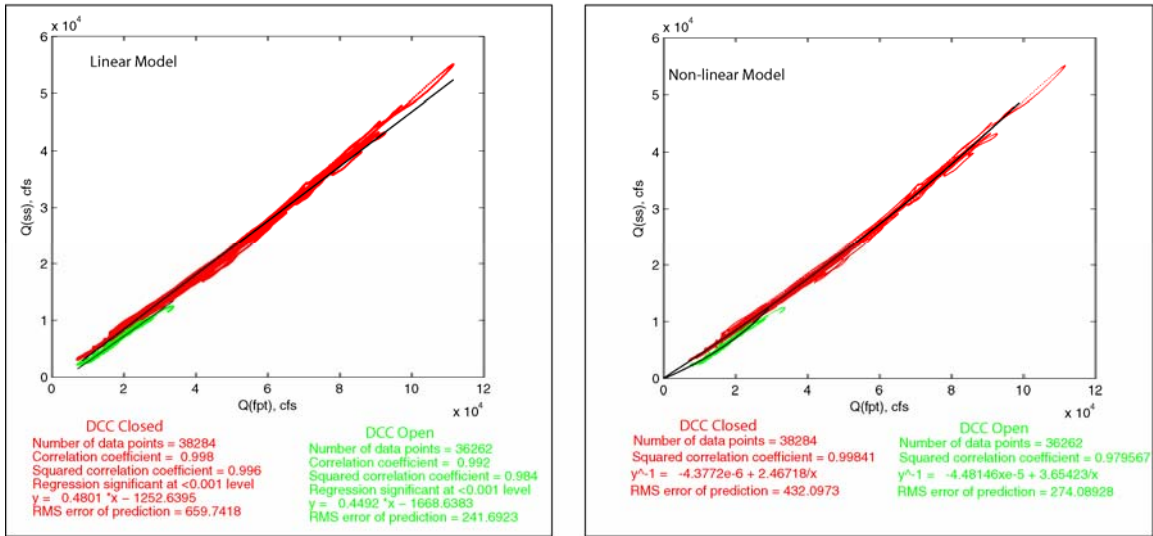


Figure 4.8 Scatter plots of the combined flow in Sutter and Steamboat Sloughs based on the difference between the net flows measured in the Sacramento River at Freeport and in the Sacramento River above the DCC (station WGA). Data were separated on the basis of DCC gate position: green = open, red = closed. Two models based on the net flow at Freeport were applied to these data sets: a linear model $Q_{SS} = aQ_{FPT} + b$ and a non-linear model $1/Q_{SS} = a + b/Q_{FPT}$, where Q_{FPT} , Q_{SS} are the discharges measured at Freeport and computed for Sutter/Steamboat Sloughs, respectively, The a's and b's were determined through least squares regression.

Station Three Mile Slough, TMS

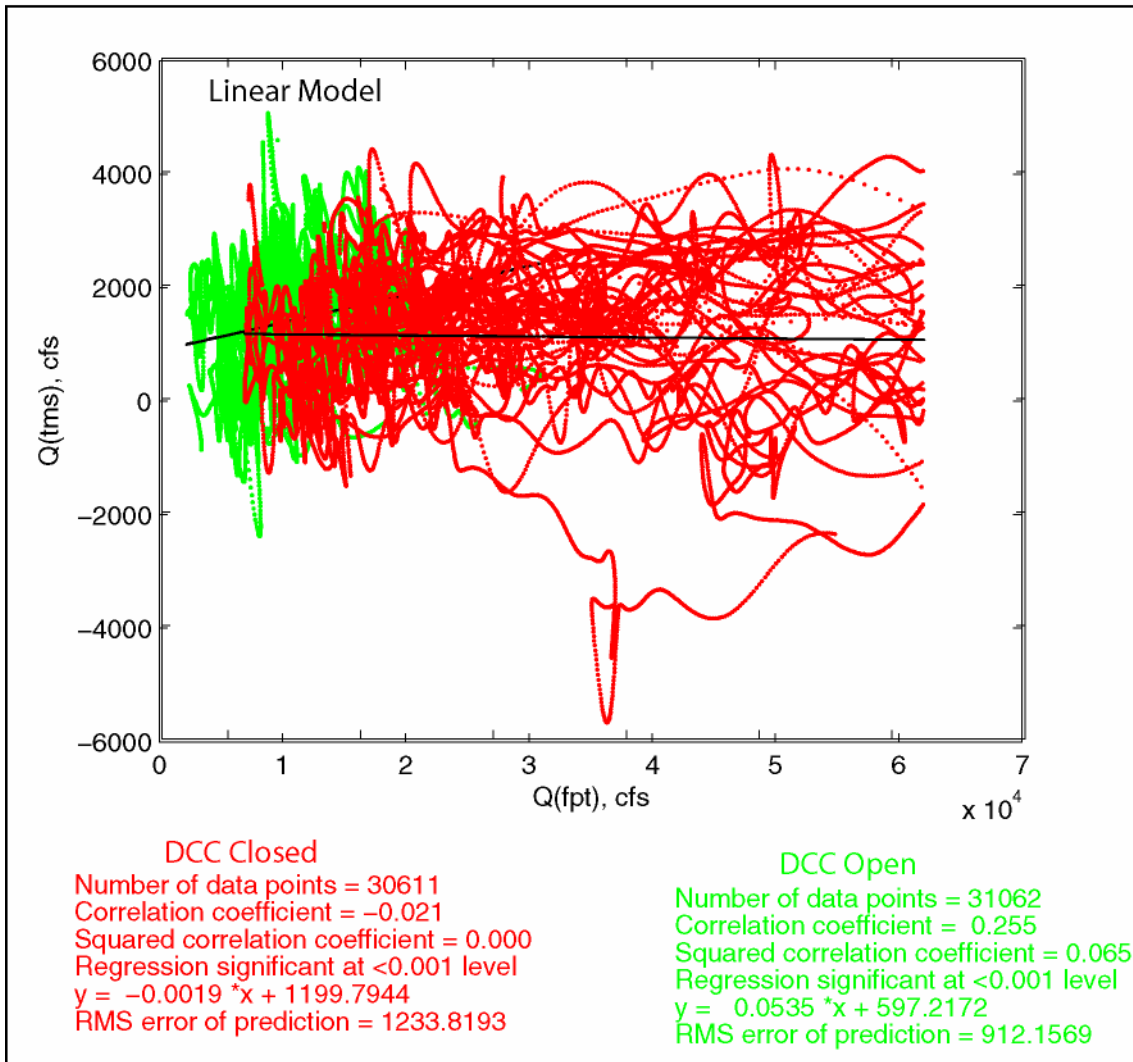


Figure 4.9 – Scatter plots of the net flow measured in Threemile Slough (station TMS). Data were separated on the basis of DCC gate position: green = open, red = closed. Two models based on the net flow at Freeport were applied to these data sets: a linear model $Q_{TMS} = aQ_{FPT} + b$ and a non-linear model $1/Q_{TMS} = a + b/Q_{FPT}$, where Q_{FPT} , Q_{TMS} are the discharges measured at Freeport and Threemile Slough, respectively, The a's and b's were determined through least squares regression.

Station WGA

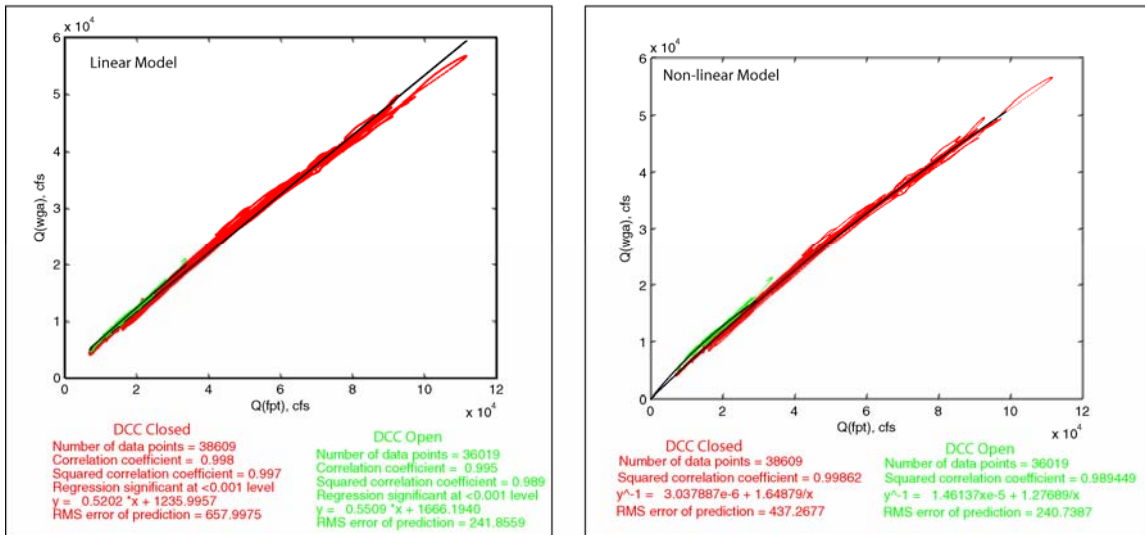


Figure 4.10 – Scatter plots of the net flow measured in the Sacramento River above the Delta Cross Channel (station WGA). Data were separated on the basis of DCC gate position: green = open, red = closed. Two models based on the net flow at Freeport were applied to these data sets: a linear model $Q_{WGA} = aQ_{FPT} + b$ and a non-linear model $1/Q_{WGA} = a + b/Q_{FPT}$, where Q_{FPT} , Q_{WGA} are the discharges measured at Freeport and in the Sacramento River above the Delta Cross Channel, respectively, The a's and b's were determined through least squares regression.

Station WGB

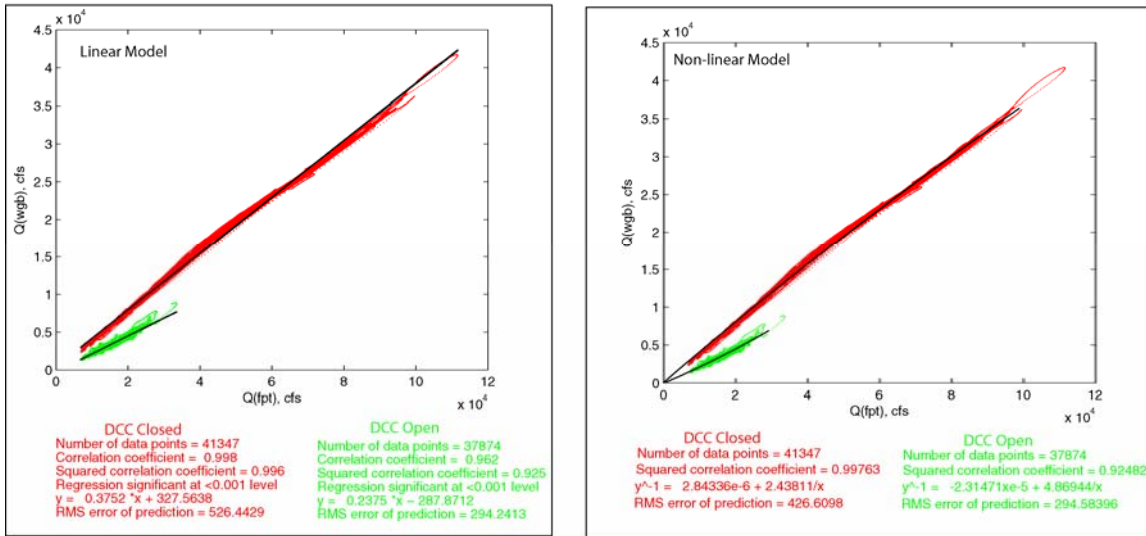


Figure 4.11 – Scatter plots of the net flow measured in the Sacramento River below Georgiana Slough (station WGB). Data were separated on the basis of DCC gate position: green = open, red = closed. Two models based on the net flow at Freeport were applied to these data sets: a linear model $Q_{WGB} = aQ_{FPT} + b$ and a non-linear model $1/Q_{WGA} = a + b/Q_{FPT}$, where Q_{FPT} , Q_{WGB} are the discharges measured at Freeport and in the Sacramento River below Georgiana Slough, respectively, The a's and b's were determined through least squares regression.

Station XGEO

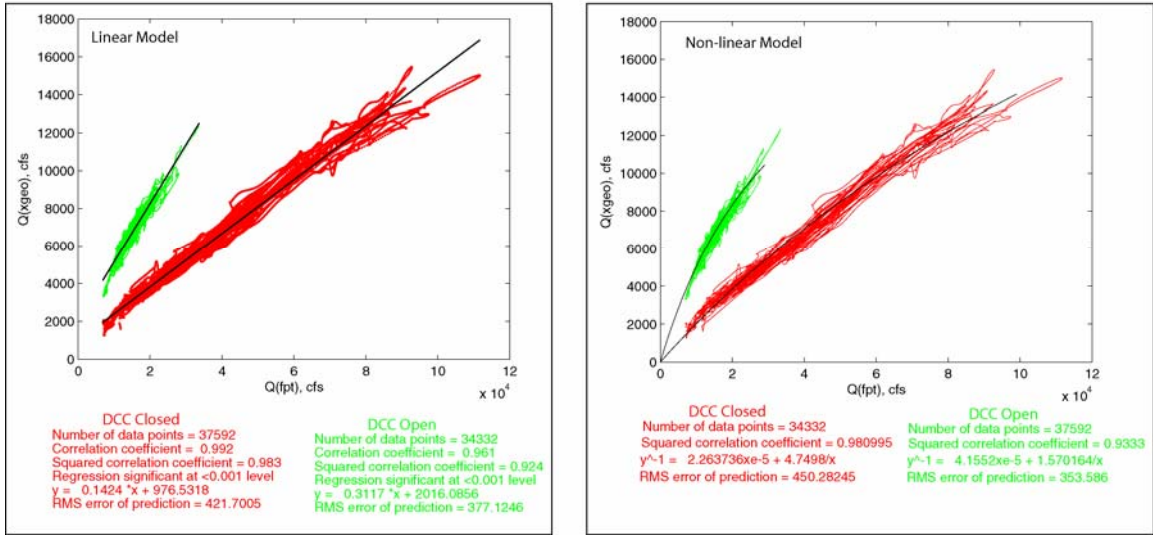


Figure 4.12 - Scatter plots of the net Delta Transfer Flow (station XGEO). Data were separated on the basis of DCC gate position: green = open, red = closed. Two models based on the net flow at Freeport were applied to these data sets: a linear model $Q_{XGEO} = aQ_{FPT} + b$ and a non-linear model $1/Q_{WGA} = a + b/Q_{FPT}$, where Q_{FPT} , Q_{XGEO} are the discharges measured at Freeport and the computed Delta Transfer flow, respectively, The a's and b's were determined through least squares regression.

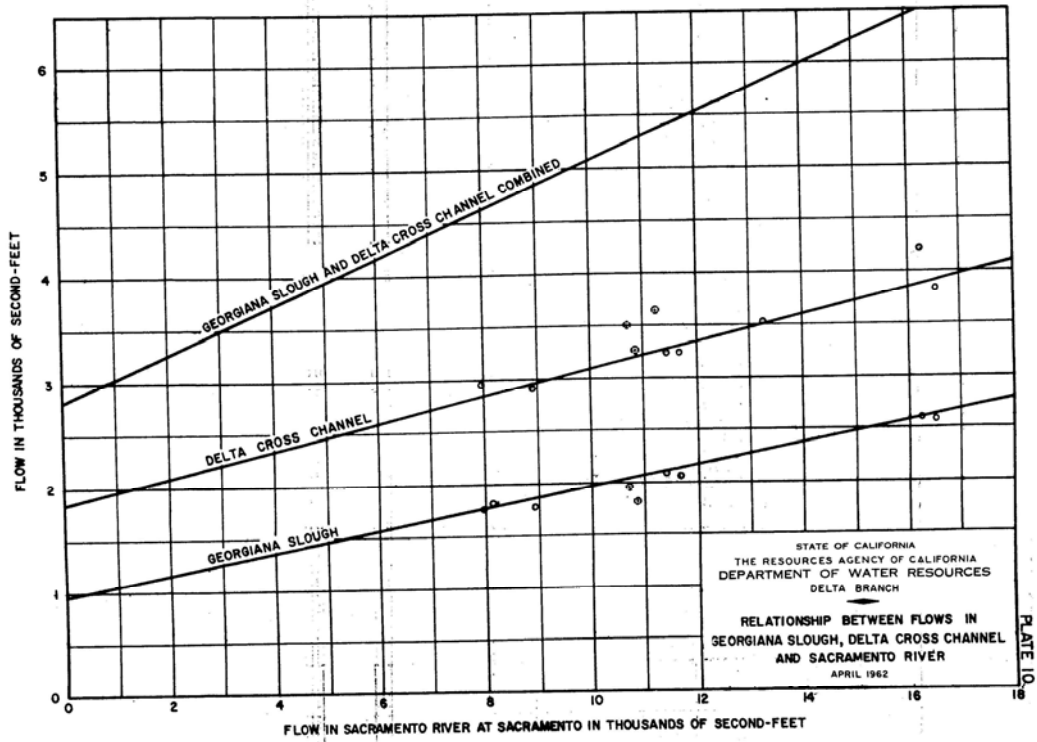


Figure 4.13 – Discharge relations computed based on tidal cycle measurements collected between 1930-1960, courtesy of [Bulletin xxx](#), DWR, 1962. (file:xgeo.1962.jpg)

FIGURE 4

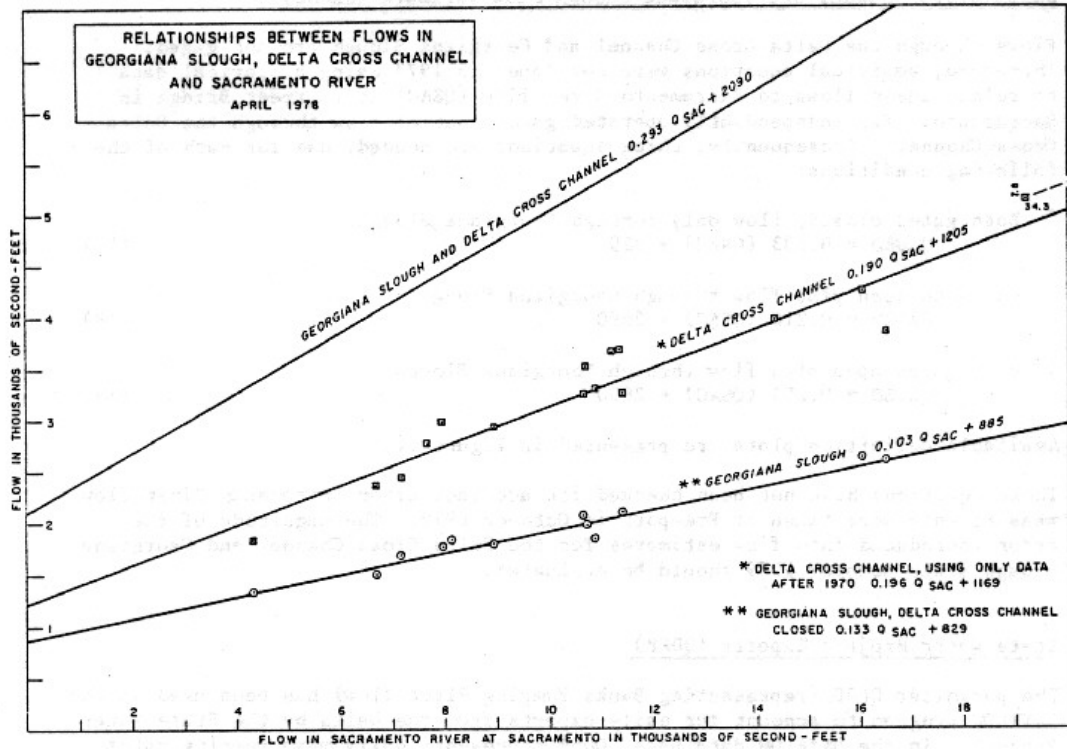


Figure 4.14 – Discharge relations for the Delta Transfer Flow, XGEO, computed based on tidal cycle measurements collected between 1930-1960, courtesy of [Bulletin xxx](#), DWR, 1978. These relations are used to compute XGEO is the DAYFLOW program, ([ref](#)).

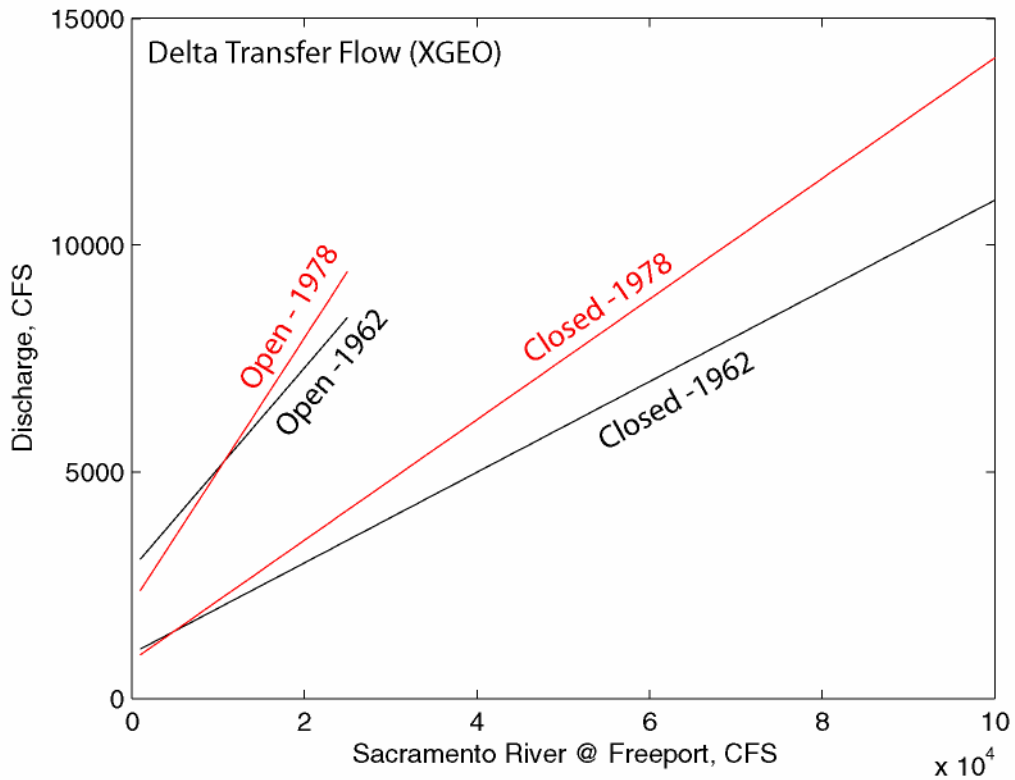


Figure 4.15 – Comparison of relations for the Delta Transfer Flow, derived by DWR in 1962 (ref) and in 1978 (ref). Open conditions compare fairly well, however, the 1962 relations significantly under predict the Delta Transfer Flow. However, this difference could be attributed to an actual change in the relation due to a significant change in geometry between 1962 and 1978.

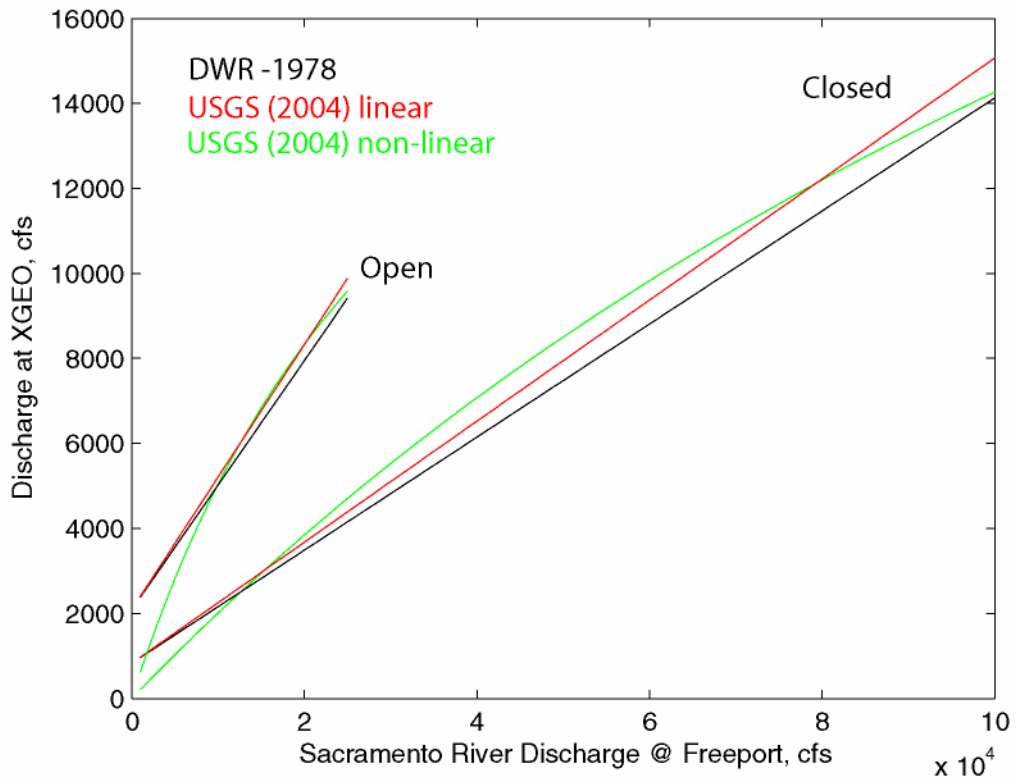


Figure 4.16 – Comparison of relations for the Delta Transfer Flow, derived by DWR in 1978 (ref) and in this paper (2004). The relations are remarkably similar, though the 1978 relations under-predict the Delta Transfer Flow.

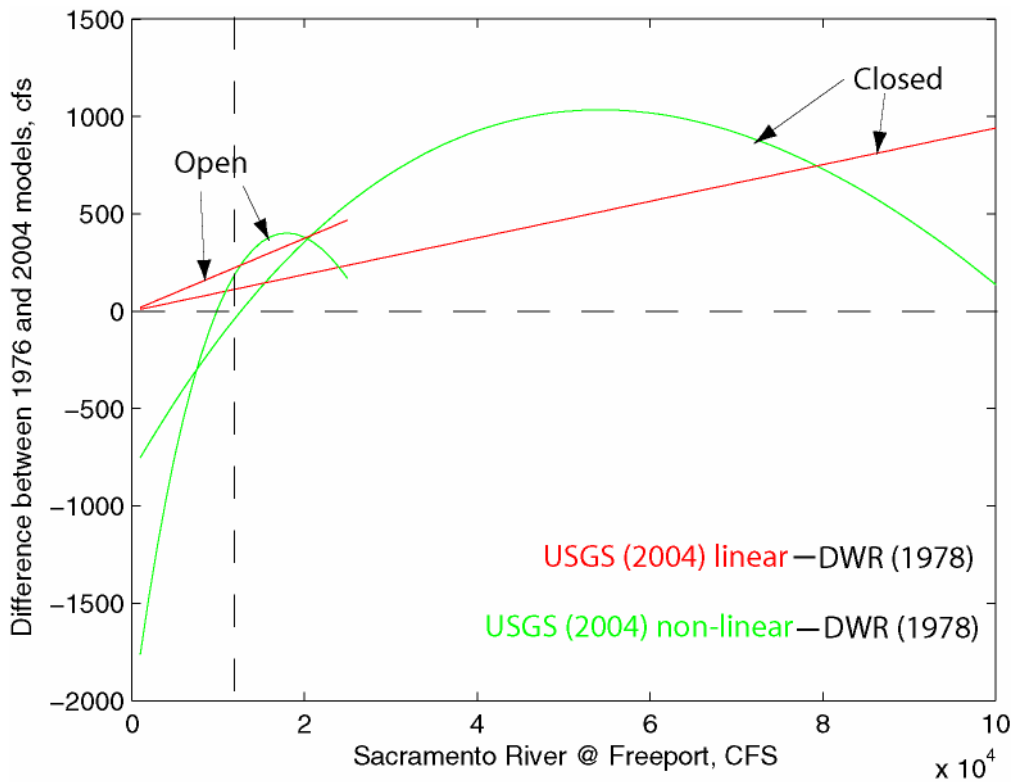


Figure 4.17 – Differences in discharge between the flows predicted by the DWR 1978 relations, [equations 22, 23](#) and the 2004 linear relations derived in this paper, [equation 18](#).

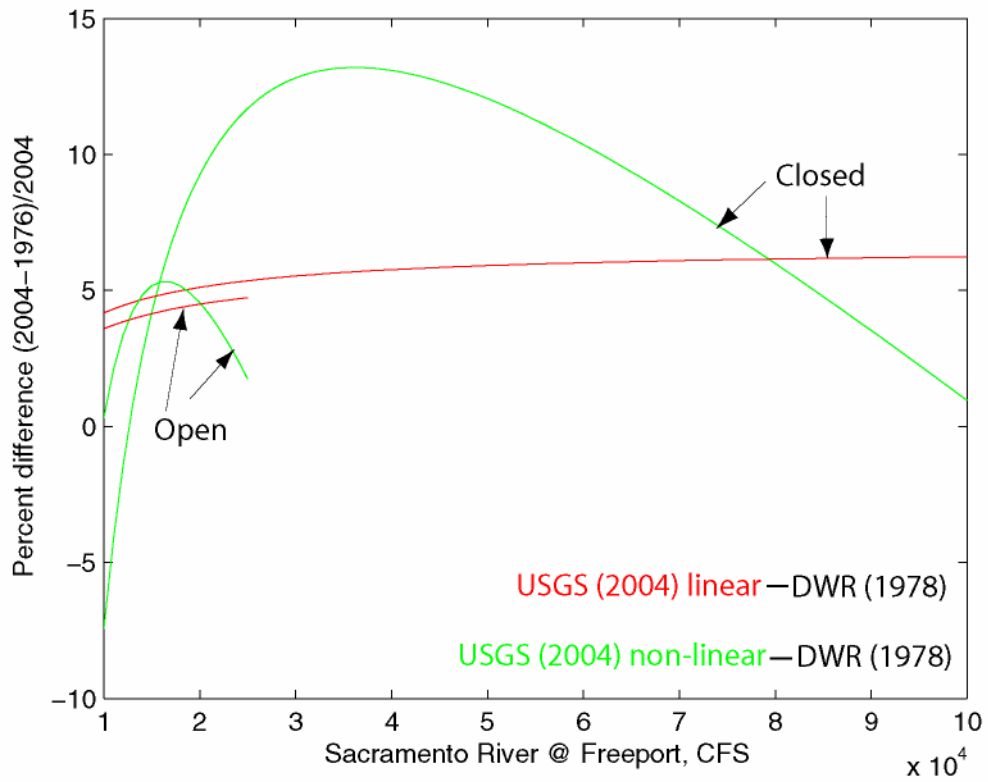


Figure 4.18 – Percent differences in discharge between the flows predicted by the DWR 1978 relations, equations 22, 23 and the 2004 linear relations derived in this paper, equation 18.

Appendix B - Summary of Mark-Recapture Modeling for North Delta Pilot Study Winter 2006/2007

Introduction

A multi-agency, multi-disciplinary team conducted a pilot study during the winter of 2006/2007 to determine the efficacy of conducting a large-scale telemetry study to estimate survival and route selection probabilities of juvenile salmon migrating through the Delta. Specific goals of the pilot study were to:

- Test and deploy Hydroacoustic Technology Inc. (HTI) acoustic telemetry equipment in the field for the purposes of estimating survival and route selection probabilities.
- Develop the statistical models necessary to estimate survival and route selection probabilities from the telemetry data.
- Use the pilot data to estimate precision and sample size for the full-scale study.
- Refine technological, field, and modeling techniques in preparation for the full scale study.

This summary describes development of the statistical model, the statistical methodology and results from applying the model to data collected during the pilot study. The statistical methodology for the full scale study will use the same approach as the pilot study, except that the spatial scale and scope will be expanded.

The study area for the pilot study focused on the North Delta because this region contains junctions critical to the migratory fate of juvenile salmon (Figure B.1). Fish migrating downstream in the Sacramento River meet their first junction at Steamboat and Sutter Sloughs. Steamboat and Sutter Slough diverts fish from the Sacramento River and converges again with the Sacramento River near Cache Slough and Rio Vista (Figure B.1). Fish that take either Steamboat or Sutter Sloughs completely bypass the second major river junction on the Sacramento River at the Delta Cross Channel (DCC) and Georgiana Slough. Fish entrained in either the DCC or Georgiana Slough are diverted to the central and southern Delta, where survival is hypothesized to be low due to longer migration distance, travel time and the possibility of entrainment in the SWP and CVP export facilities.

Methods

A limited set of HTI hydrophones (15) were strategically deployed throughout the study area to monitor approximately 250 late-fall Chinook (LFC) salmon smolts from the Coleman National Fish Hatchery (Figure B.2 and B.3). A total of 96 fish were released when the DCC was open (in December, 2006) and 150 fish were released when the DCC was closed (in January, 2007). These fish were surgically implanted with acoustic transmitters by personnel from Natural Resource Scientists, Inc., allowed to recover for 24 hours prior to being released. In an effort to allow fish to recover from handling and surgery, all fish were released at the city of Sacramento, providing approximately one day of in-river migration to resume natural migration behavior before entering the study area.

Hydrophone Deployment

Because of the limited number of hydrophones available, two distinct telemetry deployment designs were used during different DCC operations (DCC open, DCC closed), in order to maximize the amount of information collected during the study. For both sets of DCC operations

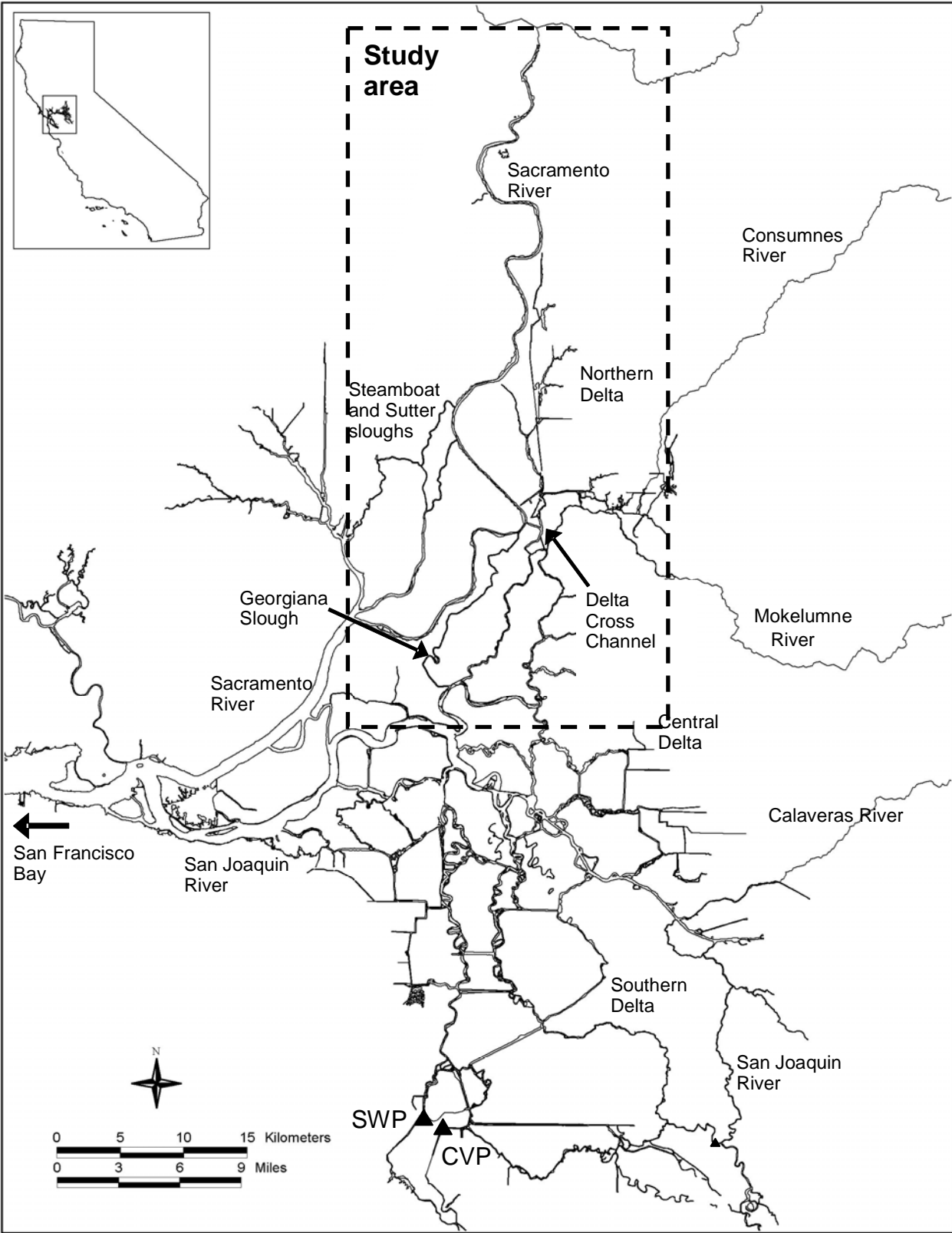


Figure B.1. Map of the San Joaquin – Sacramento River Delta showing the study area for the pilot study conducted during the winter of 2006/2007 in the Northern Delta. Also shown are major tributaries and locations of water control structures such as the Delta Cross Channel, the State Water Project (SWP), and the Central Valley Project (CVP).

Both the Sacramento River (stations 5, 8, 9, and 10 in Figure B.2; stations 5, 7, 10, and 11 in Figure B.3) and Georgiana Slough (stations 7 and 11 in Figure B.2; stations 6, 12, and 13 in Figure B.3) were monitored in the pilot. When the Delta Cross Channel was open, hydrophones were installed in the DCC and the North and South Fork Mokelumne rivers to estimate survival through this region (stations 6, 12, 13, 14, and 15 in Figure B.2). We estimated route-selection probabilities for Sutter and Steamboat sloughs (stations 1-4 in Figures B.1 and B.2) during both sets of river conditions. However, when the DCC was open, survival was not estimated for Steamboat and Sutter Slough due to the limited number of hydrophones. In contrast, when the DCC was closed, telemetry stations (hydrophones) associated with the DCC (stations 6, 12, 13, 14, and 15 in Figure B.2) were moved to Steamboat and Sutter Slough to estimate survival through that reach (stations 8, 9, and 11).

The location of telemetry stations were motivated by 1) the primary biological parameters of interest and 2) the statistical requirements needed to produce valid estimates of these parameters. In general, to estimate survival through a reach of river, that reach must be bounded by telemetry stations on the upstream and downstream end of that reach. Furthermore, at the downstream terminus of the last reach where survival is to be estimated, either one additional telemetry array must be implemented downstream, or the last array must consist of a double-telemetry array. This approach allows explicit estimation of both detection and survival probabilities in the last reach; otherwise, survival and detection probabilities can not be separated in the last reach. For example, to estimate the detection probability of the last telemetry station in Georgiana Slough, a double detection array, consisting of two independent telemetry stations were deployed (DCC closed only; stations 12 and 13 in Figure B.3). In addition, since telemetry arrays downstream of Steamboat and Sutter Slough were not specific to which slough fish entered, double detection arrays were required to estimate route selection probabilities at Steamboat and Sutter Slough (stations 1-4 in Figures B.1 and B.2). The telemetry deployment design allowed us to estimate route selection probabilities at both major junctions and survival probabilities in three reaches of the Sacramento River, one reach combined for Steamboat and Sutter Slough, the entirety of Georgiana Slough, and one reach combined of the North and South Fork Mokelumne River for fish entering the DCC (Figures B.2 and B.3).

Statistical modeling

The foundation of the statistical model is based on the classic release-recapture models of Cormack (1964), Jolly (1965), and Seber (1965). More recently, multi-strata models have been used to estimate both survival and movement probabilities between habitat areas (Brownie et al. 1993, Schwarz et al. 1993). Furthermore, the route-specific survival model (Skalski et al. 2002) comes close to emulating the model structure that is required for the Delta. This model was developed to estimate survival probabilities of juvenile salmon as they migrate through the Columbia River and pass through hydroelectric dams (e.g., see Counihan et al. 2003, Perry et al. 2006). Once fish arrive at a dam, they may pass through a number of available routes such as the turbines or the spillway. By monitoring passage routes with telemetry equipment and recording detections of tagged fish in each route, the model estimates the probability of survival through each passage route as well as the probability of passing through each route. Similarly, we are interested in estimating survival of fish through each migratory route as well as the probability of fish migrating through various routes (route selection probabilities) in the north Delta. Thus, the model we developed is a hierarchical multi-strata model similar to that of the route-specific survival model of Skalski et al. (2002).

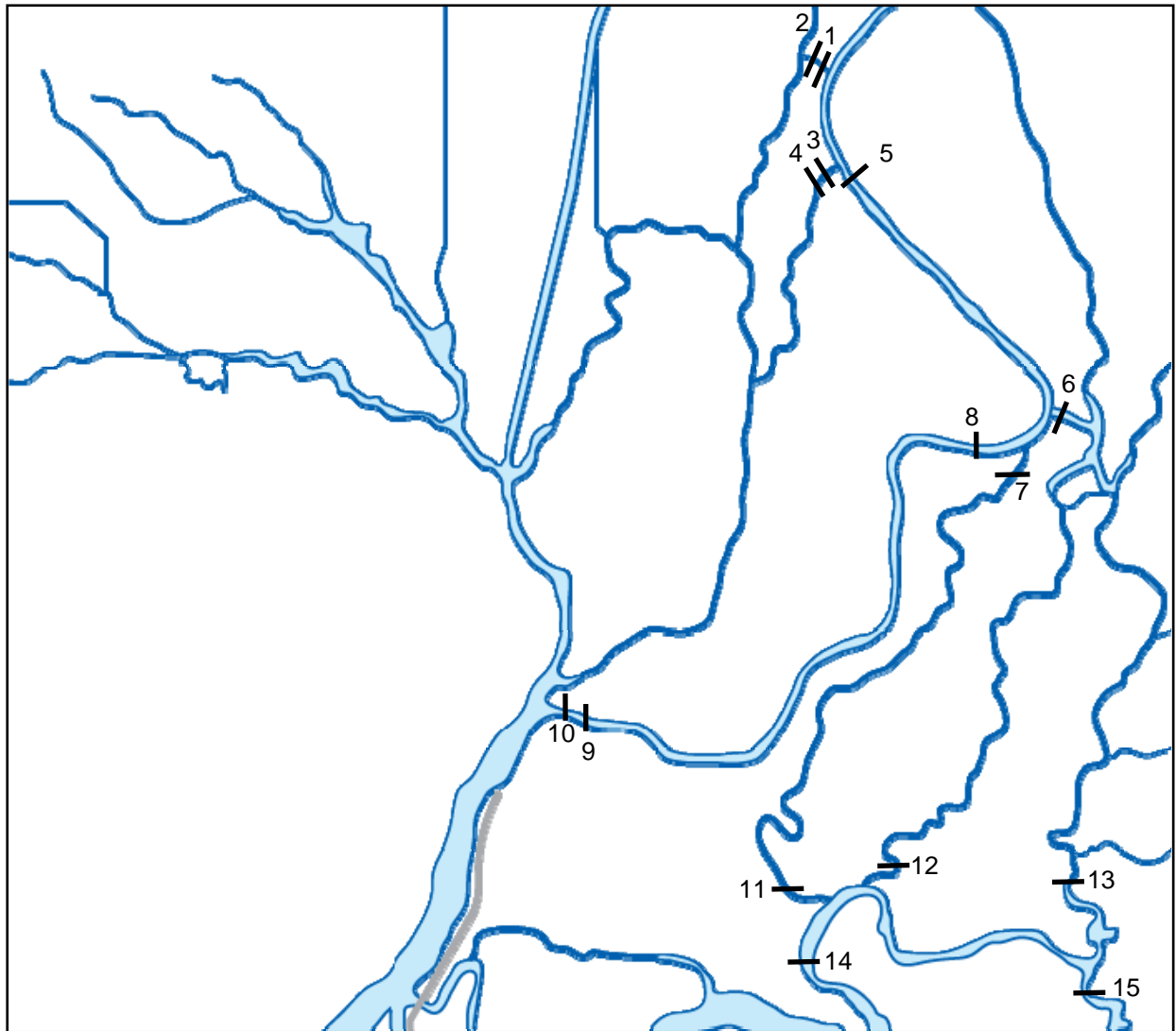


Figure B.2. Location of telemetry stations (hydrophones) with the Delta Cross Channel open for the pilot study conducted during the winter of 2006/2007.

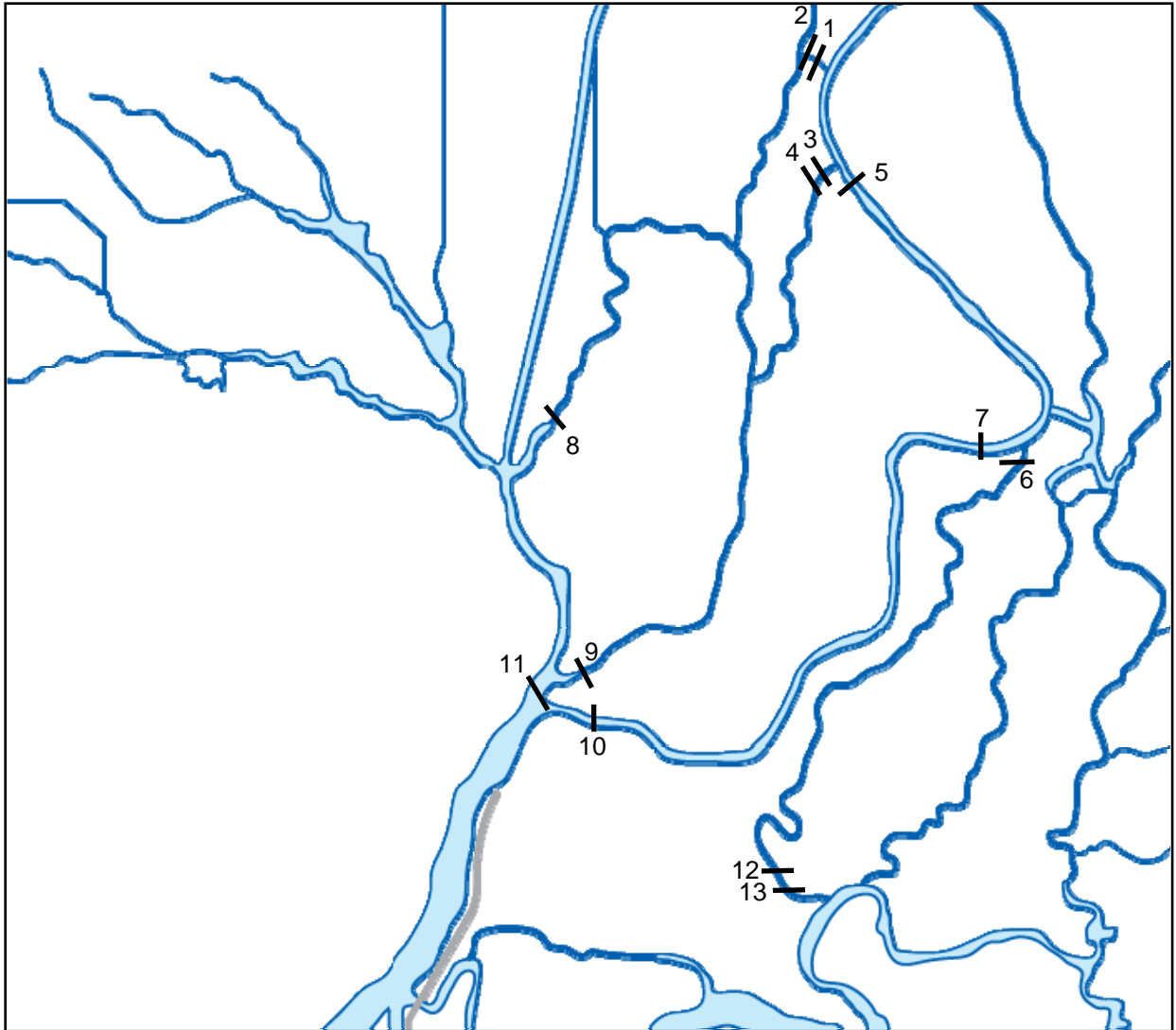


Figure B.3. Location of telemetry stations (hydrophones) with the Delta Cross Channel open for the pilot study conducted during the winter of 2006/2007.

Detection (or “capture”) histories of each fish form the basis of these models and allow for the estimation of route-specific survival, detection, and route selection probabilities. In general, parameters are estimated by:

- 1) Creating detection histories for each fish that define the unique pattern of detections .
- 2) Estimating the probability of each possible detection history from the observed frequencies of fish with each detection history.
- 3) Using likelihood methods to estimate parameters of survival, detection, and route selection probabilities that were most likely, given the observed data set of mutually exclusive and exhaustive detection histories.

Detection histories are alphanumeric codes indicating each unique migratory and detection summary of each fish. In general, we used a zero (0) to indicate when a fish was not detected and the letters A – D to indicate when fish were detected in one of four possible migratory “branches”. For example, the detection history “10BB” indicates that a fish was released (“1”), was not detected at the first junction (“0”, stations 1-5), was detected in the Sacramento River at the second junction (“B”, station 8 in Figure B.2), and was detected at the double array at the mouth of the Sacramento River (“B”, stations 9 and 10, Figure B.2).

Each unique detection history has a probability of occurrence that can be completely specified in terms of the survival, route selection, and detection probabilities. For example, if a fish was detected at a given telemetry station, then it survived through the preceding reach. Thus, the probability of this event is the joint probability that it survived (S) through the preceding reach and was detected (P) at the telemetry station ($S*P$). However, if this fish was not detected at a given receiver and there are no subsequent detections downstream, then two possibilities arise: 1) the fish died ($1-S$), the probability of not surviving; or 2) the fish survived but was not detected, $S*(1-p)$, the joint probability of surviving and not being detected. Using this approach, the probability of detection history “10BB” can be specified using survival, detection, and route selection probabilities defined based on the telemetry deployment (Figure B.4 and B.5). Specifically, detection history “10BB” indicates a fish that survived through the first reach (with probability S_1), remained in the Sacramento River at the first junction (with probability $1-A$), was not detected at telemetry station 5 (with probability $1-P_1$), survived to the second junction (S_2), remained in the Sacramento River ($(1-D)*B$), was detected in the Sacramento River at the second junction (P_{b1}), survived to the mouth of the Sacramento River (S_b), and was detected at the double array at the mouth of the Sacramento River (P_{b2} , Figure B.4)). The probability of detection history “10BB” is simply the joint probability of each of these events: $S_1*(1-A)*(1-P_1)*S_2*(1-D)*B*P_{b1}*S_b*P_{b2}$ (Figure B.4). Next, maximum likelihood methods are used, and these probability statements form the likelihood for each detection history (Figures B.4 and B.5, Tables B.1 and B.2). The joint probability of detection history frequencies form a multinomial likelihood function which is maximized to obtain the best-fit parameter estimates:

$$L(\theta | R, n_i) = \binom{R}{n_i} \prod_{i=1}^k p_i^{n_i}$$

where $L(\theta | R, n_i)$ is the likelihood of the parameters (θ) given the number of fish released (R) and the frequency of fish (n_i) with each of $i = 1 \dots k$ detection histories and p_i is the probability of each detection history defined in terms of the parameters as described above. In addition to the primary likelihood, a secondary likelihood is used for each double array to estimate the overall probability of detection at the double array.

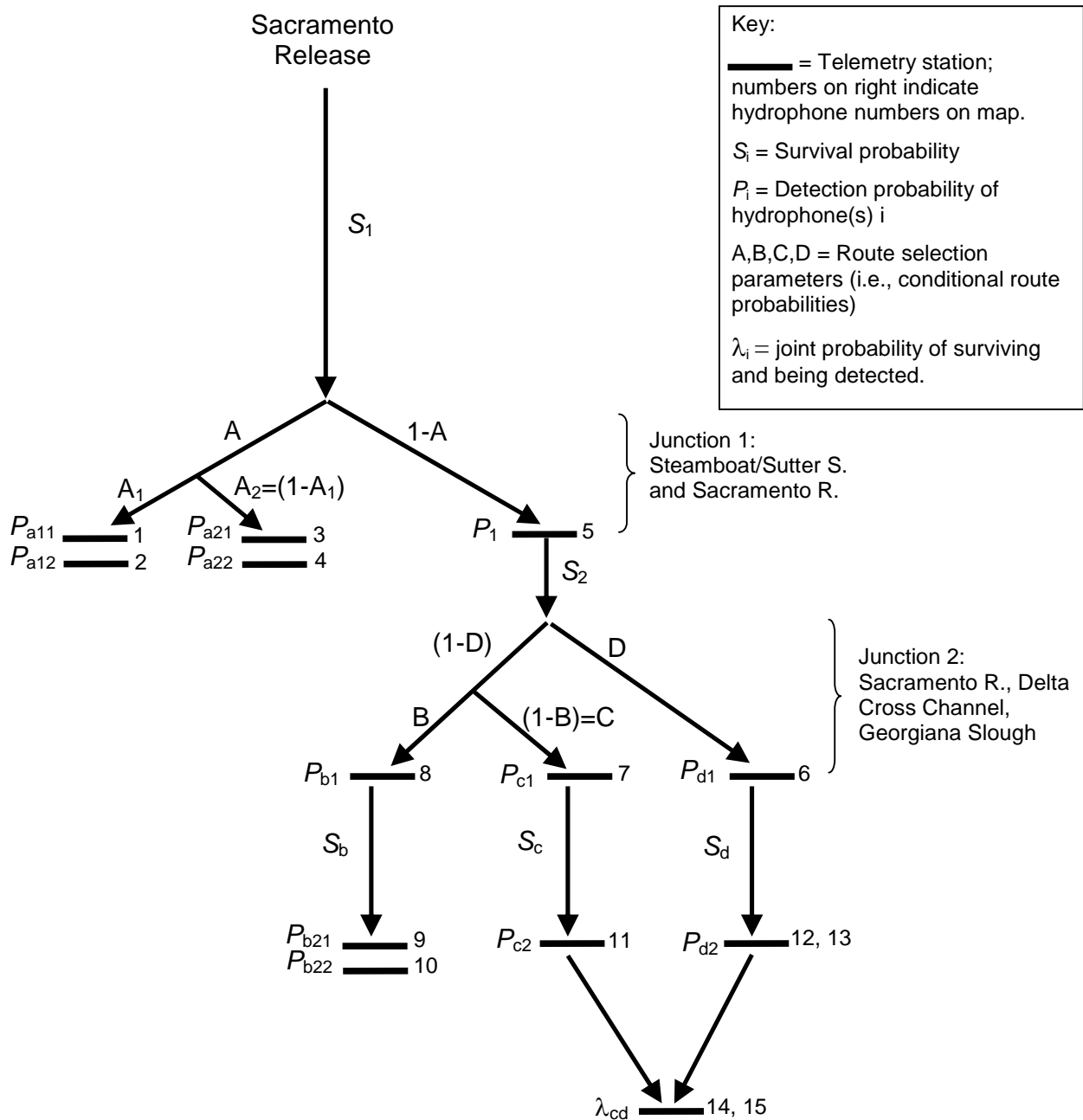


Figure B.4. Schematic representation of the survival model with the DCC open showing telemetry stations (numbers on right correspond to telemetry stations on study area map), route selection parameters at river junctions (A, B, C), survival probabilities (S_i), and detection probabilities (P_i).

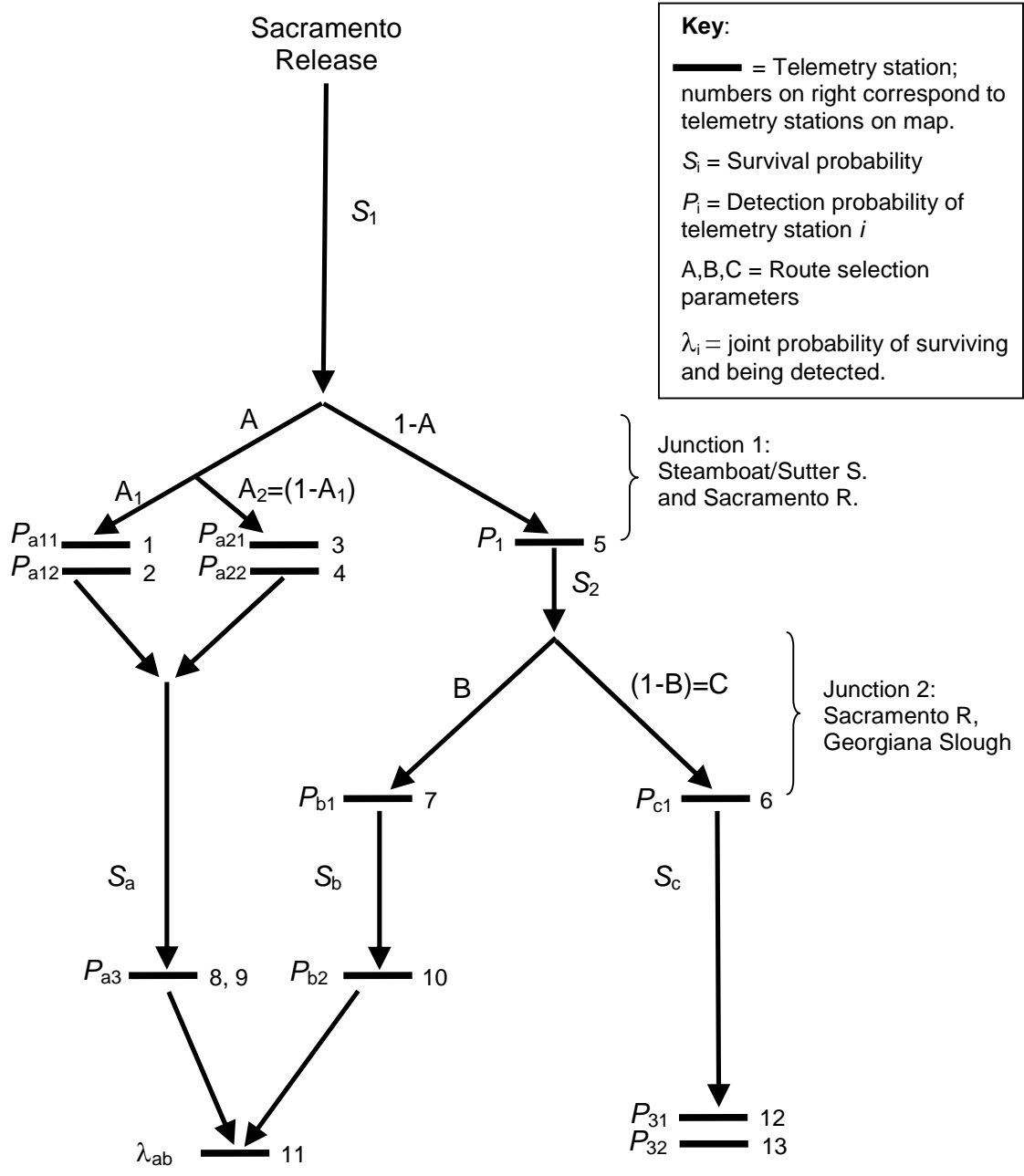


Figure B.5. Schematic representation of the survival model with the DCC closed showing telemetry stations (numbers on right correspond to telemetry stations on study area map), route-selection parameters at river junctions (A, B, C), survival probabilities (S_i), and detection probabilities (P_i).

Table B.1. Definition of parameters estimated by the survival model for the pilot study conducted by USGS during December, 2006 and January, 2007. Detection probabilities are not included below, and are defined as the probability of detecting a tagged fish at a telemetry station, given that the fish was alive at the telemetry station.

Parameter	Definition
S_1	Probability of surviving from release at Sacramento to the first junction at Steamboat and Sutter Slough. Specifically, survival is estimated to the point of detection at telemetry stations 1 – 5.
S_2	Probability of surviving from the first junction (Steamboat/Sutter Slough) to the second junction at the DCC and Georgiana Slough. Specifically, survival is estimated from telemetry station 5 to telemetry stations 6, 7, and 8.
S_a	Probability of surviving from the entrance to Steamboat and Sutter Slough at the first junction to the exit of Steamboat and Miner Slough at their confluence with Cache Slough. Specifically, survival is estimated from telemetry stations 1 – 4 to telemetry stations 8 and 9.
S_b	Probability of surviving from the second junction to just upstream of the mouth of the Sacramento River at its confluence with Cache Slough. Specifically, with the DCC open, survival is estimated from telemetry station 8 to telemetry stations 9 and 10. With the DCC closed, survival is estimated from telemetry station 7 to station 10.
S_c	Probability of surviving from the entrance to Georgiana Slough to the exit of Georgiana Slough at its confluence with the North Fork Mokelumne River. Specifically, with the DCC open, survival is estimated from telemetry station 7 to station 11. With the DCC closed, survival is estimated from telemetry station 6 to station 12 and 13
S_d	Probability of surviving from the entrance of the DCC to the exit of the North and South Fork Mokelumne rivers. Specifically, survival is estimated from telemetry station 6 to stations 12 and 13.
A	Probability of migrating through Steamboat or Sutter Slough, given that fish survived to the first junction.
(1-A)	Probability of remaining in the Sacramento River at its junction with Steamboat and Sutter Slough, given that fish survived to this junction.
A1	Probability of entering Sutter Slough, given that fish entered either Steamboat or Sutter Slough.
A2	Probability of entering Steamboat Slough, given that fish entered either Steamboat or Sutter Slough.
D	Probability of migrating through the Delta Cross Channel, given that fish survived to the second junction
(1-D)	Probability of migrating through either the mainstem Sacramento River or Georgiana Slough, given that fish survived to this junction.
B	For DCC open, probability of migrating through the mainstem Sacramento River, given that fish did not enter the DCC. For DCC closed, probability of migrating through the mainstem Sacramento River given that fish survived to the second junction.
C	For DCC open, probability of migrating through Georgiana Slough, given that fish did not enter the Delta Cross Channel. For DCC closed, probability of migrating through Georgiana Slough given that fish survived to the second junction.
λ_{ab}	Joint probability of surviving from telemetry stations 8, 9, and 10 to station 11 and being detected at station 11.
λ_{cd}	Joint probability of surviving from telemetry stations 11, 12, and 13 to station 14 and 15 and being detected at station 14 and 15.

Table B.2. Definition of probabilities that are estimated as functions of model parameters.

Parameter	Function	Definition
S_{sac}	$S_1 * S_2 * S_b$	Probability of surviving from release to the mouth of Sacramento River near its confluence with Cache Slough, given that fish remained in the Sacramento River. Specifically, survival is estimated from the release point to telemetry station 9 and 10 (for DCC open) or to station 10 (for DCC closed).
PR_{sac1}	1-A	Probability of remaining in the Sacramento River at its junction with Steamboat and Sutter Slough, given that fish survived to this junction.
PR_{sut}	$A * A_1$	Probability of entering Sutter Slough given that fish survived to this junction.
PR_{stm}	$A * (1 - A_1)$	Probability of entering Steamboat Slough given that fish survived to this junction.
PR_{sac2}	$(1 - D) * B$ or B	Probability of remaining in the Sacramento River at junction 2 given that fish survived to this junction.
PR_{dcc}	D	Probability of migrating through the Delta Cross Channel, given that fish survived to this junction.
PR_{gg}	$(1 - D) * (1 - B)$ or (1-B)	Probability of migrating through Georgiana Slough given that fish survived to this junction.
PR_{sac12}	$PR_{sac1} * PR_{sac2}$	Probability of remaining in the Sacramento after passing the first and second junction, given that fish survived between junction 1 and 2. This parameter estimates the proportion of the population that migrates through the mainstem Sacramento River, and its complement $(1 - PR_{sac12})$ estimates the proportion of the population using other routes.
PR_{cd}	$PR_{sac1} * PR_{gg}$ or $PR_{sac1} * (PR_{gg} + PR_{dcc})$	Probability of entering the central Delta. Specifically, the joint probability of remaining in the Sacramento at the first junction and entering the central Delta via Georgiana Slough or the Delta Cross Channel, given that fish survived from junction 1 to junction 2. This parameter estimates the proportion of the population entering the central Delta and accounts for fish that bypass the second junction by using Steamboat and Sutter Slough.
P_{a1}	$1 - (1 - P_{a11}) * (1 - P_{a12})$	Overall probability of detection for telemetry stations 1 & 2
P_{a2}	$1 - (1 - P_{a21}) * (1 - P_{a22})$	Overall probability of detection for telemetry stations 3 & 4
P_{b2}	$1 - (1 - P_{b21}) * (1 - P_{b22})$	Overall probability of detection for telemetry stations 12 & 13 for DCC closed
P_{c2}	$1 - (1 - P_{c21}) * (1 - P_{c22})$	Overall probability of detection for telemetry stations 9 & 10 for DCC open

Table B.3. Probability statements for each detection history that compose the maximum likelihood function of the primary likelihood for the DCC open.

Detection history	Probability function
1A1	$S_1 * A * A_1 * P_{a1}$
1A2	$S_1 * A * (1 - A_1) * P_{a2}$
10000	$1 - S_1 + S_1 * (A * A_1 * (1 - P_{a1}) + A * (1 - A_1) * (1 - P_{a2}) + (1 - A) * (1 - P_1) * (1 - S_2 + S_2 * ((1 - D) * B * (1 - P_{b1}) * (1 - S_b + S_b * (1 - P_{b2}))) + (1 - D) * (1 - B) * (1 - P_{c1}) * (1 - S_c + S_c * (1 - P_{c2}) * (1 - \lambda_{cd})) + D * (1 - P_{d1}) * (1 - S_d + S_d * (1 - P_{d2}) * (1 - \lambda_{cd}))))$
11000	$S_1 * (1 - A) * P_1 * (1 - S_2 + S_2 * ((1 - D) * B * (1 - P_{b1}) * (1 - S_b + S_b * (1 - P_{b2}))) + (1 - D) * (1 - B) * (1 - P_{c1}) * (1 - S_c + S_c * (1 - P_{c2}) * (1 - \lambda_{cd})) + D * (1 - P_{d1}) * (1 - S_d + S_d * (1 - P_{d2}) * (1 - \lambda_{cd}))))$
11BB	$S_1 * (1 - A) * P_1 * S_2 * (1 - D) * B * P_{b1} * S_b * P_{b2}$
10BB	$S_1 * (1 - A) * (1 - P_1) * S_2 * (1 - D) * B * P_{b1} * S_b * P_{b2}$
110B	$S_1 * (1 - A) * P_1 * S_2 * (1 - D) * B * (1 - P_{b1}) * S_b * P_b$
100B	$S_1 * (1 - A) * (1 - P_1) * S_2 * (1 - D) * B * (1 - P_{b1}) * S_b * P_{b2}$
11B0	$S_1 * (1 - A) * P_1 * S_2 * (1 - D) * B * P_{b1} * (1 - S_b + S_b * (1 - P_{b2}))$
10B0	$S_1 * (1 - A) * (1 - P_1) * S_2 * (1 - D) * B * P_{b1} * (1 - S_b + S_b * (1 - P_{b2}))$
11CCC	$S_1 * (1 - A) * P_1 * S_2 * (1 - D) * (1 - B) * P_{c1} * S_c * P_{c2} * \lambda_{cd}$
10CCC	$S_1 * (1 - A) * (1 - P_1) * S_2 * (1 - D) * (1 - B) * P_{c1} * S_c * P_{c2} * \lambda_{cd}$
11CC0	$S_1 * (1 - A) * P_1 * S_2 * (1 - D) * (1 - B) * P_{c1} * S_c * P_{c2} * (1 - \lambda_{cd})$
10CC0	$S_1 * (1 - A) * (1 - P_1) * S_2 * (1 - D) * (1 - B) * P_{c1} * S_c * P_{c2} * (1 - \lambda_{cd})$
11C0C	$S_1 * (1 - A) * P_1 * S_2 * (1 - D) * (1 - B) * P_{c1} * S_c * (1 - P_{c2}) * \lambda_{cd}$
10C0C	$S_1 * (1 - A) * (1 - P_1) * S_2 * (1 - D) * (1 - B) * P_{c1} * S_c * (1 - P_{c2}) * \lambda_{cd}$
11C00	$S_1 * (1 - A) * P_1 * S_2 * (1 - D) * (1 - B) * P_{c1} * (1 - S_c + S_c * (1 - P_{c2})) * (1 - \lambda_{cd})$
10C00	$S_1 * (1 - A) * (1 - P_1) * S_2 * (1 - D) * (1 - B) * P_{c1} * (1 - S_c + S_c * (1 - P_{c2})) * (1 - \lambda_{cd})$
110CC	$S_1 * (1 - A) * P_1 * S_2 * (1 - D) * (1 - B) * (1 - P_{c1}) * S_c * P_{c2} * \lambda_{cd}$
100CC	$S_1 * (1 - A) * (1 - P_1) * S_2 * (1 - D) * (1 - B) * (1 - P_{c1}) * S_c * P_{c2} * \lambda_{cd}$
110C0	$S_1 * (1 - A) * P_1 * S_2 * (1 - D) * (1 - B) * (1 - P_{c1}) * S_c * P_{c2} * (1 - \lambda_{cd})$
100C0	$S_1 * (1 - A) * (1 - P_1) * S_2 * (1 - D) * (1 - B) * (1 - P_{c1}) * S_c * P_{c2} * (1 - \lambda_{cd})$
11DDD	$S_1 * (1 - A) * P_1 * S_2 * D * P_{d1} * S_d * P_{d2} * \lambda_{cd}$
10DDD	$S_1 * (1 - A) * (1 - P_1) * S_2 * D * P_{d1} * S_d * P_{d2} * \lambda_{cd}$
11DD0	$S_1 * (1 - A) * P_1 * S_2 * D * P_{d1} * S_d * P_{d2} * (1 - \lambda_{cd})$
10DD0	$S_1 * (1 - A) * (1 - P_1) * S_2 * D * P_{d1} * S_d * P_{d2} * (1 - \lambda_{cd})$
11D0D	$S_1 * (1 - A) * P_1 * S_2 * D * P_{d1} * S_d * (1 - P_{d2}) * \lambda_{cd}$
10D0D	$S_1 * (1 - A) * (1 - P_1) * S_2 * D * P_{d1} * S_d * (1 - P_{d2}) * \lambda_{cd}$
11D00	$S_1 * (1 - A) * P_1 * S_2 * D * P_{d1} * (1 - S_d + S_d * (1 - P_{d2})) * (1 - \lambda_{cd})$
10D00	$S_1 * (1 - A) * (1 - P_1) * S_2 * D * P_{d1} * (1 - S_d + S_d * (1 - P_{d2})) * (1 - \lambda_{cd})$
110DD	$S_1 * (1 - A) * P_1 * S_2 * D * (1 - P_{d1}) * S_d * P_{d2} * \lambda_{cd}$
100DD	$S_1 * (1 - A) * (1 - P_1) * S_2 * D * (1 - P_{d1}) * S_d * P_{d2} * \lambda_{cd}$
110D0	$S_1 * (1 - A) * P_1 * S_2 * D * (1 - P_{d1}) * S_d * P_{d2} * (1 - \lambda_{cd})$
100D0	$S_1 * (1 - A) * (1 - P_1) * S_2 * D * (1 - P_{d1}) * S_d * P_{d2} * (1 - \lambda_{cd})$
1100D	$S_1 * (1 - A) * P_1 * S_2 * (D * (1 - P_{d1}) * S_d * (1 - P_{d2}) * \lambda_{cd} + (1 - D) * (1 - B) * (1 - P_{c1}) * S_c * (1 - P_{c2}) * \lambda_{cd})$
1000D	$S_1 * (1 - A) * (1 - P_1) * S_2 * (D * (1 - P_{d1}) * S_d * (1 - P_{d2}) * \lambda_{cd} + (1 - D) * (1 - B) * (1 - P_{c1}) * S_c * (1 - P_{c2}) * \lambda_{cd})$

Table B.4. Probability statements for each detection history that compose the maximum likelihood function of the primary likelihood for the DCC closed.

Detection history	Probability function
10000	$1-S_1+S_1*(A*(A_1*(1-P_{a1})+(1-A_1)*(1-P_{a2}))*(1-S_a+S_a*(1-P_{a3})*(1-\lambda_{ab}))+((1-A)*(1-P_1)*(1-S_2+S_2*(B*(1-P_{b1})*(1-S_b+S_b*(1-P_{b2})*(1-\lambda_{ab}))+((1-B)*(1-P_{c1})*(1-S_c+S_c*(1-P_{c2}))))))$
11000	$S_1*(1-A)*P_1*(1-S_2+S_2*(B*(1-P_{b1})*(1-S_b+S_b*(1-P_{b2})*(1-\lambda_{ab}))+((1-B)*(1-P_{c1})*(1-S_c+S_c*(1-P_{c2}))))$
1A1AA	$S_1*A*A_1*P_{a1}*S_a*P_{a3}*\lambda_{ab}$
1A10A	$S_1*A*A_1*P_{a1}*S_a*(1-P_{a3})*\lambda_{ab}$
1A1A0	$S_1*A*A_1*P_{a1}*S_a*P_{a3}*(1-\lambda_{ab})$
1A100	$S_1*A*A_1*P_{a1}*(1-S_a+S_a*(1-P_{a3})*(1-\lambda_{ab}))$
1A2AA	$S_1*A*(1-A_1)*P_{a2}*S_a*P_{a3}*\lambda_{ab}$
1A20A	$S_1*A*(1-A_1)*P_{a2}*S_a*(1-P_{a3})*\lambda_{ab}$
1A2A0	$S_1*A*(1-A_1)*P_{a2}*S_a*P_{a3}*(1-\lambda_{ab})$
1A200	$S_1*A*(1-A_1)*P_{a2}*(1-S_a+S_a*(1-P_{a3})*(1-\lambda_{ab}))$
10AA	$S_1*A*(A_1*(1-P_{a1})+(1-A_1)*(1-P_{a2}))*S_a*P_{a3}*\lambda_{ab}$
10A0	$S_1*A*(A_1*(1-P_{a1})+(1-A_1)*(1-P_{a2}))*S_a*P_{a3}*(1-\lambda_{ab})$
100A	$S_1*A*(A_1*(1-P_{a1})+(1-A_1)*(1-P_{a2}))*S_a*(1-P_{a3})*\lambda_{ab}$
11BBB	$S_1*(1-A)*P_1*S_2*B*P_{b1}*S_b*P_{b2}*\lambda_{ab}$
10BBB	$S_1*(1-A)*(1-P_1)*S_2*B*P_{b1}*S_b*P_{b2}*\lambda_{ab}$
110BB	$S_1*(1-A)*P_1*S_2*B*(1-P_{b1})*S_b*P_{b2}*\lambda_{ab}$
100BB	$S_1*(1-A)*(1-P_1)*S_2*B*(1-P_{b1})*S_b*P_{b2}*\lambda_{ab}$
11B0B	$S_1*(1-A)*P_1*S_2*B*P_{b1}*S_b*(1-P_{b2})*\lambda_{ab}$
10B0B	$S_1*(1-A)*(1-P_1)*S_2*B*P_{b1}*S_b*(1-P_{b2})*\lambda_{ab}$
1100B	$S_1*(1-A)*P_1*S_2*B*(1-P_{b1})*S_b*(1-P_{b2})*\lambda_{ab}$
1000B	$S_1*(1-A)*(1-P_1)*S_2*B*(1-P_{b1})*S_b*(1-P_{b2})*\lambda_{ab}$
11BB0	$S_1*(1-A)*P_1*S_2*B*P_{b1}*S_b*P_{b2}*(1-\lambda_{ab})$
10BB0	$S_1*(1-A)*(1-P_1)*S_2*B*P_{b1}*S_b*P_{b2}*(1-\lambda_{ab})$
110B0	$S_1*(1-A)*P_1*S_2*B*(1-P_{b1})*S_b*P_{b2}*(1-\lambda_{ab})$
100B0	$S_1*(1-A)*(1-P_1)*S_2*B*(1-P_{b1})*S_b*P_{b2}*(1-\lambda_{ab})$
11B00	$S_1*(1-A)*P_1*S_2*B*P_{b1}*(1-S_b+S_b*(1-P_{b2})*(1-\lambda_{ab}))$
10B00	$S_1*(1-A)*(1-P_1)*S_2*B*P_{b1}*(1-S_b+S_b*(1-P_{b2})*(1-\lambda_{ab}))$
11CC	$S_1*(1-A)*P_1*S_2*(1-B)*P_{c1}*S_c*P_{c2}$
10CC	$S_1*(1-A)*(1-P_1)*S_2*(1-B)*P_{c1}*S_c*P_{c2}$
110C	$S_1*(1-A)*P_1*S_2*(1-B)*(1-P_{c1})*S_c*P_{c2}$
100C	$S_1*(1-A)*(1-P_1)*S_2*(1-B)*(1-P_{c1})*S_c*P_{c2}$
11C0	$S_1*(1-A)*P_1*S_2*(1-B)*P_{c1}*(1-S_c+S_c*(1-P_{c2}))$
10C0	$S_1*(1-A)*(1-P_1)*S_2*(1-B)*P_{c1}*(1-S_c+S_c*(1-P_{c2}))$

Table B.5. Secondary likelihoods used for estimating detection probabilities of double detection arrays for the DCC open.

Detection History	Probability function
A10	$P_{a11}*(1-P_{a12})/P_{a1}$
0A1	$P_{a12}*(1-P_{a11})/P_{a1}$
A1A1	$P_{a11}*P_{a12}/P_{a1}$
A20	$P_{a21}*(1-P_{a22})/P_{a2}$
0A2	$P_{a22}*(1-P_{a21})/P_{a2}$
A2A2	$P_{a21}*P_{a22}/P_{a2}$
B0	$P_{b21}*(1-P_{b22})/P_{b2}$
0B	$P_{b22}*(1-P_{b21})/P_{b2}$
BB	$P_{b21}*P_{b22}/P_{b2}$

Table B.6. Secondary likelihoods used for estimating detection probabilities of double detection arrays for the DCC closed.

Detection history	Probability function
A10	$P_{a11}*(1-P_{a12})/P_{a1}$
0A1	$P_{a12}*(1-P_{a11})/P_{a1}$
A1A1	$P_{a11}*P_{a12}/P_{a1}$
A20	$P_{a21}*(1-P_{a22})/P_{a2}$
0A2	$P_{a22}*(1-P_{a21})/P_{a2}$
A2A2	$P_{a21}*P_{a22}/P_{a2}$
C0	$P_{c21}*(1-P_{c22})/P_{c2}$
0C	$P_{c22}*(1-P_{c21})/P_{c2}$
CC	$P_{c21}*P_{c22}/P_{c2}$

Table B.7. Frequencies of detection histories with the Delta Cross Channel open for the pilot study conducted during the winter of 2006/2007.

Detection history	Frequency
1A1	18
1A2	3
10000	15
11000	4
11BB	28
10BB	0
110B	0
100B	0
11B0	7
10B0	0
11CCC	4
10CCC	0
11CC0	0
10CC0	0
11C0C	2
10C0C	0
11C00	5
10C00	0
110CC	0
100CC	0
110C0	0
100C0	0
11DDD	2
10DDD	0
11DD0	1
10DD0	1
11D0D	0
10D0D	0
11D00	6
10D00	0
110DD	0
100DD	0
110D0	0
100D0	0
1100D	0
1000D	0

Table B.8. Frequencies of detection histories with the Delta Cross Channel closed for the pilot study conducted during the winter of 2006/2007.

Detection history	Frequency
10000	53
11000	9
1A1AA	11
1A10A	0
1A1A0	6
1A100	12
1A2AA	4
1A20A	0
1A2A0	0
1A200	3
10AA	0
10A0	0
100A	0
11BBB	24
10BBB	0
110BB	0
100BB	0
11B0B	0
10B0B	0
1100B	0
1000B	0
11BB0	0
10BB0	0
110B0	0
100B0	0
11B00	13
10B00	0
11CC	4
10CC	0
110C	0
100C	0
11C0	11
10C0	0

Table B.9. Detection histories for the three double detection arrays (stations 1 and 2, 3 and 4, 9 and 10, see [Figure 2](#)) used while DCC was open for the pilot study conducted during the winter of 2006/2007.

Telemetry station	Detection history	Frequency
1 and 2	11	18
	01	0
	10	0
3 and 4	11	3
	01	0
	10	0
9 and 10	11	24
	01	0
	10	4

Table B.10. Detection histories for the three double detection arrays (stations 1 and 2, 3 and 4, 12 and 13, see [Figure 3](#)) used while DCC was closed for the pilot study conducted during the winter of 2006/2007. Detection histories indicate whether fish were detected at both telemetry stations (11), just the first station (10), or just the second station (01).

Telemetry stations	Detection history	Frequency
1 and 2	11	28
	01	0
	10	1
3 and 4	11	7
	01	0
	10	0
12 and 13	11	4
	01	0
	10	0

Results and Discussion

Our telemetry deployment design succeeded in providing the data needed to estimate important biological parameters in the North Delta. Detection probabilities were very high, with most telemetry stations having detection probabilities of 1.0. High detection probabilities have positive benefits on the other parameter estimates by reducing uncertainty in the fate of each fish. Thus, standard errors of the estimates were small and confidence intervals were narrow relative to the small sample size of tagged fish used in this pilot study. Only one telemetry station at the exit of Georgiana slough (with DCC open, station 11 in Figure B.2) had a low detection probability of 0.60 (P_{c2} in Figure B.4). Low detection probabilities at this site when the DCC was open led to a large standard error of 0.178 on the survival probability of Georgiana Slough (S_c , Table B.11). In contrast, standard errors for survival probability in the Sacramento River (S_1, S_2, S_b, S_{sac}) ranged from 0.033 to 0.079 (Table B.11). This contrast in standard errors is a good example of the effect of low detection probabilities on the uncertainty of survival probability in the Sacramento River. Standard errors for the other routes were larger than those for the Sacramento River, owing largely to the smaller sample size of fish migrating through the secondary channels.

As far as we are aware, our pilot study also obtained the first quantitative estimates of how juvenile salmon are distributed among possible migration routes of the North Delta. We also observed differences among the two river conditions in the proportional use of these routes. When the Delta Cross Channel was open, about 74% of fish remained in the Sacramento river at its junction with Sutter and Steamboat Sloughs (PR_{sac1} , Table B.11, Figure B.6), with the remainder migrating via Sutter (22%, PR_{sut}) and Steamboat (4%, PR_{stm}) sloughs (Table 11, Figure B.6). In contrast, when the DCC was closed a higher proportion of fish used Steamboat and Sutter Sloughs, with 63% remaining in the Sacramento River, 30% entering Sutter Slough, and 7% entering Steamboat Slough (Table B.11, Figure B.7). At the second river junction, about 62% of the fish at that junction remained in the Sacramento River (PR_{sac2}) with the remainder split nearly equally between the Delta Cross Channel (18%, PR_{dcc}) and Georgiana Slough (20%, PR_{gg} , Table B.11, Figure B.6). When the DCC was closed, a higher proportion of fish remained in the Sacramento River (71%), but the fraction entering Georgiana Slough also increased to 29% (Table B.11, Figure B.7). Although we observed differences in these parameters among DCC operations, it is important to note that other factors (such as total river discharge) also differed, which could have contributed to the observed results.

Given the multiple migration routes, it is important to understand the fraction of the population that migrates into the Central and Southern Delta where lower survival is hypothesized relative to the Sacramento River. The route selection probabilities described above, however, are “junction specific” and do not account for the combined effect of both junctions. For example, although about 30-40% of fish at the second junction entered the Central Delta, some of the population bypassed the second junction altogether by using Steamboat and Sutter Slough. Assuming no mortality between the two junctions, if 70% remained in the Sacramento River at the first junction and 40% entered the Central Delta at the second junction, then overall, only 28% of the population entered the Central Delta (i.e., $0.70 * 0.40 = 0.28$). Therefore, taking this approach, we derived two summary statistics to estimate the combined effect of both channel junctions on fish distribution in the North Delta. The first, as described above, estimates the proportion of the population entering the Central Delta by factoring out survival between the two junctions and accounting for fish using Steamboat and Sutter Slough (PR_{cd} , see Table B.2 for equation). When the DCC was open, about

28% of the population entered the Central Delta, but when the DCC was closed 18% of the population entered the Central Delta (See PR_{cd} in Table B.11). The lower proportion with the DCC closed was due to the combined effect of a higher proportion of fish entering Steamboat and Sutter Slough and a lower proportion entering Georgiana Slough (compared to the combined proportion entering Georgiana + DCC when the DCC was open) at the second junction.

The second summary statistic estimates the proportion of the population that remains in the Sacramento River after passing both junctions (PR_{sac12} , see Table B.2 for equation), and again, survival between junctions is factored out. The complement of this parameter ($1-PR_{sac12}$) estimates the overall proportion of fish that used routes other than the Sacramento River. This parameter provides insight into how different river conditions affect the overall proportion of fish that use secondary routes to migrate through the Delta. For example, nearly equal proportions of the population used the Sacramento River regardless of whether the DCC was open ($PR_{sac12} = 0.463$) or closed ($PR_{sac12} = 0.447$, Table B.11). Although speculative at this stage, these findings could suggest that changes in DCC operations do not affect the overall proportion of fish using secondary routes, but rather affects the relative tradeoffs among the secondary routes at the first and second junction. This assertion is corroborated by observations that operation of the DCC affects not only discharge of channels at this junction, but also affects the magnitude of discharge entering Steamboat and Sutter Slough (see Appendix A).

Table B.11. Estimates of survival and route-selection probabilities for the pilot study conducted in the North Delta during the winter of 2006/2007. Parameter definitions are given in Table 1 and 2. Standard errors are shown in parentheses and 95% confidence intervals were calculated from the likelihood profile. Detection probabilities (P_j) for most telemetry stations were 1.0, and thus are not shown here.

Parameter	<u>Delta Cross Channel Open</u>		<u>Delta Cross Channel Closed</u>	
	Estimate (SE)	95% Confidence Interval	Estimate (SE)	95% Confidence Interval
S_1	0.845 (0.037)	0.763 - 0.908	0.647 (0.039)	0.568 - 0.720
S_2	0.933 (0.033)	0.850 - 0.979	0.853 (0.045)	0.750 - 0.927
S_b	0.800 (0.068)	0.649 - 0.909	0.649 (0.079)	0.488 - 0.789
S_a	NA		0.583 (0.082)	0.421 - 0.735
S_c	0.606 (0.178)	0.290 - 1.042	0.266 (0.114)	0.091 - 0.515
S_d	0.400 (0.155)	0.146 - 0.700	NA	
S_{sac}	0.630 (0.064)	0.498 - 0.745	0.358 (0.052)	0.259 - 0.460
PR_{sac1}	0.741 (0.049)	0.639 - 0.828	0.629 (0.049)	0.530 - 0.721
PR_{sut}	0.222 (0.046)	0.141 - 0.320	0.299 (0.046)	0.214 - 0.394
PR_{stm}	0.037 (0.021)	0.009 - 0.093	0.072 (0.026)	0.032 - 0.135
PR_{sac2}	0.625 (0.065)	0.495 - 0.744	0.711 (0.063)	0.580 - 0.822
PR_{dcc}	0.179 (0.051)	0.094 - 0.292	NA	
PR_{gg}	0.196 (0.053)	0.107 - 0.313	0.289 (0.063)	0.178 - 0.420
PR_{sac12}	0.463 (0.057)	0.354 - 0.574	0.447 (0.048)	0.346 - 0.551
PR_{cd}	0.278 (0.051)	0.186 - 0.384	0.181 (0.041)	0.109 - 0.272
λ_{cd}	0.750 (0.153)	0.409 - 0.953	NA	
λ_{ab}	NA		0.867 (0.051)	0.748 - 0.945

In general, survival probabilities were highest for the mainstem Sacramento River compared to secondary routes, and survival when the DCC was open was higher than when the DCC was closed (Table B.11, Figure B.6 and B.7). When the DCC was open, survival for the three reaches of the Sacramento River was 0.84, 0.93, and 0.80 (S_1 , S_2 , and S_b , respectively; Table B.11, Figure B.6). In contrast, survival for Georgiana slough was 0.61, and for fish passing through the DCC survival was 0.40 (S_c and S_d , respectively; Table B.11, Figure B.6). Combined over all three reaches, survival of fish that remained in the Sacramento was 0.63 from the point of release to mouth of the Sacramento near Cache Slough (S_{sac} , Table B.11). When the DCC was closed, survival through the three reaches of the Sacramento was 0.65, 0.85, and 0.65 (Table B.11, Figure B.7). In comparison, survival through Steamboat and Sutter Slough was 0.58, and through Georgiana Slough survival was 0.27 (S_a and S_c , respectively; Table B.11, Figure B.7). Combined over all three reaches of the Sacramento River, survival was 0.36 from the point of release to the mouth of the Sacramento River near Cache Slough.

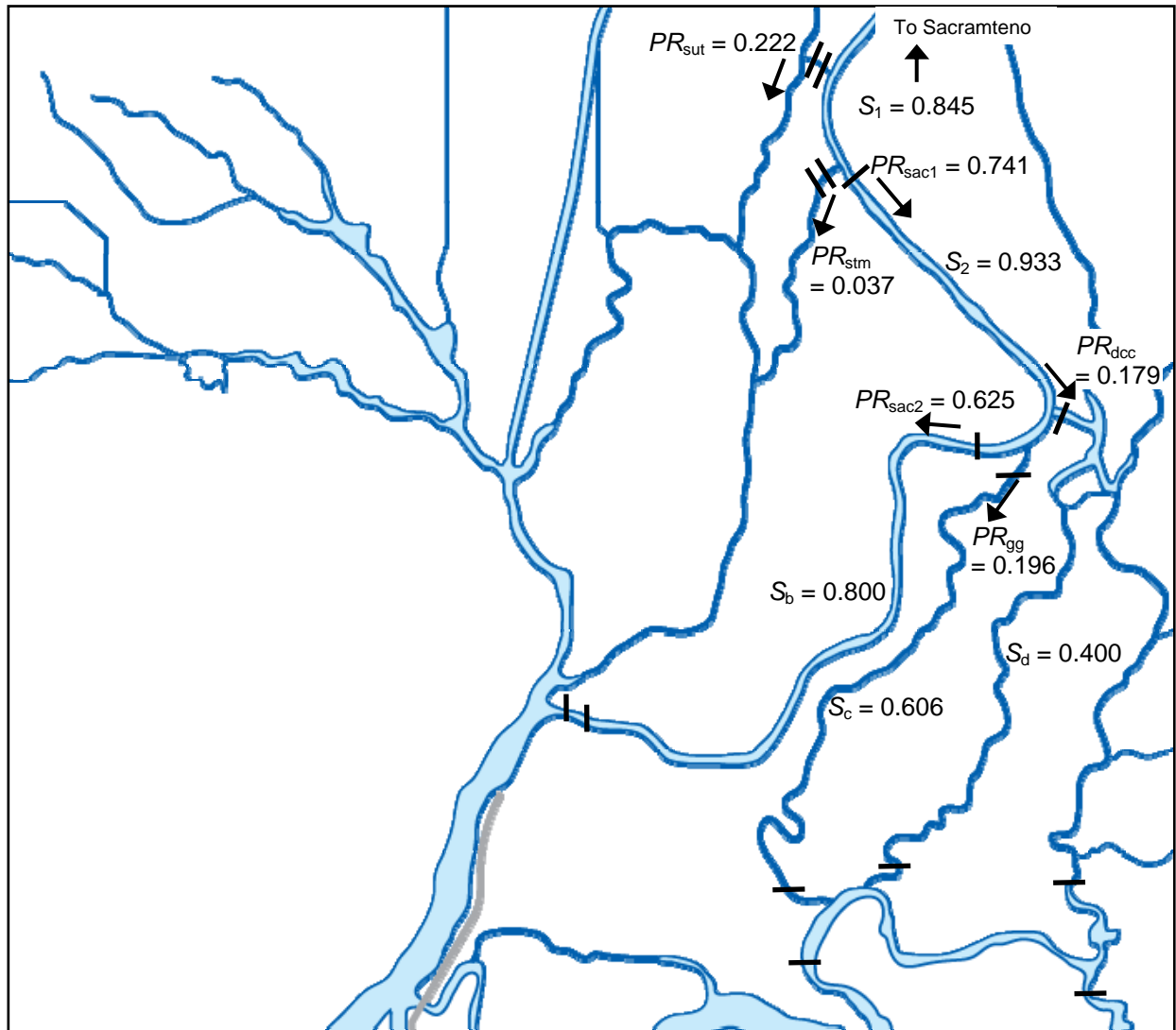


Figure B.6. Selected parameter estimates with the Delta Cross Channel open for the pilot study conducted during the winter of 2006/2007. Survival (S_i) probabilities are shown next to each reach and are bounded by telemetry stations on the upstream and downstream end of each reach. Route selection probabilities (PR_i) are shown next to arrows at each channel junction. See Table B.1 and B.2 for detailed definitions of each parameters estimate.

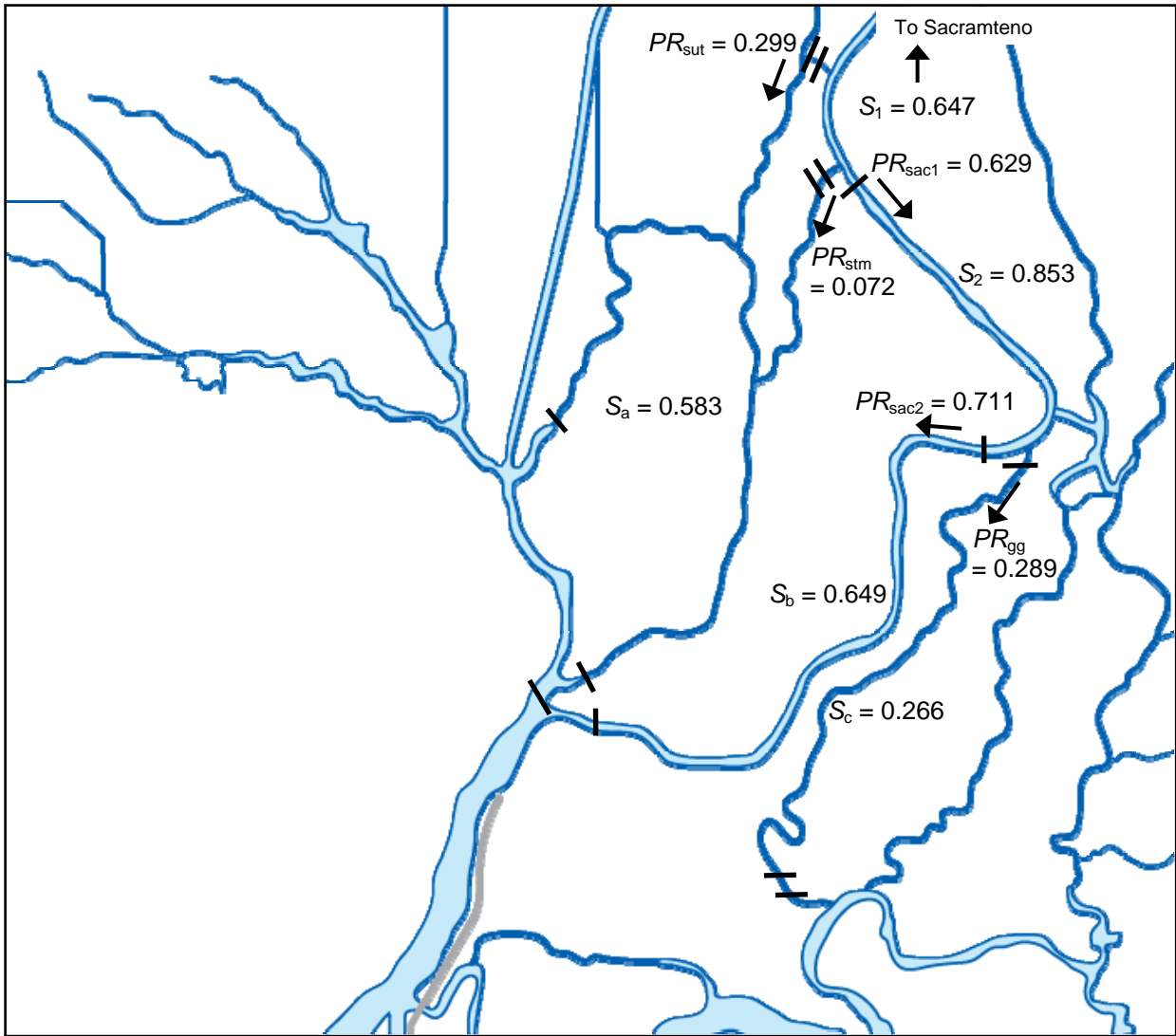


Figure B.7. Selected parameter estimates with the Delta Cross Channel closed for the pilot study conducted during the winter of 2006/2007. Survival (S_i) probabilities are shown next to each reach and are bounded by telemetry stations on the upstream and downstream end of each reach. Route selection probabilities (PR_i) are shown next to arrows at each channel junction. See Table B.1 and B.2 for detailed definitions of each parameters estimate.

References

- Brownie, C., J. E. Hines, J. D. Nichols, K. H. Pollock, and J. B. Hestbeck. 1993. Capture-recapture studies for multiple strata including non-markovian transitions. *Biometrics*. 49: 1173-1187.
- Cormack, R. M. 1964. Estimates of survival from the sighting of marked animals. *Biometrika* 51:429-438
- Counihan, T. D., Holmberg, G. S., Walker, C. E., and Hardiman, J. M. 2003. Survival estimates of migrant juvenile salmonids in the Columbia River through John Day Dam using radio-telemetry, 2003. Final Report of Research by the U.S. Geological Survey to the U.S. Army Corps of Engineers, Portland District, Portland, Oregon
- Jolly, G. M. 1965. Explicit estimates from capture-recapture data with both death and immigration-stochastic model. *Biometrika* 52:225-247
- Perry, R.W., A.C. Braatz, S.D. Fielding, J.N. Lucchesi, J.M. Plumb, N.S. Adams, and D.W. Rondorf. 2006. Survival and migration behavior of juvenile salmonids at McNary Dam, 2004. Final Report of Research by the U. S. Geological Survey to the U.S. Army Corps of Engineers, Walla Walla District, Contract W68SBV40271050, Walla Walla, Washington
- Schwarz, C.J, J. F. Schweigert, and A. N. Arnason. 1993. Estimating migration rates using tag-recovery data. *Biometrics*. 49: 177-193
- Seber, G. A. F. 1965. A note on the multiple recapture census. *Biometrika* 52:249-259
- Skalski, J. R., R. Townsend, J. Lady, A. E. Giorgi, J. R. Stevenson, and R.S. McDonald. 2002. Estimating route-specific passage and survival probabilities at a hydroelectric project from smolt radiotelemetry studies. *Canadian Journal of Fisheries and Aquatic Sciences* 59:1385-1393

Appendix C – Preliminary Results from Acoustic Tracking in Clarksburg Bend, January 2007

Fundamentals of Acoustic Tag Tracking

An explicit goal of Delta juvenile salmon studies has been to develop a tool-independent approach to analyzing juvenile outmigration dynamics, so that data from diverse physical and biological measurements can be combined in a real-world data space, with minimal effort expended on interpreting data in an instrument's native format. Past analysis of split beam transducer data acquired at the DCC and Georgiana Slough focused on interpreting four dimensional fish position data, rather than extracting information from raw echograms illustrates the significant effort required to convert a measurement into a real-world signal. Currently, this effort is considered a pre-processing step in the analysis of salmon outmigration data; however, given the quasi-experimental nature of multidimensional acoustic tag tracking technology, analysis and interpretation of this data must explicitly focus on understanding and improving the pre-processing steps. For this reason, a basic understanding of the acoustic tag tracking process is an essential foundation for interpreting and evaluating fish track data, and for discussions of future analysis needs. For the purposes of this proposal, the following discussion of the acoustic tracking process will focus on the use of HTTP's current acoustic tracking software for their 290 hardware series.

Tracking Process

Although it is in practice quite complex, the acoustic tag tracking process is conceptually simple; fish are surgically implanted with small acoustic transmitters and then released into the study reach, as fish move through the study area their tag's acoustic signal is recorded by an array of hydrophones at known locations, and the relative timing of that signal's arrival at each hydrophone is used to calculate the position of the fish. The process of collecting and processing the acoustic signals emitted by each fish (tag) is often referred to generically as "tracking", however, for clarity it is best to consider this process in three steps; echo acquisition, tag marking, and tag tracking.

Echo Acquisition

During echo acquisition analog voltage signals from each hydrophone are carried by underwater cables to the Acoustic Tag Receiver (ATR), where they are digitized by the ATR's Analog to Digital Converter (ADC) boards. The analog voltage signals from each hydrophone are the output of an analog cross-correlation filter that compares incoming acoustic signals to a model acoustic tag signal; under ideal conditions an acoustic tag echo processed by this filter should produce a near-triangular voltage signal, with the signal's peak corresponding to the arrival time for the tag's echo. Every time acoustic energy is received by hydrophones, the ADCs within an ATR digitize the cross-correlation signal from each hydrophone, analyze the digital data to find the peak of each hydrophone's cross-correlation, and report the time that the peak was detected as the arrival time of the acoustic pulse. Arrival time peaks for every cross-correlation signal are recorded in a raw data file called a RAT file, along with information on the magnitude and shape of the signal. Although these details may seem esoteric to an end user, they are important because the digitization of the cross-correlation signal determines the native resolution of the system's raw data. HTTP's family of 290 series ATRs uses ADCs with 12kHz clocks, which can resolve the peak of a near-triangular signal to +/- one clock tick. Given a nominal speed of sound in fresh water of about 1500 m/s, this temporal resolution ambiguity means that under ideal conditions the best precision the system can achieve in estimating the distance from an acoustic transmitter to an individual hydrophone is +/- .125m. It is important to note that this resolution is not the precision of a tag position estimate, but an estimate of the native resolution of the raw acoustic data used to estimate tag positions.

Tag marking

After data acquisition is finished in the field, the next step is to select, or “mark” the acoustic information in each RAT file produced by tag pings, so that tag data can be separated from background noise. Information from a RAT file associated with tag detections is stored in a TAT file, which has the same format as a RAT but without information associated with noise events. The creation of TAT files used for generating fish positions is automated using HTI’s Mark Tags software. Mark Tags does an adequate job at identifying echoes associated with persistent tag detections in environments with low ambient acoustic noise, but fails to match human performance in noisy environments, or in detecting very short tag events. Current standard operating procedures for processing TAT files for survival estimates require human verification of each automatically generated TAT file. While human proofing of TAT files has a high success of eliminating false tag detections (false positives), this process is not as likely to identify tag data missed by the automated routine (false negatives), which means that TAT generation during tag marking is likely to introduce a slightly negative bias in survival estimates based on this approach.

Tag Tracking

Once TAT files are generated, they are processed in HTI’s proprietary software to generate three dimensional estimates of tag (fish) positions. The details of this process are proprietary, but the algorithm can be summarized in 3 steps: data filtering, hydrophone choice, and position calculation. During the first step, HTI’s software checks to see if a given ping will be tracked based on a series of tests controlled by user defined filter specifications. For each ping to be tracked the software selects echo data from four hydrophones to resolve the tags position; hydrophone selection is controlled via a fuzzy logic routine that is partly driven by user inputs. The software’s choice of hydrophones has a significant effect on the tag position estimate, and as a result, the user parameters that control this process often determine the quality of the final tracking data set. At the end of the tracking process tag positions are grouped together by tag code into “tracks” (referred to as “fish tracks or “tag tracks”), and stored in a project tracking database. A complete project tracking database is the final data product of the acoustic tag tracking process, and is the starting point for juvenile outmigration analysis.

Preliminary analysis of the January, 2007, tag tracking data at Clarksburg Bend.

Hydrophone configuration

During the winter of 2006/2007 36 hydrophones were used to track acoustically tagged fish moving through the Sacramento River in the vicinity of Clarksburg, CA. Thirty-two hydrophones and two 16 port ATRs were used to instrument a pronounced, 130 degree bend in the Sacramento River known as Clarksburg Bend, and four hydrophones in conjunction with a 4 port ATR were used to instrument the river approximately 1 km upstream of the bend. The 32 hydrophones in Clarksburg Bend are shown in [Figure C.1](#). Hydrophones in Clarksburg Bend were deployed in four arrays aligned perpendicular to the direction of mean flow, and numbered upstream to downstream; the outer arrays (1 and 4) were each comprised of 6 hydrophones, the inner arrays (2 and 3) each used 10 hydrophones.

Tracking Performance

River bathymetry prevented optimal hydrophone array deployment and contributed to the inability of HTI’s tag tracking algorithm to track any of the tags detected by the 4 port system. This preliminary analysis is focused only on tracks generated by the array in Clarksburg Bend. As shown in [Figure C.2](#), HTI’s software was able to track fish well outside of the individual array sections, with only a small gap in tracking between the center arrays. [Figure C.3](#) shows a representative fish track made in this region

(code 4490), and [Figure C.4](#) shows the same track inside the second hydrophone array, plotted on a 2 meter by 2 meter grid. One can see that the track shows a clear and persistent pattern of fish movement, but that there is also consistent jitter from point to point, both in the along-track and cross-track directions. In this context, jitter is defined as the deviation of a detection's position estimate from a smooth curved line fit through a path section such that the fit values of x, y, and z are a function of time. This definition allows the estimate of both cross-track and along-track jitter. Without an independent measurement of fish position it is difficult to know how much of the apparent jitter is the result of real high frequency phenomena vs. error in the position estimate, however, it is likely that the mean amplitude of real high frequency information will remain relatively constant throughout the tracking area, so changes in jitter amplitude can be considered indicative of changes in tracking precision. Positions calculated in the immediate vicinity of the hydrophone array sections displayed jitter on the order of two meters or less. Tracks made outside of hydrophone arrays show varying amount of jitter, ranging from 2 meters to as much as 10 meters. In general, tracks made between array 1 and array 2 had lower amplitude jitter than tracks made between array 3 and array 4, and tracks in the vicinity of the upper arrays tended to have fewer large discontinuities than tracks between the lower arrays ([figures C.4 and C.5](#)).

In general, less accurate position data generated in regions outside the hydrophone arrays contain useful information about juvenile salmon outmigration, but care should be taken in interpreting higher order data products generated in the regions between arrays. For example, cross-track jitter in position estimates acts to smooth the apparent spatial distribution of fish, so that spatial distributions calculated for areas outside of the main arrays will show erroneously diffuse fish concentrations. In addition, jittery tracks introduce significant bias into estimates of fish velocity; jitter in the cross-track direction will result in a consistent over estimate of fish speed, and erroneous estimates of direction, while along track jitter will cause dramatic oscillations in speed estimates, introducing little bias into direction estimates. These effects can be seen in [figure C.6](#), which shows the distribution of calculated fish speeds for each ping, which is the sum of the actual fish speed distribution and the ping-position error distribution scaled by the average ping detection frequency. Although this distribution contains information on fish speeds, the 1 to 1 signal to noise ratio between the speed distribution and the noise distribution makes it difficult to extract meaningful information without significant analytical effort; the best estimate of mean fish velocity is the distribution mode, and even that measure is probably biased due to the net positive bias introduced by cross-path jitter.

The final consideration in evaluating the tracking results is the accuracy of the estimated vertical position of the fish. [Figure C.7](#) shows the distribution of estimated fish depths for every tag detected during the January study. The most obvious feature of this distribution is the number of tags with estimated depths outside the possible range of 0m – 12m, which is a clear indication of the high level of error in the vertical position estimates. The broad peak of the depth distribution reflects the fact that the majority of the hydrophones were between 2 and 8 meters deep, and if the samples with estimated depth values outside of the possible range were added to the distribution's tails it would resemble the probability density function (PDF) for uniform random noise. It appears that most vertical position estimates are no better than large amplitude random noise added to the depth of the nearest hydrophone to the ping. Although some position estimates made in the interior of the hydrophone arrays may contain more accurate vertical position information, the process of filtering for these points without introducing a-priori biases is non-trivial, and was beyond the scope of this preliminary analysis.

Given the resolution of the raw ping data, it is likely that much of the jitter in both the horizontal and vertical position estimates is the result of the current HTI 3D tracking algorithm. The HTI software uses a minimally constrained four-hydrophone solution to calculate tag positions, this type of solution represents the least optimal, and therefore most jittery, solution for an individual position estimate. In addition, the process of switching between different four-hydrophone geometries using a fuzzy logic algorithm is inherently noisy, and is prone to producing distinct track discontinuities. Limitations in the HTI tracking algorithm were exaggerated by the average 5:1 horizontal to vertical aspect ratio of the hydrophone array, which dramatically reduced the vertical position signal to noise ratio. Despite this limitation, examination of the January TAT files suggests that most tag pings were detected by a minimum of 6-10 hydrophones, indicating that the raw data contains enough information to support the development of a more robust tracking algorithm. In addition, the jitter in the current tracking data is introduced at a relatively high frequency with respect to fish behavior, and as such, this jitter only affects the observation of high frequency phenomena such as swim speed and rheotaxis orientation. Given the January data set's large tracking region and high tag detection rates, this data is quite valuable for observing lower frequency signals such as broad patterns in the timing of fish movement and the general spatial distribution of fish passing through the bend.

Diurnal patterns in juvenile outmigration

Over the four day period that the ATRs were recording data during the January study, a total of 133 individual tagged fish were detected and tracked in Clarksburg Bend. Patterns in the timing of the arrival and detection of these fish show a clear diurnal pattern in downstream movement. As shown in [Figure C.9](#), almost all of the fish detected during the study were present in the array during dark periods ([Figure C.8](#)), and about two thirds of the fish detected were only present during dark periods. Of the fish detected during the day, three quarters of these fish were also detected at night, with only about 10 fish out of 133 (7.5%) detected during the day but not at night. Fish that were detected during the day were in the array for much longer periods than fish that were present at night, as indicated by the extremely large number of pings detected during the day ([Figure C.10](#)). Given the ratio of individual fish to total pings for day periods and night periods, it appears that on average, fish detected at night moved through the array three to four times faster than fish that were detected during the day. This observation raises the critical question: were fish detected during the day holding inside the array, or simply moving downstream at a slower rate? If fish detected during the day were moving downstream rather than holding, then the number of fish entering the array during the day should be roughly equal to the number of fish detected during the day, and conversely, a disproportionately low number of fish entering the array during the day would indicate holding behavior.

The distribution of tag first-detections shown in [Figure C.11](#) clearly shows the proportion of fish entering the array during the day to be much lower than the proportion of fish detected during the night, and further, that the vast majority (~94%) of fish entering the array did so during dark or crepuscular periods. Displaying first detections as a time series ([Figure C.12](#)) shows that the few tags which entered the array during daylight periods only did so during times when the amount of daylight was decreasing. The single fish detected moving downstream through the array during peak daylight hours was also the first fish to arrive at Clarksburg Bend, suggesting that this fish had a greater propensity for downstream movement, probably due to increased smoltification (this fish could have also been inside a predator).

The observed patterns in fish arrivals and detections are clear evidence that study fish held during peak daylight periods, and then moved into the river during the late afternoon or evening to begin downstream migration. The pattern of diurnal outmigration observed in the January 2007 data is in

good agreement with analyses of split beam echosounder data from the 2001 and 2003 studies that showed similar patterns of fish movement (Blake and Horn, (in press)a,b). In addition, the 2007 data provides an important refinement to the hypothesis of fish outmigration proposed in the 2003 analysis; rather than conceptualizing the juvenile salmon population as having a distribution of holding periods of a fixed length (Blake and Horn, (in press)b), the January 2007 data suggests that almost the entire population holds during periods of increasing daylight, and that the observed distribution of holding times is due to variance in the population's end-of-holding behavior trigger(s). Although this might seem like a small conceptual refinement, it implies that even within a population with large variance in the over-all length of daytime holding period, there are predictable periods when the vast majority of the population holds. If this is true, this observation suggests that there are easily predicted periods when the risk of entraining downstream moving fish is minimal.

Spatial Distribution of Juvenile Salmon in Clarksburg Bend

Analysis of the temporal patterns in the January data highlighted one of the advantages of using acoustic tag tracking systems – the very large tracking volume of the hydrophone array (1000m X 100m), allowed the system to observe fish that were actively holding, providing new insights into the timing of this behavior. Thus, the large measurement volume required for Lagrangian tracking increases the resolution of Eulerian information extracted from tracking data. Another advantage of large-scale tracking systems is the ability to measure the simultaneous evolution of behaviors in space and time, which can provide more detailed insights into specific behaviors. For example, [Figure C.13](#) shows a detailed track of fish 5526, with the detections colored by date/time. Fish 5526 entered Clarksburg Bend at night moving downstream in the middle of the river, eventually it was tracked moving down the outside of the bend in array 3 just before sunrise. Immediately after sunrise, fish 5526 altered its downstream movement and was tracked entering the slow water at the inside of the bend at array 4, where it held against the bank for a short period of time. After brief holding, 5526 swam upstream along the inside bank until it reached an eddy on the inside of the bend near array 2, where it held for the rest of the day. Around dusk, fish 5526 left the eddy on the inside of the bend, and moving down river, passed through array 3 in nearly the same spot it did 10 hours prior! The track shown in [Figure C.13](#) is exciting for several reasons: first, it is a direct measurement of a fish moving to slower water velocities to hold during daylight hours and then moving back into the main flow to out-migrate at night. Second, the track suggests that there is a clear difference in the spatial location of fish during the day and night (driven by holding behavior). And third, because it shows a single fish moving down the outside of a bend and exiting the bend in the same location two times in a row!

Because the measurement of a single fish track can only be considered anecdotal with respect to quantifying population level behavior-mediated distributions, two dimensional spatial distributions of fish detections and residence times were developed to look for population level evidence of the behaviors described by track 5526. The number of individual fish (not to be confused with the number of pings) detected in each 10 meter by 10 meter section of the river is shown in [Figure C.14](#), and similar maps constructed for daylight and dark periods are show in [Figure C.15](#). The overall distribution of fish shows a clear bias in fish distribution towards the outside of the bend, and as suggested by the track of fish 5526, disaggregating this distribution into day and night periods reveals a very distinct difference between the spatial distribution of fish during the day and night. From this data it is very clear that fish are moving down the outside of the bend during dark and crepuscular periods, and holding in low velocity, near-bank areas on the inside of the bend during the day. The distinct outside of the bend bias in the distribution of the downstream moving fish supports the hypothesis that secondary velocity structures within bends act to move fish to the outside of bends as they move downstream. Examination of large numbers of individual fish tracks also supports this

hypothesis; in general, fish that enter array 1 on the outside of the bend remain on the outside of the river all the way around the bend, and fish that enter array 1 towards the inside of the bend move to the outside of the bend by the time they are detected in array 3 (Figure C.16). The tracks shown in figure C.16 (colored by daylight) also show significant inside of the bend holding behavior during daylight, and large numbers of daytime fish detections in the eddy on the inside of array 2.

Unfortunately, there was not sufficient variability in nighttime water velocities to isolate any effect that water velocity had on the spatial distribution of fish moving at night; differences between the spatial distribution of fish during the highest and lowest water velocity periods appears to be driven by sampling bias due to the nighttime water velocity distribution (Figures C.17 and C.18) rather than an observable velocity affect. It is likely that future comparison between the December (similar data were collected in December, but was not available at this writing) and January datasets will provide more information on velocity effects.

Given the preponderance of evidence indicating daytime holding behavior, the ability to predict holding habitat selection will likely be very important to future management considerations. Due to the highly channelized nature of the Sacramento River in the vicinity of Clarksburg Bend, one would expect that juvenile salmon could only hold in low velocity areas near the inside of bends, and in eddies produced by structures or unusual bathymetric features. These expectations seem to be supported by fish residence time distributions in Clarksburg Bend (Figure C.19). We note that Clarksburg Bend is one of the few locations in the Delta where significant bathymetric variability exists because it has an extremely tight radius of curvature. Most channels in the Delta exhibit very little bathymetric variability throughout their lengths, presumably providing little in the way of low-velocity habitat for holding. The only areas with residence times greater than 10 minutes in Clarksburg Bend were on the inside of the bend near the bank, and the two areas with the greatest residence time were the large eddy near the inside edge of array 2, and an intense spike in residence time underneath the research houseboat moored at pilings on the inside of the bend at array 3. When the residence time is disaggregated into daytime and nighttime periods (Figure C.20), the dramatic effect of the array 2 eddy on residence time becomes quite apparent. Based on the daytime residence time and fish detection distributions, and the detailed information provided by individual fish tracks, it appears that during the day most fish move to the inside of the river to hold, and during periods of low velocity these fish move along the bank seeking structure or low velocity areas where holding will be easier. If fish move into areas with either physical structures or velocity structures that facilitated holding they appear to stay in these areas for extended periods of time, often for the duration of their holding period (Figures C.21, C.13, and C.23). If holding fish do not encounter significant structure, they often continue to move about the edges of the river until holding behavior ends (Figures C.22, and C.24). Although a more quantitative description of this process is beyond this analysis, it appears that there is enough information in the January data set to refine and strengthen this explanation through future analytical efforts.

Evidence of Predation Events

An interesting feature of the nighttime residence time distribution shown in Figure C.20 is the extreme spike in residence time underneath the research houseboat moored on the inside of array 3. Such high nighttime residence times seem unusual considering the patterns of daytime holding behavior observed in the rest of the January data. However, analysis of the tracks from individual tags that spent large amounts of time under the houseboat at night suggest that there were several predator fish with ingested tags holding under the houseboat throughout the evening periods. The fish that were considered to be “self-tagged” predators were tag codes that moved down the outside of the bend during the night between Julian day 22 and 23, and then moved upstream into the array 24 hours later

at night. Once these tags entered the array a second time, they were observed moving rapidly along the edges of the river during the day and night, and holding for long periods under the houseboat. In addition to observations of fish that were likely to be predators with ingested tags, it appears that the January data set contains a direct observation of a predation event occurring within the array. Tag code 4280 had a pattern of detections very similar to that described above for the houseboat predators; it moved downstream normally during the late hours of Julian day 22, and then was observed moving rapidly into the array from downstream on the night of Julian day 23-24. Once in the array, 4280 moved upstream rapidly along the inside bank, where it converged with tag code 5414, which had been moving downstream on the outside of the bend and had started to move back towards the inside of the bend after passing through array 3 (Figure C.21). After the two tags converge at Julian day 24.11, they were never observed diverging, and moved rapidly together up and down the inside edge of the river, eventually swimming rapidly out of the array moving upstream (Figure C.21). These observations of likely predator fish behavior are important, as they suggest that a significant portion of the estimated mortality is due to direct predation by other fish, and further, these tracks contain valuable information on the behavior of the fish that eat out-migrating juvenile salmon.

Final Remarks

Preliminary analysis of the tag tracking data collected in January of 2007 provided significant support for the proposed study's underlying conceptual model of juvenile salmon outmigration dynamics (e.g. fish are aggregated on the outside of bends due to behavioral responses to secondary circulation), and also demonstrated the value of using acoustic tag tracking technology for studying juvenile salmon outmigration. The spatial distribution of fish detected at night showed an overwhelming majority of downstream moving fish located on the outside half of the bend, and the downstream evolution of individual fish tracks showed patterns that consistently supported and explained the population level observations obtained in previous years of research. The diurnal timing of downstream migrations observed in this data is consistent with past analysis, and given the significant management implications of the holding behaviors observed, future work should include efforts to test the hypothesis that the majority of outmigrants hold during hours of increasing daylight. Despite the jitter in individual ping position estimates, the HTI tag tracking system produced very high quality data which contains a wealth of information on juvenile outmigration behavior, and potentially significant observations of predator behaviors as well. However, it is also important to recognize that large reductions in individual position jitter will not be realized until the current tracking algorithm is replaced with one that combines all available hydrophone information with estimates of individual hydrophone parameter uncertainties to produce strongly over-constrained optimal position estimates. Thus, it is important to note that significant analysis time will be required to fully extract the information obtained in this and future tag tracking experiments.

Recommendations for future research:

- (1) The proposed research for 2007/2008 should include targeted mobile tracking and carefully designed diurnal gate operations at the DCC.
- (2) Electro fishing and/or underwater cameras to identify potential holding areas and/or predation locations
- (3) Control tags, with known locations (in X,Y and Z), such as a tag placed on drifter, should be used to assess the efficacy of the 3D array and should be compared with fish tag data.

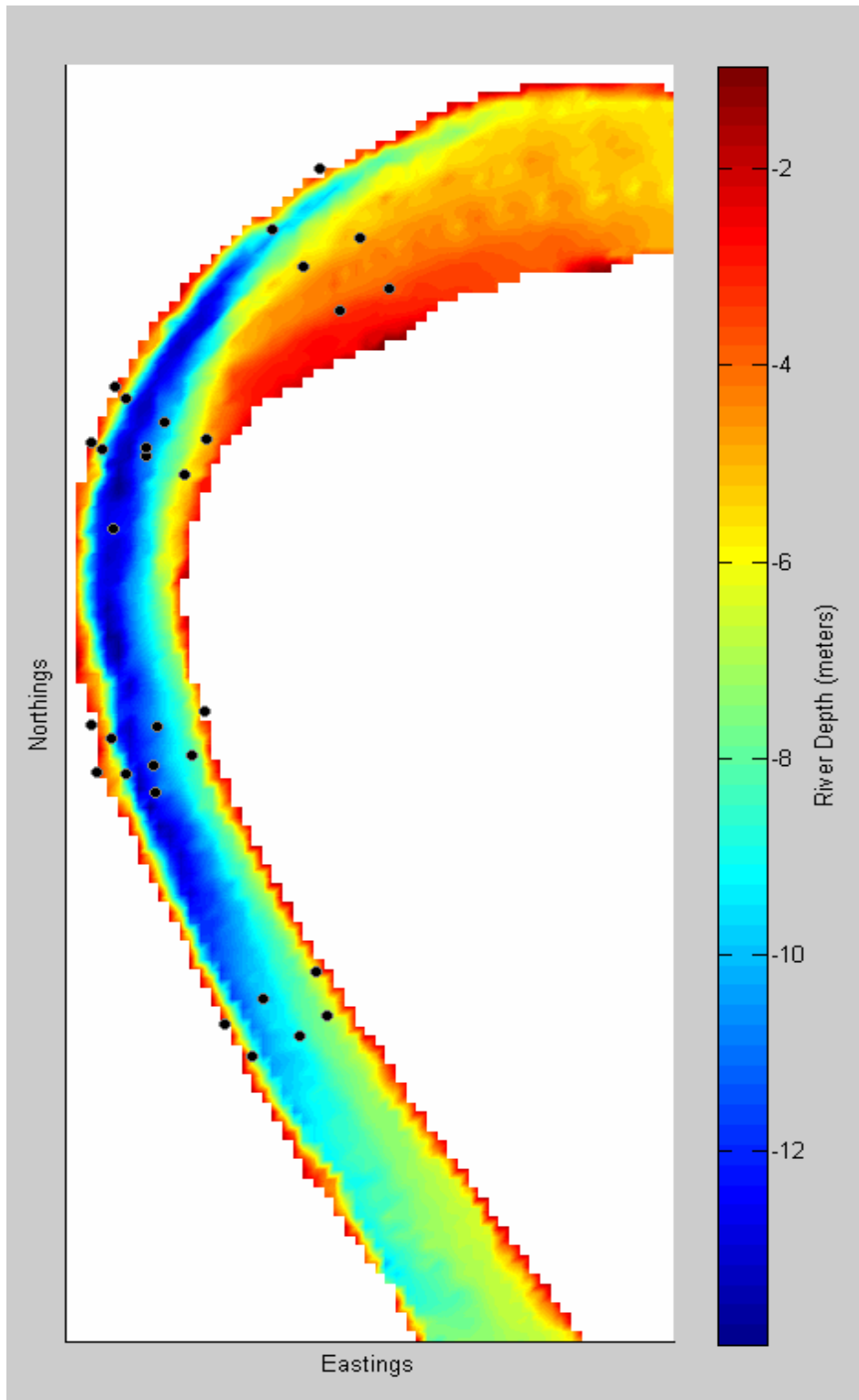


Figure C.1 – Hydrophone locations in Clarksburg Bend, hydrophones shown as black dots, river depth is represented by color.

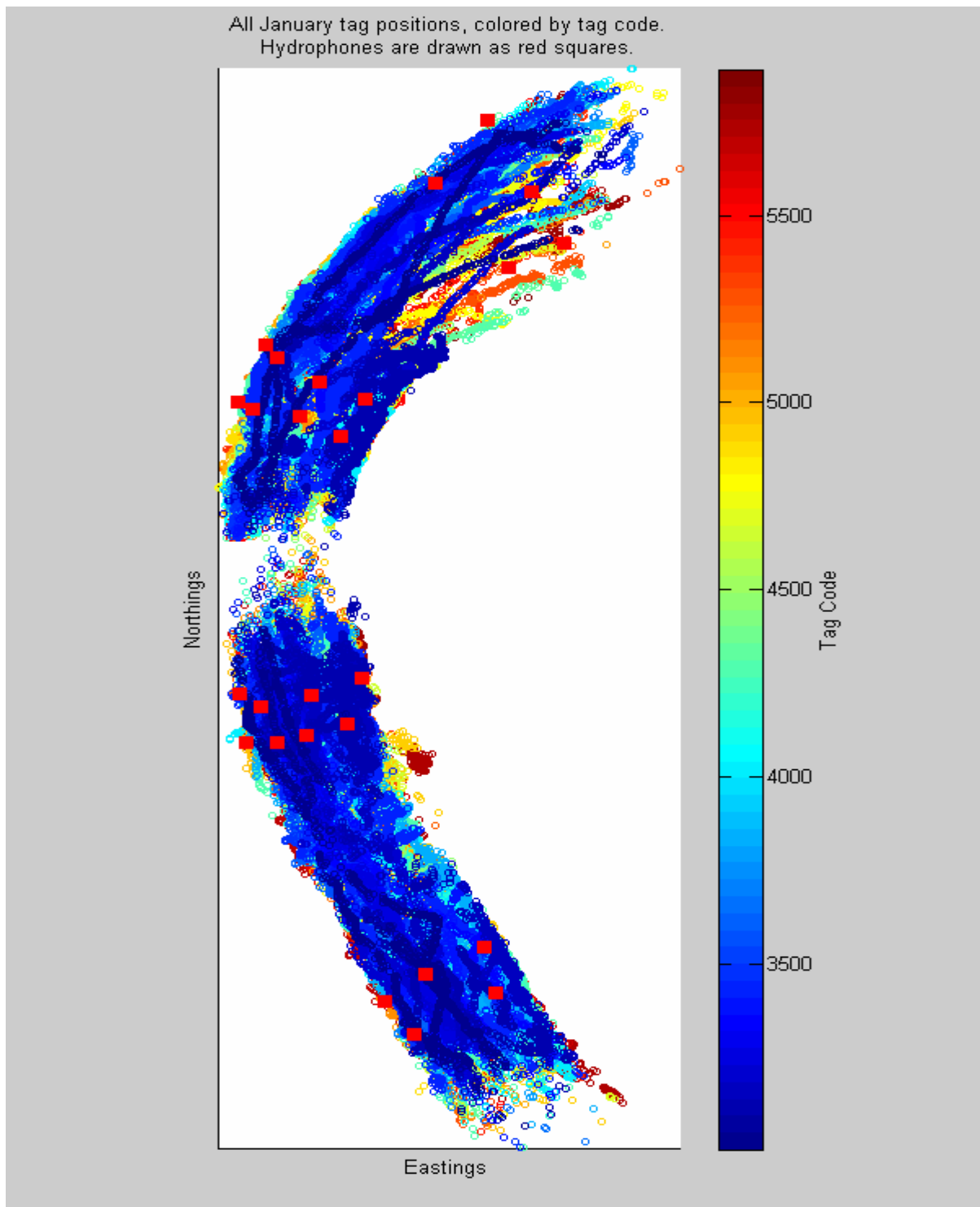


Figure C.2 – January tag positions colored by tag code, fixed hydrophones shown as red squares.

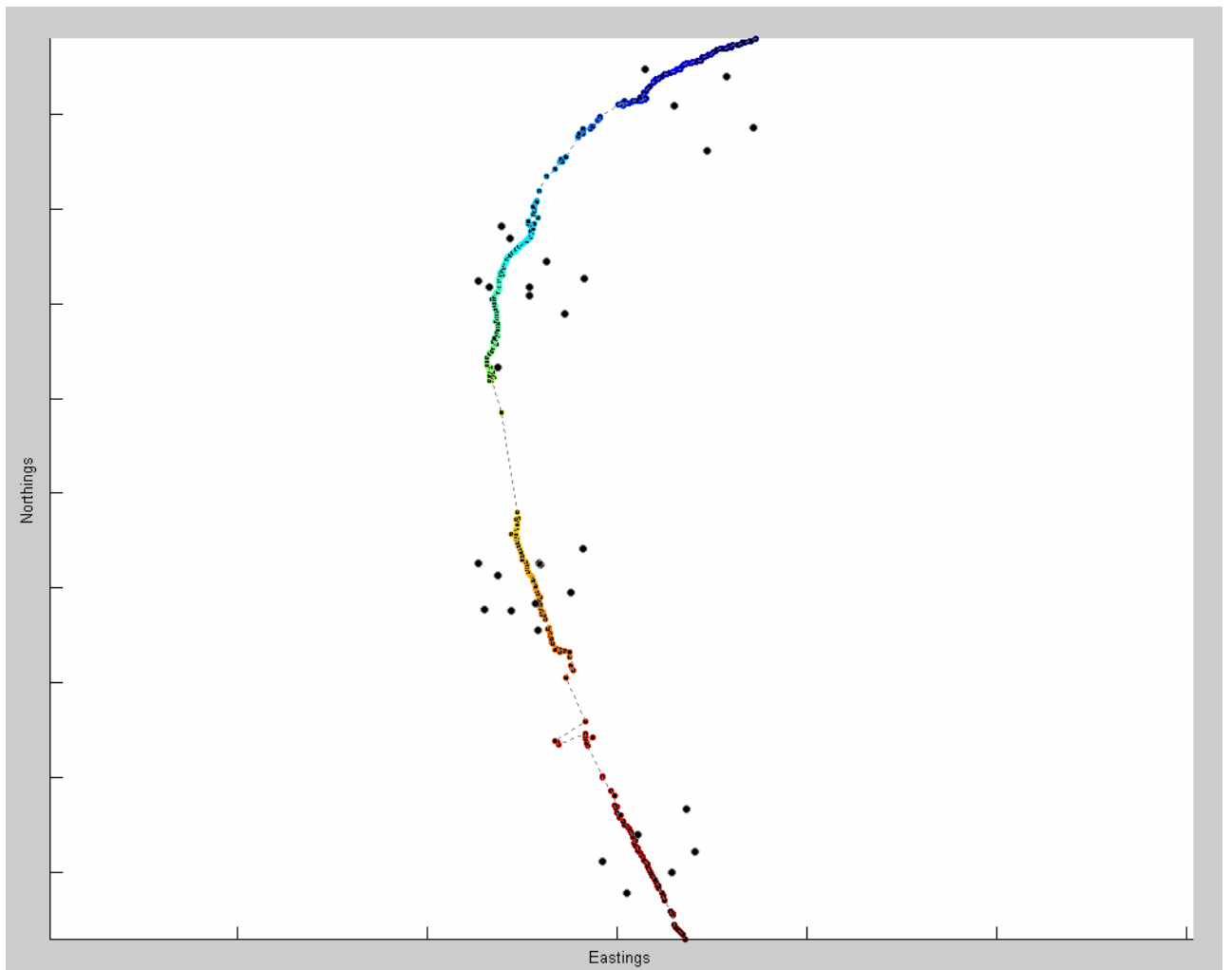


Figure C.3 – Entire track of tag code 4490, shaded by time, with “cooler” colors representing the earlier or beginning of the record and “hotter” colors representing data collected during the later times in the fish track. The quality of track 4490 is representative of average tracking performance.

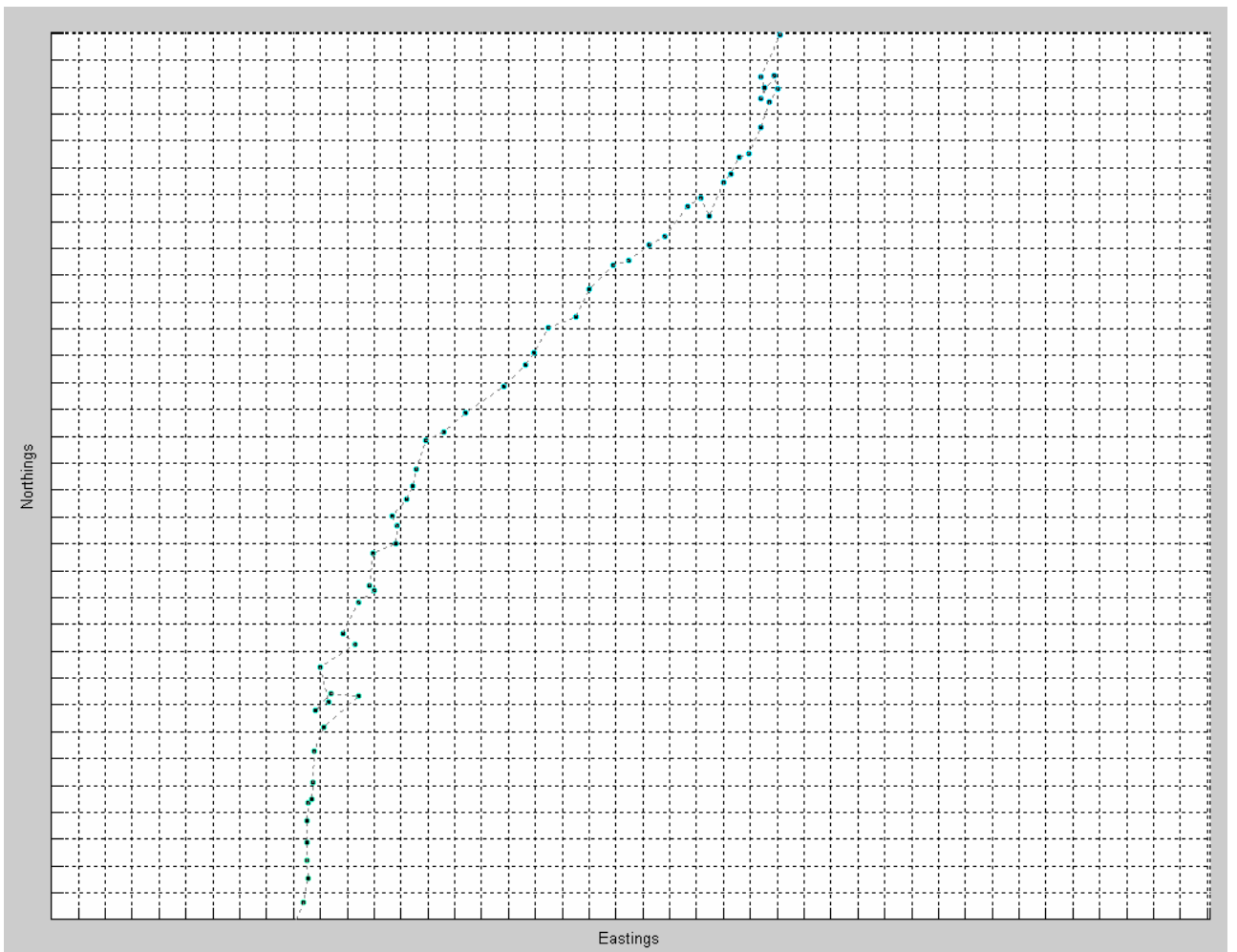


Figure C.4 – Track of code 4490 zoomed into the interior of array 2, shown on a 2 meter by 2 meter grid.

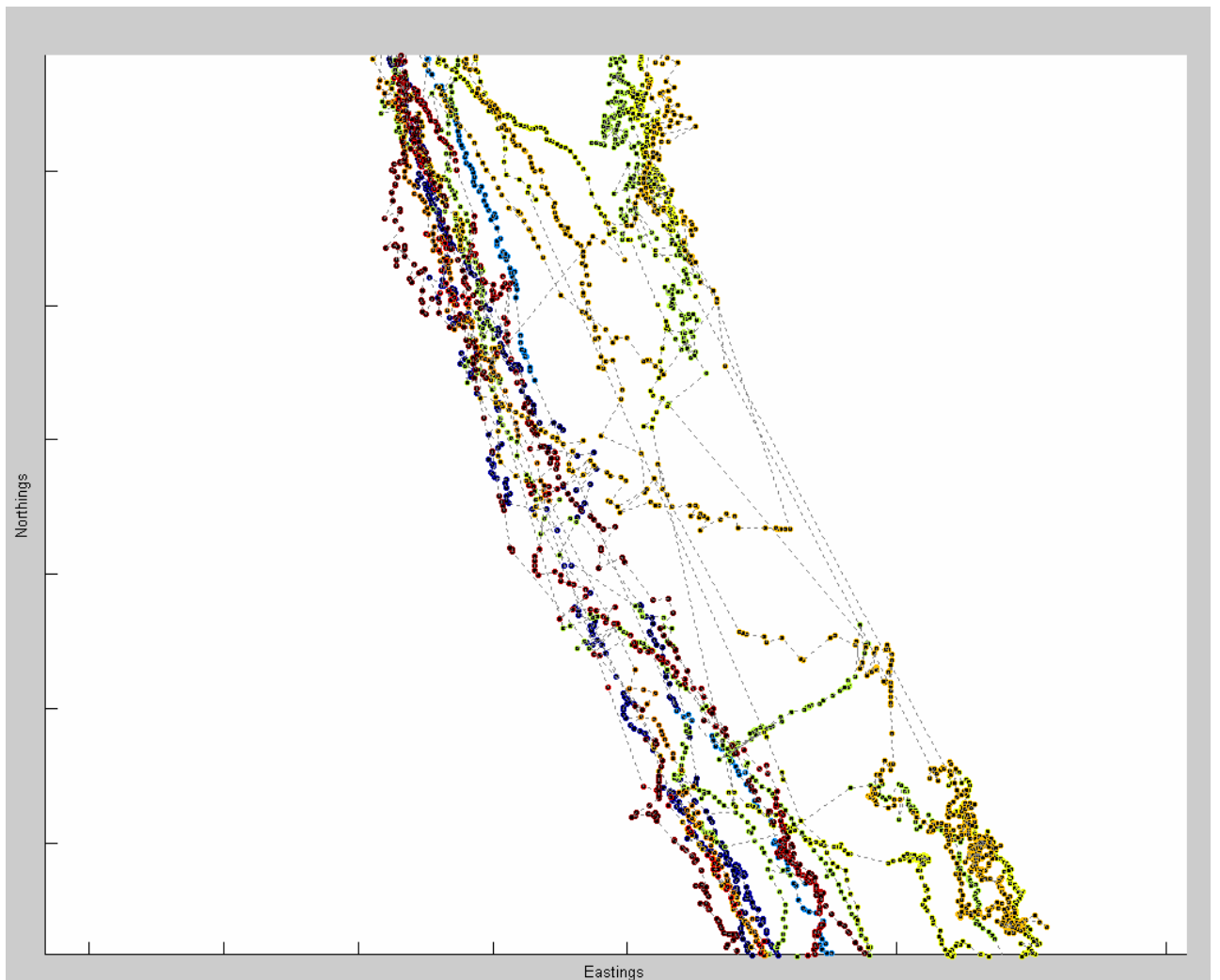


Figure C.5 – Tracks made between array 3 and array 4, colored by tag code, and with individual tracks connected by grey lines. Track quality deteriorates dramatically in the region equidistant between the two arrays.

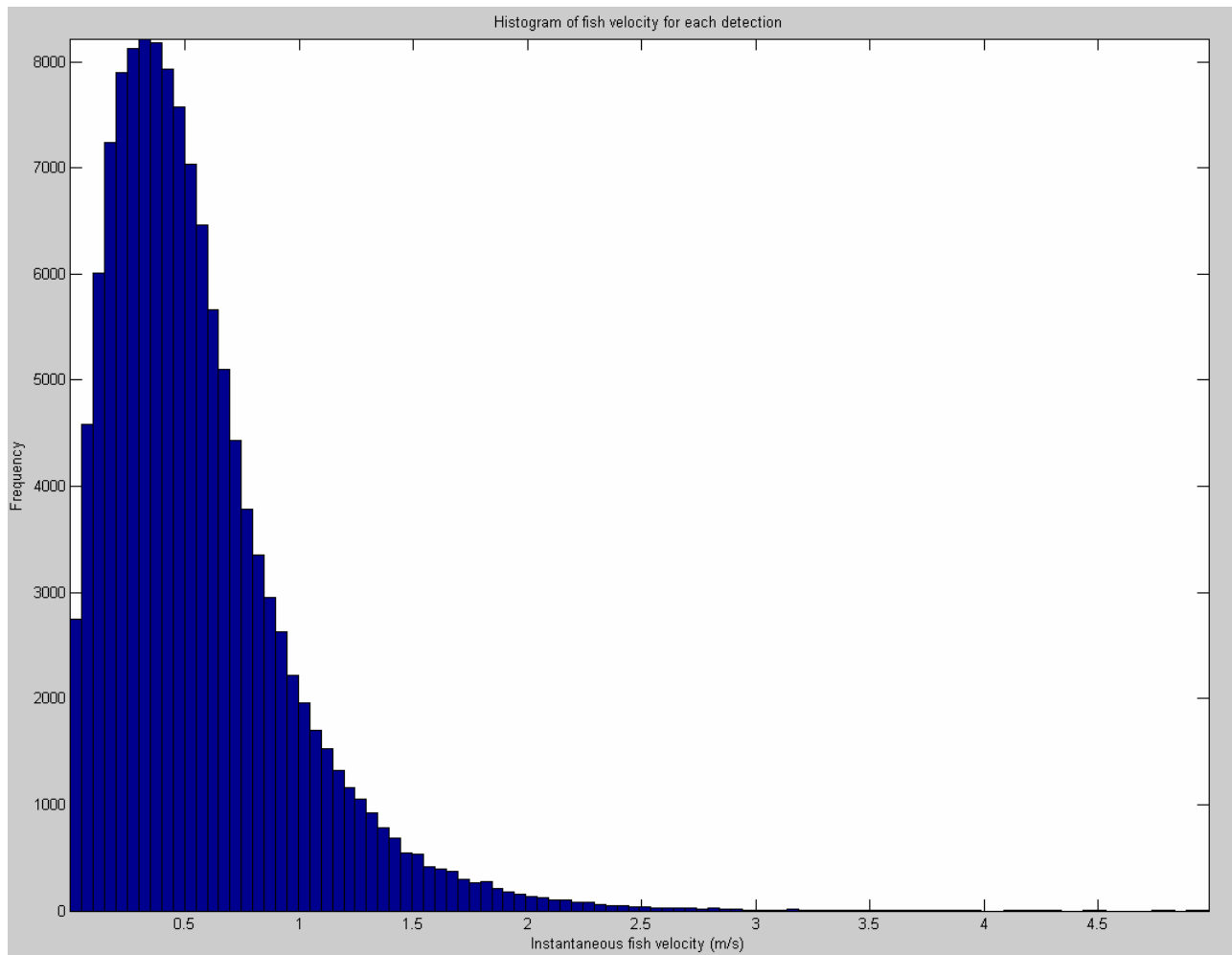


Figure C.6 – Histogram of calculated fish velocity in m/s.

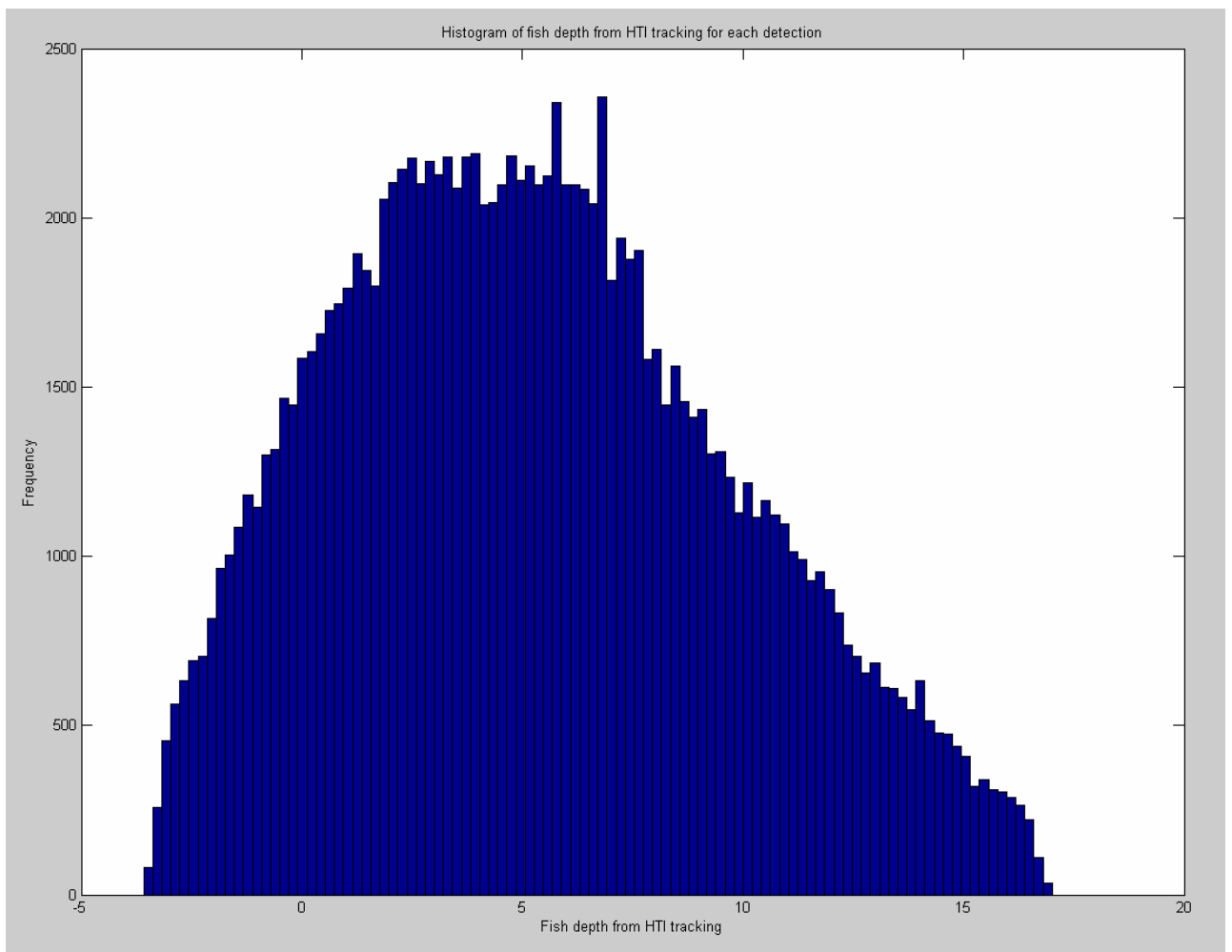


Figure C.7 – Distribution of depths calculated by HTI tracking algorithm

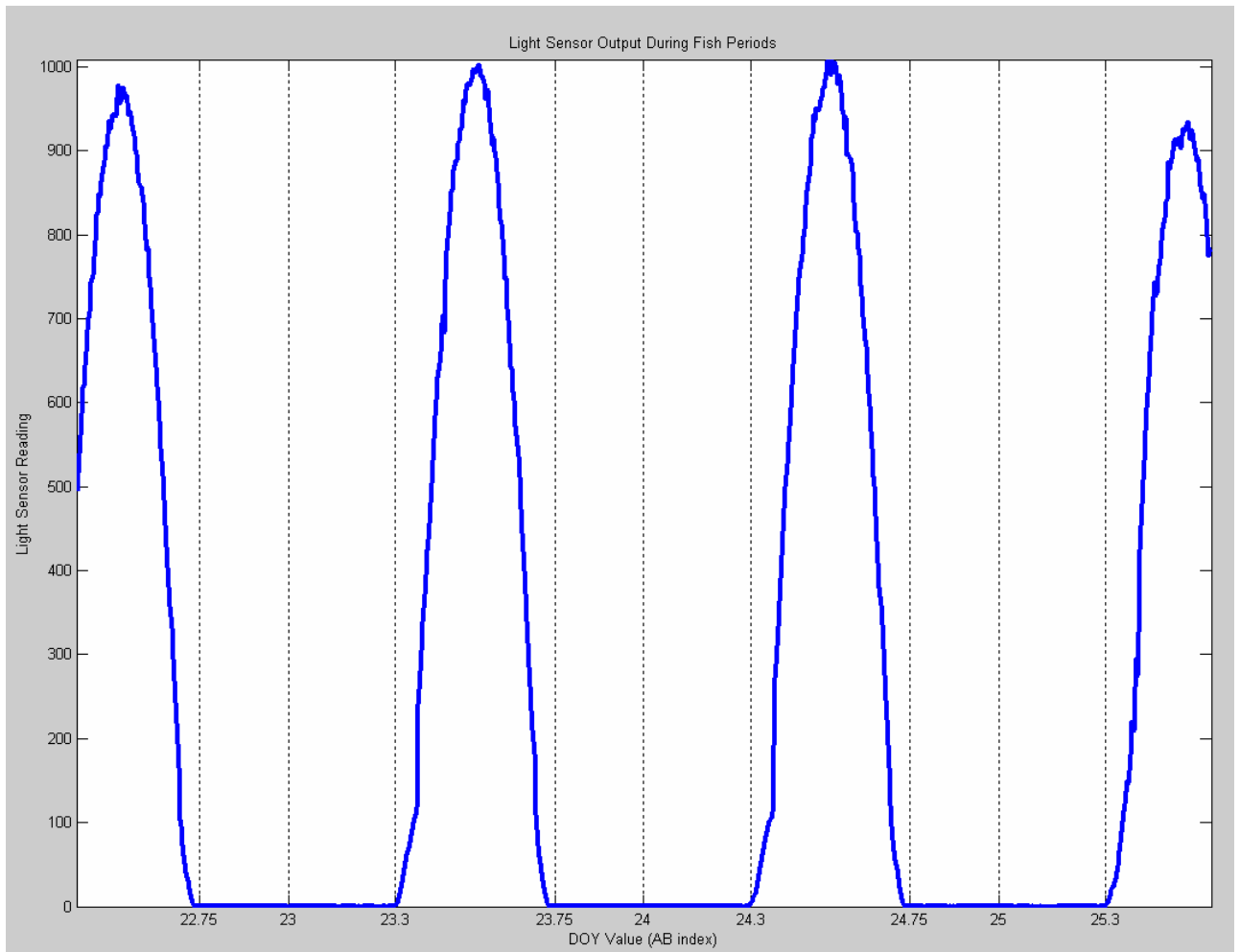


Figure C.8 – Light sensor output for the study period. Note: daylight periods are between fractional day values of about .35-.75

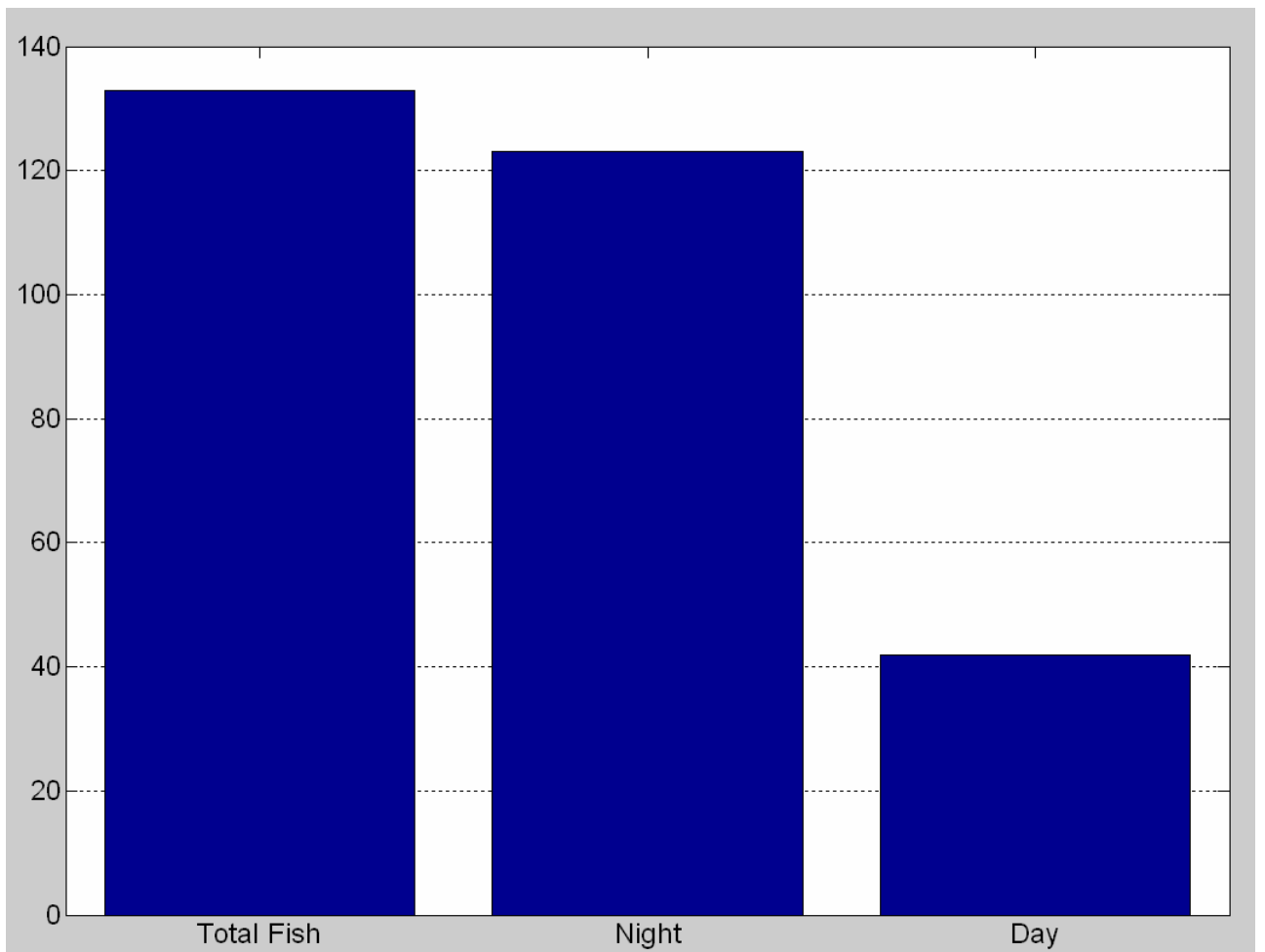


Figure C.9 – Number of individual fish detected during the entire study, during daylight periods, and during night (dark) periods.

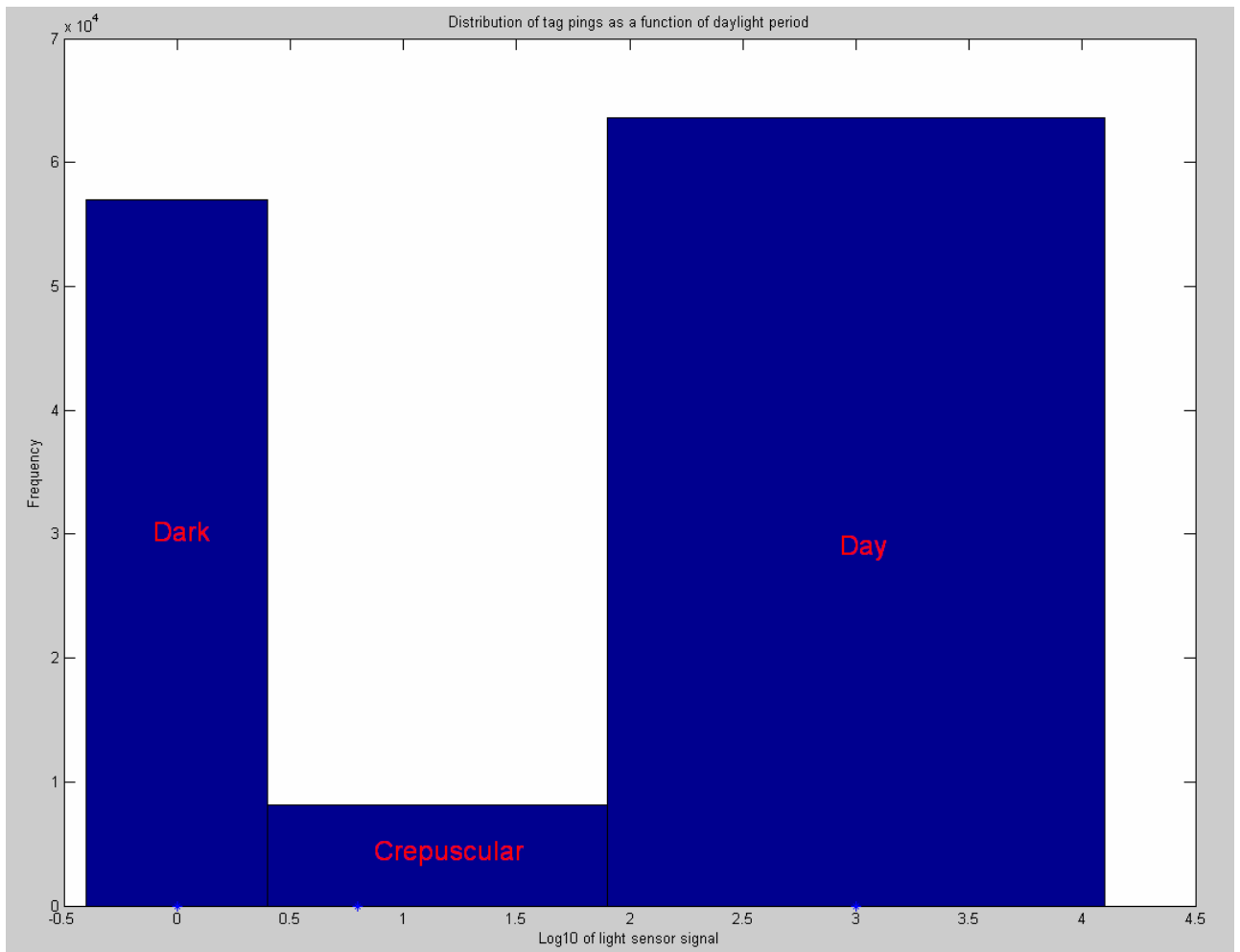


Figure C.10 – Fish ping detections, separated by daylight periods. The number of pings detected is indicative of the fish*hours in the array for a given period.

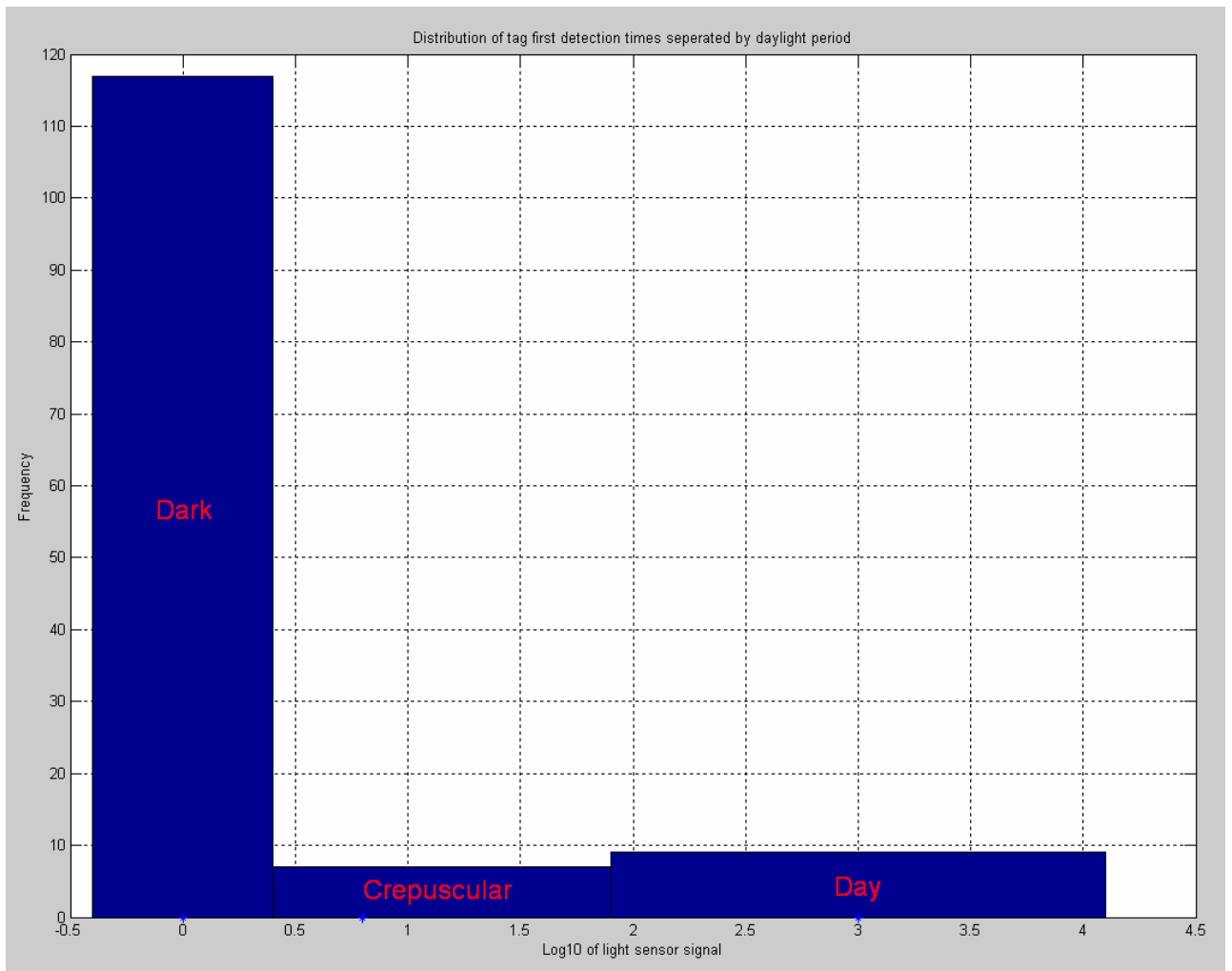


Figure C.11 – Distribution of tag first-detections by daylight period. The first time a tag code is detected is considered the time that a fish entered Clarksburg Bend. Greater than 88% of the fish enter the bend for the first time during dark periods.

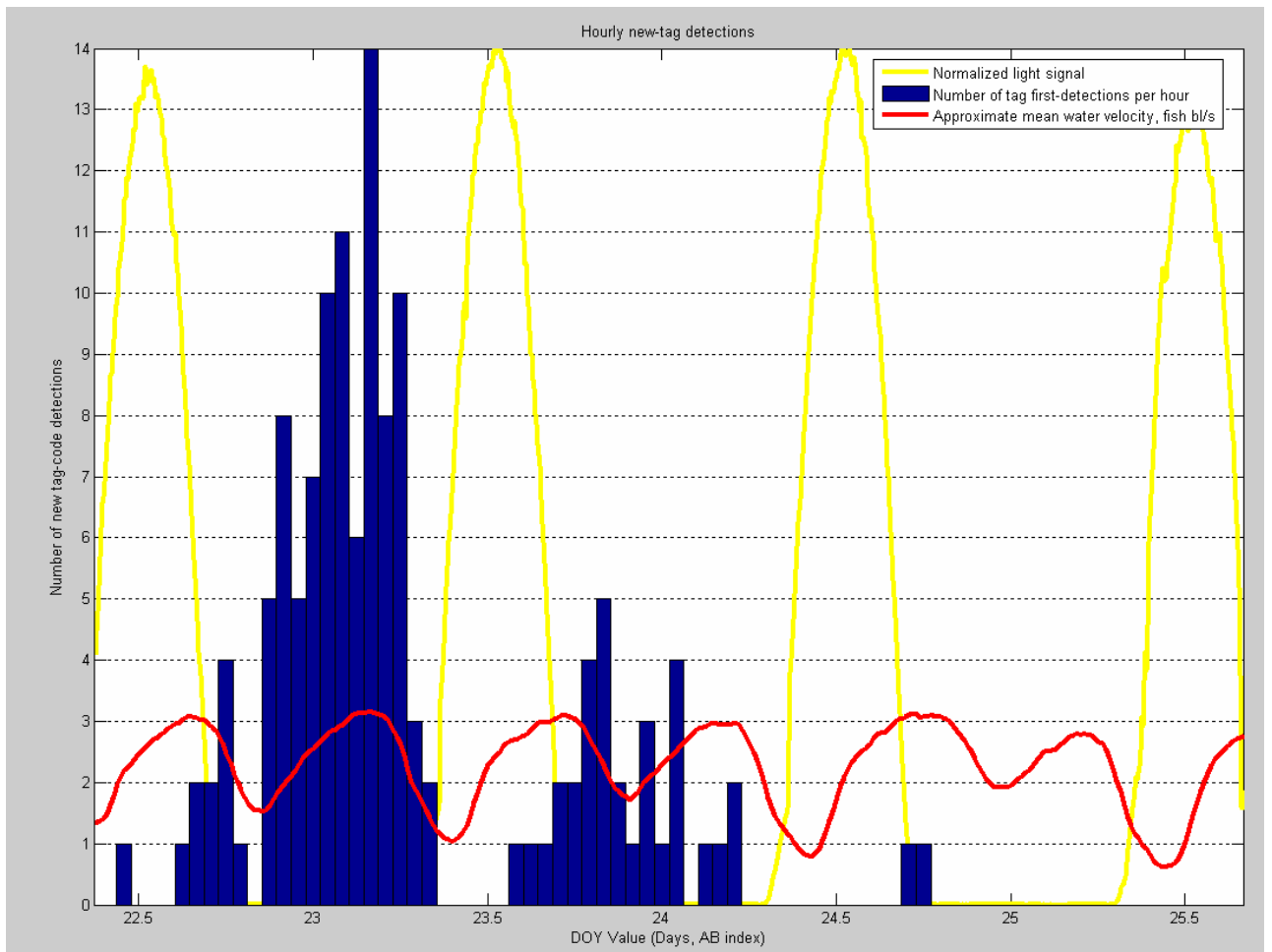


Figure C.12 – Hourly number of fish entering the array for the first time

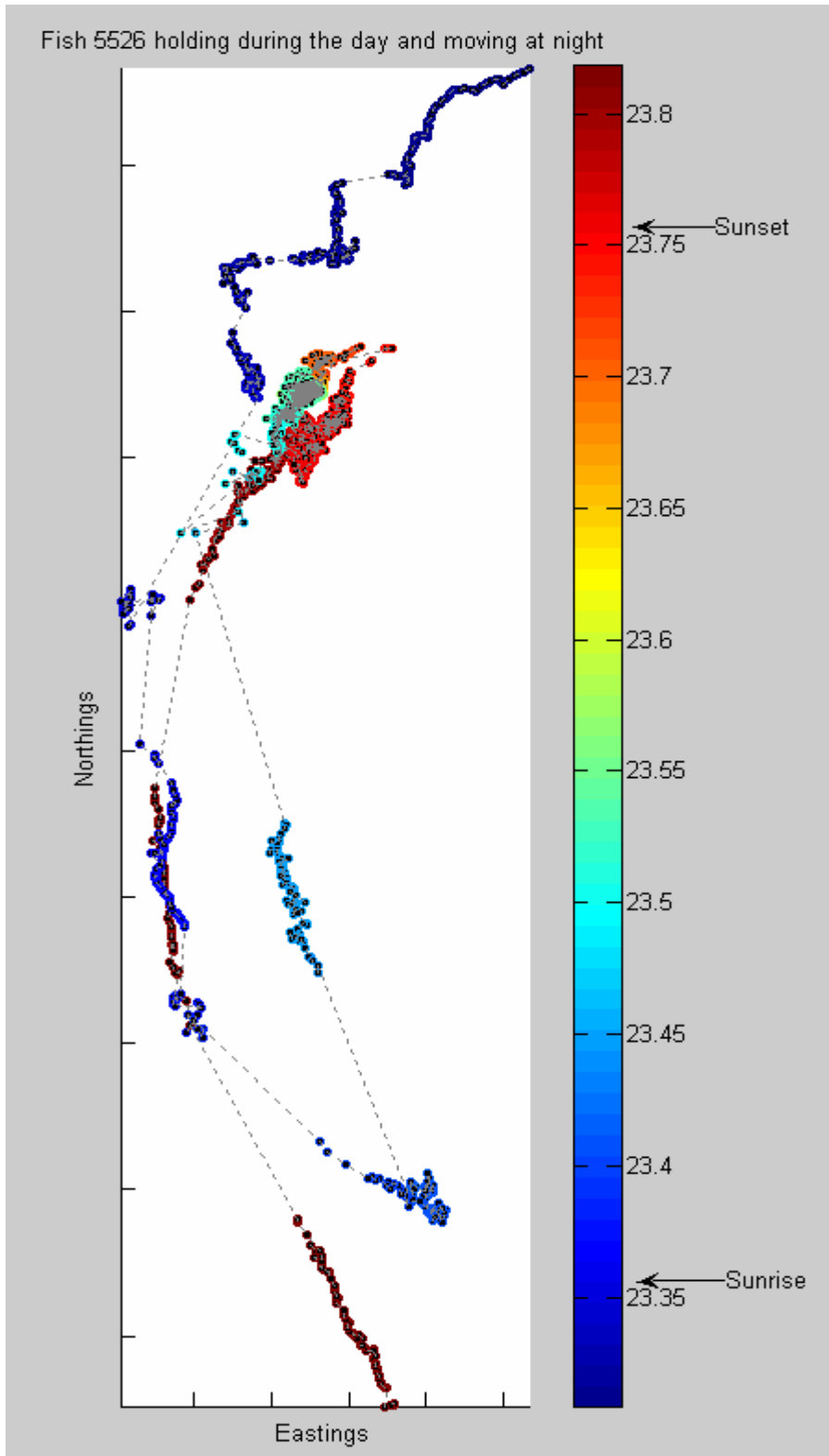


Figure C.13 – Fish 5526 holding during the day and moving at night. Fish positions are colored by Julian day value. Sunrise is just after Julian day value 23.35, and sunset just after 23.75.

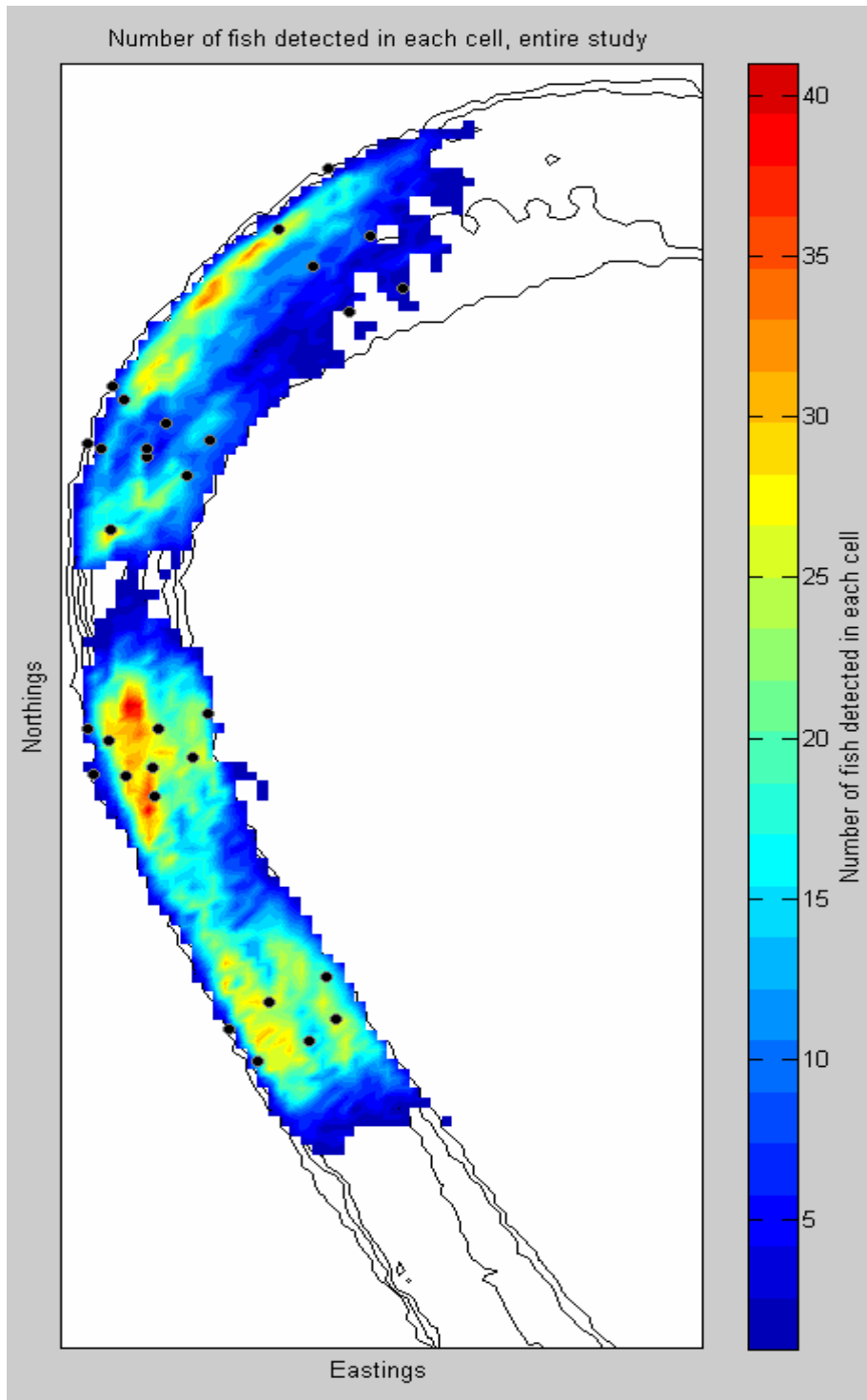


Figure C.14 – Spatial distribution of fish for the entire study. The distribution map is colored by the number of fish detected in each 10m by 10m grid, river contours are shown in black in the background.

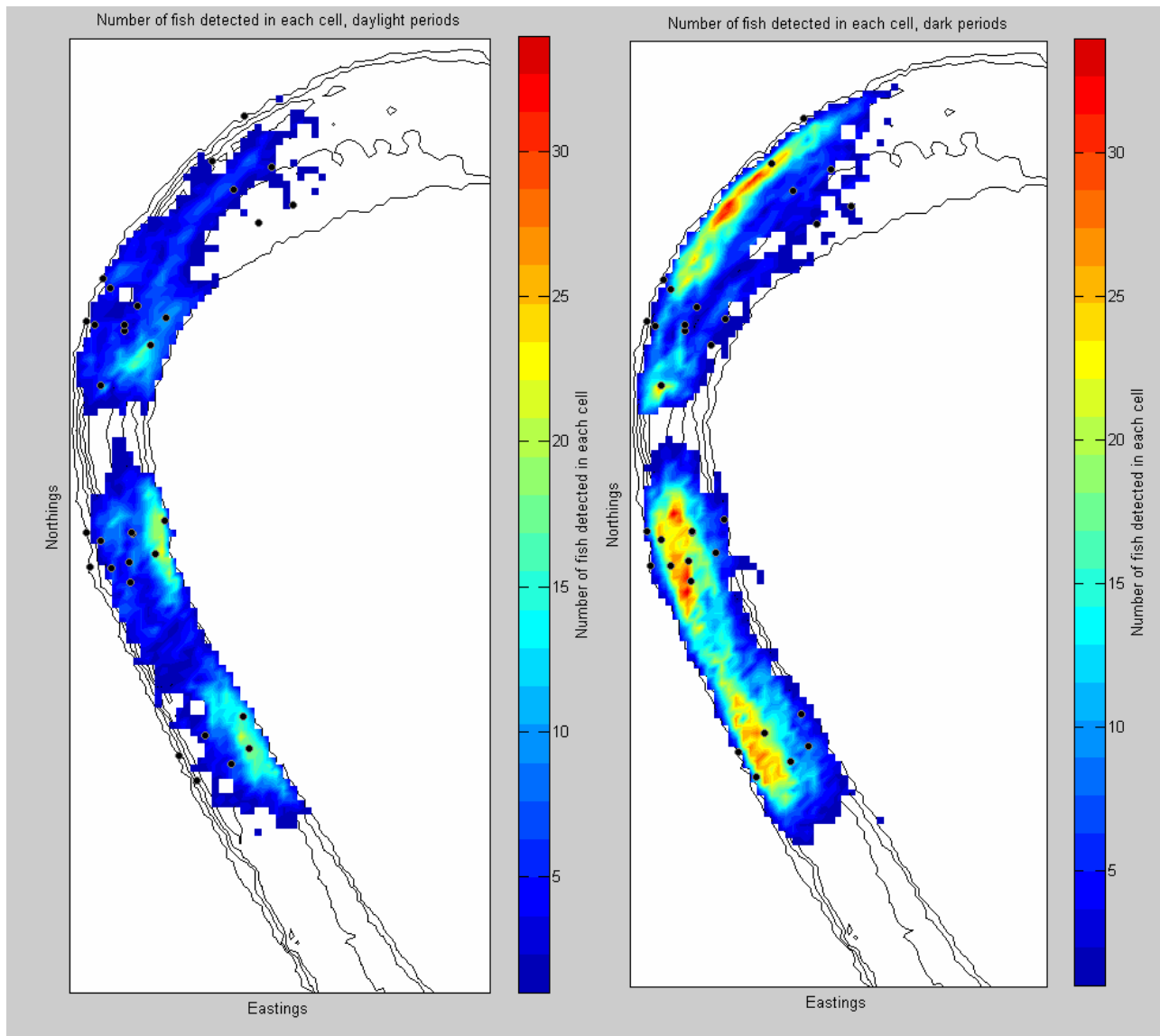


Figure C.15 – Spatial distribution of fish separated into daylight and dark periods. The distribution map is colored by the number of fish detected in each 10m by 10m grid, river contours are shown in black in the background.

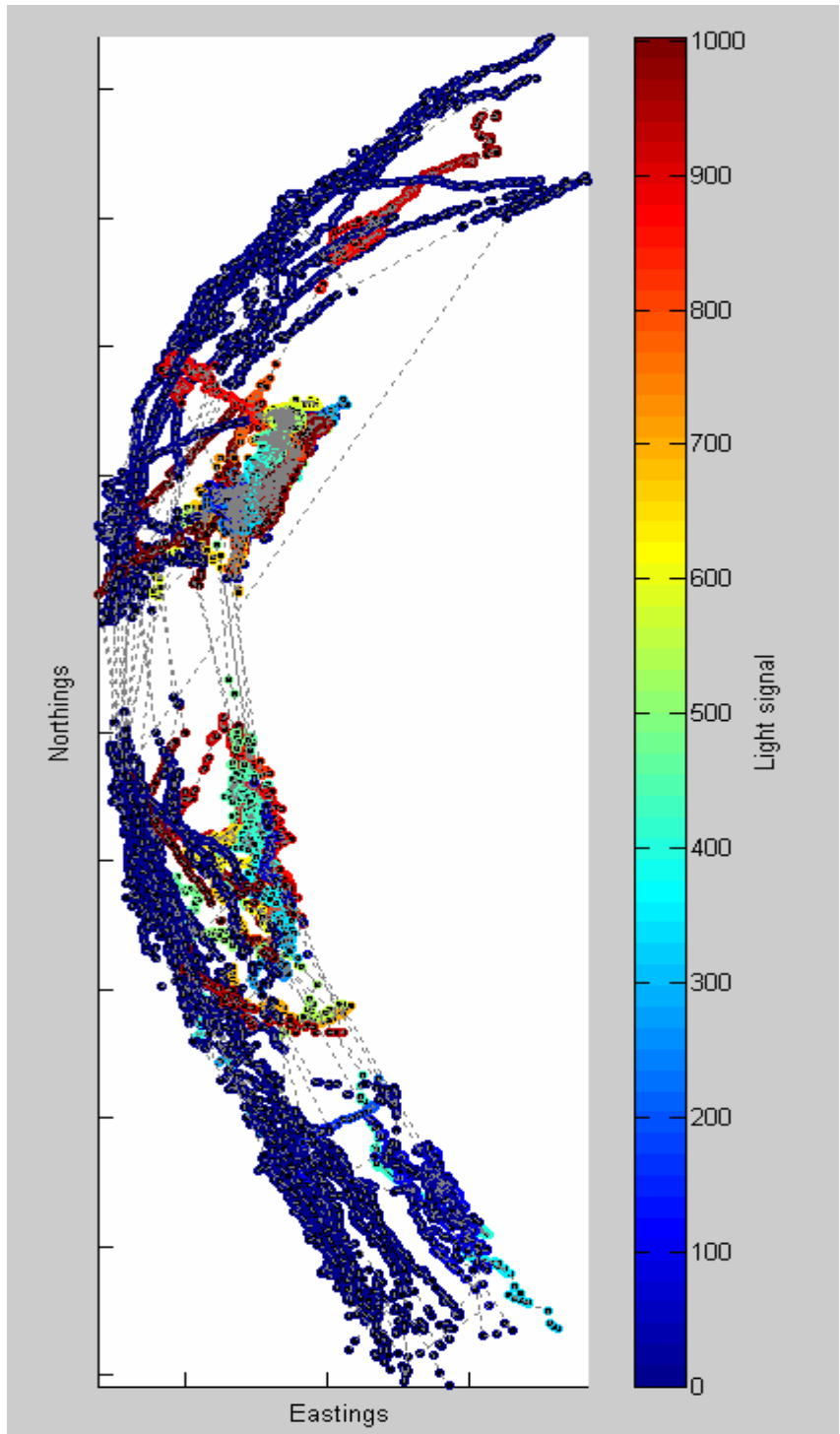


Figure C.16 – Example tracks of fish moving down the outside of the bend at night, and then moving to the inside bank during the day. These tracks are representative of the roughly 100 individual fish tracks examined during this analysis.

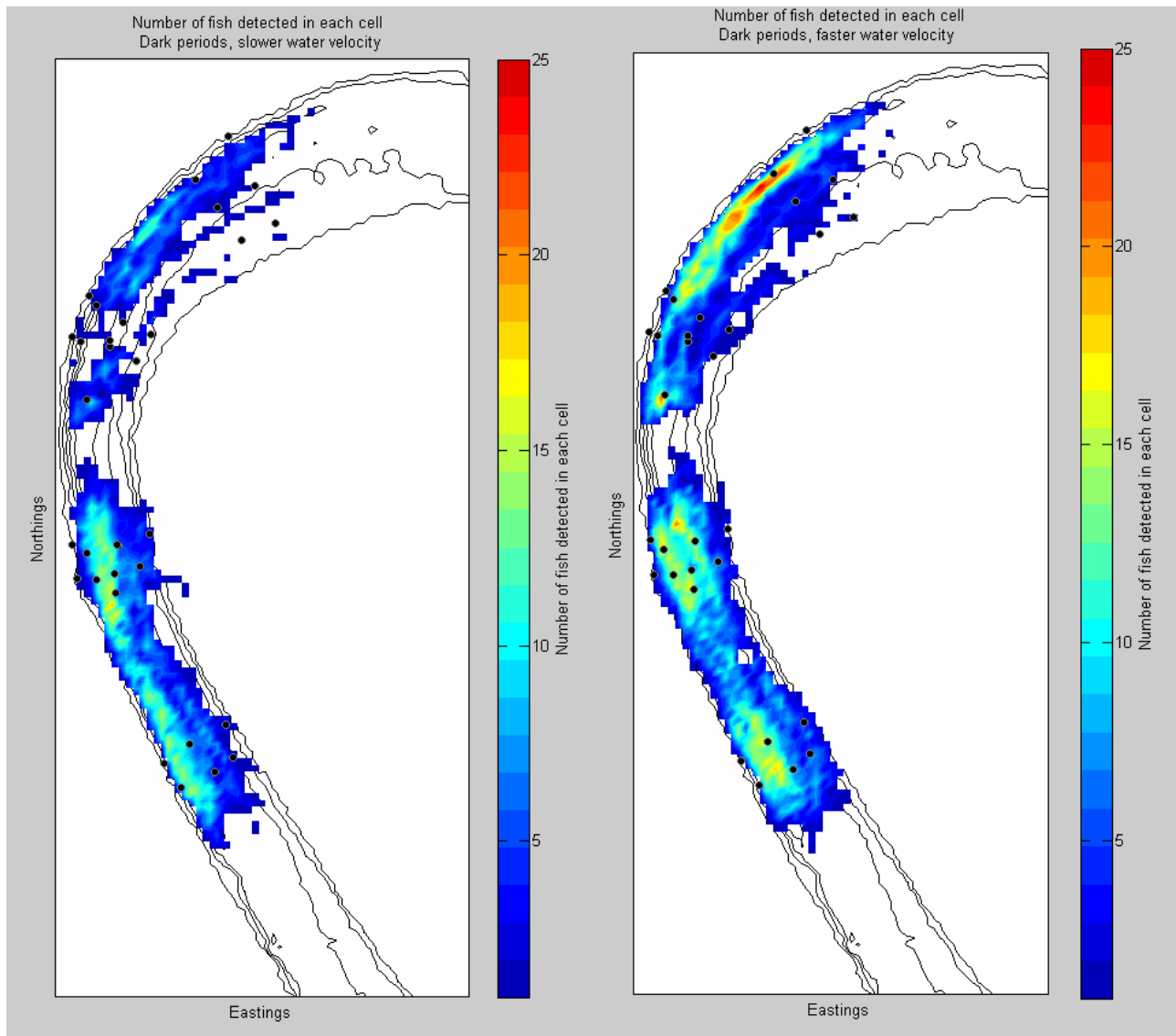


Figure C.17 – Fish spatial distributions for dark periods, separated into fast and slow water velocity periods. Fast water velocity periods are periods with water velocities equal to or greater than the mean dark water velocity. Slow periods had water velocities less than the mean dark water velocity.

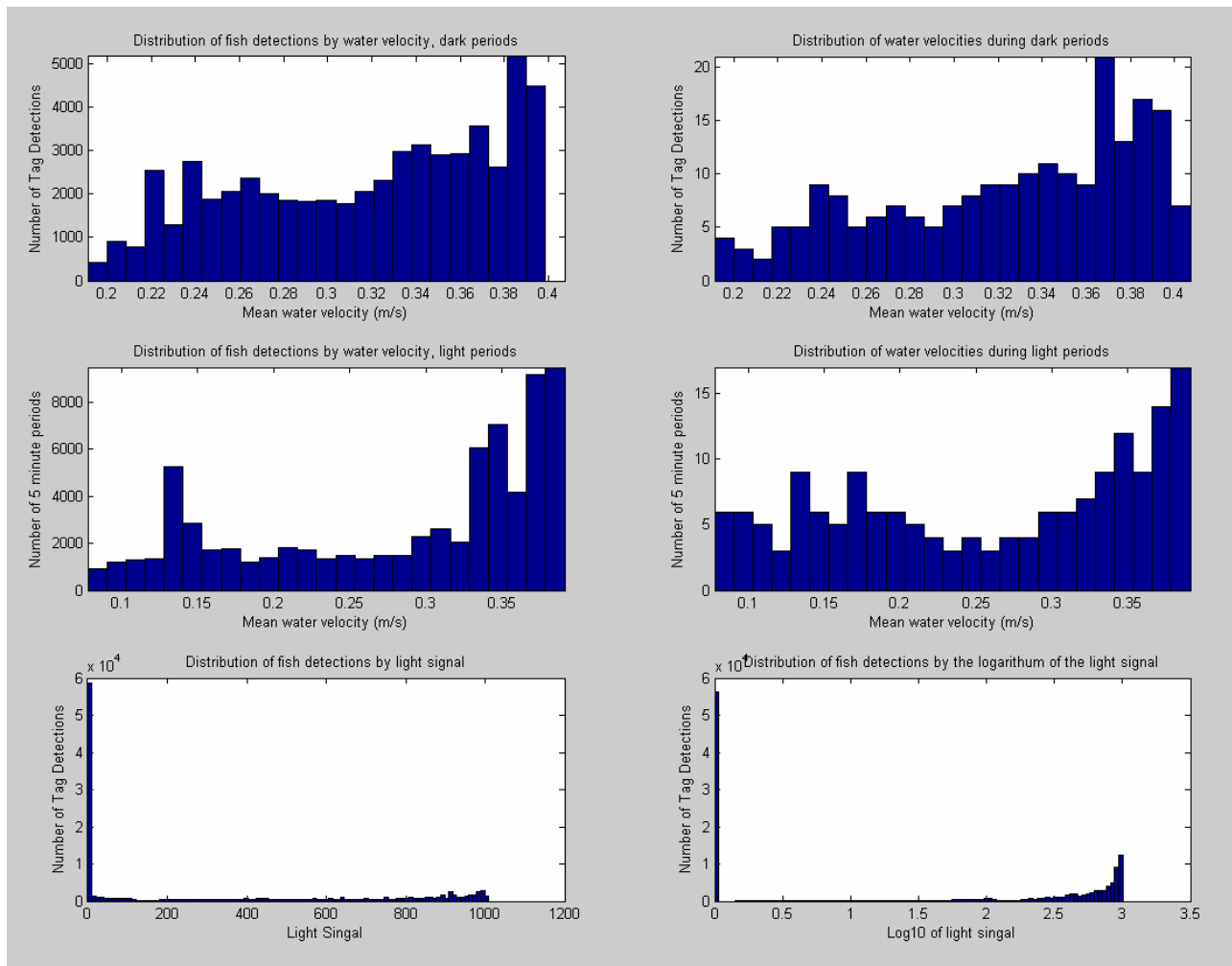


Figure C.18 – Fish detection distributions for day and night broken down by water velocity. Note that the distribution of fish detections is highly correlated with the water velocity distribution, resulting in a sampling bias during dark periods, such that most of the fish detected at night were observed during higher-velocity periods.

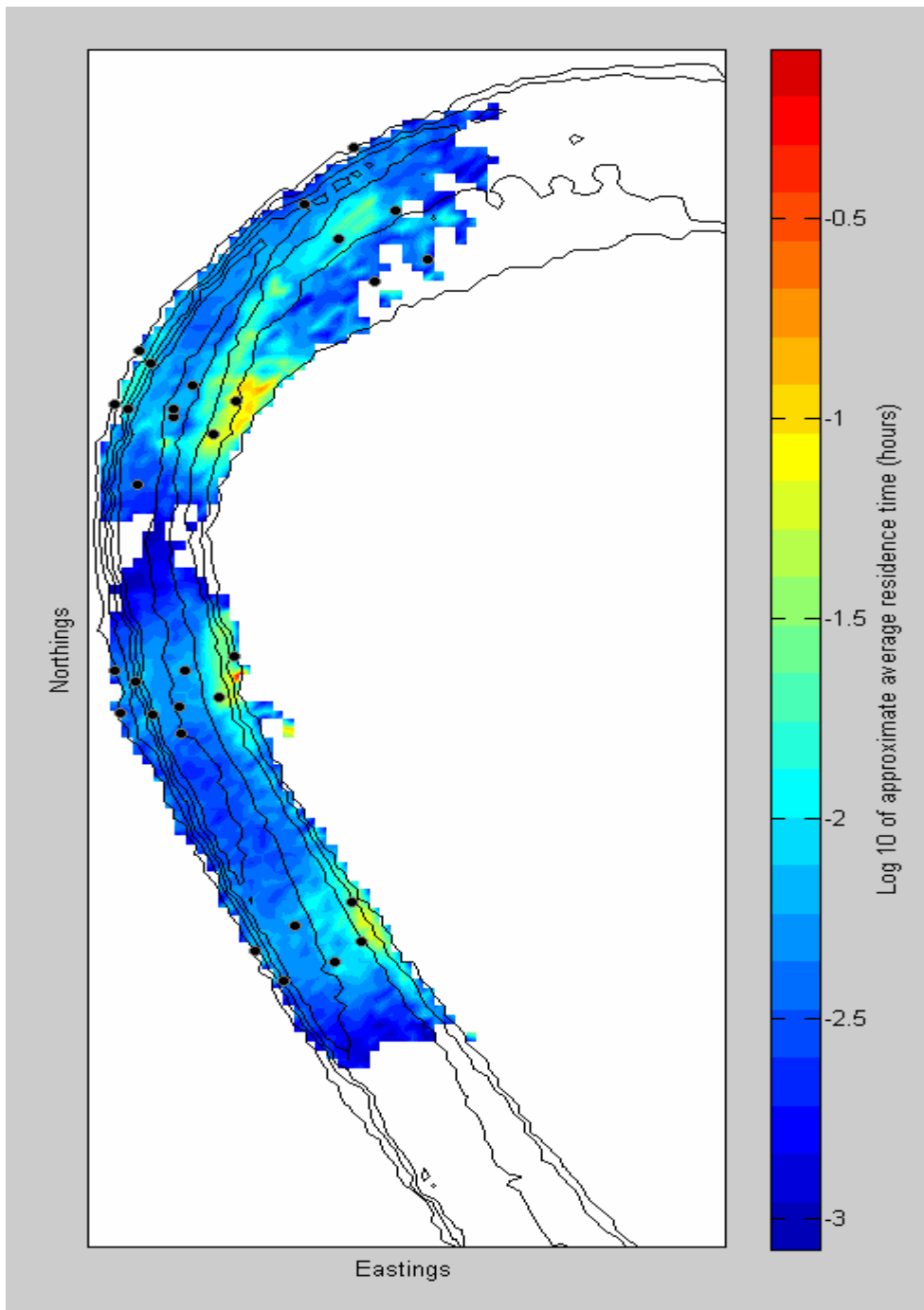


Figure C.19 – Residence time distribution for entire data set. Note that the data is displayed as the logarithm (base 10) of the average residence time per fish, in hours – a value of -3 indicates residence times on the order of seconds, -1.5 indicates times on the order of minutes, and values near 0.0 indicate times of about an hour.

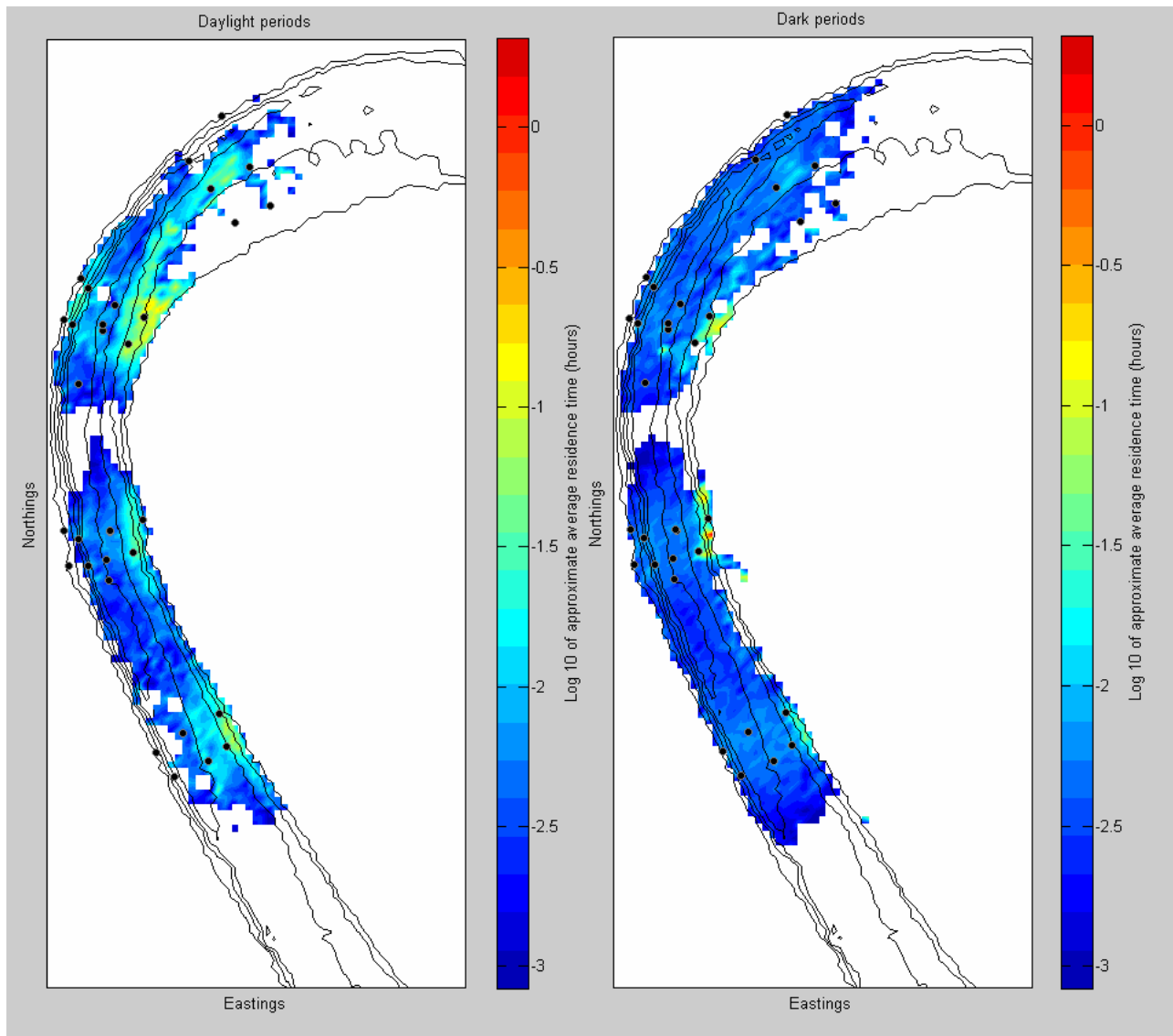


Figure C.20 – Residence time distributions separated for daylight and dark periods. Note that the data is displayed as the logarithm (base 10) of the average residence time per fish, in hours – a value of -3 indicates residence times on the order of seconds, -1.5 indicates times on the order of minutes, and values near 0.0 indicate times of about an hour.

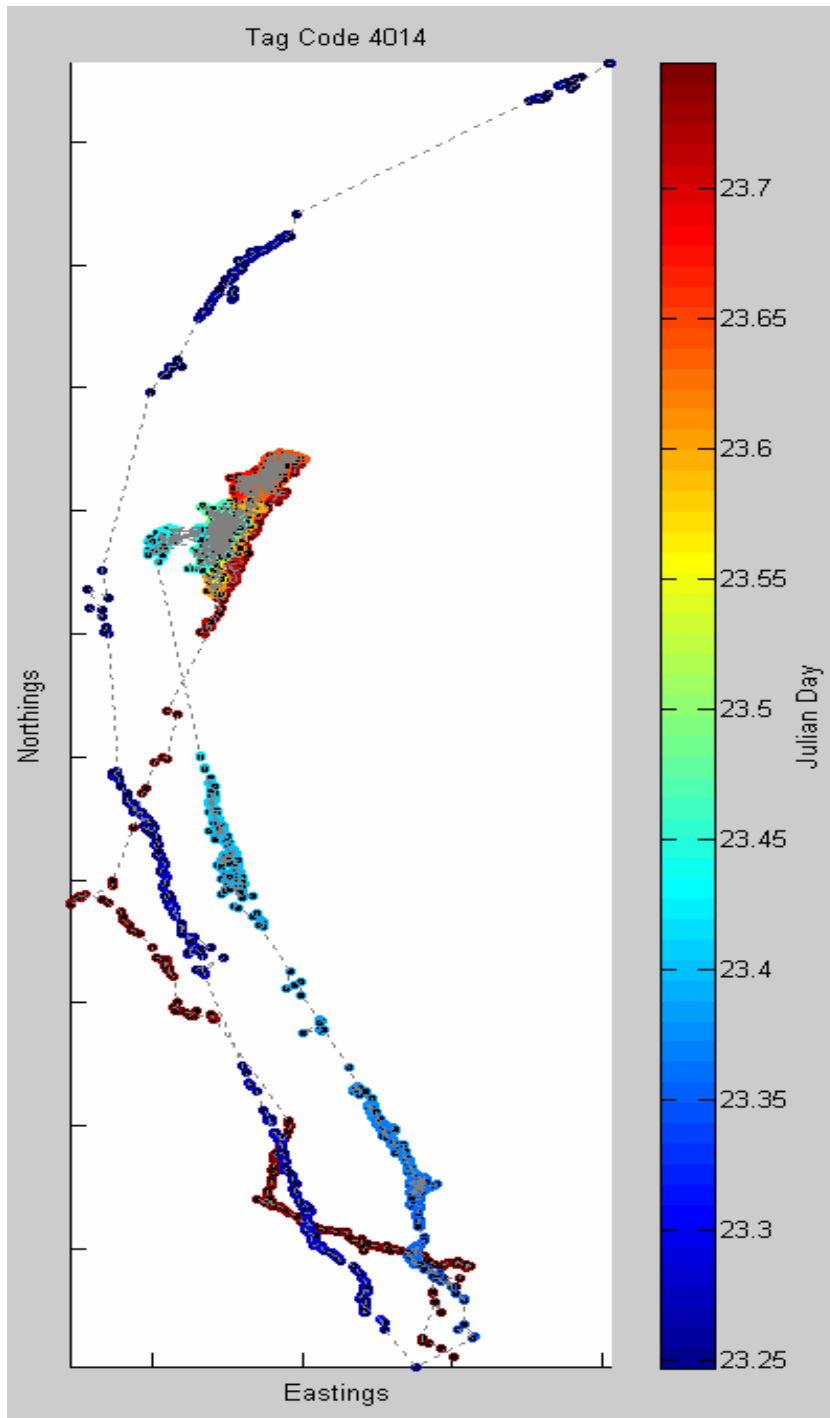


Figure C.21 – Fish 4014 holding during the day and moving at night. Sunrise is just after Julian day value 23.35, and sunset just after 23.75. Much like fish 5526, fish 4014 moved upstream during the day unit reaching the array 2 eddy, where it remained until it began downstream movement in the late evening.

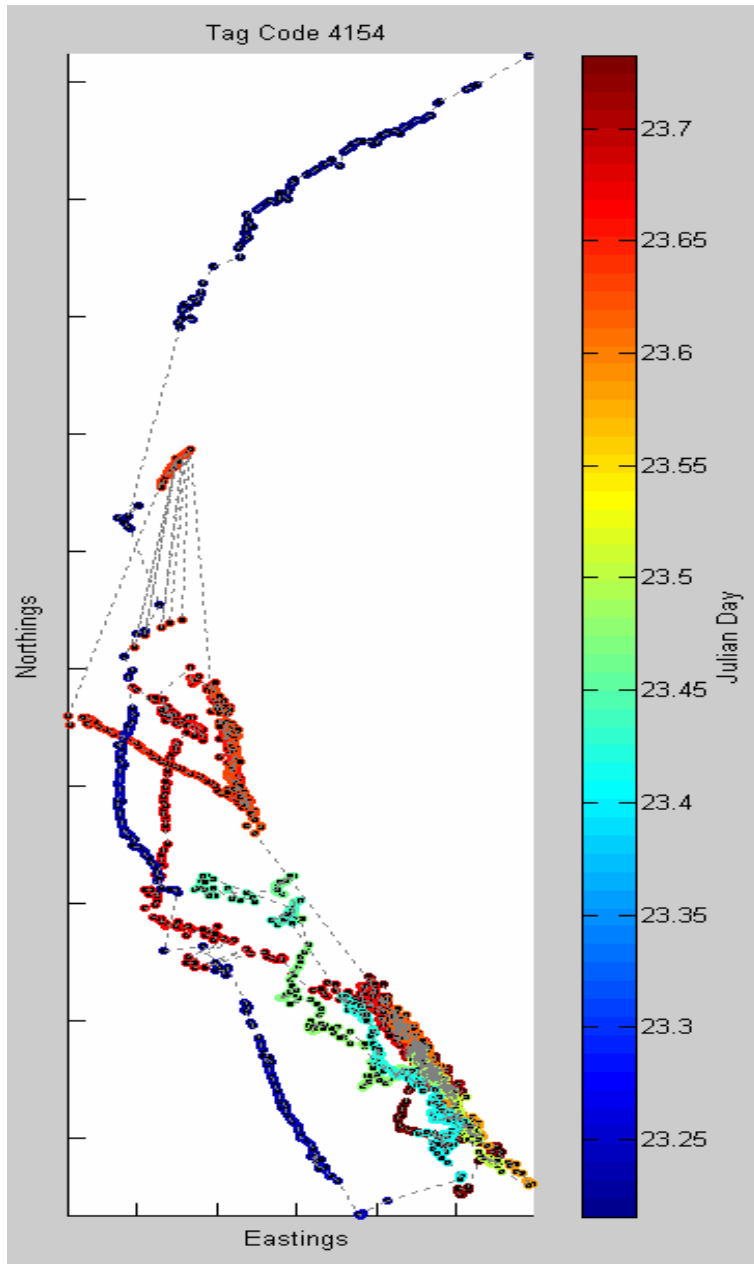


Figure C.22 – Fish 4154 holding during the day and moving at night. Sunrise is just after Julian day value 23.35, and sunset just after 23.75. Fish 4154 appears to have moved up and down the inside edge of the bend throughout the course of the day, with occasional forays to the far outside edge of the river. During movements to the outside river bank fish 4154 was advected a significant distance downstream. 4154 never stayed on the outside of the bend, most likely because water velocities were sufficiently strong to prevent holding.

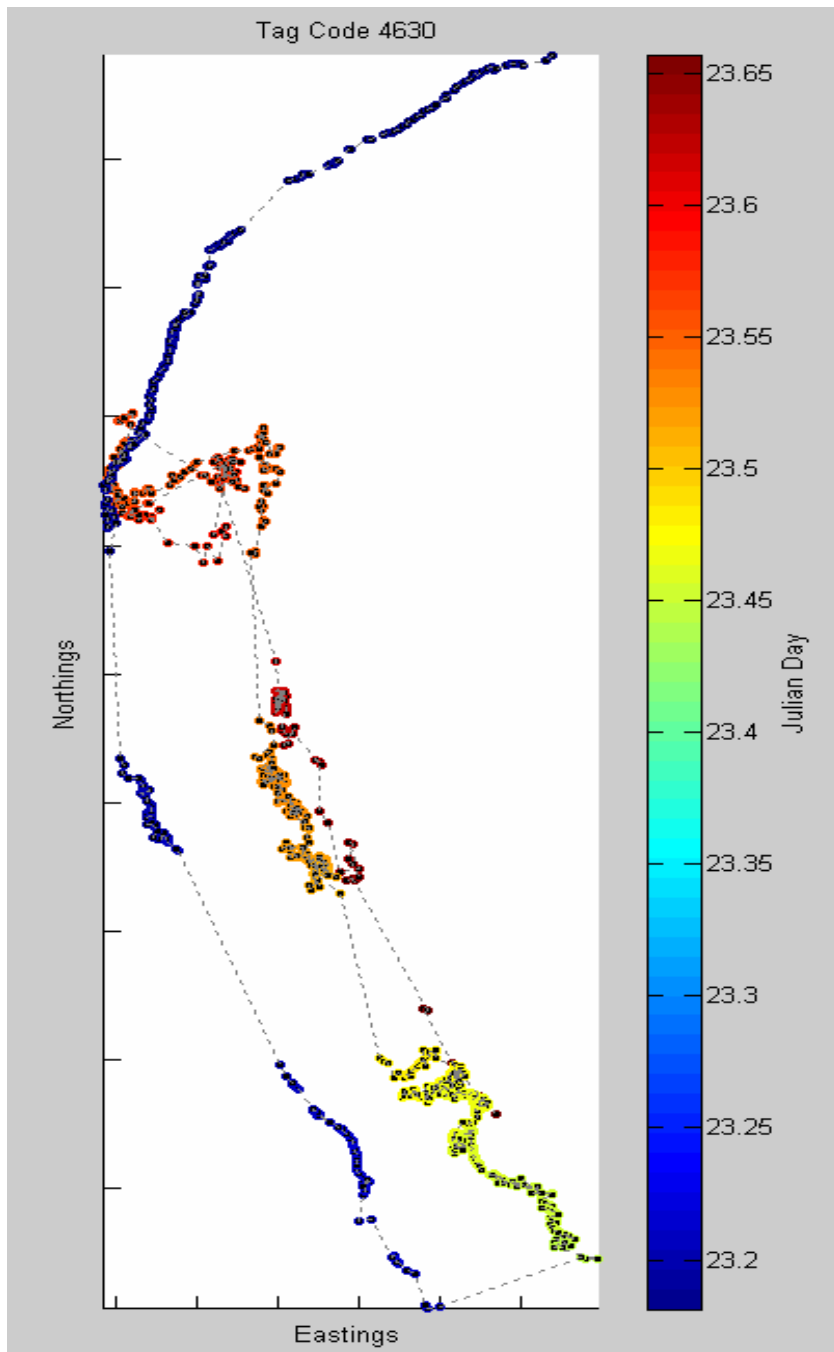


Figure C.23 – Fish 4630 holding during the day and moving at night. Sunrise is just after Julian day value 23.35, and sunset just after 23.75. Fish 4630 moved up the inside of the bend to the eddy inside array 2, held in the eddy for several hours, then moved downstream and held underneath the study houseboat for several hours, and eventually moved downstream along the inside bank and out of the array in late afternoon.

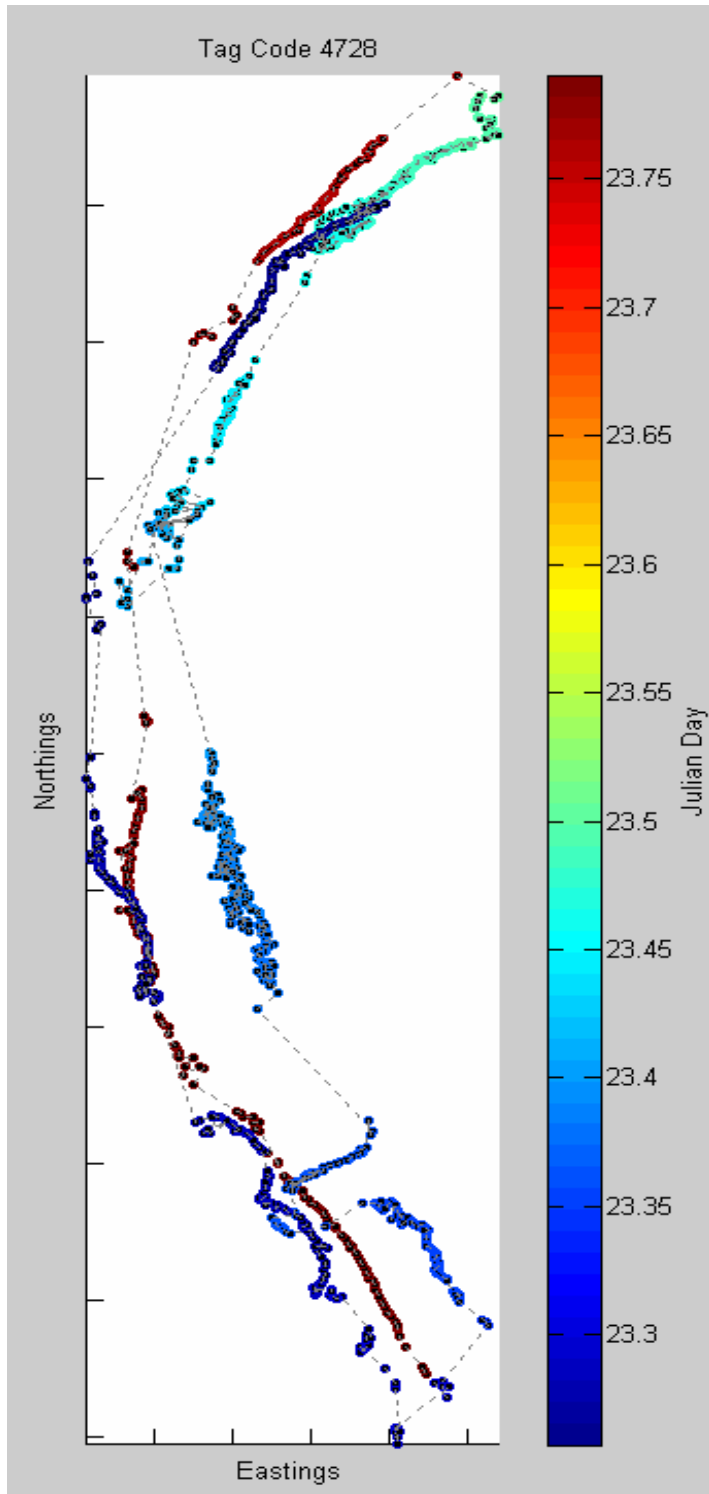


Figure C.24 – Fish 4728 holding during the day and moving at night. Sunrise is just after Julian day value 23.35, and sunset just after 23.75. Fish 4278 moved up the inside of the bend and passed out of the upstream edge of the array, and returned again moving downstream in the dark.

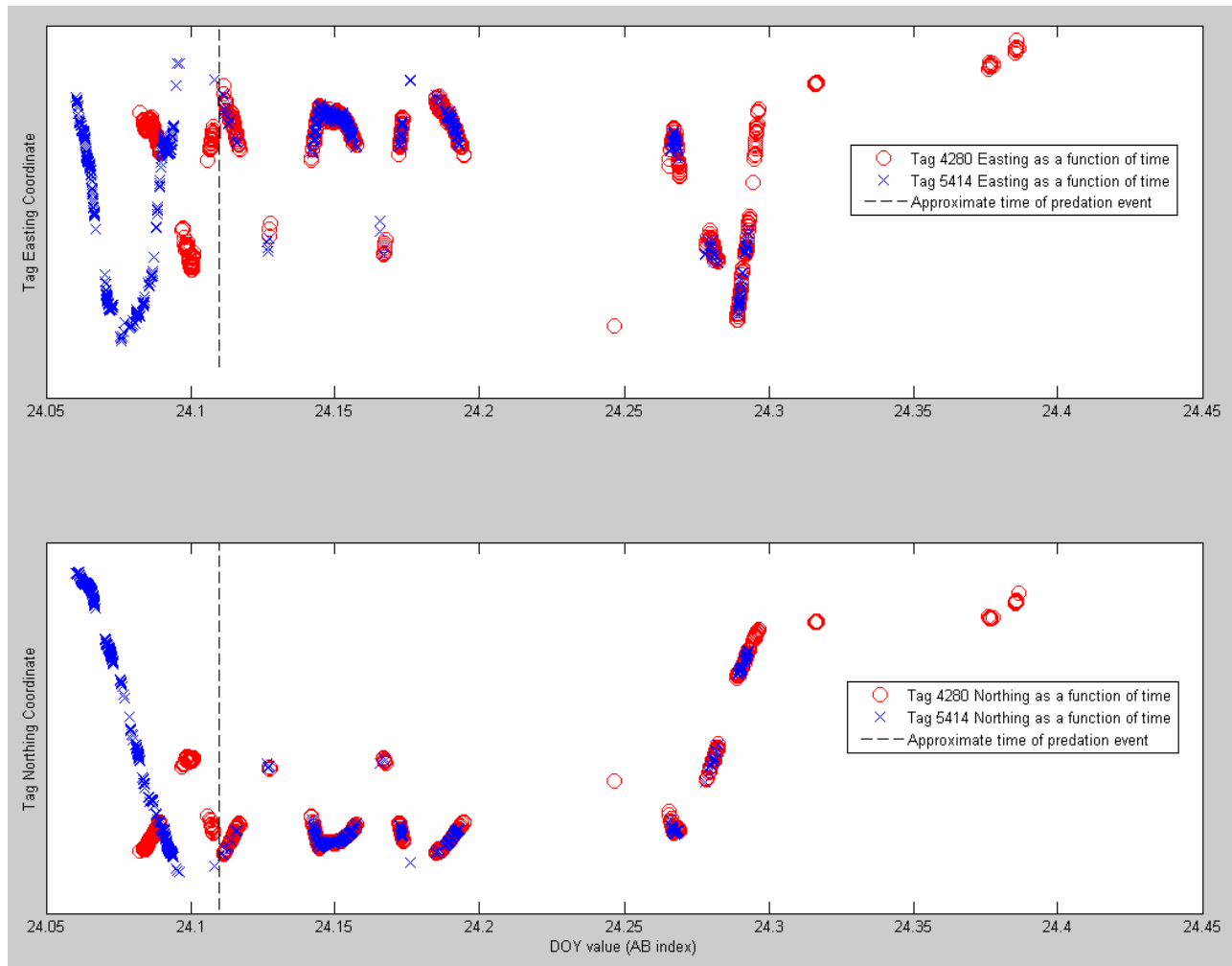


Figure C.25 – Tag 4280 eating tag 5414. Note that in the lower portion of the bend where the predation event occurred, south is towards the downstream end of the array, and east is towards the inside edge of the bend. Note that once the tag coordinates converge they never diverge. The fact that tag 4280 was tracked further at the upstream end of the array is probably due to differences in the orientation of the two tags within the predator.